UNIVERSITY OF CALGARY

Tissue Injury and Effects of Applied Vibration on the Intervertebral Disc

by

Geoffrey Thor Desmoulin

A THESIS

SUBMITTED TO THE FACULTY OF GRADUATE STUDIES

IN PARTIAL FULFILMENT OF THE REQUIREMENTS FOR THE

DEGREE OF DOCTOR OF PHILOSOPHY

DEPARTMENT OF MECHANICAL AND MANUFACTURING ENGINEERING

CALGARY, ALBERTA

APRIL, 2013

© Geoffrey Thor Desmoulin 2013

Abstract

It is thought that disc degeneration can cause spine related pain. New treatments acting at cellular levels in the intervertebral discs (IVD) may offer potential to improve long-term disc health. Hence, optimized loading that induces positive cellular changes in the disc may improve disc health delaying the onset of degeneration, thus delaying the onset of pain. This dissertation evaluates and improves a vibration based spinal intervention called the Khan Kinetic Treatment (KKT) while describing some of its mechanisms of treatment of the intervertebral disc.

Objectives of this study are to: 1) test effects of vibration on disc biosynthesis prior to device modifications (KKT_v1); 2) determine vibration conditions that are most effective in positively altering IVD gene expression; 3) implement findings from objective 2 by modifying the spinal intervention (KKT_v2) and repeating tests; and 4) design, build, validate, and experiment with a novel bioreactor so that other tissues may be targeted.

It could be concluded that the un-modified interventions (KKT_v1) vibration loading profile did not fall within the influential range that affects the cells of the bovine IVD. Objective 2 results showed that expression of certain extracellular matrix genes were significantly up regulated with specific vibration loading patterns, indicating a potential therapeutic stimulus (10 min. total duration of an equal mix of 16 Hz and a 50-80 Hz frequency sweep at a minimum of 0.4 g amplitude). Objective 3 had KKT_v1's firmware edited to drive the new frequencies found to be most effective in objective 2 making KKT_v2; results of objective 3 showed that expression of certain extracellular matrix genes were significantly up regulated when vibrated with the modified intervention (KKT_v2) indicating a potential therapeutic stimulus of the intervention itself. Objective 4 results confirmed the positive influence of mRNA expression with the new bioreactor by utilizing the optimal vibration patterns identified in objective 2.

This research has moved past the proof of concept stage as it has been shown that specific vibration conditions (10 min, 16 & 50-80 Hz, 0.4g) can influence the expression of cell genes in the IVD. The novel bioreactor built as a result of chapter 4 allows us to test other tissues, while mimicking in-vivo conditions. This information could be used to construct future experiments in protein expression or in-vivo MRI studies of human IVD.

Acknowledgements

I would like to thank the following: Optima Health Solutions International Corp. (KKT International), National Research Council of Canada's Industrial Research Assistance Program, and GTD Engineering for helping support portions of my time on this project; Dr. Simon Park for filling Dr. Christopher Hunter's shoes in administrative and dissertation support roles upon his departure from the University of Calgary to Zimmer, Inc.; and Dr. Christopher Hunter for being flexible with my time and knowing the difference between politics and progress.

Financial Disclosure: While portions of this thesis were completed while the author was an employee with Optima Health Solutions International (Optima) he is no longer an Optima employee. He currently contracts as Associate Research Director to Optima but holds no shares nor received any bonuses outside the hourly rate given for portions of work herein. The author is also president and senior engineer at GTD Engineering and is the primary shareholder for the company but GTD Engineering does not hold shares in Optima and paid only for the author's time on portions of work herein. Important note is that GTD Engineering received remuneration from Optima for portions of work performed herein but was solely on a contract basis. GTD Engineering and Optima continue to work together on related projects.

Table of Contents

List of Tables

List of Figures and Illustrations

List of Symbols, Abbreviations and Nomenclature

Symbol	Definition
ADAMTS	A Disintegrin And Metalloproteinase with Thrombospondin Motifs
AF	Annulus Fibrosus
ANOVA	Analysis of Variance
CAD	Computer Aided Design
cDNA	Complimentary Deoxyribonucleic Acid
CEP	Cartilaginous End Plate
CFD	Computational Fluid Mechanics
DAQ	Data Acquisition System
EMG	Electromyography
FDA	Food and Drug Administration
GAPDH	Glyceraldehyde-3-Phosphate Dehydrogenase
GLM	General Linear Model
HHD	Hand Held Device
IVD	Intervertebral Disc
kDa	KiloDalton
KKT	Khan Kinetic Treatment
LCAM	Linear Current Amplifier Module
MAR	Mean Axis of Rotation
MMPs	Matrix Metalloproteinases
MRI	Magnetic Resonance Imaging
mMRI	Messenger Ribonucleic Acid
NP	Nucleus Pulposus
PCR	Polymerase Chain Reaction

PID controller	Proportional gain, Integral gain, Derivative gain controller.
RMS	Root Mean Square
RT	Real Time
TUNEL	Terminal deoxynucleotidyl transferase Nick End Labeling
TZ	Transitional Zone
VEP	Vertebral Endplates
WBV	Whole Body Vibration

CHAPTER 1: INTRODUCTION AND HYPOTHESIS

1.1 Introduction

Back pain is often associated with degeneration of the intervertebral discs and abnormal spinal joint pivot points (Amevo, Worth, & Bogduk, 1991; Wiesel & International Society for Study of the Lumbar Spine., 1996). It was initially thought that whole body vibration (WBV) or repetitive low intensity impacts were possible causes of premature disc degeneration and eventual back pain (Alem, 2005; M. Fritz, Fischer, & Brode, 2005; Oborne, 1983). However, the results of subsequent epidemiological studies are mixed (Lings & Leboeuf-Yde, 2000; Okunribido, Magnusson, & Pope, 2008; Palmer et al., 2008; Robb & Mansfield, 2007; Tamrin et al., 2007; Tiemessen, Hulshof, & Frings-Dresen, 2008; Videman, Simonen, Usenius, Osterman, & Battie, 2000). Further, some clinicians have used vibration of the spine and WBV successfully in treating back pain without completely understanding how it affects the disc tissue or vertebrae positioning (G.T. Desmoulin, Hunter, Hewitt, Bogduk, & Al-Ameri, 2012; G.T. Desmoulin, Yasin, & Chen, 2007; Fontana, Richardson, & Stanton, 2005; Iwamoto, Takeda, Sato, & Uzawa, 2005; Rittweger, Just, Kautzsch, Reeg, & Felsenberg, 2002). Although spinal adjustments, such as those applied by a sinusoidal vibration that replace abnormal joint pivot points are important for acute changes in patient symptoms (G.T. Desmoulin, Szostek, et al., 2012), new treatments that act at the cellular level in the intervertebral discs (IVDs) are required to maintain the spinal joint corrections and improve long term disc health.

By up-regulating genes responsible for producing proteins accountable for disc matrix maintenance, the primary goal, it may be possible to change the overall health of the disc itself. Therefore, optimized vibration loading that induces positive cellular changes in the disc could improve the current health of the disc delaying the onset of degeneration, thus delaying the onset of associated pain. A vibration-based spinal intervention system exists called the Khan Kinetic Treatment (KKT). The system utilizes specific vibration for treatment of acute back pain but has yet to be evaluated or its mechanisms described. This dissertation investigates the intervention while describing some of its mechanisms of treatment on the intervertebral disc.

1.2 Intervention

The Khan Kinetic Treatment (KKT), manufactured by Starfish Medical Inc., is a spinal and upper cervical treatment device consisting of a controller mounted on top of an impulse delivery mechanism, or device head, which is mounted on a movable armature to a fixed stand Figure 1-A. The device head generates the waveforms (sine waves at 50-110 Hz) and the stylus located at the base of the device head mechanically transduces the waveforms through the skin and ultimately to the spine. The vibration reaches multiple tissues as the stylus is placed over a spinal bony landmark, causing minor vibration of the vertebrae and minor repetitive stretching of the attached soft tissues (Figure 1-B and 1-C). The device head may be freely moved in three dimensions so that the stylus may be positioned appropriately on the skin. The stylus movement is controlled by a touch screen setting, which also controls the amplitude of current that is supplied to the stylus actuator. As the device head is fixed in location during treatment, a collapsible rod provides a necessary element of safety to the patient. The rod has been designed to collapse under sufficient force that indicates a non-clinical incident (i.e., the patient moves out

of position). A Hall effect sensor tracks the position of the rod. Thus, if the rod collapses, the device turns off within a few milliseconds.

The intervention is being used clinically and is being further developed by Optima Health Solutions International Corporation (KKT International). Device design, research, development, and manufacturing operations conform to the International Organization for Standardization (ISO) standard 13485:2003 (No. 9309). The intervention currently has class 2 approvals by the Medical Devices Bureau of Health Canada (No. 68884) and 510(k) clearance from the Center for Devices and Radiological Health of the US Food and Drug Administration (No. K060043).

Patients typically undergo a protocol that consists of individual treatments two or three times per week for a period of four to six weeks with each treatment lasting approximately 10 minutes. A more detailed description of the device has been published previously (G.T. Desmoulin et al., 2007).

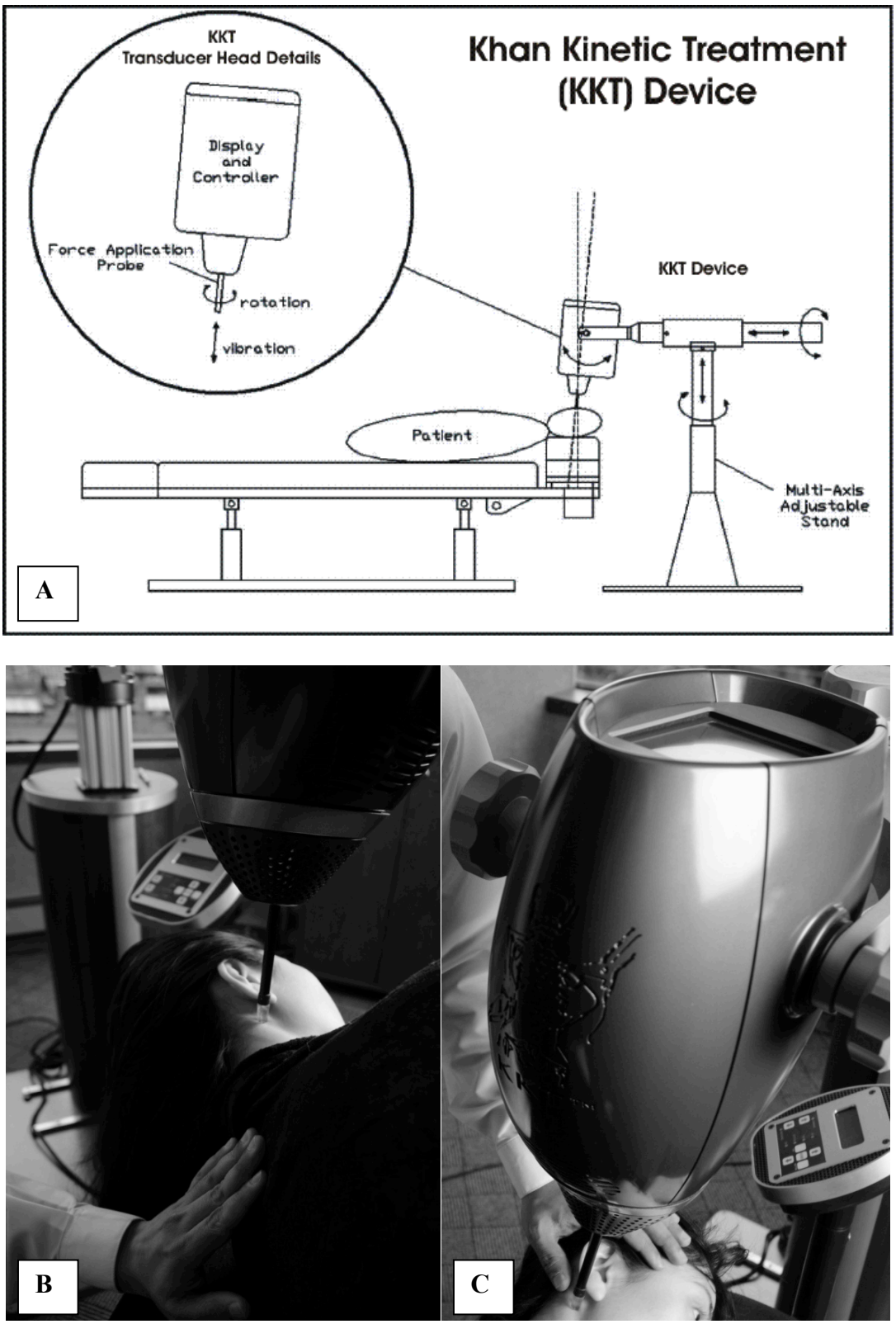

Figure 1: KKT clinical set-up. (Figures were obtained from Optima Health Solutions International Corporation and the Copyright Permission for use of said figures has been attained (See Appendix))

1.3 Motivations

It is known that disc degeneration can cause spine related pain and is related to abnormal spinal joint pivot points. The manufacturer believes that spinal joint adjustment using low amplitude high rate techniques, such as vibration to replace abnormal pivot points, are critical in causing acute changes in patient symptoms such as pain. However, new treatments that act at the cellular level in the intervertebral discs (IVD) are required to maintain these improved pivot point alignments and improve the overall health of the disc for long-term benefits to occur. The object is to find the appropriate vibration protocol that up-regulates genes responsible for producing proteins accountable for disc matrix maintenance. Once this is found, it may be possible to change the overall health of the disc itself by offsetting the initiation of degeneration or in fact restoring tissue and combating chronic pain at its root cause, the disc. Finding the optimized mechanical loading that induces positive cellular changes in the disc will improve the current health of the disc delaying the onset of degeneration, thus delaying the beginning of pain. The research performed here may allow us to optimize the mechanics necessary to induce the changes in the disc that are required to delay this onset of degeneration as well as implement beneficial findings into an existing FDA/Health Canada cleared intervention for use at the clinic level.

1.4 Objectives

The overall objective is to find the appropriate vibration protocol that up-regulates genes important for disc health and implement that protocol into an existing intervention to assess its efficacy. The primary focus of this study is to determine the imparted mechanics to the disc that

optimize biosynthetic response and implement them into the clinical intervention (KKT). We expect the optimal vibration will not cause harm to the cells that we monitor. This feature will be indicated by no significant increases in cell death rates determined via staining techniques and no significant increases in the expression of genes typically found in low magnitudes in the nucleus and high magnitudes in scar tissues such as Collagen I.

To further the research that is performed in this dissertation, a novel bioreactor was built that improves on current prototypes. It was envisioned that the bioreactor would have the ability to load multiple ex-vivo discs at the same time and hold appropriate CO_2 gas control, temperature control, and medium fluid exchange control systems in place. Finally, it was expected that the loading would also be more precise via displacement control and have automatic frequency changes at specific conditions.

Hypothesis: Specific vibration loading patterns between 0-200 Hz, 0-60 min, and 0-5 g delivered to vertebrae up-regulate bovine disc genes designed to produce proteins that affect tissue maintenance.

While this dissertation has specific objectives to address the above stated hypothesis, we have already performed some experiments that begin to explain the complex relation between disc, vertebrae vibration and disc cellular response. Two experiments were run for the initial evaluation of the unmodified spine treatment (KKT_v1) that vibrates the spine between 50-110 Hz: 1) a clinical experiment deriving spinal pivot points or mean axes of rotation (MAR) from x-rays both prior to and after a typical treatment period, and 2) a bovine tail experiment. While the clinical study fell outside the scope of this dissertation, KKT_v1 vibration corrected 62 percent of abnormal MARs with significantly larger MAR vector magnitude differences [pre-post] at the C5-C6 level than shams and MAR correction was significantly related to improving pain across

all human subjects. Hence, we give biomechanical evidence to the term spinal "re-alignment" (G.T. Desmoulin, Hunter, et al., 2012; G.T. Desmoulin, Szostek, et al., 2012). However, the bovine study (second study) was included as one of the objectives in this dissertation and is described in the experimental summary below.

Objective 1: Test vibration effects on specific bovine nucleus pulposus gene mRNA expression in KKTs unmodified state (prior to any device modifications).

This objective tests the unmodified interventions (KKT_v1) vibration pattern on bovine discs prior to any device alterations. The following gene expression profile was the assay of choice: aggrecan, collagen type I, collagen type II, biglycan, decorin, and versican. The KKT_v1 operated and was applied as it was designed, in a frequency range of 50-110 Hz, large amplitudes (>0.5g) for a duration (30 s & 10 min) typical of actual clinic treatments.

This bovine tail experiment found that the initial version of the device (KKT_v1) does not operate in the ideal 'window' for stimulating extracellular matrix gene synthesis in the bovine intervertebral disc (IVD). Only collagen I was differentially expressed as opposed to controls, with both 36 s and 10 min of application *inhibiting* expression. KKT_v1 vibration did not detectably change any other genes.

Objective 2: Perform a matrix of tests to identify parameters necessary to stimulate maximum gene mRNA up-regulation.

Using a free axial vibration prototype, load bovine disc segments at 0-5g; 0, 8, 16, 20, 30, 40, 50, 60, 70, 80, 160, and 200 Hz for 0, 10 min, and 1 hr to determine the window of vibration patterns for stimulating mRNA upregulation using the same gene assay as Objective 1 above.

To address the passive disc gene response of KKT_v1 vibration, a comprehensive loading parameter experiment was performed on bovine caudal IVD while measuring apoptosis or cell death rates monitored the safety of the vibration. Since KKT_v1 had a strict frequency range and no means of controlling the environment of ex-vivo tissue samples, a custom voice coil system was designed, which generated motion in the axial direction only but allowed for tissue to be inside an incubator (37°C, 5% CO_2). Gene mRNA expression in the nucleus pulposus of the bovine tissue was assessed using real time (RT) polymerase chain reaction (PCR) and apoptosis (cell death) was assessed using TUNEL staining. Expression of mRNAs for biglycan, collagen type I, collagen type II, decorin, and versican were significantly affected by vibration duration, frequency, and amplitude, while aggrecan was unaffected. Of the three factors, amplitude had the largest and widest effect. Statistical analysis concluded that expression of extracellular matrix genes was significantly up-regulated at high amplitudes (>0.4 g) in as little as 10 minutes, peaking in two frequency windows: one at around 8-16 Hz and the other between 50-80 Hz without increases in cell death rates. This may indicate a potential therapeutic stimulus. Periodic application of controlled vibration could positively influence matrix maintenance (G.T. Desmoulin, Hunter, et al., 2012; G.T. Desmoulin, Reno, & Hunter, 2010).

Objective 3: Implement information of objective 2 loading patterns to modify the intervention and use it to apply the vibration. The function of the original intervention (KKT_v1) required modification to version KKT_v2 by allowing the implementation of objective 2 loading patterns. The implemented changes could then be characterized by measuring the imparted mechanics through accelerometers and a load cell. Further, re-testing the modifications based on the basic research knowledge that we gained from Objective 2 could

assess their affects on gene expression using the same gene assay used for Objectives 1 and 2 experiments.

Using the knowledge obtained from Objective 2, we implemented the optimal levels of the vibration parameters into the KKT device creating KKT_v2. We then re-ran the initial bovine disc experiment of Objective 1. Results showed that expression of mRNAs for aggrecan, collagen type II, and versican were significantly affected by the modified device (KKT_v2) while collagen type I, biglycan and decorin were unaffected. It was concluded that expression of bovine nucleus pulposus extracellular matrix genes were significantly up-regulated when vibrated with the intervention under the specific loading patterns found in the earlier experiments, indicating a potential therapeutic stimulus (G.T. Desmoulin, Hunter, et al., 2012; G.T. Desmoulin, Reno, & Hunter, 2011).

Objective 4: Develop a more efficient, accurate in-vivo bioreactor for multi-sample loading.

The intervention is not a research tool nor does it allow for incubator conditions of tissue samples; hence this aim involved a major development project; design, assemble, and validate a novel bioreactor that can apply vibration at 0-200 Hz, a 0-1 mm stroke in one axis to isolated IVD samples ex vivo, using closed-loop control. This included the use of CAD software (SolidWork™) to visualize the design, machining to create the specialized parts, electronics to drive the actuators, pumps to create an artificial circulatory/nutritive system for the discs themselves, LabVIEW™ programming for control of loading patterns, and eventual validation of the system with an external sensing system.

The design also improved fluid flow between bioreactors, was capable of loading up to four discs independently, and could switch vibration-loading patterns instantly and automatically. By confirming the positive influence of bovine disc mRNA expression from applied vibration patterns with an entirely new device regardless of loading orientation, this research has demonstrated the methods and ideas feasibility (G.T. Desmoulin, Enns-Bray, Hewitt, & Hunter, 2013). However, the current data remain unable to determine whether the gene expression changes translate into altered protein expression. For a full compilation of assumptions and limitations to these studies please see section 5.5 Limitations and Assumptions. Despite the positive research results of the above summary there are limitations of working with strictly bovine tissue and therefore this research should be continued at the human tissue and in-vivo levels.

1.5 Expected Novel Contributions

The research work is expected to show that specific vibration amplitudes, durations, and frequencies have positive effects on the disc cell gene expression. In this case, significantly increased expressions of genes accountable for disc matrix maintenance are hypothesized to have positive effects. This is important since current literature debates any amount of vibration exposure as being healthy (addressed in Chap. 2). However, vibration that positively influences genes of disc cells will signify the first step in the ability to create a non-invasive therapy for disc degeneration and suggest a regenerative effect of the intervention. Since it is thought that disc degeneration is associated with chronic back pain, the novel therapy will be one of the first of its kind to treat the problem at its root cause, the disc.

This research is also expected to show that it is possible to "tune" loading patterns to the intervertebral disc tissue. Having shown that it is possible to test the ability of other specific vibration conditions to "tune" the intervention to treat within other tissues of the spine such as ligaments and bone. This would help create a holistic treatment system that involves all subject tissue to treat the root of the cause and not just the symptoms.

We expected to build a novel bioreactor that could be validated with the IVD data collected previously but could also be used as a research tool to investigate the loading patterns most beneficial to other tissues of the spine as well. The novel bioreactor more accurately mimics in-vivo conditions by circulating cell culture medium (0.05 L/min) and increases research productivity by allowing for multiple tissue samples to be loaded in one testing cycle.

The value of this research was amplified when considering the key information was transferred immediately to the general public via a regulatory cleared intervention. All findings will help increase the effectiveness of the intervention.

1.6 Organization of Thesis

The thesis is organized based on the flow of experiments that occurred. Chapter 2 consists of a detailed literature survey. Topics include disc anatomy, tissue injury, non-invasive tissue repair, the disc as a mechanical system, pathogenesis of disco-genic pain, current treatment options, and known effects of tissue vibration. Chapter 3 details the effects of disc vibration research performed in the first three of the dissertation's four objectives. Since it was previously shown that the KKT non-invasive intervention helped correct "abnormal" motion in spinal joints (G.T. Desmoulin, Hunter, et al., 2012; G.T. Desmoulin, Szostek, et al., 2012), we wanted to test if the device could maintain that "alignment" for long-term health by restoring disc tissue.

Hence, we tested how the non-invasive intervention would affect disc metabolism in its current state prior to any loading capability modifications. Then, we optimized the loading pattern to maximize the amount of positive gene expression while monitoring the potential for disc injury. The KKT's loading protocol was modified as a result and used in a subsequent experiment as the actual vibration source. Chapter 4 summarizes the design, assembly, validation, and experimentation of a bioreactor for multi-platform loading of tissues. Since, an optimal loading protocol was identified for disc tissue it was desired to find similar "windows" where other types of tissues might respond best. Hence, a multi-platform bioreactor was designed and built to accommodate a wide frequency range (0-200 Hz) and controlled loading so as to be able to assess multiple tissue types. In Chapter 5 the data are considered across all experiments, summarized across experiments, the novel outcomes and limitations from the research are detailed as well as potential future work. Amalgamating the data were performed to both see the effects of the animals that were used in the various experiments but also to build on the results in Chapter 3 and further identify what level of each parameter (frequency, load, and duration) would cause the greatest amount of gene expression for each gene in the assay.

CHAPTER 2: LITERATURE SURVEY

2.1 Introduction

This chapter reviews the body of literature required to both outline the questions that the research will address and information necessary to complete the objectives. Sections include information on the structure of the intervertebral disc (IVD), the complexity of IVD mechano-biology, understanding traumatic disc injury, and potential for non-invasive regeneration. There are also sections looking at the disc as a mechanical system and how disc degeneration affects the disc mechanically. Then the pathogenesis of discogenic back pain is reviewed along with justification for the gene assay utilized in this study. Current treatments are discussed and finally, the importance of vibration in the musculoskeletal tissues surrounding the spine, such as the effect on paraspinal muscles and vertebrae position, is considered.

2.2 Structure of Intervertebral Disc (IVD)

The IVD consists of three tissues: the nucleus pulposus (NP), the annulus fibrosus (AF), and the cartilaginous end plate (CEP) (Figure 2); the first two tissues are surrounded inferiorly and superiorly by the CEPs. The annulus fibrosus is a complex array of layered fibrocartilage. Each layer consists of obliquely oriented, regularly arranged, collagen fibre bundles. The collagen fibres of adjacent layers are arranged in opposite directions crossing obliquely. Lying in the center of the disc, the nucleus pulposus is surrounded by the annulus fibrosus and is constrained by the end plates on both the cranial and caudal surfaces**.**

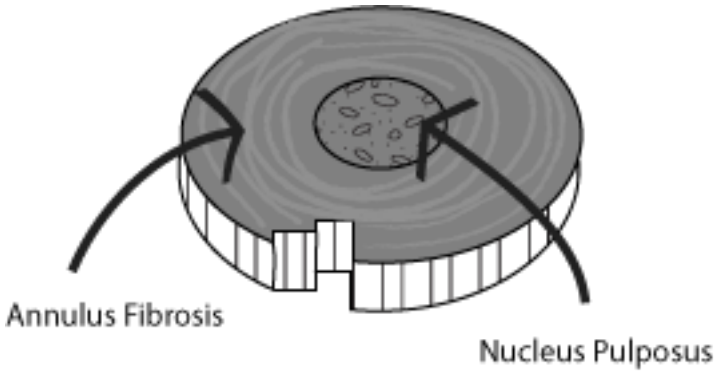

Figure 2: Structure of intervertebral disc. Anterosuperior view with the anterior half of the disc and the right half of the end plate removed.

2.2.1 Nucleus Pulposus

The Nucleus Pulposus (NP) is soft, highly hydrophilic, and is contained within the central zone of the IVD. It is typical that the NP be thought of as an inflated car tire between the two CEPs, thereby explaining vertebral movement with 6 degrees of freedom and providing resistance to compressive loads in its healthy state.

Discography allows radiographic visualization of the disc in a living subject. However, the results of discography reveal that in adults the NP shape varies (M. Adams, Dolan, & WC., 1986). The stratified distribution of the Annulus Fibrosis (AF) can extend somewhat into the central region albeit with decreasing intensity (Rabischong, Louis, Vegraud, & Massacre, 1978). There are many differences between the two regions but the main difference is density, with the NP containing a specific population of proteoglycans and sulfation, enabling it to retain fluids and turgid pressure (Roughley, Melching, Heathfield, Pearce, & Mort, 2006). Although there is no distinct separation between the NP and AF, we use the following three regions for simplicity: AF, NP, and the section between the AF and NP referred to as the transitional zone (TZ) (Taylor,

Ghosh, & GR., 1981). Taylor et al. (1981) describes this zone as sensitive to physical forces and is an area of NP remodeling, since the NP can only increase at the expense of the inner annulus. Using MRI, it is possible to see the variation of both the location and size of the NP: this may be linked to some aspect of function, but the trend is for the NP to be centrally located in cervical discs and posteriorly located for lower lumbar discs (Rabischong et al., 1978). The NP is a heterogeneous structure composed of proteoglycans, collagen fibers, mineral salts, water, and cellular elements. In early life a water content of 80-88% is usually quoted; however, from about the fourth decade (> 40 years old) onward an increasing proportion of subjects show a progressive decrease in the water content until it is about 70% (Keyes & Compere, 1932; Lindahl, 1948).

Electron microscopy studies (H. Inoue, 1973; Sylven, Paulson, Hirsch, & Snellman, 1951; Takeda, 1975) have shown that the healthy gelatinous NP has a three-dimensional structure. The tissue embedded fibrils (collagen and decorin) are irregularly oriented, with diameters in the range of 0.1-0.15 μm in the adult. Proteoglycans become trapped in the fibrils and enable them to imbibe water. The entrapped proteoglycan system modulates water content by both static and dynamic effects. Therefore, changes in the composition of proteoglycans would be expected to have mechanical consequences and since the NP is much richer in proteoglycans than the AF, the NP would be expected to cause the greatest mechanical effect.

Differences in the physical forces applied to the disc may be reflected by differences in the cellular and biochemical composition of the IVD, but how variations occur are still unclear (Taylor et al., 1981). In the NP the cells are enmeshed in a loose three dimensional network and unlike the annulus cells, they appear not to be subjected to any obvious unidirectional stress (Happey, Johnson, Naylor, & Turner, 1964). Consequently, they preserve their spherical shape

and produce new fibrils with apparently random orientation. Although if loads are asymmetrical (15°) with respect to the end-plate and vertebral plane this causes deleterious effect on both tissue and cells.

2.2.2 Annulus Fibrosis (AF)

The AF surrounds the NP. The three-dimensional architecture of the AF is a series of fibrocartilaginous bands whose geometry varies as a function of vertebral level. Macroscopically, the angle of the band is greatest in the inner most layer of any given disc. The number of layers and their size, thickness, and angle of arrangement show variations for any given band within different parts of the same disc, for any particular anatomic level, and from individual to individual. However, in general the thickness of the layer varies from 200 to 400 μm, increasing from inside to outside (H. Inoue, 1973). The fibrils (dia: 0.1-0.2 μm) are uniformly arranged within each layer. The collagen fibres are regularly oriented in alternate sheets crossing at about 60° (Horton, 1958). In electron microscopy (EM) studies, a similar value (50°) for the crossing angle has been determined (H. Inoue, 1973). The question that presents itself is whether the orientation observed is predetermined or is mechanically induced when movement occurs. It is probable that the mechanical phenomena, particularly torsion, are largely responsible for the structure seen in the adult.

The layered bands do not form complete rings, but split and/or merge to interlock with other bands. The posterolateral regions of the AF are both thinner and appear to have marked irregularities. Thus the AF is weakest in these posterolateral regions, thereby predisposing to NP herniations (Kazarian, 1981). The elastic fibres in human discs are circularly, obliquely, and vertically arranged within the AF (E. Johnson, Chetty, Moore, Stewart, & Jones, 1982).

It is thought that alterations in the type of collagen present may be involved in detection of certain disease processes, for example scoliosis (Taylor et al., 1981). The total collagen content decreases from the outer layers of the AF toward the NP. However, the proportion of type II to type I collagen increases from the outer layer of the AF to the NP. Adams et al. (1977) found type I collagen in the outermost regions of the AF and type II in the innermost, whereas the nucleus contained type II collagen only (P. Adams, Eyre, & Muir, 1977). Since type I collagen is typical of tendons and type II of articular cartilage, where large transient compressive forces are generated, the tensile strength of the annulus is probably provided by type I collagen, while the compressive component probably involves type II. In the inner one-third of the AF obliquely oriented fibrillar bundles of lamellae interconnect with the CEP, while in the outer two-thirds these bundles are firmly anchored to the vertebral bodies. Such an arrangement is therefore weak to horizontal shearing forces.

2.2.3 Cartilage End Plate

The cartilage end plate (CEP) is found at each end of the vertebral body and represents the anatomic limit of the disc. It is approximately 1 mm thick at the periphery and decreases toward the centre (Saunders & Inman, 1940). The CEP has three main functions: 1) It appears to protect the vertebral centrum from pressure atrophy (Kazarian, 1981). 2) It confines the AF and NP within their anatomical boundaries. 3) It acts as a semipermeable membrane to facilitate fluid exchanges between the annulus fibrosus, nucleus pulposus, and vertebral body via osmotic action (Armstrong, 1958). However, permeability studies using dyes or radioactive substances appear to indicate that only the central portion of the CEP is permeable and as the person ages localized calcification may reduce the permeability reducing nutritional fluid exchange (Ferguson & Steffen, 2003; A. Nachemson, Lewin, Maroudas, & Freeman, 1970).

2.3 Bovine vs. Human Intervertebral Disc Tissue

The relations between various mechanical inputs and intervertebral disc (IVD) structure, composition, and metabolism are critical to detailing the nuances of disc mechano-biology in both health and disease. Developing a model to test the mechano-biology of IVDs ex-vivo is a complex task, as chemical and mechanical boundary layers are difficult to replicate in-vitro. Further complexity arises from structural differences of the annulus fibroses and the nucleus pulposes of the IVD. Bovine discs have been considered a prime candidate for IVD mechano-biology studies over other animal discs because of their large size, similar aspect ratio, diffusion distance, and resting pressure (0.2-0.3 MPa) as compared to human discs. Bovine discs have also been found to be similar in composition, hydration, collagen profile, proteoglycan profile, and similar rate of proteoglycan synthesis to human discs (Demers, Antoniou, & Mwale, 2004; Oshima, Ishihara, Urban, & Tsuji, 1993). Additionally, coccygeal bovine discs are inexpensive, can be quickly obtained, and are easier to extract than lumbar discs.

Since the future end-goal of this work was to assess how vibration might affect IVD cells in humans, experiments performed have all bovine spine positions "loaded" despite their orientation with respect to gravity. The static tare loads that were applied to bovine IVDs were to recreate resting musculature load and relaxed standing loads that would be present in-vivo for humans even during "unloaded" positions such as lying down. This is important since its likely gene response changes if tissue is loaded statically, dynamically or both.

A difference between bovine and human discs is that a subpopulation of notochordal-like cells remains in the bovine disc (Gilson, Dreger, & Urban, 2010). Notochordal cells affect cell matrix production, which is an important factor in cell therapies aimed at increasing activity in

the nucleus pulposes. Previous research has shown that different loading regimes (C.L. Korecki, Jeffrey, & Iatridis, 2007) and limited nutrition (Jünger et al., 2009) also have a significant effect on overall disc degeneration. Thus, maintaining a controlled culture medium during IVD loading protocol is necessary to fully understand the mechano-biology of IVDs.

2.4 Understanding Disc Injury and Potential for Healing

This section discusses tissue injury and growth or regeneration potential from an engineering perspective. The former is relevant to understanding impact loads that cause tissue failure and the latter pertains to treatment and healing. The belief is that tissue injury and repair is related to physical stress, especially load bearing tissue, as it has known mechano-biological processes that stimulate gene expression on a regular basis. Hence, the body's response to physical stress is biological by nature (Nahum & Melvin, 2010).

Trauma to a person or tissue is similar to that of any physical structure. Since, engineers have studied physical structures for generations there is a general consensus among them that stress and the resulting strain is the most critical values when it comes to failures in physical structures. Hence, the capacity of a structure is viewed as the stress at every point within the structure relative to the strength of the material being stressed.

The magnitude of the impact or mechanical loading acting on tissues, specifically the disc, as previously mentioned, is best described in terms of stresses and pressures. Stress is force per unit area acting on a solid and can vary with location and direction. Pressure is the force per unit area acting in a fluid, and is typically the same as measured in different directions and locations because fluids deform to equalize the pressure. The nucleus pulposus of normal intervertebral discs behaves like a fluid exhibiting hydrostatic pressure (A. L. Nachemson, 1960), but it is also

capable of stress gradients typical of solids (Skrzypiec, Pollintine, Przybyla, Dolan, & Adams, 2007). This is important because stress concentrations and gradients can disrupt tissue architecture, which can lead to structural failure. Further, cell metabolism is sensitive to stress and pressure. For example, chondrocytes in the nucleus pulposus increase matrix synthesis in response to moderate hydrostatic pressure, but decrease their synthesis and produce more proteases (Handa et al., 1997a) if the stresses become too high, such as occurs during a traumatic impact (Hall, Urban, & Gehl, 1991). Hence, it is apparent that both tissue failure leading to injury and positive cell responses leading to tissue maintenance depend on the characteristics of the imparted stress.

2.4.1 Understanding Mechano-biology

Mechanical factors like stress influence the biological response of intervertebral disc (IVD) tissue through changing metabolic activity and eventually matrix integrity (J. C. Iatridis, J. J. MacLean, P. J. Roughley, & M. Alini, 2006). Some research groups suggest, as with other tissues of the body, the IVD has a threshold of mechanical loading beyond which structural damage occurs and biological activity shifts towards being catabolic (A. J. Walsh & J. C. Lotz, 2004) however, it remains unclear as to whether damage and the resulting biological consequences are dependent more on load magnitude or the manner in which the load occurs. For example, when relatively large compression magnitudes (up to 2.5 MPa) were applied to IVDs it increased cell metabolism with a relatively slow rate of accumulation of degenerative changes (C. L. Korecki, MacLean, & Iatridis, 2008). In other words, compression loads up to 2.5 MPa are not overly dangerous. Torsion does not appear to be particularly damaging to the IVD either as the amount of rotation needed for structural failure of the human lumbar IVD (±10°) is

five times greater than that experienced physiologically (±2°) (M. A. Adams & W. C. Hutton, 1981). Further, relatively large magnitudes of torsion did not induce negative biosynthetic activity in a rat-tail model (Barbir et al., 1976). Together, these results suggest that the IVD can tolerate relatively large amounts of loading in a single direction.

A combination of multiple loading directions, or complex loading, develops in many physiological spinal motions such as bending with compression (e.g., deadlift). The complex loading that develops in hyperflexion has been implicated in IVD injury with a potential mechanism being the development of both shear and compressive strain (Costi et al., 2007). The concept of vulnerability during complex loading was further demonstrated with the combination of axial torque with flexion-extension fatigue loading and found that the combined loading accelerated injury in porcine motion segments (Drake, Aultman, McGill, & Callaghan, 2005)). Load to failure evaluations on the IVD determined that extreme loading could lead to herniation or other pathologies but with limited understanding of the biological consequences. Hence, improved understanding of the interaction of biomechanical and biological factors with loading is required to create effective strategies that provide functional restoration of intervertebral discs and prevent progressive degeneration.

2.4.2 Tissue Stress becomes Irregular Following Injury

Injury to the bony section of the spine is less common than injury to the soft tissues of the spine during traumatic loading at least during automobile accidents. Further, disc rupture tends to be induced by repetitive stress rather than due to a single incident. Nonetheless, high stress loading leading to damage to an intervertebral disc or a fracture to its subchondral bone causes an immediate large reduction in pressure in the nucleus pulposus. Nucleus decompression

averages 25% of pre-loaded pressures (M. A. Adams, B. J. Freeman, H. P. Morrison, I. W. Nelson, & P. Dolan, 2000). As the decompression phenomenon occurs, high stress concentrations develop as a result in various locations of the disc (Luo et al., 2007). Damage to a vertebral endplate increases the volume of space developed by the injury and causes a relatively large drop in pressure (Brinckmann & Horst, 1985), and studies of disc injuries show that stress distributions are influenced more by endplate injury than by injuries of the outer annulus (Przybyla, Pollintine, Bedzinski, & Adams, 2006). These findings have consequences, which give insights into the nature of disc degeneration.

The results of measuring the stress profile of the disc over time suggest that disc degeneration represents what seems to be a progressive structural failure leading to stress concentrations. Stress concentrations could cause pain, and could encourage continued physical damage and injury to propagate throughout the tissue. This point is emphasized when the literature around disc rupture is reviewed. Early papers (Brinckmann, 1986; Henzel, Mohr, & H.E., 1968; Roaf, 1960) show that disc ruptures, where nucleus matter is extruded, do not occur as the result of a single loading event unless there is massive accompanying bony fractures. Although more recently it has been shown that ligament tears and disc disruption can occur in impacts with an average deceleration as small as 3.3g (ΔV = 4.4 m/sec) but it is still likely a strong initiator of this repetitive process rather than the sole cause (Yoganandan, Cusick, Pintar, & Rao, 2001). More specifically stress concentrations have negative influence on disc cell metabolism because both extreme high and low pressures decrease matrix synthesis (Ishihara, McNally, Urban, & Hall, 1996). Cells in a nucleus experiencing stress concentrations and overall decompression produce less proteoglycans, leading to a larger difference between stress variations and additional decompression. In effect, disc cell metabolism becomes aberrant

because nucleus cells largely responsible for imbibing water to maintain disc pressure respond negatively to their abnormal local mechanical environment (M. A. Adams & P. J. Roughley, 2006). Tissue studies show that high stresses that could cause structural damage increase the synthesis of degrading enzymes (Handa et al., 1997b), and interestingly, the activity of such degrading enzymes is increased most in regions of structural failure leading to further differences in stress variations (Weiler, Nerlich, Zipperer, Bachmeier, & Boos, 2002).

Stress measurement provides insight into the initiation and progression of disc degeneration as most animal models of disc degeneration start with structural damage to either the annulus or the endplate (Holm, Holm, Ekstrom, Karladani, & Hansson, 2004; Ulrich, Liebenberg, Thuillier, & Lotz, 2007).

2.4.3 Potential for Regeneration

The potential for the non-invasive stimulation of tissue regeneration seems plausible when considering that the body itself regulates tissue maintenance daily when loads are transferred through the body by external reaction forces during activities of daily living. Isolated cell culture systems, like the one built in this dissertation, have been an important tool to delineate the relationship between mechanical stimuli and cellular response. When intervertebral disc (IVD) cells are subject to compressive static loads there is zonal or location specific increases in gene expression as measured by changes in mRNA (Chen J, 2004). It is hypothesized that this increase in gene expression can be maximized and could stimulate tissue remodeling (G.T. Desmoulin, Hunter, et al., 2012).

It is hypothesized that gene expression of proteins in the intervertebral disc is a quantitative function of intervertebral joint forces and it is dependent on magnitude, frequency,

and duration. Potential gene expression responses to continuous loading could occur when experiments of mRNA levels following compression loading in vivo are observed. A) There could be an on/off response of gene expression to mechanical loading as gene-expression response increases to a maximum and stays upregulated as long as the mechanical stimulus is continued. This was observed by annulus cells in response to continued mechanical loading at 1 MPa and 1 Hz in a petri dish (Roughley, 2004). B) Other studies have shown that in the pulposus there was a maintenance effect with an initial upregulation followed by a return to control levels when loaded to 1 MPa at 1 Hz (MacLean, Lee, Alini, & Iatridis, 2005). C) There could be an adaptation effect as well, which demonstrates an upregulation followed by equilibrium at a new steady state above that of the control levels. D) Finally, the effects of mechanical loading could result in no response from the cells and therefore no change in mRNA levels. However, a response similar to any of the first three types of changes (A-C) in mRNA levels could lead to changing the outcome levels of proteins (G.T. Desmoulin, Hunter, et al., 2012). The changes in protein levels could manifest itself several ways. It is hypothesized that either a) conditions promote protein synthesis but only to the level of replacing those lost resulting in a null change in overall protein levels; or b) conditions promoting increases in overall protein levels.

2.5 Intervertebral Disc as a Mechanical System

To gain insight into how the disc behaves under cyclical load a review of mechanical models of the disc and vertebrae system is presented below. Generally the intervertebral discs provide mobility and a degree of shock absorbance to the spinal column. They also transmit the majority of loads between the adjacent vertebrae (with lesser contributions from the vertebral processes and articulating facets). It has been shown that the mechanical properties of the

intervertebral discs play an important role in their functionality (Cheung, Zhang, & Chow, 2003; A.J. Walsh & J.C. Lotz, 2004).

At its most basic level, a spinal joint including an intervertebral disc can be viewed as a classical second order mechanical system. A second order mechanical system consists of a damped mass-spring system under an applied force or in this case a forced vibration (Figure 3).

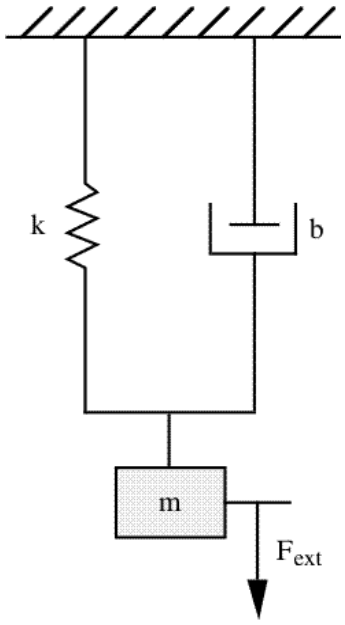

Figure 3: Second order system. k- stiffness; b-damping; m-mass; F-force.

2.5.1 Frequency Response Function

When a vertebrae being loaded by applied force experiences acceleration, the system's apparent mass develops a corresponding D'Alembert (inertial) force. This force acts on and displaces the spring component of the system a distance and the damper provides a resistance force that is proportional to the velocity of the motion. Therefore, the response of the spine model can be found by summing the forces acting on its apparent mass (Figure 4).

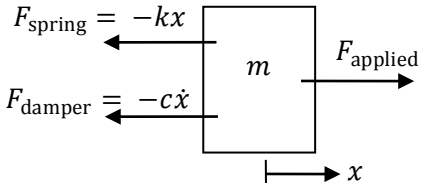

Figure 4: Summing the forces on the apparent mass of the second order system.

The equation of motion can be shown to be (Morril, 1957)

[2.1]

$$\ddot{x} + 2\xi\omega_{\text{n}}\dot{x} + \omega_{\text{n}}^2 x = \frac{F_{\text{applied}}}{m}.$$

where acceleration, velocity and displacement are defined as $\ddot{x}, \dot{x}$, and x respectively and the natural (angular) frequency, ω_{n}, and the damping ratio, ξ, of the system are defined by

[2.2]

$$\omega_{\text{n}} = \sqrt{\frac{k}{m}}$$

where k and m are stiffness and mass respectively and

[2.3]

$$\xi = \frac{c}{2\sqrt{km}}.$$

where c is the damping coefficient. Taking the Laplace Transform shows:

[2.4]

$$\frac{\mathbb{X}(s)}{\mathbb{F}(s)} - \frac{sx(0) + (1 + 2\xi\omega_{\text{n}})\dot{x}(0)}{(s^2 + 2\xi\omega_{\text{n}}s + \omega_{\text{n}}^2)\mathbb{F}(s)} = \frac{1/m}{s^2 + 2\xi\omega_{\text{n}}s + \omega_{\text{n}}^2},$$

where $\mathbb{X}(s)$ and $\mathbb{F}(s)$ are the Laplace Transform of x and F_{applied}, respectively, and $x(0)$ and $\dot{x}(0)$ are the initial conditions. Considering the steady-state response, *i.e.*,

[2.5]
$$\frac{\mathbb{X}(s)}{\mathbb{F}(s)} = \frac{1/m}{s^2 + 2\xi\omega_{\text{n}}s + \omega_{\text{n}}^2}$$

and substituting in $s = j\omega$ leads to the frequency response function,

[2.6]
$$\mathbb{H}(\omega) = \frac{\mathbb{X}(\omega)}{\mathbb{F}(\omega)} = \frac{1/m}{(\omega_{\text{n}}^2 - \omega^2)^2 + (2\xi\omega_{\text{n}}\omega)^2}(\omega_{\text{n}}^2 - \omega^2 - j2\xi\omega_{\text{n}}\omega),$$

with a magnitude of

[2.7]
$$|\mathbb{H}(\omega)| = \frac{1/m}{\sqrt{(\omega_{\text{n}}^2 - \omega^2)^2 + (2\xi\omega_{\text{n}}\omega)^2}}$$

and phase of

[2.8]
$$\phi(\omega) = \tan^{-1}\left(\frac{-2\xi\omega_{\text{n}}\omega}{\omega_{\text{n}}^2 - \omega^2}\right).$$

The value of k can be determined at $\omega = 0$, where $|\mathbb{H}(0)| = 1/k$. In turn, the value of ξ can be determined at $\omega = \omega_{\text{n}}$, where $|\mathbb{H}(\omega)|$ is at its maximum with a value of $|\mathbb{H}(\omega_{\text{n}})| = 1/(2\xi k)$.

Like the above model of the disc other more complex models lump masses of anatomical structures into concentrated masses interconnected by ideal springs and dampers. While these models do not necessarily correspond well to the actual anatomy of the disc many have proven effective in capturing functional biodynamic properties. Coermann (1962) developed the classic single degree-of-freedom (DOF) model like the one presented above (Coermann, 1962). Since,

anatomical masses are concentrated into a single lumped mass and connected to the vibration application probe the model will predict one resonant frequency in the transmission of vibration.

The type of model discussed above produces linear responses. Mertens (1978) developed a multi-DOF model that simulates the non-linear mechanical response of biological tissue with reasonable accuracy (Mertens, 1978) where the individual parameters of the model represent different anatomical parts. The values for the mass and spring elements were obtained from experimental data and transmissibility was calculated for the model and compared with experimental data from nine cadaveric samples.

Many attempts have been made to develop more accurate but consequently more complex nonlinear models; for instance, a complex multi-degree-of-freedom model was proposed by Muksian & Nash, 1974 (Muksian & Nash, 1974). However, the model is incapable of assessing conditions involving random vibration. In 1994, Qassem et al. (1994) presented an extension of Muksian and Nash's (1974) model that comprised of a multi-part, two-axis model (Qassem, Othman, & Abdul-Majeed, 1994). This model could predict the response from a combination of horizontal and vertical vibrations either separately or together. The model showed good correlation with experimental data in the vertical plane but not the horizontal plane between 4-40 Hz. So, in 1994, Smith increased the models complexity again by adding a quasi-static nonlinear component (Smith, 2006).

The importance of anatomically accurate models was emphasized in the above model review, as this allows a better understanding of the effect of vibration on spinal joints. However, it was also emphasized that this rule of thumb should not preclude the use of simple models to establish the general response to vibration, as these model types are relatively easy to develop

and interpret. The application of this information is that it allows us to interpret the results of the following experiments more accurately. By knowing the energy transmission will change with various frequencies helps determine what the cell response should be. For example, this allows us to predict variability in discs of a range in size, density, and composition as the amount of vibrational energy reaching the cells would be different in each case.

2.5.2 Transmissibility

Disc vibration transmissibility is defined as the ratio of the output spectrum over the input spectrum and was calculated below in a sweeping frequency from 0 to 100 Hz using a base excitation model.

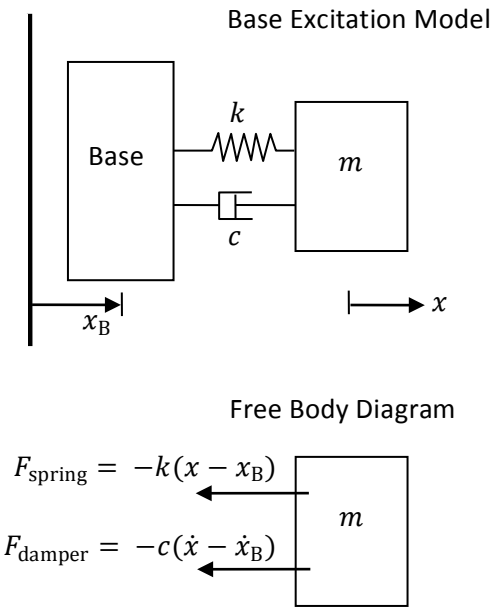

Figure 5 Base excitation model and free body diagram of net forces to demonstrate disc transmissibility.

The equation of motion of the system can be shown to be (Morril, 1957):

[2.7]

$$\ddot{x} + 2\xi\omega_{\mathrm{n}}\dot{x} + \omega_{\mathrm{n}}^2 x = 2\xi\omega_{\mathrm{n}}\dot{x}_{\mathrm{B}} + \omega_{\mathrm{n}}^2 x_{\mathrm{B}} .$$

Taking the Laplace Transform of the equation of motion and then rearranging terms give

[2.8]

$$(s^2 + 2\xi\omega_{\mathrm{n}}s + \omega_{\mathrm{n}}^2)\mathbb{X}(s) - [sx(0) + (1 + 2\xi\omega_{\mathrm{n}})\dot{x}(0)] = (2\xi\omega_{\mathrm{n}}s + \omega_{\mathrm{n}}^2)\mathbb{X}_{\mathrm{B}}(s) - 2\xi\omega_{\mathrm{n}}\dot{x}_{\mathrm{B}}(0) ,$$

where $\mathbb{X}(s)$ and $\mathbb{X}_{\mathrm{B}}(s)$ are the Laplace Transform of x and x_{B}, respectively, and $x(0)$, $\dot{x}(0)$ and $\dot{x}_{\mathrm{B}}(0)$ are the initial conditions. We consider the steady-state response, *i.e.*,

[2.9]

$$(s^2 + 2\xi\omega_{\mathrm{n}}s + \omega_{\mathrm{n}}^2)\mathbb{X}(s) = (2\xi\omega_{\mathrm{n}}s + \omega_{\mathrm{n}}^2)\mathbb{X}_{\mathrm{B}}(s) .$$

Substituting in $s = j\omega$ and rearranging terms lead to the transmissibility,

[2.10]

$$\mathrm{TR}(\omega) \stackrel{\text{def}}{=} \left|\frac{\mathbb{X}(\omega)}{\mathbb{X}_{\mathrm{B}}(\omega)}\right| = \sqrt{\frac{\omega_{\mathrm{n}}^4 + (2\xi\omega_{\mathrm{n}}\omega)^2}{(\omega_{\mathrm{n}}^2 - \omega^2)^2 + (2\xi\omega_{\mathrm{n}}\omega)^2}} .$$

The value of ξ can be determined at $\omega = \omega_{\mathrm{n}}$, where TR is at its maximum with a value of

[2.11]

$$\mathrm{TR}(\omega_{\mathrm{n}}) = \sqrt{1 + \frac{1}{4\xi^2}} .$$

TR < 1 when $\omega > \sqrt{2}\omega_n$ means that the base excitation is isolated when $\omega > \sqrt{2}\omega_n$. Figure 6 below was generated using the MATLAB code found in the appendix when $\omega_n = 2$, $\xi = 0.1$, and ω ranged from 0-6 to highlight the transmissibility effects when excitation frequency nears natural frequency of the system.

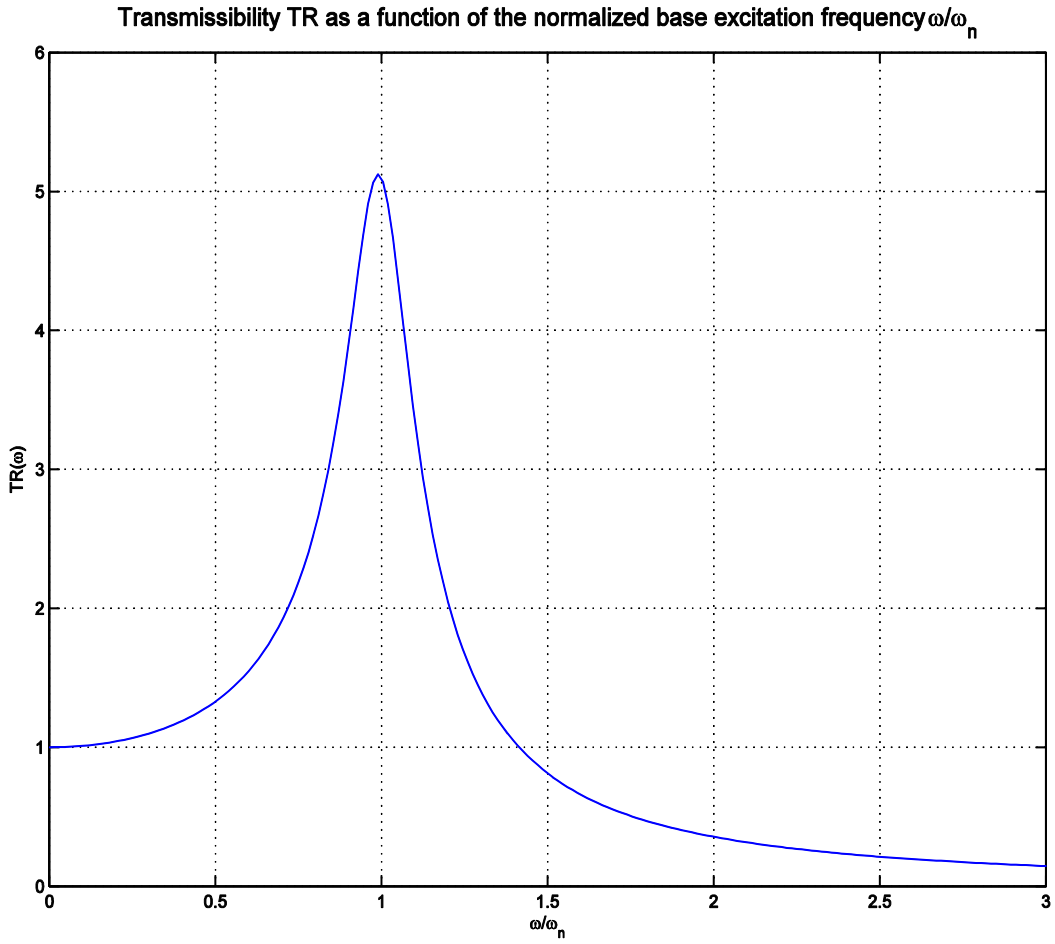

Figure 6. Disc transmissibility diagram using a base excitation model

In order to obtain these values experimentally a number of approaches can be used. Static models have significance, but dynamic models are more accurate in that they characterize the *in situ* nature of the tissues. Some researcher groups have studied dynamic disc loading using

biomedical performance and fatigue failure methods (M.A. Adams & W.C. Hutton, 1981), while other researchers reported on the mechanical parameters of discs under high frequency vibration (Hult, Ekstrom, Kaigle, Holm, & Hansson, 1995). Another study which found the mechanical parameters (stiffness, damping, and natural frequencies) using experimental modal analysis and the receptance coupling method (Malekian, Park, & Hunter, 2008). The identified parameters in the axial direction were a natural frequency of 8 Hz, 0.23 damping ratio, a 134 N/m stiffness in the first mode of the response, and 12.6 Hz, 0.065, and 1360 N/m in the second mode of the response. Izambert and colleagues (Izambert, Mitton, Thourot, & Lavaste, 2003) tested cadaveric human lumbar IVD preloaded with 400 N; they found a single natural frequency peak between 8 and 10.4 Hz. Kasra et al. (M. Kasra, Shirazi-Adl, & Drouin, 1992), accounting for torso loading, used both experimental methods and finite element models to assess resonant frequencies and spinal joint motion damping in the axial direction. They showed that resonant frequency increases about 10 Hz with axial load ranging from 50-700N, dynamic stiffness increases almost 4 fold (~600-2100 N/m) with the same pre-loads, but the damping ratio remains relatively constant (~0.08) throughout the pre-load range. An elegant in vivo study performed by Kaigle et al. (Kaigle, Ekström, Holm, Rostedt, & Hansson, 1998) utilizing porcine models in health, acute disc injury and disc degeneration, found resonant frequency to be 25 Hz. Dynamic stiffness increased significantly with each repeated pre-loading protocol and increased about 10-15% over the frequency range tested (0.05-25 Hz), which is typical of a viscoelastic material. However, there was no significant increase in stiffness of the disc in the axial direction, when comparing from healthy to the acute injured state, but there was a highly significant increase in stiffness when comparing across the healthy disc (~170 N/m) and degenerated disc (~230 N/m).

This mechanical summary of spinal joints, including the intervertebral disc, highlights the facts that while damping ratios are relatively large, stiffness is largely dependent on the static and dynamic loading magnitude and loading history. Also, the biomechanical properties of the disc segment under loading are significantly affected over time due to disc degeneration. This summary was of assistance when determining what frequencies should be tested. The University of Calgary's Vibrations Laboratory cited above and assisted by the author (Malekian et al., 2008) found that the bovine model (vertebrae-disc-vertebrae) system has a natural frequency of 8Hz in the axial direction. Hence, it was desired to see if vibration at that frequency would be different than others selected. Further, all of the summary's information was of assistance when interpreting data and attempting to understand human response during actual treatment.

2.6 Pathogenesis of Discogenic Back Pain

Studies examining the problem from different directions, (e.g., examination of volunteers) (Kelgren, 1977) and patients (Kuslich, Ulstrom, & Michael, 1991), imaging investigations (Luoma et al., 2000), and trials of intervention (Barrick, Schofferman, & Reynolds, 2000) have produced evidence implicating the intervertebral disc (IVD) in a significant proportion (>40%) of cases of chronic spinal pain, leading to the use of the term '*discogenic back pain*'.

The nucleus pulposus (NP) tissue changes include; increased breakdown of matrix, altered matrix synthesis (consisting of type II to type I collagen synthesis and decreased synthesis of aggrecan), and cell loss through apoptosis and clonal replication of surviving cells to form clusters (M. Adams & P. Roughley, 2006; W. Johnson & Roberts, 2007; Le Maitre, Pockert, Buttle, Freemont, & Hoyland, 2007). As the amount of aggrecan and swelling pressure of the NP fall, loss of disc height alters joint loading patterns eventually leading to microtrauma and pain.

The microtrauma damages both the AF and the bone into which the fibers of the AF insert, allowing blood vessels and nerves a route into the IVD (Hilton & Ball, 1984). When the spacing effect of the normal NP is lost and the vertebral bodies approximate to one another, abnormal movement and loading occurs throughout the entire motion segment (vertebrae-disc-vertebrae) causing traumatic damage to the facet joints and other structures (M. Adams, Pollintine, Tobias, Wakley, & Dolan, 2006; Brown, Pollintine, & Adams, 2008). This dysfunction of the motion segment is mediated by disturbances in the biology of the cells of the NP and AF (Zhao, Wang, Jiang, & Dai, 2007).

These cellular disturbances can be broken down to six main mechanisms:

(i) Diffusion of nutrients and oxygen across the IVD matrix.

(ii) Soluble regulators of cell function.

(iii) Genetic influences.

(iv) Senescence.

(v) Mechanical load.

(vi) Nerve ingrowth.

(i) Diffusion of nutrients and oxygen across the IVD matrix.

Cells of the IVD receive oxygen and nutrients by diffusion across the disc matrix. The diffusion length to cells in the center of the disc can be long (up to 1 cm) and while the cells are believed to be adapted to function in an environment that is relatively oxygen and nutrient poor (Soukane, Shirazi-Adl, & Urban, 2007), any other conditions reducing this nutrient flow accelerates disc degeneration (Freemont, 2009). The exact pathways need to be elucidated, but there is a strong relationship between reduced blood flow and early disc degeneration due to

factors such as smoking (Cong, Pang, Xuan, & Tu) or injury to the Cartiladge End Plate (CEP) (Baranto, Hellstrom, & Sward).

(ii) Soluble regulators of cell function.

In degeneration, there is a breakdown in Interleukin-1 (IL-1) regulation with increased production of IL-1 isoforms by native disc cells associated with a failure to up-regulate IL-1Ra. This imbalance in the IL-1 system has been shown to be able to induce all the tissue changes associated with degeneration. These include:

- Up-regulation of zinc-based matrix degrading enzymes, notably matrix metalloproteinases (MMPs), a disintegrin and metalloproteinase with thrombospondin motifs **(**ADAMTS) (Anderson, Izzo, & Hall, 2002; Jimbo, Park, Yokosuka, Sato, & Nagata, 2005; Shen, Melrose, Ghosh, & F., 2003; Studer et al., 2008).
- Abnormal synthesis of aggrecan and collagen II and their replacement by collagen I (Goldring & Goldring, 2004; Le Maitre, Pockert, et al., 2007).
- Angiogenesis or the development of vessels where vessels are not normally found (Maruotti, Cantatore, Crivellato, Vacca, & Ribatti, 2006; Voronov, Carmi, & Apte, 2007).
- Neuronogenesis or innervation where nerves are not normally found (Brisby, 2006).
- Apoptosis of native IVD cells (Zhao, Liu, Li, Jiang, & Dai, 2007).

TNF-α is particularly expressed by cells of a prolapsed disc. An explanation for the role of TNF-α in back pain comes from a recent study in a TNF-α deficient mouse that has provided evidence that TNF-α can induce sensory nerve growth into the IVD (Hayashi, Taira, & Inoue, 2008), which is of considerable interest as it has been previously noted that nerve in-growth is a feature of the painful degenerate IVD (Freemont et al., 1997). However, the IVD cells that would be the putative target do not express its receptor (Le Maitre, Hoyland, & Freemont, 2007), and anti-TNF does not inhibit in situ matrix degrading activity (Hoyland, Le Maitre, & Freemont, 2008).

(iii) Genetic influences.

Twin and other studies have shown that a significant proportion of IVD degeneration cases can be explained on the basis of genetic factors alone (Battie´, Videman, Levalahti, Gill, & Kaprio, 2007; MacGregor, Andrew, Sambrook, & Spector, 2004). This means that a large proportion of the variance between subjects with or without disc degeneration can be accounted for by genetics.

(iv) Senescence.

Disc cell numbers and viability decrease in degenerate IVD. This has been attributed to apoptosis and cellular senescence. Senescent cells lose their ability to divide, they are viable and synthetically active, although gene expression is different from that in normal cells. The accumulation of senescent cells in-vivo, together with their changed pattern of gene expression implicates cellular senescence in age-related pathologies (Repanti, Korovessis, Stamatakis, Spastris, & Kosti, 1998) of other chondroid tissues such as articular cartilage in osteoarthritis

(Martin & Buckwalter, 2002), where chondrocyte senescence correlates with disturbed matrix homoeostasis. This has raised the possibility that the changes seen within the diseased IVD are also senescence related.

(v) Mechanical loads.

There is increasing evidence that load has a profound and fundamental influence on the biology of IVD cells (Wang, Jiang, & Dai, 2007) and that 'normal' mechanical loading is essential for maintaining a normal phenotype (Johannessen, Vresilovic, Wright, & Elliott, 2004; Setton & Chen, 2006). Excessive spinal loading however, can lead to the development of the radiological and biochemical features of degeneration (Pye, Reid, Adams, Silman, & O'Neill, 2007). Not only does excessive load lead to changes in the IVD but other factors such as significant traumatic injury (M. Adams & P. Roughley, 2006) and scoliosis (Meir, McNally, Fairbank, Jones, & Urban, 2008), which alter the load in other ways do as well. The precise mechanisms linking load and cell function in the IVD are poorly understood (Hill, Desmoulin, & Hunter, 2009). However, increasing interest in mechanotransduction is gradually aiding an understanding of how the altered mechanical environment in the IVD; a) causes (M. Adams, B. Freeman, H. Morrison, I. Nelson, & P. Dolan, 2000) and is caused by degeneration (M. Adams & Dolan, 2005); b) translates into altered cell and matrix biology (J. Iatridis, J. MacLean, P. Roughley, & M. Alini, 2006); and c) can also be employed in therapeutic regeneration (Schnake, Putzier, Haas, & Kandziora, 2006).

(vi) Nerve ingrowth.

A factor that has been a reoccurring finding in the analysis of excised painful IVD has been the presence of nerves and to a lesser extent blood vessels within the aneural and avascular tissues of the IVD (Aoki et al., 2006; Aoki, Ohtori, Ino, et al., 2004; Aoki, Ohtori, Takahashi, et al., 2004; Aoki, Takahashi, et al., 2004; Freemont, 2009; G. Inoue et al., 2006; Ohtori et al., 2001; Ohtori et al., 1999; Salo et al., 2008; Sugiura et al., 2008). An important aspect of these studies is that nerves with the structure and biology of nociceptive nerves are only seen in IVD that has been classified clinically as 'pain level discs'. By this, it means that probing these discs specifically reproduces the patient's symptoms of back pain. IVD showing similar degrees of degeneration but that did not come from 'pain levels' do not show nerve ingrowth.

Johnson and co-workers (W. Johnson et al., 2002) examined the in vitro effects that aggrecan removed from normal human disc tissue and altered aggrecan had on neurite outgrowth. They showed that aggrecan derived from normal IVD inhibited the growth of neurites, but deglycosylated aggrecan, similar to that found in the degenerate IVD, had a reduced inhibitory effect. This implies that normal aggrecan is an inhibitor of nerve ingrowth into the IVD, and that in degeneration nerve ingrowth may occur as a consequence of changed aggrecan biology. Aggrecan from both the AF and NP were inhibitory but aggrecan from the AF was more inhibitory.

As the above review highlights, there is an association if not a clear link implicating the IVD in a significant portion of chronic spinal pain cases. The '*discogenic back pain*' occurs as a result of disc degeneration, which is becoming more understood as several main mechanisms have been identified. The main mechanisms of disc degeneration involve the disruption of: a) nutrient flow to disc tissue, b) regulators of disc cell function, c) disc cell viability, and d)

mechano-biology with specific loads. While genetics plays a large role in the rate of disc degeneration the mechanisms mentioned above lead to nerve ingrowth that is likely the sole source of '*discogenic back pain*'. However, aggrecan, a protein that is responsible for the mechanical health of the disc and shown to be reduced with disc degeneration, has been shown to retard this nerve ingrowth. Hence, a therapy that non-invasively upregulates aggrecan as is discussed in this study may help and even prevent '*discogenic back pain*'.

2.7 Justification of Gene Assay

The gene assay utilized in this study is comprised of six genes considered to be most important because they are the most directly related in the cascade of genes that produce proteins that maintain disc structure and matrix. The six genes are: aggrecan, biglycan, versican, collagen I, collagen II, and decorin.

An overview of the concept is that aggrecan and versican are the most highly expressed in the nucleus pulposus of a healthy disc, therefore we hypothesize that increased expression for these genes would be expected to correlate to tissue maintenance or repair; conversely, healthy nucleus pulposi exhibit low collagen I expression, as its presence usually indicates formation of scar tissue in response to possible damage. An explanation as to why we are using each gene in the assay is defined below.

Aggrecan is a very large proteoglycan (>2800 kDa) with a primarily mechanical function in the tissue matrix (Benjamin & Ralphs, 2004; Rufai, Benjamin, & Ralphs, 1995). The absence of aggrecan has been shown to be critical in disc health; analysis of excised painful IVD has shown the presence of nerves and blood vessels within the usually aneural and avascular tissues of the IVD, which has been suggested to be a result of altered aggrecan biology (Freemont,

2009). Hence, monitoring aggrecan is important to gain insight into how the disc may increase function mechanically by increased expression but also how increased expression may have a protective effect from the pathological effects of neural ingrowth.

Versican is also a large proteoglycan (1000 kDa) similar to aggrecan, but with a less clear function. It is involved with cell adhesion and cell signaling (Sztrolovics et al., 2002), however a decrease in versican expression occurs at various stages of disc degeneration (Cs-Szabo, Ragasa-San Juan, Turumella, Masuda, & Thonar, 2002) in the same way as aggrecan, making it an important gene to monitor.

As the function of larger proteoglycans such as aggrecan become more understood greater attention is being paid to the smaller proteoglycans, the most abundant being biglycan and decorin. Leucine-rich core proteins and total molecular weights of about 40 kDa (atomic mass unit) characterize these small proteoglycans. They were monitored since they are believed to play important roles in the regulation of the function of the extracellular matrix of the disc.

A recent in-vivo study looking at whether or not biglycan has a role in maintaining the structural integrity of the disc shows that decreased expression caused early onset disc degeneration (Furukawa et al., 2009). More specifically, biglycan deficient knock out mice had significantly greater degenerative scores than wild type at 4 and 9 months of age. Indicating that biglycan deficiency accelerates disc degeneration and as a result increased expression should help maintain disc matrix.

Decorin is more understood and is involved in the organization of collagen fibrils leading to increased tensile strength of the tissue. Specifically, in the modulation of collagen metabolism and in interactions with various glycoproteins and growth factors (Gotz et al., 1997). Decorin is found in greater concentrations in denser more fibrillar regions of the disc. Since decorin is

tightly coupled to collagen metabolism and ultimately the tensile strength of the disc it may be important to see how its expression changes with "good" (type II) and "bad" (type I) collagen.

Collagen type II, a structural protein, is the dominant collagen in the nucleus. However changes in collagen type II during disc degeneration remains unclear (Kluba, Niemeyer, Gaissmaier, & Grunder, 2005), and may not mirror the loss of proteoglycans. Collagen type II forms a fibrillar network to entrap proteoglycans in order to provide tensile strength to the tissue, therefore a net down regulation of its expression could be interpreted as a negative consequence to loading and vise versa for up-regulation.

Collagen type I is normally not highly expressed in the nucleus pulposus as it is typically reserved for the healing process after traumatic injury and the development of scar tissue. In a study looking at conditions that increased the amount of load and load durations on the disc it was found that collagen type I increased with increasing loads and load durations while conversely proteoglycans such as aggrecan decreased (Hutton et al., 1998). Hence, monitoring collagen type I acts as an early screen to injury response. A result of proteoglycan up-regulation with no associated change in collagen I could be interpreted as being beneficial to the tissue.

It is important to understand that while we assume (see Table 1) that significant gene expression increases found in this study represent eventual increases in protein expression, the expression of mRNA actually does correlate to protein expression (Guo et al., 2008). While the correlations over all 71 genes tested in Guo et al. 2008 had significant relationships to respective protein expression ($r=0.235$; $p<0.0001$), the noise was relatively large as mRNA could only explain about 5% of the variance of the protein expression. However, looking specifically at genes responsible for extracellular regions of tissues (15 in total) similar to the ones used in this study, there was a significant improvement in the accounted variation to approximately 41%

(r=0.643; p<0.0001). While relying on mRNA expression to predict protein expression is not perfect it would be considered reliable and valid in this case.

Table 1 Summary of changes in gene expression that would be considered beneficial (Good), harmful (Bad), and neutral if no change is detected based on the hypothesis.

Gene Expression Hypothesis						
	Aggrecan	Versican	Biglycan	Decorin	Collegan II	Collegan I
Good	increased	increased	increased	increased	increased	no change
Bad	decreased	decreased	decreased	decreased	decreased	increased
Effect	mechanical functino	cell adhesion/signaling	regulation of matrix	organization of collagen	tensile strength	injury response

2.8 Current Treatment Options

Traditionally, back pain has been treated using many different approaches. The more conservative approaches include applications of ice and heat (Melzack, Jeans, Stratford, & Monks, 1980), bed rest of no more than two days (Arnau et al., 2006), general exercise and specific conditioning of back and abdominal muscles to help stabilize hyper-mobile regions (Geisser, Wiggert, Haig, & Colwell, 2005; Peate, 1994; Skikic & Suad, 2003), spinal manipulation to increase the range of motion for hypo-mobile regions (J. Fritz, Whitman, & Childs, 2005; Licciardone, Brimhall, & King, 2005; Perle & Kawchuk, 2005), massage therapy (Cherkin et al., 2001; Ernst, 1999; Furlan, Brosseau, Imamura, & Irvin, 2002), and transcutaneous electrical nerve stimulation (Fox & Melzack, 1976; Khadilkar et al., 2005; Melzack, Vetere, & Finch, 1983).

More invasive treatment involves the use of medications such as over-the-counter analgesics, opiates, anticonvulsant agents, antidepressants (Katz, Pennella-Vaughan, Hetzel,

Kanazi, & Dworkin, 2005; Mens, 2005; Peloso, Fortin, Beaulieu, Kamin, & Rosenthal, 2004), acupuncture (Cherkin et al., 2001; Furlan et al., 2002; Kerr, Walsh, & Baxter, 2003), epidural, and facet joint corticosteriod injections (R. Haigh & AK. Clarke, 1999), spinal nerve blocking techniques (Hodge, 2005; Pang, Ho, & Huang, 1999; Robert et al., 2004), and depending on the diagnosis, surgery may consist of procedures ranging from microdiscectomy (Figure 7A) and spinal fusion (Figure 7B) to a full laminectomy (Figure 7C) (Derby et al., 2005; Strayer, 2005; van Tulder, Koes, Seitsalo, & Malmivaara, 2006) . Although spinal fusion has some efficacy in pain management, spine biomechanics are ultimately compromised leading to adjacent level disc degeneration. While some total disc replacement prosthesis are approved for human use in the United States, their longevity is unknown and inherently limited due to their inability to biointegrate.

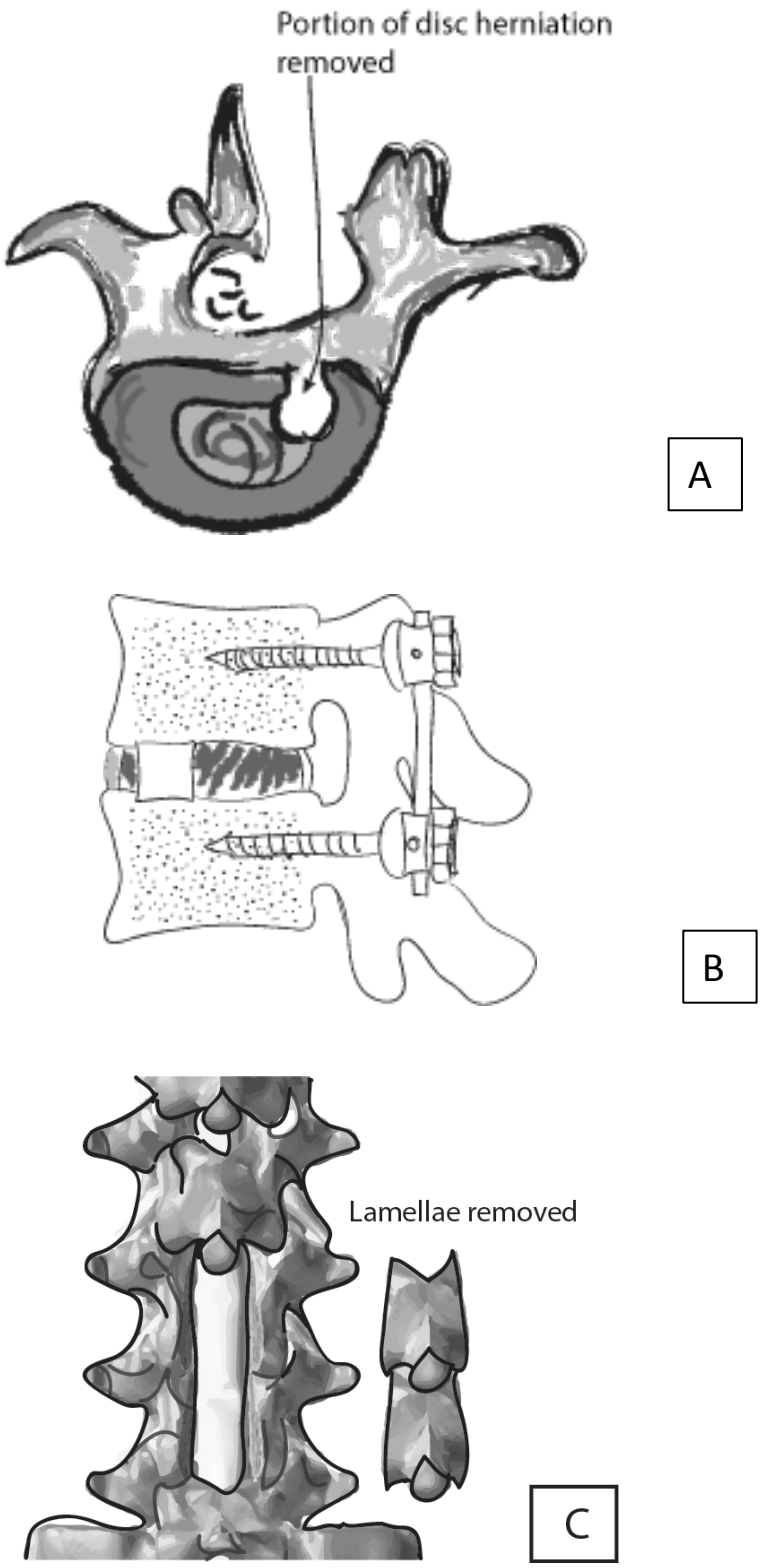

Figure 7: Surgical procedures. A) Microdiscectomy; B) Spinal Fusion; C) Full Laminectomy.

Despite the multitude of treatments and clinical studies, back pain still remains one of the most elusive ailments of our time and lacks available standardized guidelines for treatments that achieve acceptable results (Arnau et al., 2006). In fact, within the framework of evidence-based medicine [high-quality blinded randomized trials being conducted], the best treatment for chronic low back pain (LBP) remains cognitive intervention combined with physical exercises specific for stabilizing the lumbar spine (Licciardone et al., 2005; Peate, 1994; Sharma, Sing, Sharma, & Mittal, 2003; van Tulder et al., 2006). Therefore, the need for further high-quality studies of new approaches is required for the advancement of patient care in the area of spine related pain.

2.9 Prior Art Review

Traditionally, prior to vibration based therapies, spinal manipulation or impulse [low amplitude high velocity] treatment was performed using bare hands (Assendelft, Morton, Yu, Suttorp, & Shekelle, 2003). As the number of investigations using the bare hands methodology increases, it is becoming evident that the variability of patient outcomes implementing this type of treatment can be significant (Assendelft et al., 2003; R. Haigh & AK. Clarke, 1999). These results may be due to the variability in the pressure applied by the hand due to variations in practitioner hand anatomy (Perle & Kawchuk, 2005), variability in patient anatomy, or the variability of the application itself (Kawchuk & Herzog, 1993).

Spinal impulse treatment devices trying to circumvent these problems have been experimented with (Dungan, May 8, 2001; Elliot, April 8, 1997; Evans & Moore, June 27, 1989; Sweat, July 24, 1984; Tucek, Aug 5, 2003; Wing, October 29, 1985). United States Patent Number 4,461,286 describes a percussive prototype operated by a trigger (Sweat, July 24, 1984).

A practitioner would position the hand held device (HHD) on the patient considering both location and direction which are known to be important elements in delivering impulses (Perle & Kawchuk, 2005). The linear force impulse of the device is delivered by a loaded spring that would have a tendency to drift over time as the mechanical properties of the spring began to fail. This device is also completely dependent on the reactive force holding the prototype in place. United States Patent Number 4,841,955 is also a HHD but uses solenoids as a means to improve accuracy and repeatability of the linear force impulse (Evans & Moore, June 27, 1989). These devices only deliver a single force impulse and no vibration.

The HHD US Patent Number 4,549,535 was designed to deliver multiple linear force impulses [pulse width, frequency, and amplitude] with a square wave (Wing, October 29, 1985). Using a square wave presents several drawbacks, most importantly, abrupt forces to sensitive areas of the body that are considered undesirable. In addition, a perfect square wave places excessive performance requirements on the electronic and mechanical systems that attempt to produce them. As a result, high frequency artifacts in the impact pin may occur.

United States Patent Number 5,618,315 also describes multiple linear force impulses as well as rotational forces. However, draw backs are again its use of a square wave form to drive the impact pin and the uncertainness of a HHD (Elliot, April 8, 1997). In addition, there are no fail-safe mechanisms built into the device.

Other devices exist [US Patent 6,228,042 and 6,602,211] but neither incorporates feedback on device position (Dungan, May 8, 2001; Tucek, Aug 5, 2003). As no clinical data could be found on these devices it is unknown as to their efficacy.

The intervention assessed in this study has the ability to apply controlled vibration and preliminary studies identify patient benefits. However, the interventions effect on the disc remains unknown, until now.

2.10 Importance of Vibration in Musculoskeletal Tissues

This dissertation focuses on the effects of vibration on the intervertebral discs (IVD). However, it is important to note that, in the clinic, vibration will travel to surrounding tissues as well as the discs. In fact, the intervention is applied to the spine through bony prominences of the vertebrae via the skin. Hence, we must consider the vertebrae, the muscles attached to the vertebrae, and also the nervous system that controls the muscles attached to the vertebrae.

2.10.1 Gamma Motor Neuron Modulation

As a result of induced muscle pain, muscle firing patterns or coordination between flexors and extensors change significantly to reduce motion of the segment (Graven-Nielsen, Svensson, & Arendt-Nielsen, 1997; Lee, Desmoulin, Khan, & Park, 2011a, 2011b). It has also been shown that gamma motor neuron sensitivity increases during induced muscle pain (Matre, Sinkjaer, Svensson, & Arendt-Nielsen, 1998). While this increase in sensitivity may not lead to excessive electromyography (EMG) at all contraction levels, it most certainly increases reflexive activity. This enhanced sensitivity may act to create load asymmetries on the spine.

Since the vertebrae are moved during the treatment, they stretch the attached muscles. As found previously in animal models, the vibratory aspect results in the application of sinusoidal stretches to the tendons of the muscles attached to the vertebrae resulting in decreases to gamma motor neuron input mediated by Renshaw cells activated during vibration (Fromm & Noth, 1976; Fromm, Noth, & Thilmann, 1976; Pompeiano, Wand, & Sontag, 1975; Rymer & Hasan,

1981). These researchers discovered that the inhibition increased as vibration frequency increased. The frequencies tested ranged from 100 to 300 Hz. As well, Pompeiano et al. discovered that Renshaw cell activity maximized at frequencies between 150 and 250 Hz (Pompeiano et al., 1975). Although, micrometer displacements are typical for these types of experiments Pompeiano et al. (1975) used amplitudes ranging from 180 μm to 12 mm, none of which showed a difference in Renshaw cell activity, hence the phenomenon is frequency dependent and displacement independent (Pompeiano et al., 1975). As gamma motor neuron input decreases so does the stretch reflex input for contraction. It has been shown that this reflex activity entering the medial branch of the dorsal ramus at one spinal level cause's similar activity across 1 or 2 adjacent levels (Kang, Choi, & Pickar, 2002). Hence, not only does a vibration translate as a wave down the spine at multiple spinal levels, the reflex activity involved in that translation also acts at multiple spinal levels. So, if the paraspinal muscles are undergoing a pain-spasm-pain cycle (Cobb, deVries, Urban, Luekens, & Bagg, 1945) or have enhanced gamma motor neuron sensitivity and are responsible for asymmetric loads on the spine, then appropriately applied vibrations to the spine may reduce the load asymmetry (Maigne & Vautravers, 2003).

2.10.2 Cellular Biosynthesis

There is some evidence to show that vibration affects biosynthesis of chondrocytes (M. Kasra, Goel, Martin, Wang, Choi, & J., 2003; Liu et al., 2001). Liu et al. (2001) using a sinusoidal wave form of 1.4 g acceleration at 200 through 1600 Hz found that at 200 and 300 Hz the mechanical vibration of chondrocytic culture in a petri dish promoted DNA and proteoglycan synthesis, although frequencies above 400 Hz suppressed it (Liu et al., 2001). As well, Kasra et

al. (2003) discovered that collagen and protein synthesis of annulus fibrosus (outer layer of intervetebral disc) cells was promoted when 3 MPa loads were delivered at the higher frequencies (~20 Hz) tested (M. Kasra, Goel, Martin, Wang, Choi, & Buckwalter, 2003).

2.10.3 Central Mechanisms

Specific frequency mechanical vibration applied transcutaneously reduces chronic pain (Ekblom & Hansson, 1985; Guieu, Tardy-Gervet, & J., 1991). Although the mechanism is not truly understood (Guieu, Tardy-Gervet, & Giraud, 1992) vibration analgesia relies at least in part on central nervous system processes rather than local mechanisms (Roy, Hollins, & Maixner, 2003; Tardy-Gervet, Guieu, Ribot-Ciscar, & Roll, 1993). It is believed that the input transduced by the mechanoreceptors in the skin interrupts central nervous system processing of the pain signal (Roy et al., 2003). This reasons as several researchers have discovered that lower frequency vibration does not cause analgesia as well as higher frequency vibration suggesting efficacy is stimulus specific (Ekblom & Hansson, 1985; Roy et al., 2003).

This information supports the Melzack and Wall (1965) gate-control theory of pain where by cutaneous input from Ia afferent nerve fibers act to close the "gate" or interrupt pain signals being sent through A-delta and C fibers to be perceived in the cortex (Melzack & Wall, 1965). Although, the gate-control theory must continually be revised to accord with new information, it has been a major impetus for stimulating fruitful research and none the less useful in attempting to explain vibration analgesia (Bishop, 1980; Dickenson, 2002). This mechanism is important because it is believed to act on the circuitry of the spinal cord where permanent plastic changes can occur (G. Desmoulin & Khan, 2007).

2.10.4 Vertebrae Position

Patients with neck and back pain typically do not exhibit obvious abnormalities in plain radiographs (Friedenberg & Miller, 1963; Gore, Sepic, & Gardner, 1986; Heller, Stanley, Lewis-Jones, & Heller, 1983). Noting the lack of effectiveness of range of motion investigations, investigators began exploring the notion of the quality of motion of the vertebrae, they reasoned that while range of motion may be normal, abnormalities of spinal joints including disc degeneration might be revealed by abnormal motion patterns within individual joints (Bogduk & Mercer, 2000; Ferguson & Steffen, 2003). It emerged that 72% of patients with neck pain exhibited at least one abnormally located cervical pivot point or mean axes of rotation (MAR). The relationship between axis location and pain was highly significant statistically ($p < 0.001$). It can be shown that the location of any, normal or abnormal cervical MARs are governed by the net effect of compression forces, shear forces and moments acting on the moving segments, largely influenced by disc health and degeneration (Bogduk, Amevo, & Pearcy, 1995; Ferguson & Steffen, 2003). Therefore, an abnormal MAR can only occur if the normal balance of compression loads, shear loads, or moments is disturbed and is typically exaggerated during disc degeneration (Ferguson & Steffen, 2003). This allows the location of a MAR to be interpreted in anatomical and pathological terms. In addition to using MAR location to assist diagnosis we demonstrate that MAR's can be corrected with the use of vibration and this correction relates highly to decreases in pain ($p = 0.024$) despite which group (sham or treatment) the patient was in (G.T. Desmoulin, Hunter, et al., 2012; G.T. Desmoulin, Szostek, et al., 2012).

It is important to note that the above stated vibration effects on the musculoskeletal and nervous tissue surrounding the spine garnered from the literature focus primarily on the benefits of the application. It should be also noted, especially for clinicians implementing the results of

this thesis, that results here-in pertain only to the bovine IVD and while results are meant to benefit humans vibration applied to other tissues may not be suitable.

2.11 Summary

While the structure and function of the disc is relatively well known, its injury and the ability to induce self-repair are less understood. There is a clear relationship however to disc pathology and related pain. Current treatment for this 'discogenic' back pain is varied and has mixed results at best. While there is a long history of investigations to determine the effects of vibrations on the human spine, data has been confusing, with mixed results and conflicting conclusions. Taken collectively, the data surveyed suggests that the effect of vibrations may be highly dependent upon the loading parameters of frequency, amplitude, and duration of exposure, and may be highly sensitive to subject mechanical variability. Some vibration patterns are not overtly harmful, in that they do not statistically correlate to the incidence of reported discogenic back pain, this however, does not mean that all vibrations are harmless. Therefore, it is our opinion that further study is required to isolate the effects at least from a therapeutic point of view. Our approach includes the evaluation and further development of an FDA and Health Canada approved medical device called KKT. KKT is a clinical treatment that focuses on the use of vibration as a means of correcting 'abnormal' motion in spinal joints, reducing pain, and increasing mobility through various mechanisms. KKT's effect on the discs are being investigated first, since they are known to be involved in back pain and a high percentage of patients seen at KKT clinics present with some level of disc degeneration. The following experiments detail the effects of KKT and specific vibration on disc metabolism.

CHAPTER 3: VIBRATION EFFECTS ON DISC BIOSYNTHESIS

3.1 Introduction

This chapter entails the crux of the vibration evaluation and development experiments. The three major experiments are broken into three different objectives and cover a) the evaluation of version 1 of KKT in its current state at the time of testing (KKT_v1); b) finding the parameters (load, frequency and duration) that maximize up-regulation of gene expression (considered to positively affect the IVD) without tissue injury; and c) examining how KKT_v1 affects disc metabolism once it is modified to operate as KKT_v2 to perform the 'optimal' loading pattern. These experiments are summarized in Figure 8 then presented chronologically and individually so that results of each major experiment can be discussed in detail. However, in chapter 5 the data of all experiments, including those of chapter 4, are amalgamated so that data are considered across all experiments of the dissertation. Note: that raw data from all objectives and full output ANOVA tables from Objective 2 and the entire data set can be found in the Appendix.

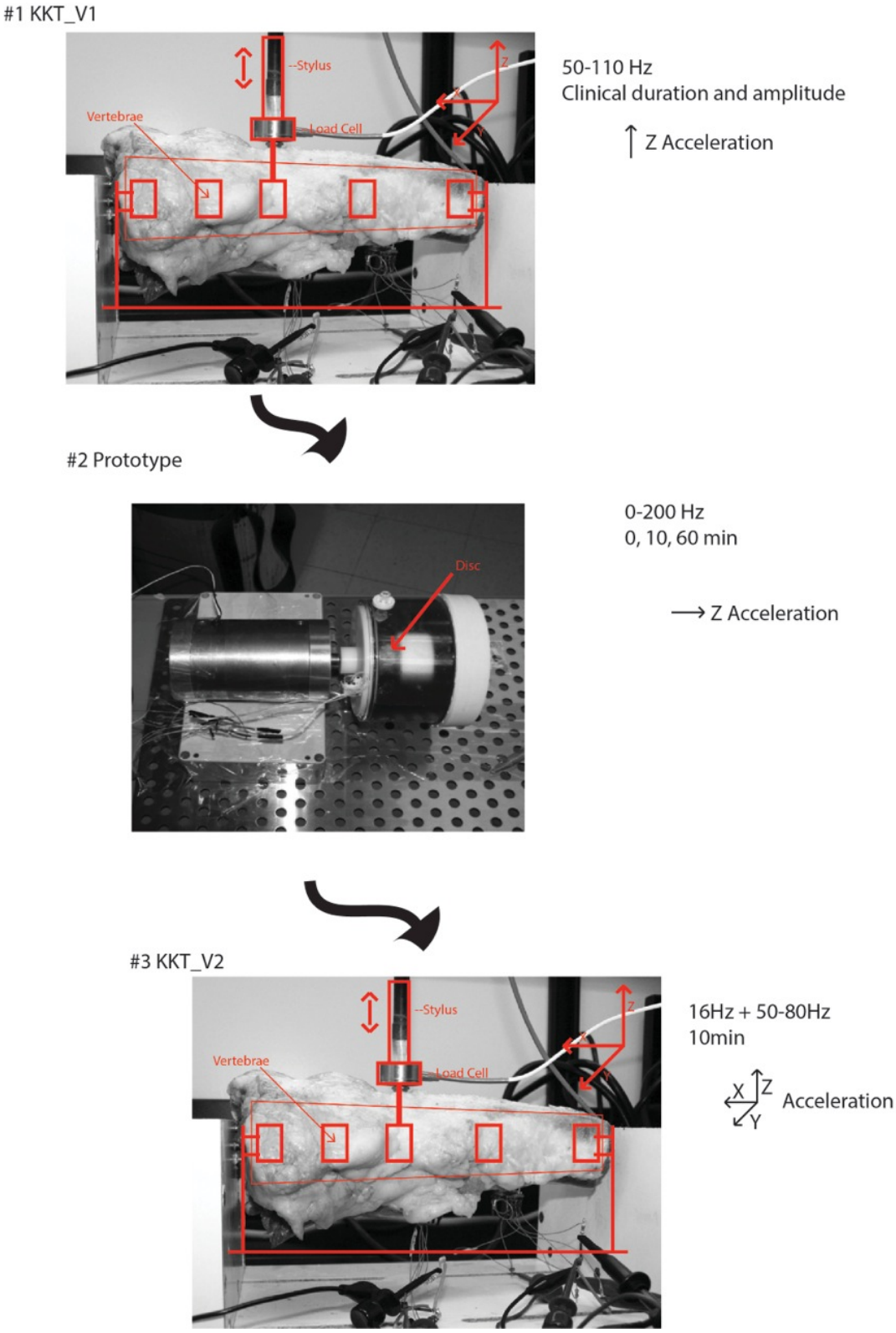

Figure 8: Chapter 3 experimental summary. Experiment number with abbreviated device name (top left); coordinate system and disc identifiers (in frame); experimental conditions and measured acceleration (right hand side).

3.2 Objective 1 Experiment – Clinical Intervention (v1) Mechanics and Gene Influence

This experiment evaluates the KKT (clinical intervention) in it original form (KKT_v1) and function by having it sweep through the original designed frequencies of 50-110 Hz at an amplitude and duration similar to that used in the clinic. Measures include the imparted forces and accelerations to the vertebrae and the resulting changes, if any, to disc tissue gene expression.

3.2.1 Experimental Goal

Determine the interventions imparted mechanics and the effect the intervention has in altering IVD gene expression prior to device (KKT_v1) modifications.

3.2.2 Intervention

To briefly reiterate the explanation from Chapter 1, the Khan Kinetic Treatment (KKT) is a cervical treatment device consisting of a controller mounted on top of an impulse delivery mechanism, or device head, which is mounted on a movable armature to a fixed stand. For this experiment the device head generated waveforms [sine waves at 50-110 Hz] and transduced them mechanically to a bony prominence of the subject spinal joint in a clinical manner. It is important to note at this time that the KKT device used for this experiment was the original design of the device, hereafter referred to as "KKT_v1". In later experiments the intervention's (KKT_v1) firmware was modified to incorporate other necessary frequencies.

3.2.3 Tissue

Tails from skeletally mature cattle were obtained from a local slaughterhouse within 6 hr of death. The muscle, fat, fascia, and vertebrae remained intact when shipping though the abattoir removed the skin. Prior to testing, the experimenter allowed two thin (approximately 3 mm thick) slices of the connecting proximal and distal vertebrae to remain on either side of each 5-segment tail section to provide grip to the fastening device. Using this intact 5-segment bovine tail section, we applied vibration by the KKT intervention (KKT_v1) prior to any device modification, as it would be in the clinic. Research methods of this experiment were reviewed and approved by the University of Calgary's Animal Care Committee.

3.2.4 Methods

KKT_v1 vibrated the spine by sweeping through 50-110 Hz (Figure 9), as it was originally designed but never assessed quantitatively until this study, and was applied to intact bovine tails (4-6 per condition (low, med, high amplitude using qualitative clinical setting on the intervention, at 36 sec and 10 min duration) including control group). The mechanical coordinate system defined the direction of gravity as the z-axis and was the direction of vibration loading of the stylus. The imparted mechanics of the stylus input was quantified using intact bovine tails in a clinical emulation set-up, three-dimensional accelerometers (Analog Devices, Massachusetts, USA), and a 450 N (100 lb.) load cell (MN# WMC-100-456, Honeywell, New Jersey, USA; Figure 10). The accelerometers were calibrated using a 1 g shaker plate (Type 4291 – 1 g Accelerometer Calibrator, Brüel & Kjaer, Copenhagen, Denmark) and the load cell was statically calibrated using several known masses. The imparted mechanics set-up mirrors the KKT_v1 treatment, where mechanical vibrations are transmitted to the spinal system via the devices stylus

tip. The load cell and accelerometers were attached directly to vertebrae in order to achieve accurate measurements.

More specifically, the bovine tail segment had five (5) vertebrae in total. A tissue holder that resembled a vice with several spikes and a thumbscrew at each end were used to embed into the vertebrae when squeezed together would hold two in place. However to avoid non-physiological compression forces, a thumbscrew was used to secure the tissue holder to the end vertebrae. Attaching the tail segment in this manner would alleviate the need for high compression forces to embed the spikes into the vertebrae and allow the tail segment to be relatively suspended; similar to the cervical section of the human spine would be when the intervention is used in the clinic.

The load cell was placed between the stylus of the intervention and the target bony prominence of the tail segment with an 11 N (2.5 lb.) static load on average in order to measure the loads directly applied to the vertebrae. Cleaning tissue away from the vertebrae to the bone ensured a rigid connection between the load cell and vertebrae. Cyanoacrylate was used to glue the load cell to the vertebrae. The accelerometer configuration ensured that the ±18 g range of each axis would not saturate as the units were mounted on a 45° angle. Further, PCB layouts were designed and implemented in order to facilitate mounting of the chip and soldering of the appropriate connections for both power supply (2.5 V) and voltage output.

The effect of treatment on gene expression was determined by application of two typical clinical treatment durations (36 s and 10 min).

3.2.4.1 RT-PCR

At the end of the experimental period, discs were harvested and separated into nucleus pulposus (NP) and annulus fibrosus (AF), flash-frozen in liquid nitrogen, and stored at -80 ^{o}C until extraction of total RNA. Time between flash freezing and PCR analysis varied from one to four weeks. A letter and number system tracked the tissue samples. “A” stood for annulus fibrosus; “T” for tunnel staining; “P” for nucleous pulposus followed by a sequential number. All discs were visually inspected at the time of RNA harvest and found to be approximately equal to a human Thompson Grade II disc (opaque fibrous nucleus, clear nuclear/annular demarcation, and distinct lamellae). Only the NP was analyzed for the current study; AF samples were stored for future testing, as pilot studies indicated minimal changes in the AF (data not shown). The frozen tissue was ground in Trizol reagent; full details of the protocol are provided elsewhere (Reno, Marchuk, Sciore, Frank, & Hart, 1997). Briefly, total RNA was isolated using the Trispin method and quantified using the Ribogreen assay (Invitrogen). A sample containing 5µg of RNA was reverse-transcribed using poly-T primers (First Strand Synthesis Kit, Stratagene). The resulting cDNA was probed with custom intron-spanning primers for aggrecan, biglycan, collagen type I, collagen type II, decorin, GAPDH, and versican (Table 2). Real-time PCR was performed using SYBR green chemistry (SYBR Green Premix, Bio-Rad) on an iCycler IQ system (Bio-Rad). Starting quantity was determined using the ddCt method, as calculated by the iCycler software. All data were normalized to GAPDH expression and then normalized to control sample set. In more detail, the PCR machine generates numbers for each set of primers used. These numbers are the "threshold cycle" (CT) at which the amount of template starts to rapidly double in number with each machine PCR cycle. Specifically, the quantitative approach is termed the comparative ddCT method. This involves comparing the CT values of the samples

of interest with a control or calibrator such as normal tissue or in this case we used a non-treated sample. The CT values of both the control and the samples of interest are normalized to an appropriate endogenous housekeeping gene, in this case we used GAPDH.

The comparative ddCT method can be reduced to the following equation, where

$$ddCT = dCTsample - dCTreference$$

Here, 'dCTsample' is the CT value for any sample normalized to the endogenous housekeeping gene (GAPDH) and 'dCTreference' is the CT value for the control also normalized to the endogenous housekeeping gene.

Table 2: PCR primers and thermocycler settings.

Gene	Forward Primer	Reverse Primer	Annealing temperature
GAPDH	GGC GTG AAC CAC GAG AAG TAT AA	CCC TCC ACG ATG CCA AAG T	60
Aggrecan	GAG TGG AAC GAT GTC CCA TGT	GCA TTG ATC TCG TAT CGG TCC	50
Biglycan	GCT CCT CCA GGT GGT CTA TC	GCT GAT GCC GTT GTA GTA GG	50
Collagen I	AAG AAC CCA GCT CGC ACA TG	GGT TAG GGT CAA TCC AGT AGT AAC CA	50
Collagen II	GCA TTG CCT ACC TGG ACG AA	CGT TGG AGC CCT GGA TGA	50
Decorin	TGA CTT TAT GCT GGA AGA TGA G	TGG ACA ACT CGC AGA TGG	50
Versican	GAG AGT GTC GGT GCC TAC	GTC CTG TGT GTC TTC AAT CC	50

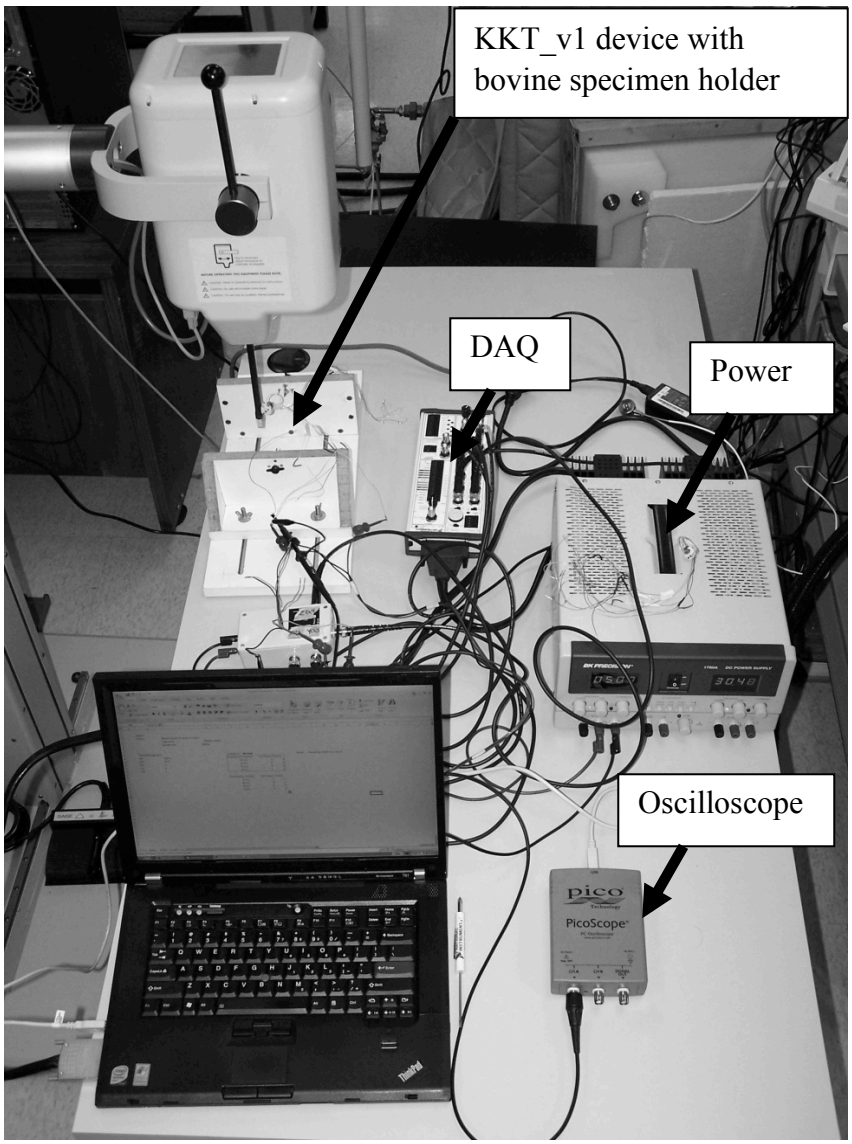

Figure 9: KKT bench testing set-up.

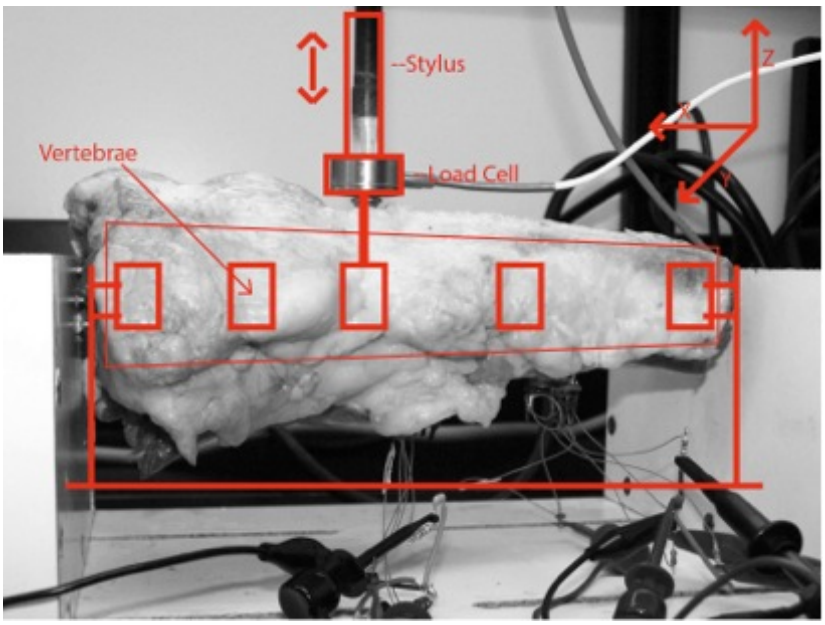

Figure 10: Imparted mechanics set-up with assigned coordinate system. Load cell is attached to cleaned section of central vertebrae [five vertebrae in total; central vertebrae is loaded] and aligned with stylus of the device. Three-dimensional accelerometer mounted on central vertebrae measures stylus affects on in situ vertebrae.

3.2.5 Results

Imparted Mechanics: the force applied to the central vertebrae of the 5-segment in situ bovine tail averaged peak force of 10.3 N (2.3 lb) and the resulting z-axis acceleration was 21.48 m/s^2 (2.19 g) (Table 3).

Table 3: Quantifying imparted mechanics using in situ bovine tail and direct stylus contact with the central vertebrae (5 in total) of the specimen. Treatment in humans is applied at a clinical setting called 'intensity' and was programmed to 0.5 and so the results here accurately represent its mechanical input.

Condition	Force on Vertebrae (peak-N)	SD	Z-axis Acceleration of Vertebrae (peak-G)	SD
Treatment	10.3	1.9	2.19	0.62

Condition – Defines amount of current sent to the actuator (i.e. intensity).
Force on Vertebrae – averaged peak force of vibration over 100 cycles
Acceleration of Vertebrae – averaged peak acceleration (g) over 100 cycles
SD – Standard deviation

Gene Expression: Only collagen I was differentially expressed as opposed to controls, with both 36 s and 10 min *inhibiting* expression in the nucleus pulposus. KKT_v1 vibration did not detectably change any other genes.

Overall: Prior to the device modifications the KKT_v1 device did not operate in the ideal 'window' for stimulating extracellular matrix gene synthesis in the IVD. This first experiment determined that while KKT_v1 did inhibit collagen I gene expression this did not fit the hypothesized positive consequences. Hence, there remains a need for determining which vibration parameters are required to cause the most gene expression. Specifically, in genes responsible for producing proteins that maintain disc matrix as it is hypothesized up regulation of these genes will correlate to a healthier disc. These parameters are identified in Objective 2 below.

3.3 Objective 2 Experiment – Basic Research of Optimal Parameter Magnitudes

The above experiment evaluated the KKT_v1 (clinical intervention) in its original form, which swept through the frequencies of 50-110 Hz at an amplitude and duration similar to that when used in the clinic. The results clearly showed that the imparted mechanics did not elicit a

positive influence over gene expression as no significant up regulation could be detected. Further, while the amplitude is editable, KKT_v1 had no way to change the frequency sweep manually due to fixed parameters in its firmware. Hence for objective 2 experiments, it was necessary to build a prototype capable of exploring a large range of amplitudes, frequencies, and durations to determine the optimal window for stimulating increased gene expression. The prototype includes improvements in the loading system such as temperature-controlled cell culture medium and carbon dioxide control but was only capable of loading individual intervertebral discs. Measures included the ability to monitor frequency, amplitude (acceleration) and duration to the individual vertebrae-disc-vertebrae joint section and the resulting changes, if any, to disc tissue metabolism.

3.3.1 Experiment Goal

Determine the vibration conditions that are most effective in altering individual intervertebral disc gene expression. This was done using general trend statistics and if significance was found then post-hoc comparisons with control treatments were performed. The loading parameters with the greatest gene expression (most significant response) of key genes were noted.

3.3.2 Tissue Isolation

As section 3.2.3. above with the exception that individual IVDs were cut free using a handsaw, leaving approximately 2-5 mm of bone on either side. The isolated IVDs were then stored in phosphate-buffered saline at 4 °C until ready for experimentation.

3.3.3 Vibration

Design specifications of the prototype used for vibration loading were: a) capable of 0-200Hz frequencies and 0-1 g acceleration magnitudes; b) secure a single bovine IVD segment surrounded by cell culture medium in a biocompatible container; c) apply a tare load of 40N to the IVD segment; d) allow medium to be in contact with environmental atmosphere for CO_2 exchange; e) able to fit inside, be controlled within, and withstand the humidity and temperature of a standard environmental control chamber. Once built and tested axial vibration was applied by placing individual discs into the prototypes chamber (Nalgene) filled with cell culture medium (Figure 11). The lid on the chamber was fixed with a spring (k = 26.2 N/cm) that applied static axial load (Mean 40.6 N) on the discs during the unconstrained vibration. The static axial load was calculated using the average thickness of the vertebrae-disc-vertebrae section and the spring stiffness. Similarly to Liu et al., 2001 (Liu et al., 2001), the chamber had a ±1.7 g accelerometer (ADXL 203, Analog Devices Inc., Norwood, MA) fixed to it to track the vibration load when the chamber was mounted to a voice coil (#NCM05-28-180-2LB, H2W Tech Inc., Vanencia, CA) (Figure 11). The accelerometer was previously calibrated using a "1g shaker" (B&K Type 4291). The vibration of the voice coil was controlled with the output of a Linear Current Amplifier Module (LCAM-1, Quanser, Markham, ON), which received its command signal from a function generator (PicoScope2203, Pico Technology, St Neots, Cambridgeshire). The LCAM was powered by 27 V and cooled by a 7.06 CFM fan (#2412PS-12W-B30, NMB-MAT, China) to eliminate temperature fluctuation of the output. The voice coil and chamber were secured with damping to a shelf in a 37 ^{o}C and 5% CO_2 via an environmental control chamber. The control signal to the voice coil and the accelerometer output was monitored in real-time via an oscilloscope (PicoScope2203, Pico Technology, St Neots, Cambridgeshire)

during the loading. Vibration was applied at various frequencies (0, 8, 16, 20, 30, 40, 50, 60, 70, 80, 160, 200 Hz) and acceleration amplitudes (0-0.54 g RMS) for either 10 or 60 minutes. Stroke length and force was not measured. The order of both amplitude and frequency selection was randomly assigned to eliminate any time-dependent trends due to sample storage. All conditions were run on a minimum of 5 separate and individual discs (from at least two different tails).

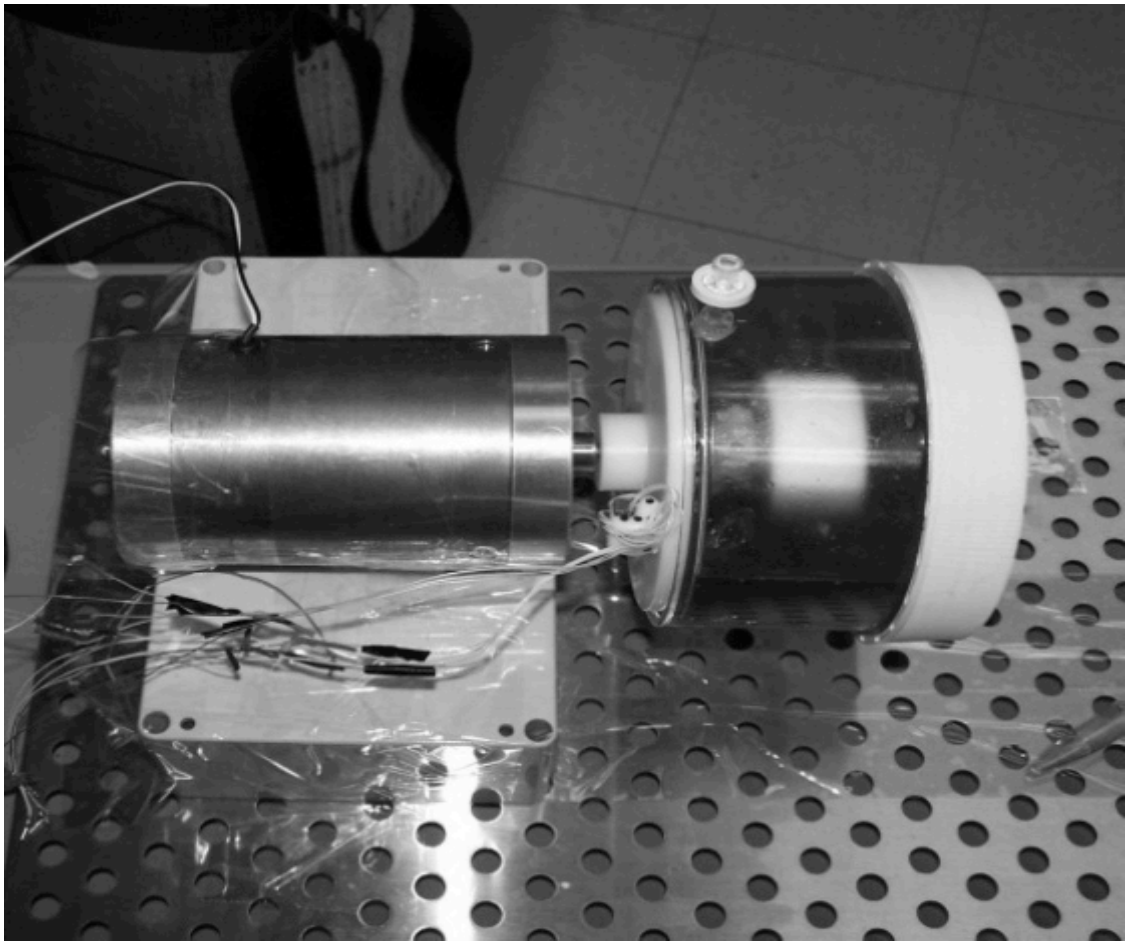

Figure 11: The vibration culture system. The individual IVD lies inside the polycarbonate culture chamber (right), immersed in DMEM culture medium. The culture chamber rests on the actuator end of the calibrated voice coil (left) and moves freely through the axial direction during vibration.

3.3.4 RT-PCR

As stated above in section 3.2.4.1 RT-PCR.

3.3.5 TUNEL

A subset of discs (1 per treatment for 0, 8, 16, 30, 40, 60, 80, 160 and 200 Hz) were separated from the bone and fixed in 10% neutral buffered formalin. These discs were embedded in paraffin, sectioned at 8 μm, and mounted on glass slides. Random transverse sections throughout the disc were stained with either mercuric trichrome or TUNEL (Roche In Situ Cell Death Kit). TUNEL-positive and -negative cells were manually enumerated by two different observers on an upright microscope with a 40x objective.

3.3.6 Data Analysis

Due to the number of frequency groups, contingency tables of the data determined that a full model (not complete factorial) with interactions could not be run. Instead, data were analyzed using the General Linear Model (GLM) to determine significant factors. The normality assumption was verified using normal probability plots and histograms of residuals. In those cases where substantial non-normalities were detected, Box-Cox analysis was performed and a suitable transform applied prior to re-analysis. Linear regression coefficients were determined to identify general trends in frequency or amplitude effects, and Tukey's post-hoc test was used to compare individual treatments to control. Comparisons were considered significant at or below the $p=0.05$ value. Bar plots are depicted with a vertical error bar that represents the standard error of the mean, which is an estimate of the true standard deviation of the distribution. For example, the standard error of the mean is the standard deviation of those sample means over the samples

drawn from the population. In practical applications, such as this dissertation, the true value of the standard deviation is unknown. As a result, the standard error will be used to estimate this unknown quantity.

3.3.7 Results

The GLM analysis indicated that frequency significantly affected expression of collagen type II, and decorin mRNA (Figure 15). The regressions for each of these genes were not significant. Amplitude significantly affected expression of biglycan, collagen type I, collagen type II, decorin, and versican mRNA. The regression slopes for these genes were significant and positive for all, with the exception of versican, which was not significant. Duration significantly affected expression of biglycan and versican, though neither regression slope was significant (Tables 4 and 5).

Due to the lack of a general trend in frequency response and the number of possible pairwise comparisons, only certain comparisons are presented here. Pairwise comparisons via Tukey's post-hoc analysis indicated that collagen type II was upregulated at 80 Hz across all loads and durations, while decorin was likewise upregulated at 8 Hz and downregulated at 40 Hz across all loads and durations ($p=0.027$, 0.047, and 0.041, respectively) (Figure 15). In general, expression trends appeared to change around 4.8 m/s^2 (0.49 g), so samples were lumped into general categories of 'control', 'low', and 'high' amplitudes and tested across all frequencies and durations. Biglycan was significantly downregulated by vibration below 4.8 m/s^2 (0.49 g), and upregulated above 4.8 m/s^2 (0.49 g) ($p=0.011$ and 0.020), while collagen type II and decorin were upregulated above 0.49g ($p<0.001$ and $p=0.003$), and versican was downregulated above 0.49g ($p<0.001$) (Figure 15). No pairwise comparisons were significant for biglycan ($p>0.17$ in

all three comparisons). Versican was unchanged after 10 minutes of vibration but significantly down regulated after 60 minutes (p=0.41 and p=0.040) (Figure 16). The bar shown in Fig. 15 indicates significant difference between the conditions found under its edges ($p < 0.05$).

In histological sections, the NP and AF were clearly defined and well formed, with no signs of degenerative changes, annular fissures, or other gross damage (not shown). TUNEL analysis indicated a mean background apoptosis rate of 10+/-0.7% (mean+/-standard error). There was no significant difference between frequencies (p=0.08), amplitudes (p=0.44), or annulus/nucleus (p=0.53) (Figure 12).

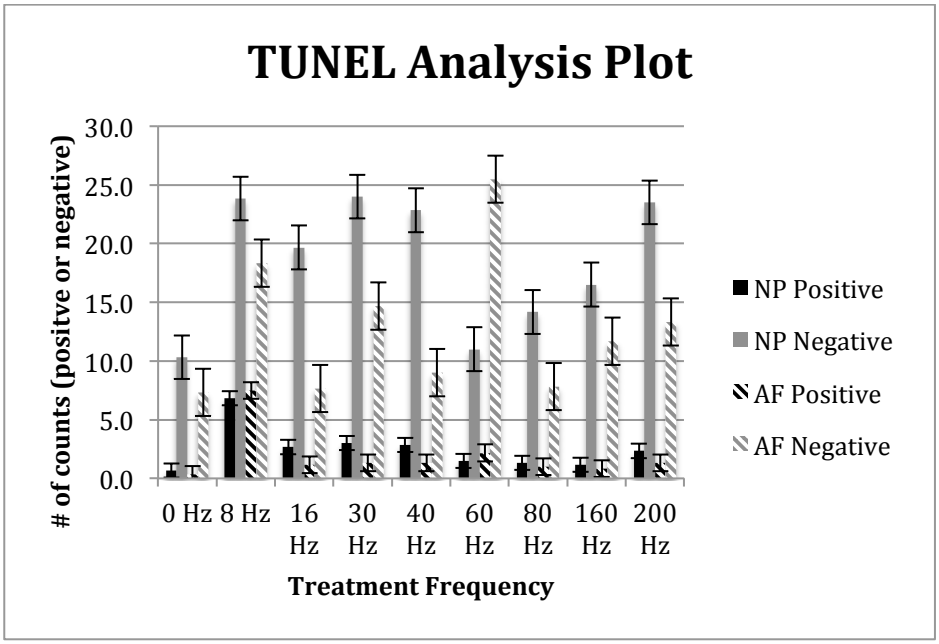

Figure 12: Raw TUNEL data are plotted with 1 standard error bar as SD estimate. The number of counts (positve apotosis or negative apotosis) are shown for each treatment frequency and area of disc (Nucleus Pulposus = NP; Annulus Fibrosus = AF).

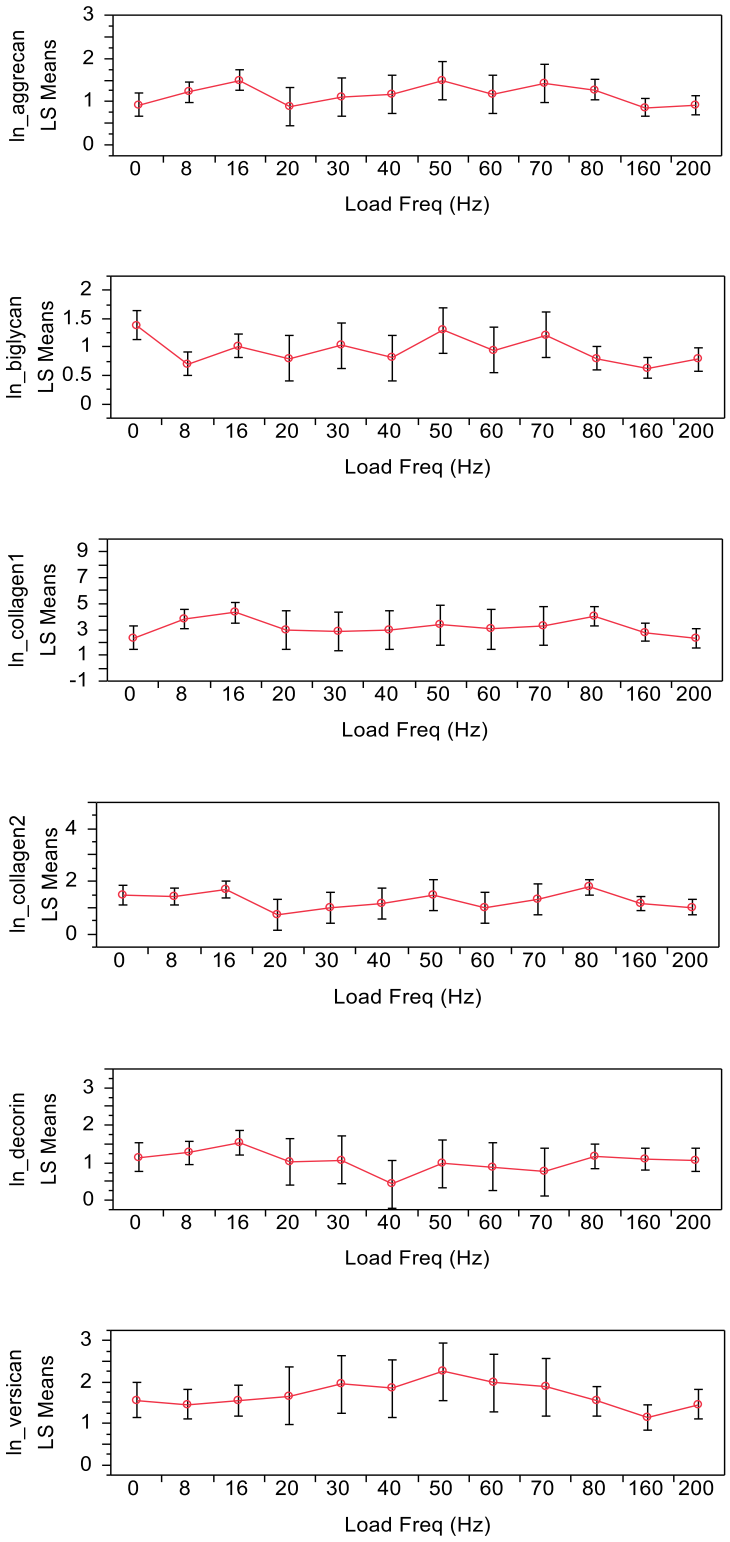

Figure 13: Mean plus 2 standard error plots of tested frequencies vs. the transformed gene expression of interest. No obvious qualitative trend exists.

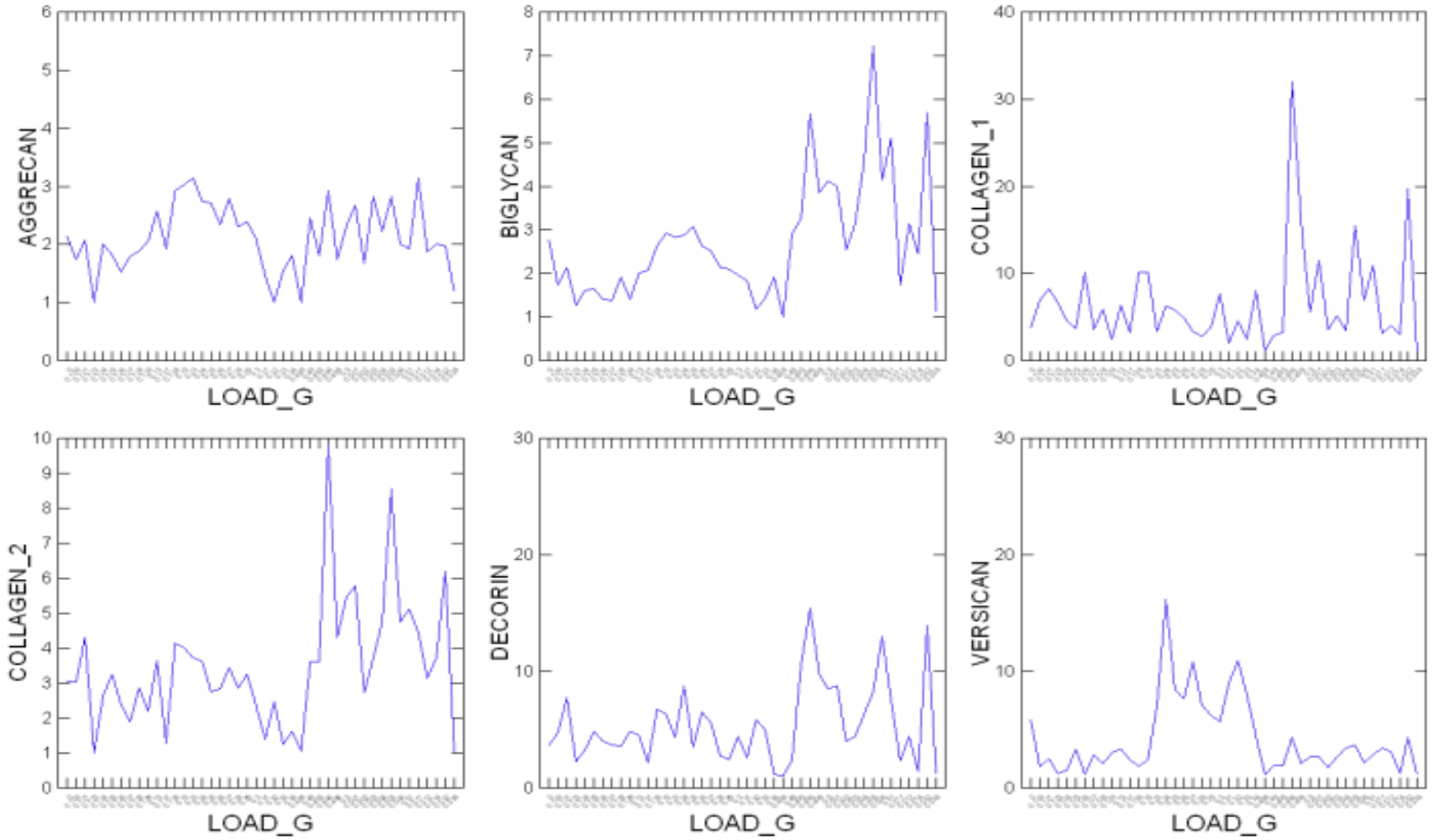

Figure 14: Qualitative analysis suggested a threshold effect around 0.4g; therefore subsequent analysis sorted the treatments into control (no vibration), low amplitude (<0.4g), and high amplitude (>0.4g) conditions.

Table 4: P-values for individual factors and genes from the GLM analysis.

	Aggrecan	Biglycan	Collagen type I	Collagen type II	Decorin	Versican
Frequency	0.139	0.417	0.237	0.033	0.004	0.007
Load	0.914	<0.001	<0.001	0.010	0.026	<0.001
Duration	0.348	0.050	0.838	0.464	0.088	0.014

Table 5: Regression coefficients for the significant factors found in the GLM analysis.

	Aggrecan	Biglycan	Collagen type I	Collagen type II	Decorin	Versican
Frequency	n/a	n/a	n/a	ns (p=0.266)	ns (p=0.057)	ns (p=0.359)
Load	n/a	1.605 (p=0.001)	4.209 (p=0.036)	1.623 (p=0.025)	8.383 (p<0.001)	ns (p=0.622)
Duration	n/a	ns (p=0.124)	n/a	n/a	n/a	ns (p=0.206)

ns – indicates difference not statistically significant
n/a – regression not run due to non-significant GLM analysis

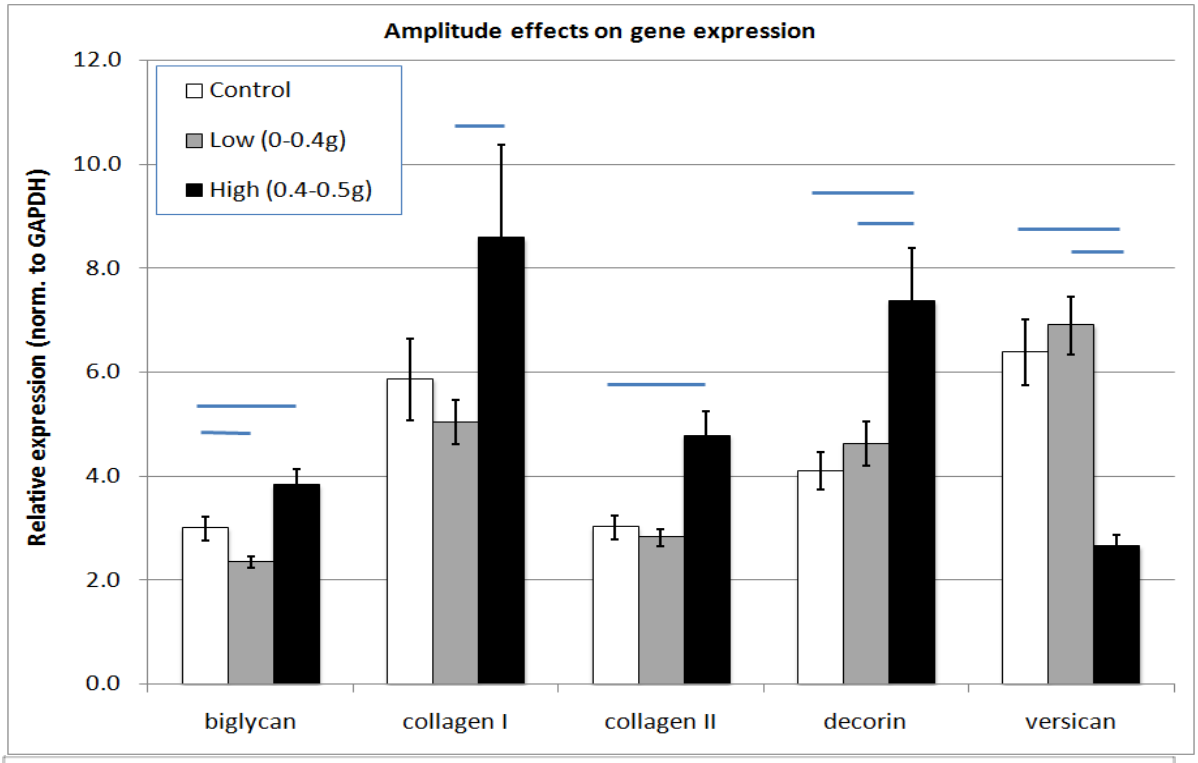

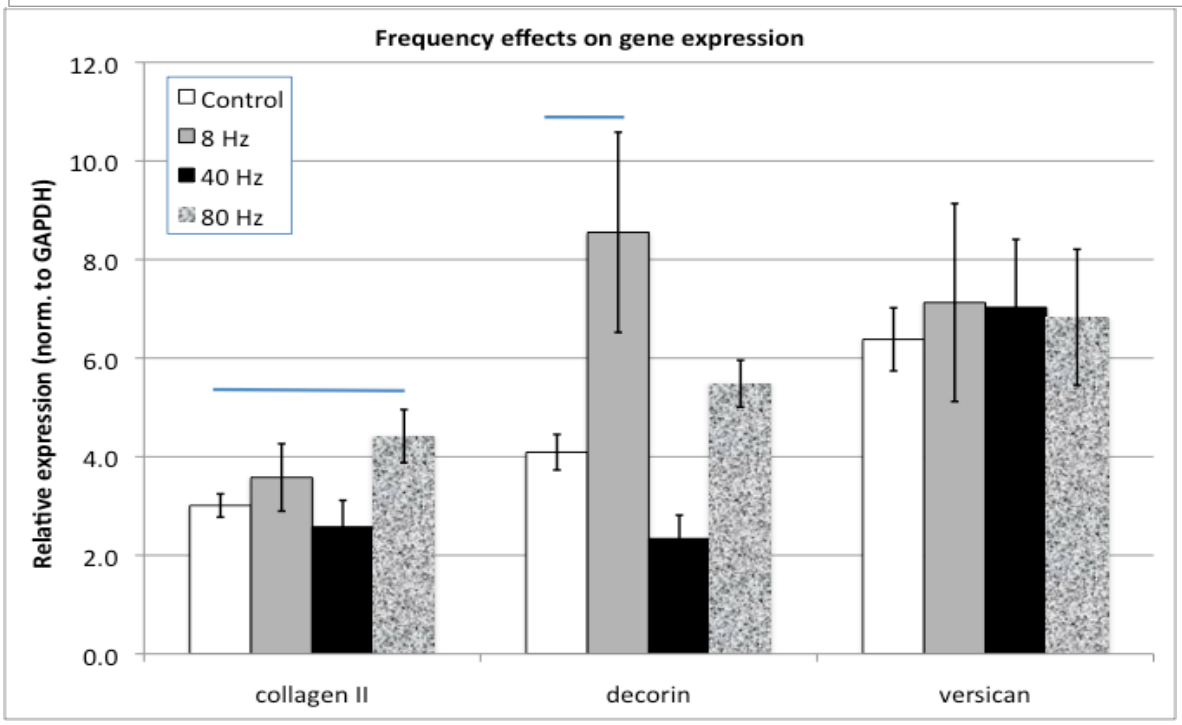

Bar – indicates significant difference between conditions under bar edges ($p < 0.05$).

Figure 15: (Top) GLM analysis indicated a significant effect of vibration amplitude on expression of biglycan, collagen type I, collagen type II, decorin, and versican mRNA (bars: $p<0.05$). (Bottom) GLM analysis indicated a significant effect of vibration frequency on expression of collagen type II, decorin, and versican mRNA. Pairwise analysis indicated that collagen type II was significantly upregulated at 80 Hz, decorin was significantly upregulated at 8 Hz, and decorin was significantly downregulated at 40 Hz (bars: $p<0.05$).

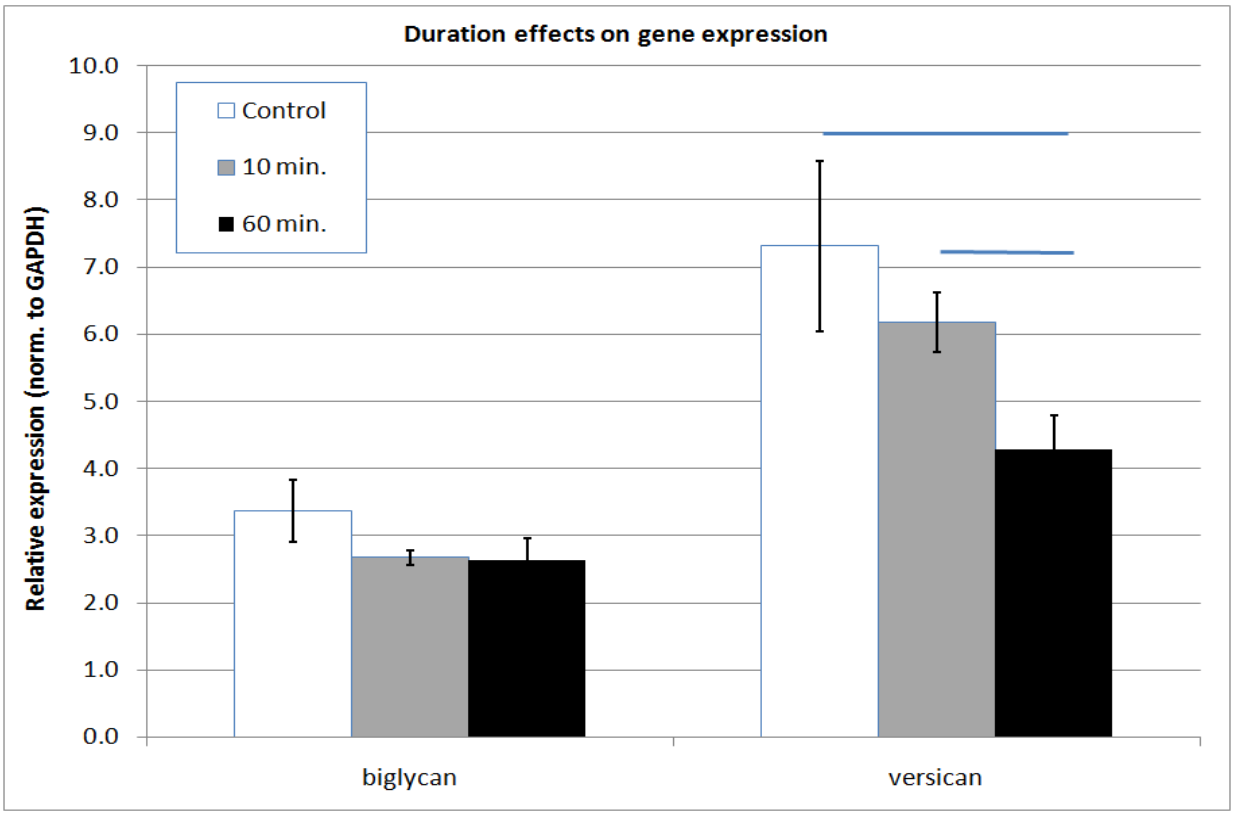

Bar– indicates significant difference between conditions under bar edges ($p < 0.05$).

Figure 16: GLM analysis indicated a significant effect of vibration duration on expression of biglycan and versican mRNA, however only versican demonstrated significant pairwise comparisons (bars: $p<0.05$).

3.3.8 Discussion

Vibrations may have beneficial or adverse effects upon musculoskeletal tissues. Studies have variously suggested an increased risk of disc degeneration (Jensen et al., 2008), no effect (Kumar et al., 1999), or even an analgesic effect (G.T. Desmoulin, Hunter, et al., 2012; G.T. Desmoulin, Szostek, et al., 2012; G.T. Desmoulin et al., 2007) of vibrations. Thus, further investigations of the cell- and tissue-scale processes are warranted.

In general, the results presented here indicate a positive effect of axial vibration on extracellular matrix gene expression in bovine nucleus pulposus (NP), which is the first step in

creating a vibration-based therapy for humans. This concept was justified in section 2.6 and is briefly reiterated here. It is important to understand that the expression of mRNA does correlate to protein expression (Guo et al., 2008). Looking specifically at genes responsible for extracellular regions of tissues (15 in total) similar to the ones used in this study, there is a significant portion of the variation accounted for (41% ($r=0.643$; $p<0.0001$)). Hence, while relying on mRNA expression to predict protein expression is not perfect it is considered reliable and valid in this case.

Continuing, the results show that most genes were at or above control levels for most frequencies and amplitudes, with the notable exceptions of biglycan and versican. Both of these genes exhibit complex expression patterns with high and low regions throughout the amplitude spectrum (Figure 14). Regardless of frequency and amplitude, versican expression was reduced after 60 minutes of exposure.

Most of the genes analyzed in this study are normally highly expressed in the NP therefore increased expression would be expected to correlate to tissue maintenance with vibration. However collagen type I is normally expressed at a low level in healthy NP. Therefore, increased expression of collagen type I, and decreased expression of versican may suggest a potential adverse affect of vibration. Further studies are required to determine whether the positive effects (biglycan, collagen type II, and decorin) outweigh the negative effects (collagen type I and versican).

It is interesting to note that the small proteoglycans (i.e. biglycan, decorin, and versican) were influenced by vibration while the largest proteoglycan (i.e. aggrecan) was not affected. The current data are insufficient to determine whether the gene expression changes translate into

altered protein expression. These results may suggest a fundamental difference in the functionality of the large versus small proteoglycans during mechanical loading.

It should be noted that this study applied unconstrained vibration; this is distinct from other systems, which apply oscillating axial compression. A 40.6 N mean value tare load was applied to the disc, and the entire culture chamber was vibrated in the axial direction. The static axial load was calculated using the average thickness of the vertebrae-disc-vertebrae section and the spring stiffness. Rapid motion of the chamber induces eddy currents in the culture medium and presumably increases nutrient transfer through the disc. A similar phenomenon would occur via convective pumping in the axial compression case, but the microenvironment will be different in the two cases (unconstrained vibration and oscillating axial compression).

Taken as a whole, objective 2 results indicate that vibration influences extracellular matrix gene expression. Increased gene expression in bovine discs may not translate well to human discs and does not necessarily mean increased protein synthesis. Further, increased protein synthesis does not mean a translation to a healthier disc in-vivo. Hence, additional work should be carried out to answer these questions. Capability of performing the loading parameters that maximize gene expression is the first step in developing such a therapy. In Objective 3, the firmware of KKT_v1 was modified (KKT_v2) to include the capability of 16 Hz as part of the loading parameters and to determine if the intervention could reproduce similar results.

3.4 Objective 3 Experiment – Implementation of Basic Science into Intervention (KKT_v2)

3.4.1 Goal of Experiment

Modify the interventions capability to apply optimal vibration parameters found in Objective 2 and both characterize its imparted mechanics and determine the effect the intervention has in altering intervertebral disc (IVD) gene expression.

3.4.2 Tissue

As section 3.2.3. above with the exception that the tail segment containing 5 vertebrae were weighed. On average the 5 vertebrae tail segments weighed 49.5 N (11.1 lb) with a 10.3 N (2.3 lb) standard deviation. Each tail segment was then fixed to a device that held it in a way that emulated clinical positioning of the human cervical spine (Figure 17). Figure 17A shows how the device is used in the clinic, head and shoulder fixed on treatment bench with neck freely suspended; similarly Figure 17B shows the clinical emulation test set-up using the bovine tail fixed at either end. The center vertebra of each segment was loaded with the treatment device.

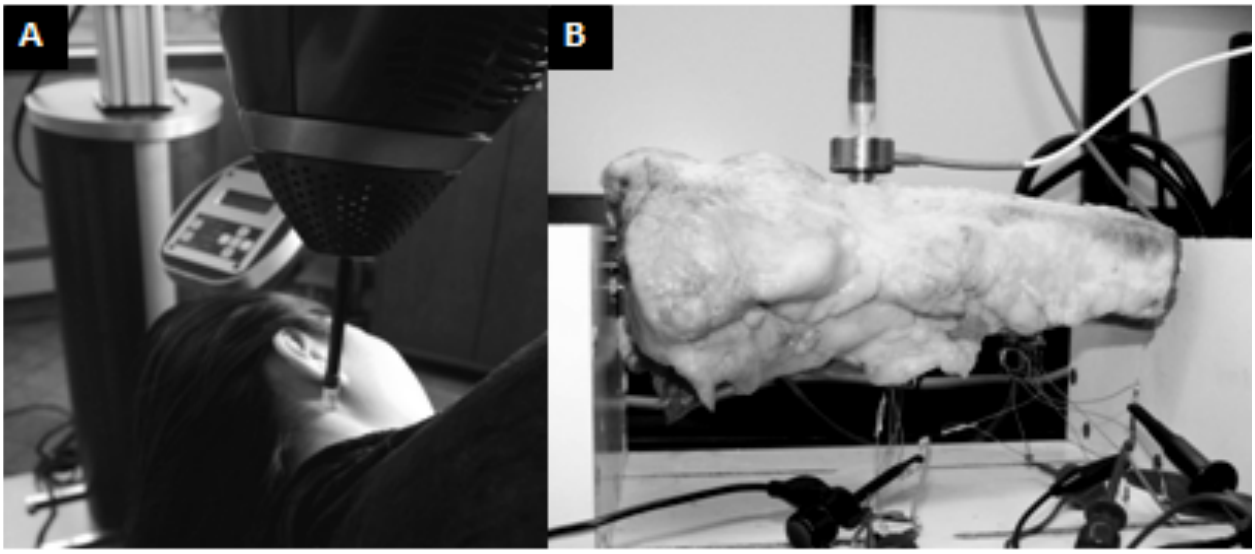

Figure 17: (A) KKT unit being used in the clinic on a patient. (B) 5 segment bovine tail clinical emulation set-up.

3.4.3 Vibration Loading

Similar to the first experiment detailed at the beginning of this chapter, vibration was applied to discs via the intervention through the center vertebrae (KKT_v2). KKT_v2's stylus was placed on the sensitive region of a strain gauge based load cell (450 N (100 lb)) (MN# WMC-100-456, Honeywell, Morristown, NJ). The load cell was fixed to the center spinous process of the 5 segment bovine tail (Figure 17B). In contrast to the first experiment summarized in section 3.2, three-dimensional accelerations were recorded as opposed to single axis acceleration. To perform this ±10 g accelerometers (#MMA7261QT, Freescale Semiconductor Inc., Austin, TX) were mounted on a cube which was oriented with a coordinate system that aligned with the axes of the disc (X-axis = axial compression/tension; Y-axis = shear 90 deg out of alignment with applied load, Z-axis = shear parallel with applied load). The cube was glued directly to the bone using cyanoacrylate in order to track acceleration of both the loaded and adjacent vertebral bodies. The accelerometers were previously calibrated using the same technique as previously explained.

The data from the load cell and accelerometer were collected via a PCMCIA data acquisition card (National Instruments, Austin TX), at the sample rate of 3000 Hz using LabVIEW^{TM} and processed to produce three dimensional disc strain using DIAdem^{TM} 10.2 software packages (National Instruments, Austin, TX). KKT_v1's internal control was bypassed in order to obtain the specific vibration conditions determined to be optimal for gene expression in objective 2 of this chapter. The voice coil producing the vibration from within the KKT_v1 unit was controlled with the output of a Linear Current Amplifier Module (LCAM-1, Quanser, Markham, ON), which received its command signal from a function generator (PicoScope2203, Pico Technology, St Neots, Cambridgeshire). The LCAM was powered by 27 V, and cooled by a

7.06 CFM fan (#2412PS-12W-B30, NMB-MAT, China) to eliminate temperature fluctuation of the output. The intervention's stroke length was not measured. Electrical current to the voice coil, and the accelerometer output was monitored in real-time via an oscilloscope (PicoScope2203, Pico Technology, St Neots, Cambridgeshire) during the loading.

Imparted vibration was tested at four different current values (~0.9-1.9 Amp driving current) although stroke length was not a measured variable. Testing vibration was applied at two constant frequencies (0 or 16 Hz) and/or one sweep frequency (50-80 Hz) that started at 50 Hz and would step up by 2 Hz every two cycles of oscillation reaching 80 Hz. These frequency ranges are based on the "optimal" windows for gene expression determined in the objective 2 and summarized in section 3.3 above. Each frequency treatment was applied for 10 minutes; one treatment combined frequencies of 16 Hz for 5 minutes and 50-80 Hz for 5 minutes to maintain the overall 10-minute application. All amplitudes were sustained at 0.5-5 g peak RMS of the vertebrae directly receiving the load. This is similar to clinical treatments using the device, and corresponds to those stimuli eliciting peak responses in previous experiments (G.T. Desmoulin et al., 2010).

The order of control samples versus actual vibration samples were randomly assigned to eliminate any time-dependent trends due to sample storage. All conditions were run on a minimum of 6 separate individual discs from at least three different tails. Control discs were treated equally in order to perform as true unloaded controls (stored, handled, dissected, and snap-frozen).

3.4.4 RT-PCR

As stated above in section 3.2.4.1 RT-PCR.

3.4.5 Data Analysis

Imparted Mechanics: Raw voltage from the load cell and accelerometers were converted to average peak Newtons of force, and average peak g's respectively in the data collection software. Post processing analysis consisted of converting g's to m/s^2, integrating the signal twice, and scaling it to mm so that relative strain could be estimated along all three axes of the adjacent disc.

RT-PCR: Data were first analyzed using General Linear Model (GLM) analysis; substantial non-normalities were detected using normal probability plots. Therefore the analysis was revised using the Kruskal-Wallis nonparametric test. A Box-Cox analysis was performed in order to conduct post-hoc analyses on the non-normal data. In all cases a transform of lambda=0.5 was found to be optimal. The transformed data were then analyzed using ANOVA and Tukey's post-hoc test. The results of the original Kruskal-Wallis test and the transformed ANOVA test were consistent in all cases, indicating that the transform was effective in normalizing the data. Pairwise comparisons were considered significant at or below the p=0.05 value. All bar graphs plot the mean ± standard error.

3.4.6 Results

Imparted Mechanics: Table 6 shows that for similar current amplitudes sent to the voice coil, the KKT stylus, which is fixed to the coil, applies a similar force to the tissue sample despite the difference in frequencies (16 and 50-80 Hz). The accelerations of the measured vertebrae were also similar across current amplitudes despite different frequencies. The relative strains along the X and Z-axes tend to differ over the two frequency levels, at 16 Hz the relative strains tend to be larger across the same current values than at 50-80 Hz. The largest shear strain

occurred in the Z-axis (3.28% peak strain) that was parallel to the loading axis, with substantially less shear strain in the Y-axis (transverse shear, 0.13% peak strain). Linear strain in the X-axis was measured at 2.56% peak strain.

Table 6: Imparted mechanics and resulting relative disc strain.

Amp (to actuator)	Frequency (Hz)	Force on Vertebrae (peak-N) - Avg.	SD	Acceleration of Vertebrae (peak-g) - Avg.	SD	Relative Strain of Disc (%) X- Avg.	X-SD	Relative Strain of Disc (%) Y- Avg.	Y-SD	Relative Strain of Disc (%) Z-Ave	Z-SD
~0.946	16	5.8	1.4	1.17	0.21	0.00	0	0.00	0.00	0.24	0.39
~1.132	16	9.3	2.5	1.77	1.14	0.34	0.56	0.07	0.12	0.55	0.67
~1.522	16	10.6	2.0	2.49	0.81	0.85	1.70	0.00	0.00	0.55	0.67
~1.898	16	12.2	1.9	2.79	0.39	2.56	3.40	0.00	0.00	3.28	3.69
~0.936	50-80	5.5	1.0	0.93	0.15	0.25	0.29	0.10	0.17	0.20	0.24
~1.122	50-80	6.9	1.1	1.27	0.28	0.47	0.53	0.13	0.23	0.57	0.39
~1.484	50-80	11.1	1.7	2.81	0.96	0.23	0.32	0.00	0.00	0.63	0.39
~1.864	50-80	12.2	1.9	3.03	1.09	0.55	0.35	0.00	0.00	0.90	0.39

RT-PCR: Both the Kruskal-Wallis test and the ANOVA on transformed data indicated that there were significant effects on aggrecan, collagen type II, and versican expression ($p=0.039$, 0.039, and 0.001, respectively) (Figure 18), but no significant effects on biglycan, collagen type I, and decorin expression ($p=0.113$, 0.182, and 0.128, respectively) (Figure 19).

Post-hoc analysis indicated that aggrecan expression was significantly higher than control at the combined frequencies (16 Hz and 50-80 Hz) ($p=0.016$). Collagen type II expression was significantly different between the 16 Hz and the combined (16 Hz and 50-80 Hz) treatments ($p=0.0347$) but neither was significantly different from control. Versican expression was significantly higher at 16 Hz than control ($p=0.0257$) and the combined frequencies (16 Hz and 50-80 Hz) ($p<0.001$). At 16 Hz versican was also significantly higher than the 50-80 Hz frequency sweep ($p=0.0146$). No other comparisons were statistically significant at $p>0.05$.

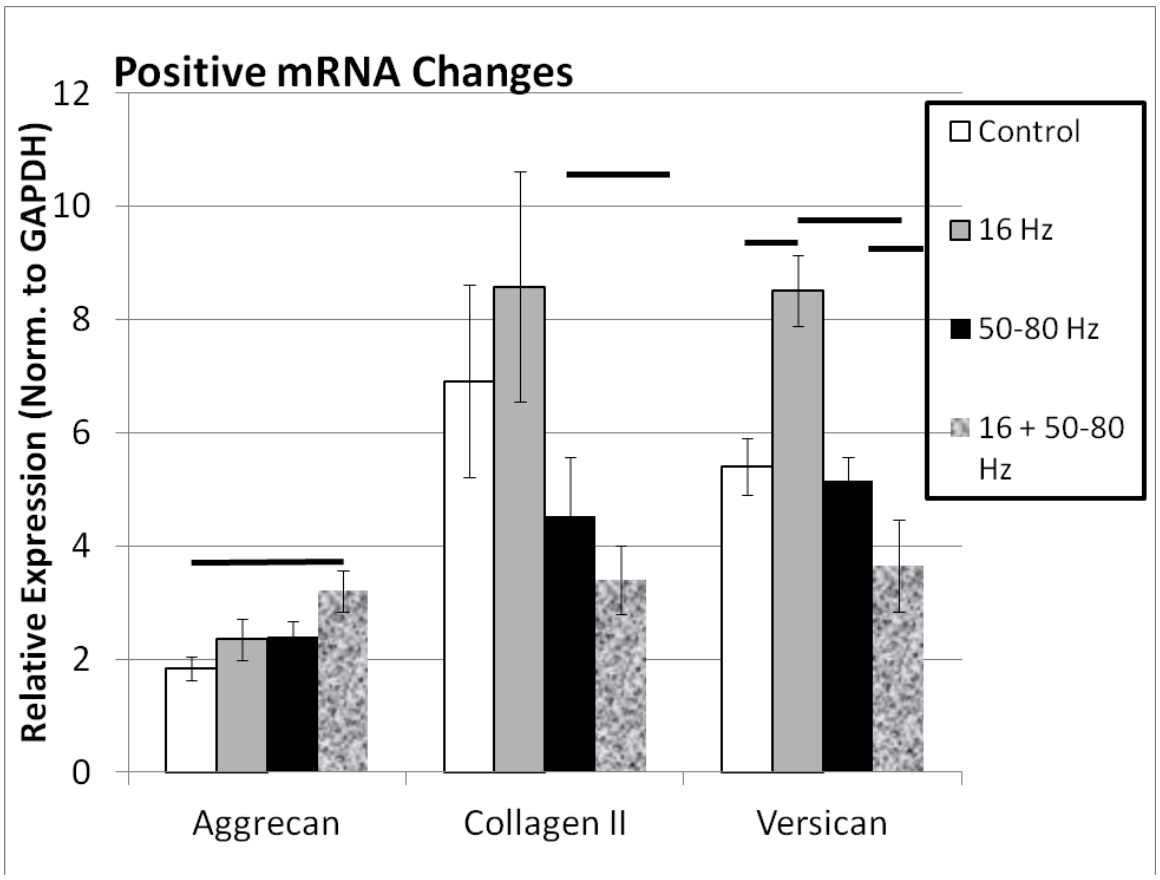

Bar– indicates significant difference between conditions under bar edges ($p < 0.05$).

Figure 18: Positive mRNA expression changes included the genes Aggrecan, Collagen type II, and Versican.

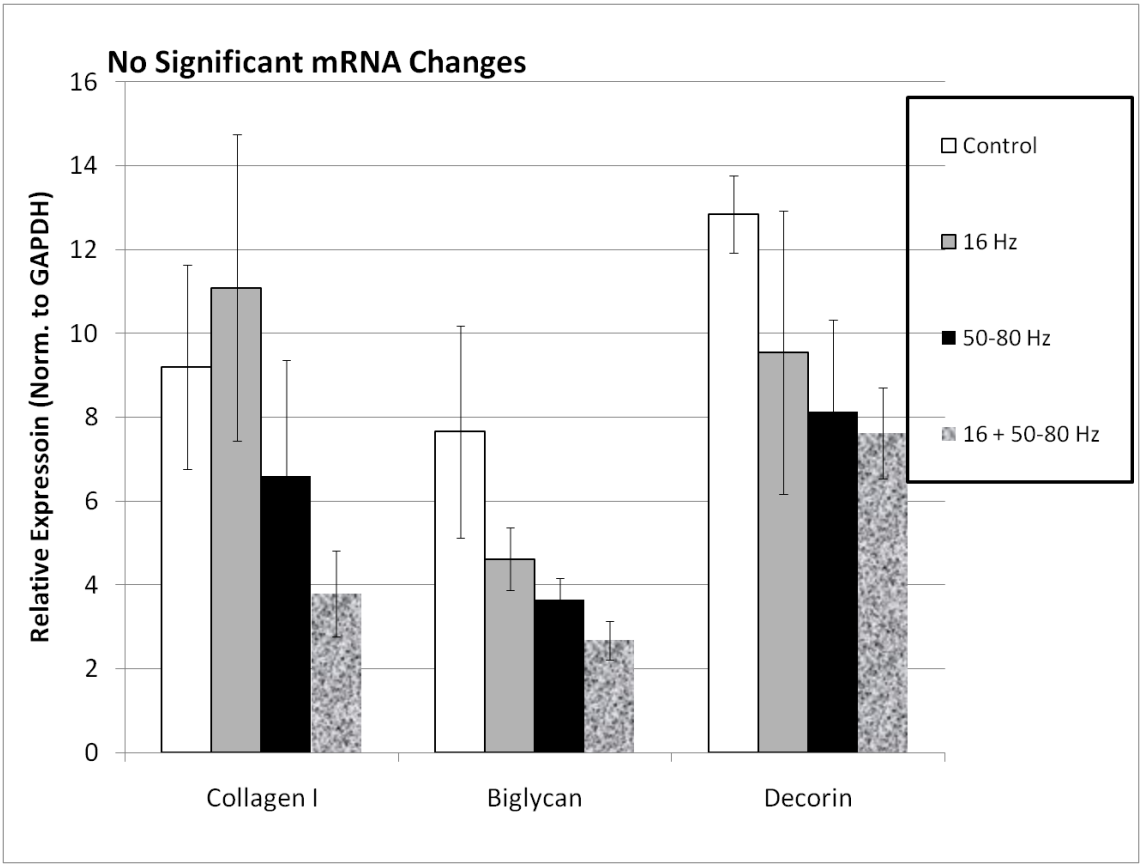

Figure 19: No significant mRNA expression changes included the genes Collagen I, Biglycan, and Decorin.

3.4.7 Discussion

Vibrations may have beneficial effects upon intervertebral disc (IVD) tissue, though the explanation to date is still confusing (Hill et al., 2009). Evaluating the mRNA changes is challenging, since mRNA does not always correlate to functional protein changes. However, as discussed in Chapter 2, there is evidence that matrix gene expression correlates significantly to protein expression (Guo et al., 2008). Hence, in the present study, we accepted any statistically significant change as noteworthy. Under this definition, the current findings indicate potential for this approved clinical tool to beneficially influence gene expression in the IVD under certain loading patterns (G. T. Desmoulin & Hunter, 2010).

The experimental set-ups for objectives 1 and 3 were physically different than the set-up for objective 2. There were physical differences to how the tissues were loaded at an organ level, which may also alter the effect of vibrations at the cellular level. While current data cannot determine the differences, theory does support that equal pressure differentials should have been experienced by the randomly oriented nucleus pulposus cells across all experiments. Differences between objective 2 and 3 experimental results would be expected since the loading patterns applied to disc tissue were different with each case and only objective 3 combined loading patterns. Further, the optimal loading patterns implemented in objective 3 were not discovered until after objective 2 results were analyzed appropriately. A more relevant comparison would be that of objective 1 and objective 3 where the load application vector, disc set-up, and amplitudes were identical. The results show a dramatic increase in expression of genes important for producing proteins that maintain disc integrity. A "tuning" effect occurred with the optimal loading pattern developed by objective 2 data and utilized in objective 3.

In general, the results presented here indicate that a particular window of vibration may have a positive effect on extracellular matrix gene expression when applied using the KKT_v2 device. Aggrecan and versican, important for disc health, were above control levels for the specific frequencies and combination of frequencies tested.

Aggrecan, collagen type II and versican are highly expressed in the nucleus pulposus (NP) of a healthy disc, therefore increased expression of these proteins genes could correlate to tissue maintenance or repair. In contrast, collagen type I is normally expressed at low levels in healthy NP. Consequently the combination of non-significant changes in expression of collagen type I and increased expression of aggrecan and versican suggest a potential beneficial effect of the current vibration loading pattern tested with KKT_v2 in this study (G. T. Desmoulin & Hunter,

2010). Further studies will be required to elucidate any clinically relevant effect of specific vibration loading patterns.

As previously mentioned, a bovine tissue is considered the best candidate for gene expression experiments ex vivo however, increased gene expression in bovine discs may not directly translate to human discs, and increased gene expression does not necessarily result in greater protein expression. Not withstanding these caveats, objective 3 demonstrated that when the firmware of KKT_v1 was modified to include the ideal loading parameters it produced similar results to those determined to be optimal in objective 2 (as illustrated in section 3.3).

The current data are insufficient to determine whether the gene expression changes translate into altered protein expression or clinically relevant changes in pathology. It is clear that the loading patterns tested with KKT_v2 positively influence mRNA expression in genes responsible for disc health and avoid increasing expression of genes that control proteins that are normally found in low quantities in a healthy disc (Table 7). Furthermore, the use of sustained vibrations to manipulate gene expression has moved past the proof of concept stage and warrants investigation in-vivo either in animals or humans if feasible as KKT_v2 is currently being used in clinics. Additional clinical study is recommended to determine how these up-regulations actually affect disc health in humans. This could be performed using advanced analysis of MRI indices of disc degenerations (Zobel et al. 2012) with regular KKT_v2 treatment over the long-term, or in cross-section, but would need to control for age and time related co-factors.

3.4.8 Results Summary

As discussed above, chapter 3 experimental results indicate a window of vibration that stimulates bovine nucleus pulposus extracellular matrix gene expression to significantly up-

regulate. This "window" of vibration was determined to be 16-80 Hz frequency, >0.4 g acceleration amplitude, and 10 minutes duration and was determined to maximize gene expression of the array tested as a whole. While the above stated loading pattern affected the gene array as a group there were also individual genes of the same array that significantly responded (up-regulated) to more specific loading patterns not necessarily the pattern outlined above that was best for the group. For example, versican was up regulated at 16 Hz only; biglycan had a load dependent relation only (>0.4 g); decorin required specific load and frequency requires (>0.4 g and 8 Hz); similarly collagen type II required load and frequency requirements of a different range (>0.4 g and 80 Hz); while collagen type I, hypothesized to be a negative response if up-regulated, remained neutral throughout testing under these conditions (10 min duration and compared to controls only). Table 7 below briefly summarizes these findings. Note: all raw data from all objectives and full ANOVA tables from Obj. 2 and all data points can be found in the Appendix.

Table 7 Summary of changes in gene expression (Hypothesis v. Results) compared to control at 10min duration.

Gene Expression Influence (Hypothesis vs. Results)						
	Aggrecan	Versican	Biglycan	Decorin	Collagen II	Collagen I
Hypothesis	si/up	si/up	si/up	si/up	si/up	neutral
Results (ch3 experiments)	si/up	si/up	si/up (◆)	si/up (γ)	si/up (γ)	neutral

si = significantly influenced
neutral = no change
up = up-regulated compared to control
down = down-regulated compared to control
◆ = load dependent.
γ = load and frequency dependent.

CHAPTER 4: DESIGN, ASSEMBLY, VALIDATION, AND EXPERIMENTATION WITH NOVEL BIOREACTOR

4.1 Introduction

The experiments outlined in chapter 3 demonstrated that it is possible to "tune" loading patterns to up-regulate genes of bovine discs non-invasively, these genes tend to be variably sensitive to amplitude, duration and frequency. Which led to the belief that it was likely possible to "tune" the loading patterns to up-regulate genes for other load bearing tissues. As a requirement of testing additional tissues, it was desirable to design a novel bioreactor that can load tissues with a wide range of parameter magnitudes while mimicking an in-vivo environment. Further, we integrated the experience from the un-modified/modified KKT intervention and the prototype bioreactor into more comprehensive design requirements. The first major step was to design, assemble, validate, and experiment with a bioreactor using bovine disc tissue to confirm past experiments was completed in this study. The results of this first step have been published in the Journal of Biomechanics (G.T. Desmoulin et al., 2013).

4.2 Design Requirements and Experiment Introduction

The relationships between various mechanical inputs and intervertebral disc (IVD) structure, composition, and metabolism are critical to detailing the nuances of disc mechano-biology in both health and disease. Previous research has shown that different loading regimes (C.L. Korecki et al., 2007) and limited nutrition (Jünger et al., 2009) also have a significant effect on overall disc degeneration. Thus maintaining a controlled culture medium during IVD loading protocol is necessary to fully understand the mechano-biology of IVDs.

Previous biomechanical studies reported in chapter 3 increased expressions of mRNA in healthy IVDs in response to mechanical vibrations (G.T. Desmoulin, Hunter, et al., 2012; G.T. Desmoulin et al., 2010, 2011). These experiments determined an optimal window for bovine IVD vibration of 16-80 Hz frequency, 40 N tare load, and 10 minutes duration, which maximized specific gene expression. However, the experiments detailed in chapter 3 utilized a simplified bioreactor that did not consider the benefits of circulating culture medium and was controlled with an open loop loading protocol (G.T. Desmoulin et al., 2010, 2011). For this study (chapter 4), a fully automated device was designed to improve accuracy and efficiency of experiments. This was achieved by loading four discs: a) simultaneously; b) in constantly circulating culture medium; c) while applying different loading regimes automatically; and d) with a higher degree of numerical accuracy under closed loop control. Improving experimental controls such as temperature, air quality, and culture medium were also added to preserve the viability of ex vivo tissue in order to produce more accurate results. The system was designed to maximize mRNA expression within tissues treated with sustained axial vibration loading. The efficacy of the system was validated in part by comparing independent experimental data to previous studies showing vibration loading at 16-80 Hz positively affects mRNA expression in bovine NP (G.T. Desmoulin et al., 2010, 2011). This chapter summarizes the design, validation, and experimental results, technical advantages, and research limitations of this novel vibration-loading platform (Bioreactor).

4.3 Bioreactor Device Design and Validation

The novel test device used a quadruple bioreactor system that circulated culture medium between the four chambers, each of which contained a vibrating pushrod that loaded the discs

(Figure 20). The 1.5 L of phosphate buffered saline medium was circulated at ~0.05 L/min using tubing that connected all four chambers and a pump (Master Flex #HV-07575-10**,** Cole-Palmer, Montreal). The device was designed to fit within a standard cell culture incubator (470x450x470mm) (Figure 21), and the medium circulation rate, constant temperature (37 ^{o}C), and constant environmental CO_2 level (5%) achieved within the incubator were chosen to best represent in-vivo conditions (Kofoed & Levander, 1987). The CO_2 levels were controlled using an automatic gas regulator from a CO_2 tank and a CO_2 monitor for feedback and monitor display. Disc nutrients are achieved through diffusion in-vivo. Hence, the circulating medium and increased CO_2 devised here ensures uniform conditions surrounding the disc.

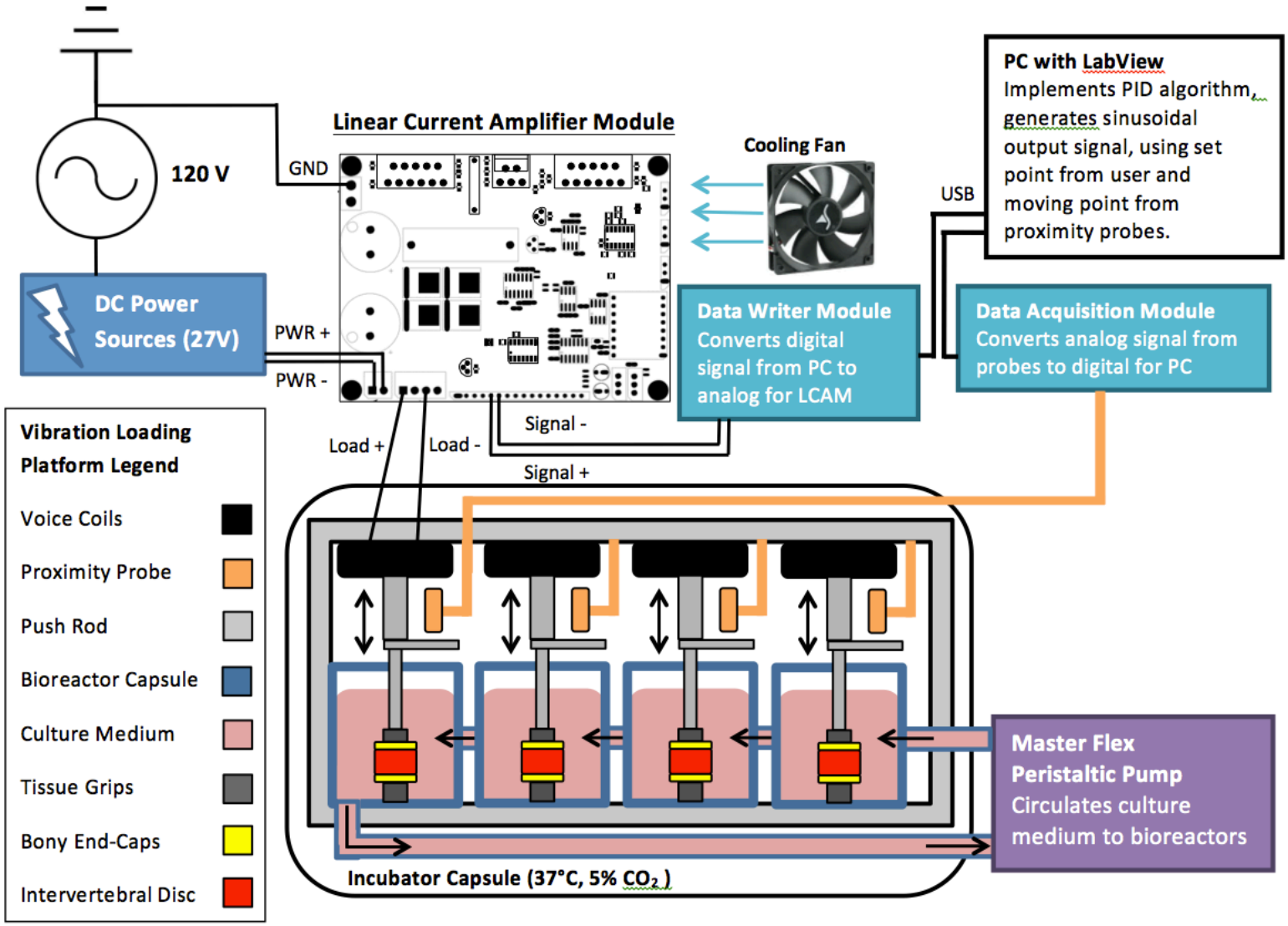

Figure 20 Bioreactor Design Schematic (Vibration Loading Platform).

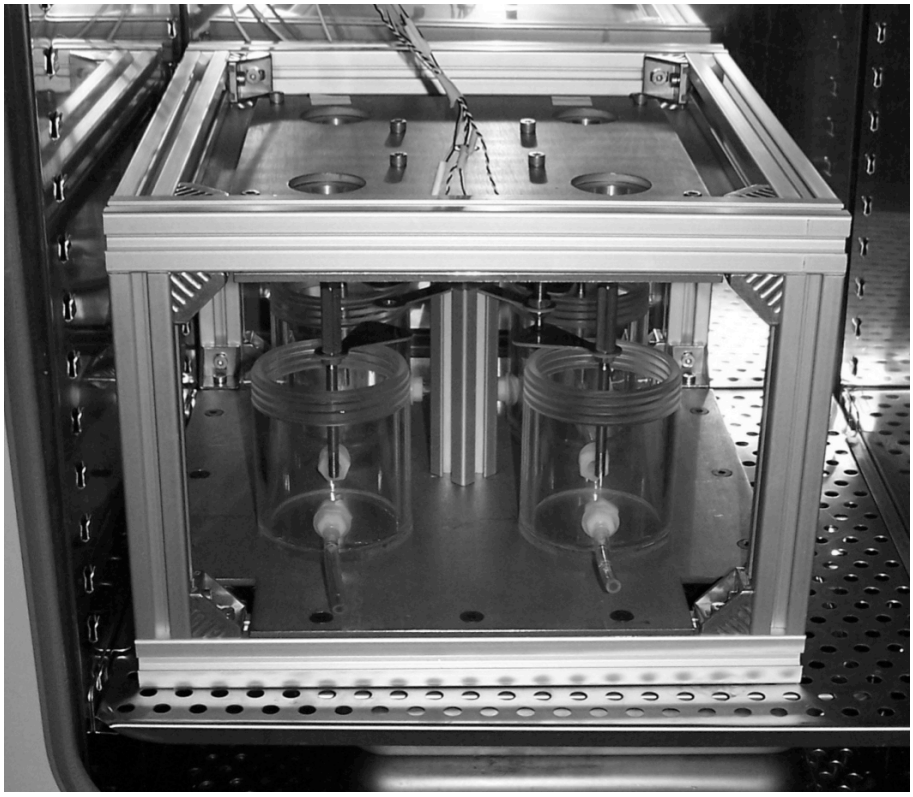

Figure 21: Device with bioreactors inside standard incubator to ensure in-vivo temperature.

The bioreactors were designed as modular with removable components allowing for easy separation from the device for cleaning and replacement. The stainless steel frame and polymethylpentene containers were autoclavable, non absorbing, and chemically inert to the tissue samples and culture medium.

The Bosch framing elements (30 mm Rex Roth PN. 3 842 990 742, Canada) that give the four bioreactors their structure were chosen to accommodate the forces experienced, while allowing for scalability and ease of disassembly for transport. The frame design was assessed in SolidWorks™ CAD software using simulation FEA, load tests were specifically performed using the "automatic" solver in FFEPlus™, which is a simulation solver within SolidWorks ™. The

static load tests were performed at a simulated 289 Kelvin (i.e. 15.85 °C). The applied static loads to specific parts simulated forces that would actually be experienced once built; 160 N for the upper plate (assuming 40 N per actuator), 160 N for the frame, and 40 N for a beam element (Figure 22). In figure 21, the dark arrows are the direction of force and the light arrows are the fixed points according to the design. The plate is upside down to show the fixed faces and the loads. The resulting deflection was a maximum of 3.8 μm in any frame element. The natural frequency of the frame and plate stainless steel elements was estimated to be 5136 Hz, well above the 200 Hz capacity frequencies of the voice coils.

The push-rod linkage between the tissue sample and the voice coil would experience axial forces imparted by the coil and the reaction of the sample. Given that the push-rod linkage force would only see a potential axial load on the 6.4 mm (0.25 inch) diameter steel rod of approximately 40 N and the part had a minimum tensile strength of approximately 984 MPa and a yield strength of 724 MPa, it was determined the part was adequately strong and did not need physical testing.

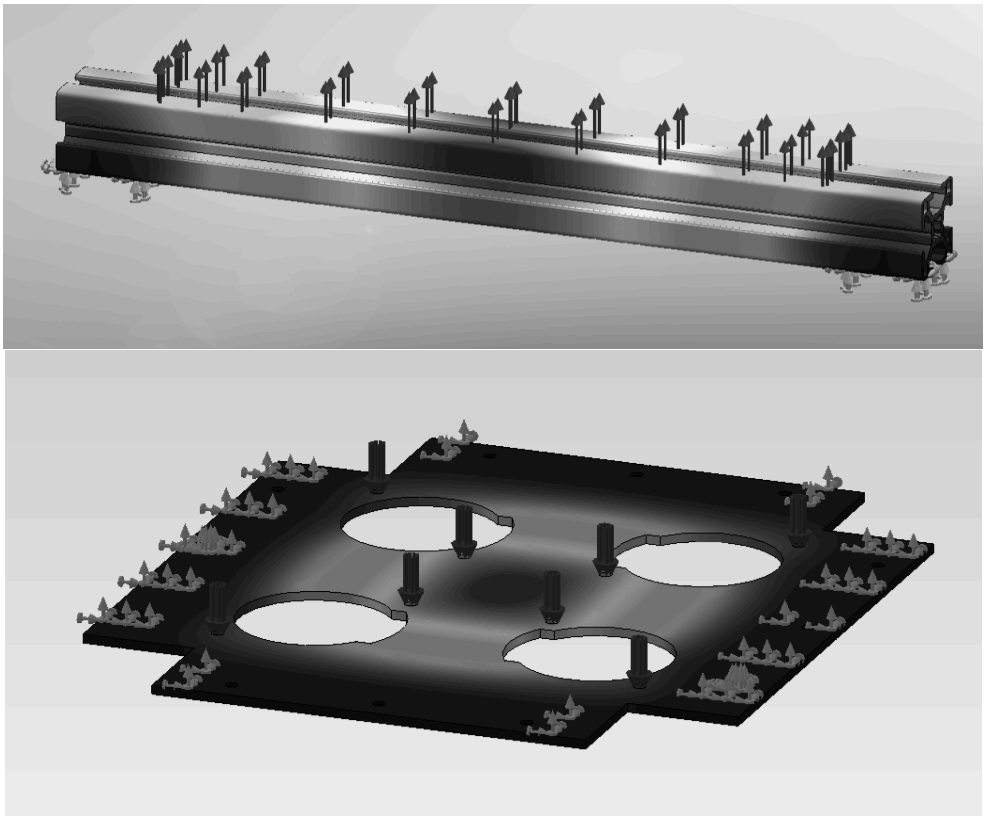

Figure 22: Solid Works Simulation FEA results for a beam element and upper plate (maximum displacement = 3.8 μm).

Flow Simulations in SolidWorks™ is based on solving time-dependent Navier-Stokes equations iteratively through moments in time or time steps. A table method is used for accelerating the iterative solution convergence and suppressing parasitic or incorrect anomaly data. For example, the table can be likened to an Excel spreadsheet that looks at each iteration, if there is a statistical anomaly it disregards it (similar to finding the best fit curve of scatter plot data that has some outliers). The 3D model or computational mesh is designed as a parallelepiped (rectangular mesh) enveloping the model. The 3D mesh is refined to better resolve the model features, such as high-curvature surfaces in contact with fluid, thin walls surrounded by fluid, and narrow flow passages (gaps). Upon subsequent calculations during the solving of the problem the computational mesh can be additionally refined (if that is allowed by the user-

defined settings) to better resolve the high-gradient flow (large relative rate change) and solid regions revealed in these calculations allowing for adaptive meshing to increase accuracy.

Any flow simulation calculation is performed in a rectangular 3D mesh computational domain. The resulting computational mesh consists of cells of the following types:

- Fluid cells are the cells located entirely in the fluid.
- Solid cells are the cells located entirely in the solid.
- Partial cells are the cells that are partly in the solid and partly in the fluid.

4.3.1 Controller

Voice coils, capable of 10 N of dynamic loading (40 N tare load prototype, Crowson Technology, LLC, Carpinteria, USA), drove the push rods compressing the IVD. The voice coils were powered by Linear Current Amplifier Modules (LCAM-1, Quanser, Markham, ON) controlled by a custom LabVIEW^{TM} program through a Compact DAQ Output Module (NI 9263, National Instruments, Texas, USA) (Figure 23). The LCAM was powered by 27 V source, and cooled by a 7.06 CFM fan (#2412PS-12W-B30, NMB-MAT, China) to eliminate temperature fluctuation of the output.

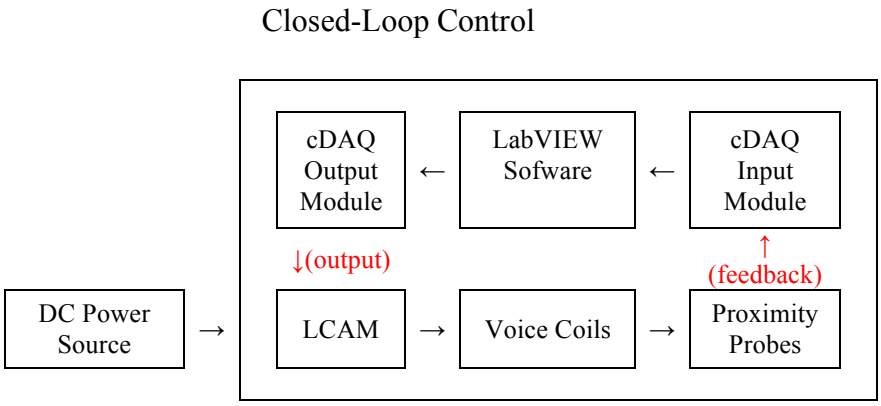

Figure 23: Hardware Set-up with feedback loop.

Vertical translation of the push rod was measured at 1000 Hz with eddy current proximity probes that provided feedback for closed loop control and came from a 10 mm Rotor kit (# 126376-01, Bently Nevada, USA) (Figure 22). The probes were individually calibrated using a device that measured the analog output over a distance of 1-10 mm (Figure 24). The sensors measured displacement of steel projections attached to the pushrod, rather than the coils themselves, to avoid electrical interference from the coil's magnetic field (Figure 25). LabVIEW^{TM} (version 9.0.1, National Instruments, USA) was used to calculate the compression applied to the IVDs by converting analog output from the probes into displacements using calibration data.

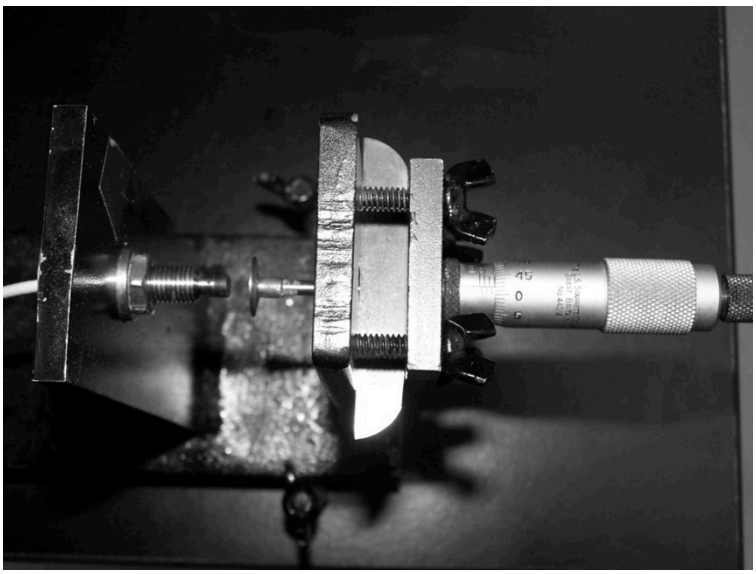

Figure 24: Proximity Probe Calibration Set-up

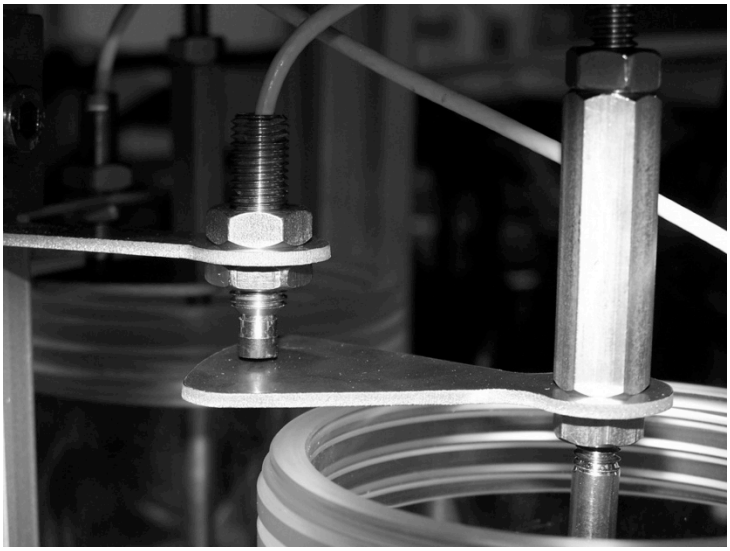

Figure 25: Proximity Probe with steel projection

Measuring the displacement response via two independent methods validated system frequency and amplitude. The National Instruments Compact DAQ Input Module (NI 9215, National Instruments, Texas, USA) and LabVIEW™ software values were compared to a PC Oscilloscope (PicoScope 2203, Pico Technology, UK), and PicoScope™ software (version

5.19.1, Pico Technology, UK) values, for frequency and displacement. Sensor feedback data were measured over a range of output frequencies and amplitudes for LabVIEW™ and PicoScope™ software separately (Table 8). There was a maximum 5.4% difference in measured amplitude voltage (0.018 mm), and identical frequency readings between LabVIEW™ and PicoScope™ software at maximum output.

Table 8: Software Validation Results

Output Freq (Hz)	cDAQ Output (V)	LabVIEW Freq (Hz)	Picoscope Freq (Hz)	LabVIEW Amp (mV)	Picoscope Amp (mV)	% difference
25	0.75	25	25	480	456.5	5.2
25	1	25	25	650	616.5	5.4
25	1.25	25	25	833	802.5	3.8
50	0.5	50	50	321	306.5	4.7
50	0.75	50	50	491	479	2.5
50	1	50	50	672	647.5	3.8
50	1.25	50	50	862	855.5	0.8
100	0.5	100	100	404	412.5	-2.1

LabVIEW's ™ proportional-integral-derivative control virtual instrument (PID.vi) was used to create a closed-loop PID control of the coil's displacement amplitude. A "VI" is a virtual instrument that combines CPU power with flexible software and specific hardware that meet application needs. Feedback data from proximity sensors were used by the Single Tone Extractor Virtual Instrument to determine amplitude and frequency of a generated waveform that optimally fits the sampled data. Specifically, the Single Tone Extractor VI allows hardware to take a signal in, find the single tone with the highest amplitude, and returns frequency, amplitude and phase to the CPU for display. The frequency remained in open loop control due to its high stability and on-screen display. User specified amplitude also enters the PID controller as the Set Point (displacement amplitude), along with user specified PID parameters (proportional, integral,

and derivative gain). The PID algorithm generates an output that is fed into the next iteration of the loop, which occurs once per second.

Figure 26 below shows a flow chart describing the flow of data in the LabVIEW™ program. The PID parameters were obtained experimentally to prevent any overshoot, while reaching 95% of desired amplitude in fewer than 10 seconds.

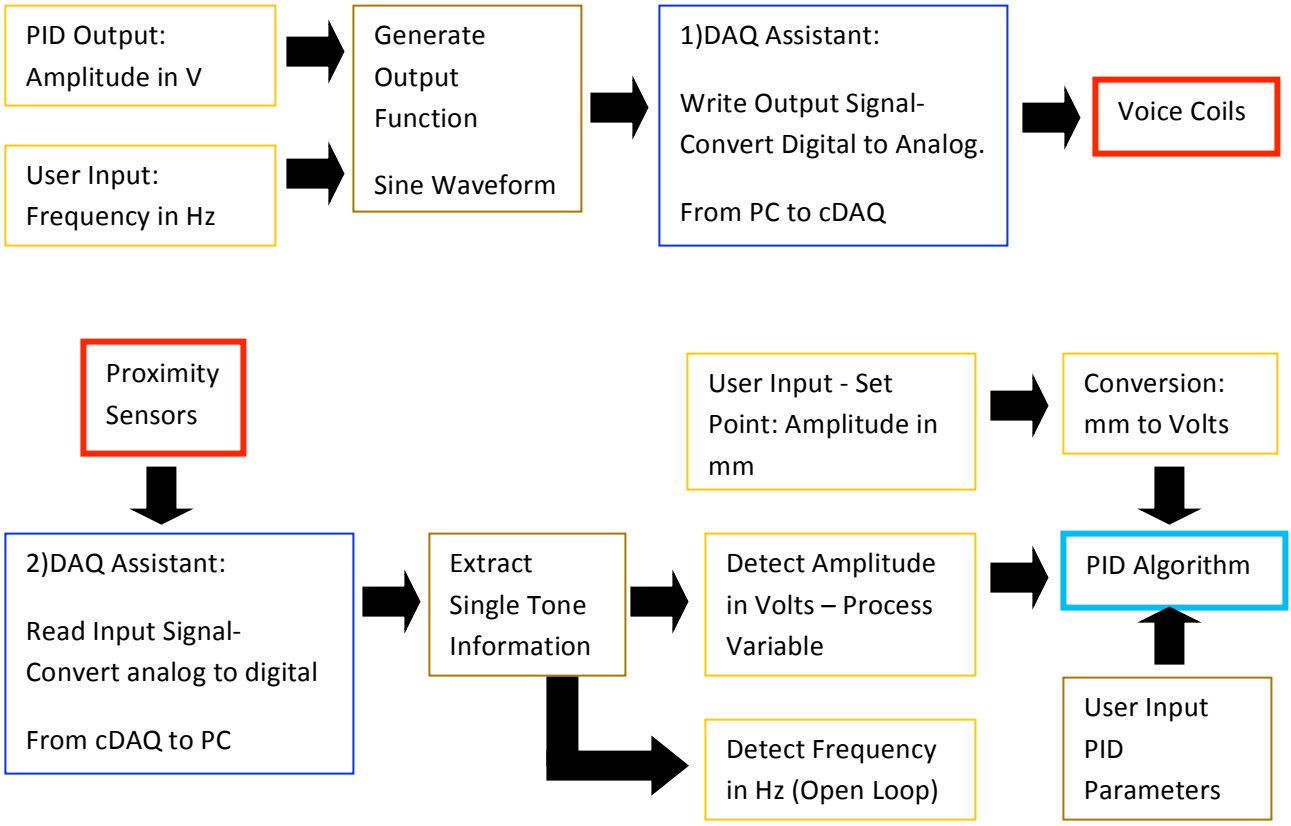

Figure 26: LabVIEW Controller Flow Chart.

4.3.2 Additional Features

The control loop collected data at 1000 Hz and iterated the LabVIEW™ PID algorithm to determine new output voltage based on the detected amplitude. The LabVIEW™ VI was

designed to run two sets of parameters, frequency and amplitude, for a desired duration. It would also automatically switch to a second set of parameters, running continuously until a specified end time. This allowed for two loading regimes that mimic periods of vibration treatment and activities of daily living. Daily activities such as walking or running produce low frequency vibration on the spine (<10Hz) (Schmidt, Shirazi-Adl, Galbusera, & Wilke), while treatments such as the Khan Kinetic Treatment (KKT) use higher frequency vibrations (>16Hz) to improve neck pain (G.T. Desmoulin, Hunter, et al., 2012; G.T. Desmoulin, Szostek, et al., 2012; G.T. Desmoulin et al., 2007). Thus, the controller was able to automatically switch loading patterns that mirror these two different loading regimes. Further, other tissues may respond to a different window of vibration parameters, therefore the device was designed to load tissue in a full 0-200 Hz range of frequencies for maximum capabilities.

4.4 Bioreactor Experiment Materials and Methods

4.4.1 Tissue

As in section 3.3.2 above.

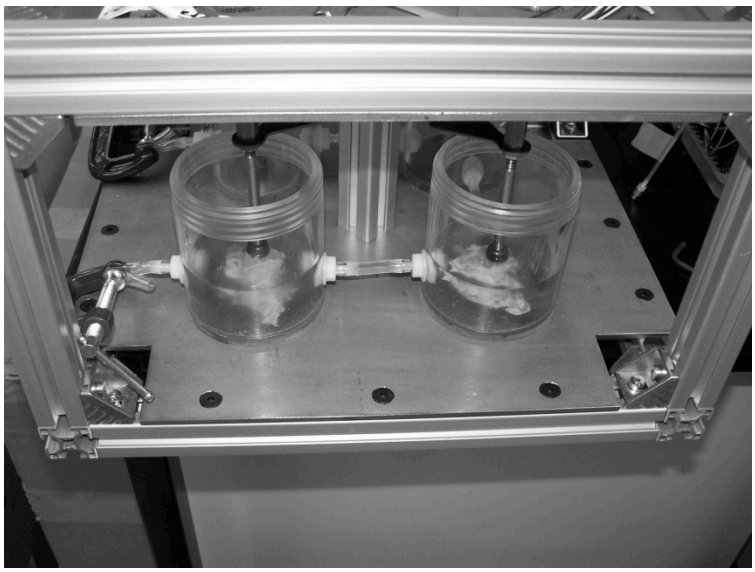

Figure 27: IVD within bioreactor, with PBS culture medium, ready for loading.

4.4.2 Vibration Loading

To demonstrate the device's efficacy identical: a) tissue preparation; b) displacement; c) frequency; d) loading duration; and e) reverse transcription polymerase chain reaction (RT-PCR) assay were used as the study outlined in chapter 3 (G.T. Desmoulin et al., 2011). Six IVD samples were compressed on average by 0.6 mm peak-to-peak compression at 16 Hz for the first 5 minutes, and 65 Hz for the next 5 minutes since these were the profiles that maximized expression in previous experiments. Six control discs from different animals were dissected and housed in the bioreactors without loading for the same duration of time and then snap-frozen, identically to loaded discs in a randomized order to eliminate time-dependencies. All bovine samples used in this experiment were acquired, extracted, loaded, dissected, and frozen in one day to minimize morphological changes and time-dependencies in IVD tissue after death. All conditions were run on a minimum of 6 separate discs from different bovine tails. The goal of this experiment was to yield maximum expression of target mRNA to provide supporting

evidence that optimal vibration parameters affect cellular activity, which could possibly translate to future treatments. The effect of the experimental loading regime was compared to unloaded tissues held in the bioreactor under the same conditions.

While displacement was controlled during experimentation, load was not. To characterize the force during experimentation the force output of the device on the IVD tissue was tested without laboratory controls; these tests were performed immediately after dissection to compensate for the absence of bioreactors and culture medium. A 450 N load cell (Electroforce 3200, Bose, USA) designed for application of force up to 200 Hz was utilized. The load cell had a natural frequency of 2000 Hz at 2.2 kg and 28000 Hz at 45.4 kg and was attached between the IVD sample and the base of the vibration platform (Figure 28).

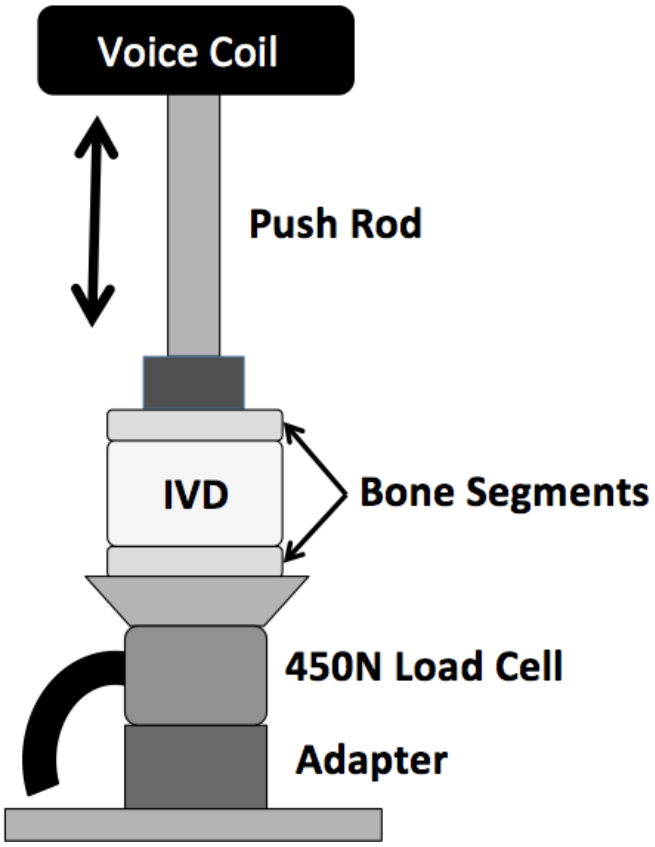

Figure 28: Load Cell Attached to Vibration Platform.

The output force transmitted through the push rod and IVD was detected by the load cell at a sampling rate of 700 Hz. Loading profiles were measured at maximum output from voice coils at low and high frequency (Figure 29). The average initial tare load was approximately 40 N, which gradually decreased to 30 N due to stress relaxation of the disc. The applied force during sustained vibration was consistently between 40-50 N, measured on three different bovine discs. The applied force from the system is comparable in magnitude to pressure in human lumbar discs during relaxed standing, for an average bovine disc diameter of approximately 25 mm (Wilke, Neef, Caimi, Hoogland, & Claes Lutz, 1999). When frequency was increased, the peak-to-peak amplitude of the loading profile decreased from approximately 2 N to <1 N.

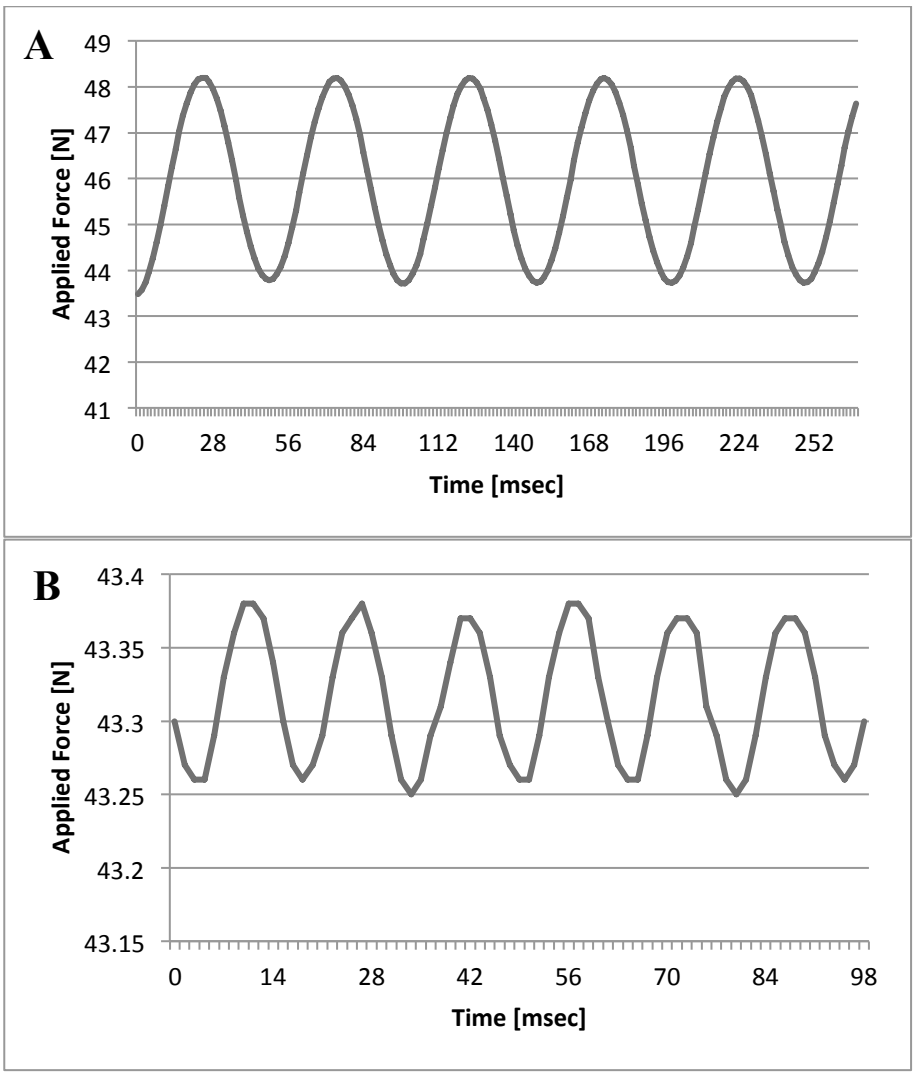

Figure 29 Exemplary Loading Profiles for Maximum Output at 20Hz (A) and 65Hz (B).

4.4.3 RT-PCR

As stated above in section 3.2.4.1 RT-PCR.

4.5 Data Analysis

As stated above in section 3.3.6 Data Analysis.

4.6 Medium Flow

SolidWorks™ Flow Simulation was used to conduct a Computational Fluid Dynamic (CFD) analysis. CAD assembly parts were defined for either internal or external flow analysis ('Internal' meaning flow should be analyzed internally to the part and vise versa for 'external'). After assembly parts were defined, and a working fluid was chosen from a library of common liquids and gases, in this case water that would be likely identical to the medium comprised of a solution of phosphate buffered saline solution. Velocity at the inlet was chosen to be 0.05 L/min based on previous experimentation. Boundary pressure conditions at inlet and outlet mimicked experiment conditions (1 Atm.) and a "steady-state" approach was used to run the model. Assumptions included that: a) the effect of the push rods would be nil and hence were left out of the model; and b) the vertebrae-disc-vertebrae tissue sample was modeled as a cylinder and defined for external flow analysis.

4.7 Results

4.7.1 Medium Flow

A Computational Fluid Dynamic (CFD) test was performed to qualitatively investigate any stagnation points or high flow regions. The goal was not to simulate normal fluid flow in the body but rather to ensure uniform distribution of nutrients and removal of waste products around each disc.

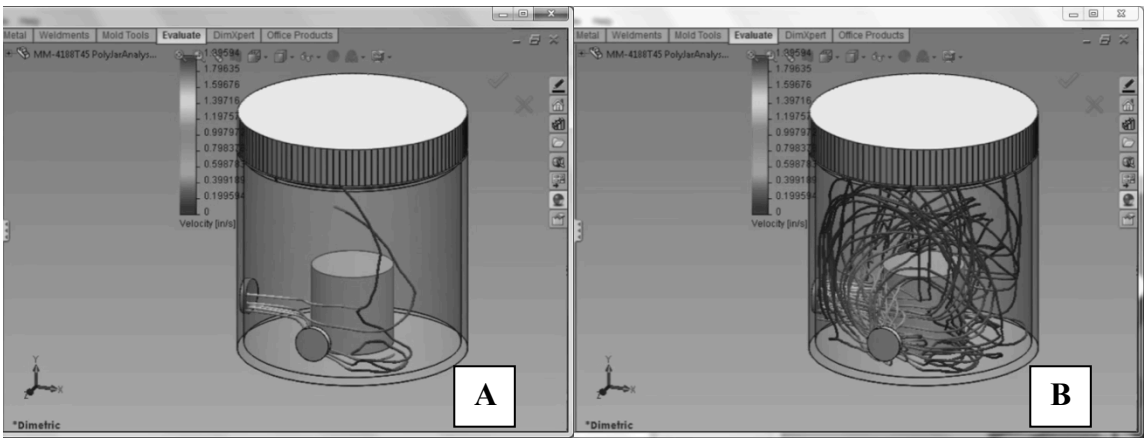

Figure 30: CFD results. A) Start of flow. B) After 1min.

Given the experimental flow of ~0.05 L/min and a density/viscosity similar to water, flows showed no stagnations affecting the samples (Figure 30). Despite the CFD models simplicity there was a substantial increase in the confidence of the systems ability to achieve uniform distribution of the fluid, at least enough to assemble the parts and test the system.

4.7.2 RT-PCR

Both the Kruskal-Wallis test and the ANOVA on transformed data indicated that there were significant differences between treatment and control for aggrecan, decorin, and versican ($p=0.045$, 0.044, and 0.008, respectively) but no significant differences for biglycan, collagen type I or collagen type II ($p=0.052$, $p=0.49$ and 0.14 respectively) (Figure 31).

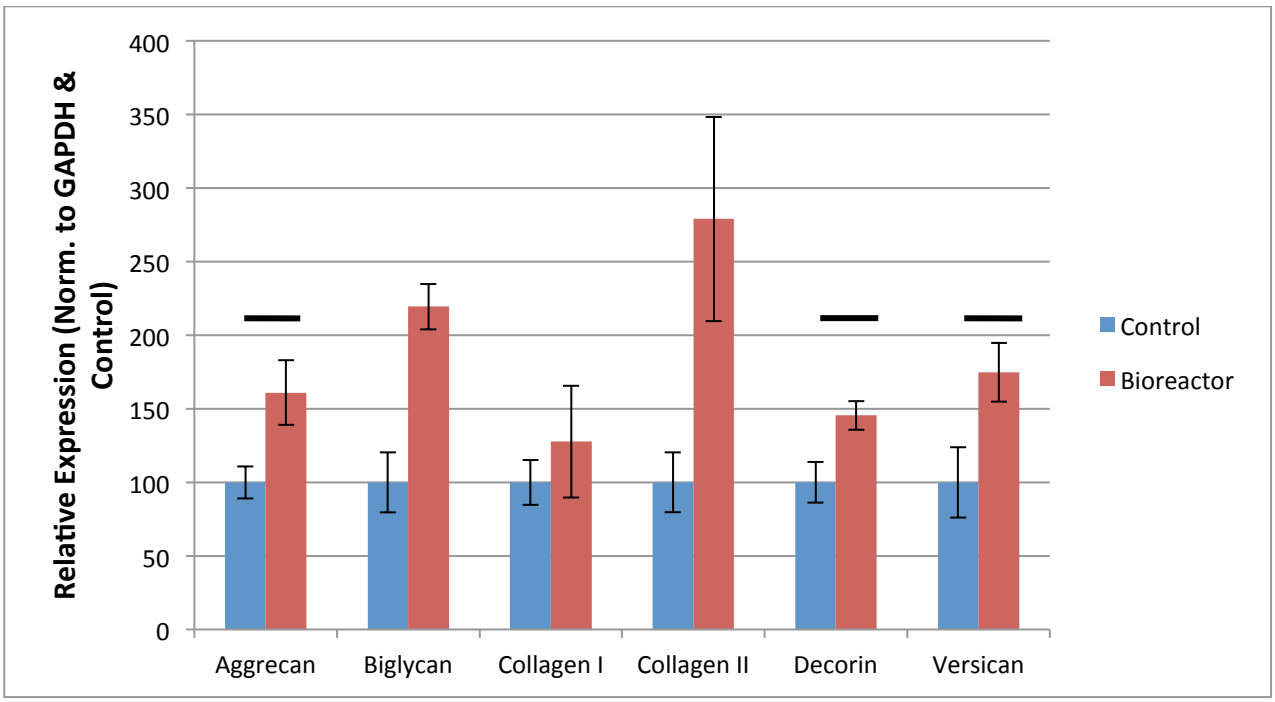

Figure 31: Gene expression levels normalized to GAPDH levels and to control values (black bars represent significant difference $p<0.05$; error bars represent 1 standard error).

4.8 Discussion

The experimental multi-unit vibration-loading platform (bioreactor) successfully accomplished its intended purpose by achieving similar increases in target mRNA expression in the IVDs due to applied vibration loading. The efficacy of the system was validated using similar loading parameters as previously reported, and by demonstrating a similar biological response in IVD tissue (G.T. Desmoulin et al., 2010, 2011). The similarities can be seen below (Table 9).

Table 9 Load condition vs gene expression.

	Gene Expression					
Load Condition	**Aggrecan**	**Biglycan**	**Collagen I**	**Collagen II**	**Decorin**	**Versican**
Complex Shear	s/up	ns	ns	ns	ns	s/up
Constrained Axial	s/up	ns	ns	ns	s/up	s/up

s = significant compared to control
ns = non-significant compared to control
up = upregulated

Five of six genes had identical responses. However, decorin was significantly up-regulated when tested with constrained axial loading and was unaffected when tested with complex shear loading. Since the NP behaves like a fluid, exhibiting hydrostatic pressure (A. L. Nachemson, 1960), it could be expected that loading at the tissue level, regardless of orientation, would have the identical effect at the cellular level. However, in the constrained axial experiment there was a tare load of 40 N that was not present in the complex shear experiments. Since it is known that the NP does not act purely like a fluid and is also capable of stress gradients typical of solids (Skrzypiec et al., 2007), it may affect the cells when the tissue is loaded at different orientations. As discussed in chapter 2, decorin is involved in the organization of collagen fibrils leading to increased tensile strength of the tissue (Gotz et al., 1997). Consequently, decorin mRNA expression may have been more sensitive to the tare load that was experienced in the constrained axial load experiments.

The ability to load four tissue samples independently was highly advantageous; the accelerated experimental method allowed the loading of more discs in less time. This is an important factor when testing tissues taken ex-vivo, as maximum viability must be maintained in order to demonstrate the biological effect of mechanical loading. The loading platform also improved the in-situ testing environment by controlling temperature and humidity in the

incubator, and by equalizing medium quality through constant circulation. The fully automated LabVIEW™ (See Appendix) control program also included a built-in timer allowing for more complex loading regimes, which enabled the seamless switch of vibration parameters at specific time points during testing. The goal of these additions was to enhance experimental controls and preserve tissue quality by accelerating the testing procedure.

To demonstrate the utility of the system, this study presented pilot data that is consistent with scientific literature. Several mRNA expressions were increased within the cells of IVD tissue in response to applied mechanical vibrations, supporting that gene expression is responsive to mechanotransduction. Aggrecan, decorin, and versican mRNA expressions were significantly increased above control levels. Biglycan, Collagen types I and II mRNA expression showed no significant difference compared to the control group. These results are largely consistent with previous studies, where aggrecan, decorin, and versican mRNA expression were also increased in response to vibration loading (G.T. Desmoulin et al., 2011). This independent experimental data were able to demonstrate similar effects in bovine IVD tissue using a completely new device, thereby achieving design goals.

A possible limitation of the fluid circulation system of this design is the fact that individual bioreactor cells "share" the same fluid medium. Therefore, it is recommended that the identical loading pattern be applied to each cell in the bioreactor for a given run and that the tissue sample cell location is recorded so that this random variable can be accounted for during the data analysis phase of test results.

4.8.1 Effects on mRNA Expression

Aggrecan and versican are highly expressed in the nucleus pulposus of a healthy disc, therefore we hypothesize that increased expression for these genes would correlate to tissue maintenance or repair; conversely, healthy nucleus pulposi exhibit low collagen I expression, as its presence usually indications formation of scar tissue in response to possible damage. This study reported non-significant changes in expression of biglycan, collagen types I and II mRNA, and increased expression of aggrecan, decorin, and versican, which suggests that externally applied vibrations may produced a beneficial effect on disc health.

4.9 Conclusion

A new fully automatic vibration-loading platform was designed and constructed with four independent bioreactors in order to increase experimental efficiency, incubator compatible dimensions, and circulating culture medium (G.T. Desmoulin et al., 2013). By using the previously reported vibration parameters, the device achieved positive influence of mRNA expressions, thus demonstrating its efficacy. The evidence provided by this study supports the use of this device for vibration loading experiments of tissues perhaps outside the realm of IVDs. Current data remain unable to determine whether gene expression changes translate into altered protein expression, and further research is still required to determine how these increased mRNA expressions actually affect long-term disc health. However, to our knowledge the combination of the above stated abilities, are novel. Future work on IVDs could investigate directional vibration loading other than axial loading to explore the effect of directional loading on different mRNA expression. This methodology should also be expanded beyond IVDs, and optimal vibration parameters should be investigated in other tissues as well.

CHAPTER 5: CONCLUSIONS

5.1 Introduction

Chapter 5 synthesizes all the results of all tissue samples (KKT_v1, Prototype, KKT_v2, and Bioreactor) and therefore additional analysis could be performed. Specifically, data from every experiment was considered to investigate the effects of the individual animals used in each experiment but also to identify what level of each parameter (frequency, load, and duration) caused the greatest amount of gene expression for each gene in the assay. Further, interactions between the fixed effects factors (frequency, load, and duration) were considered (Figure 32). Also in the following summary, the novel outcomes as a result of this dissertation are highlighted with their associated published article, the limitations and assumptions are outlined, and future work that could stem as a result of the research presented in this dissertation are covered.

The experiments began with evaluation of a spinal intervention that used cervical biomechanics, self-reported pain, and disability as clinical outcomes. While this study is not detailed as part of this thesis, it has been peer reviewed and was an important preliminary study that gave direction to the idea that spinal mechanics were an important phase in the treatment process (G.T. Desmoulin, Hunter, et al., 2012; G.T. Desmoulin, Szostek, et al., 2012). For long-term spinal health however, it was hypothesized that the improved spinal mechanics would require maintenance in the form of tissue restoration. Since about 40% of patients seen by clinicians using the intervention show signs of disc degeneration, investigation of the device as a means of non-invasive tissue regeneration was warranted.

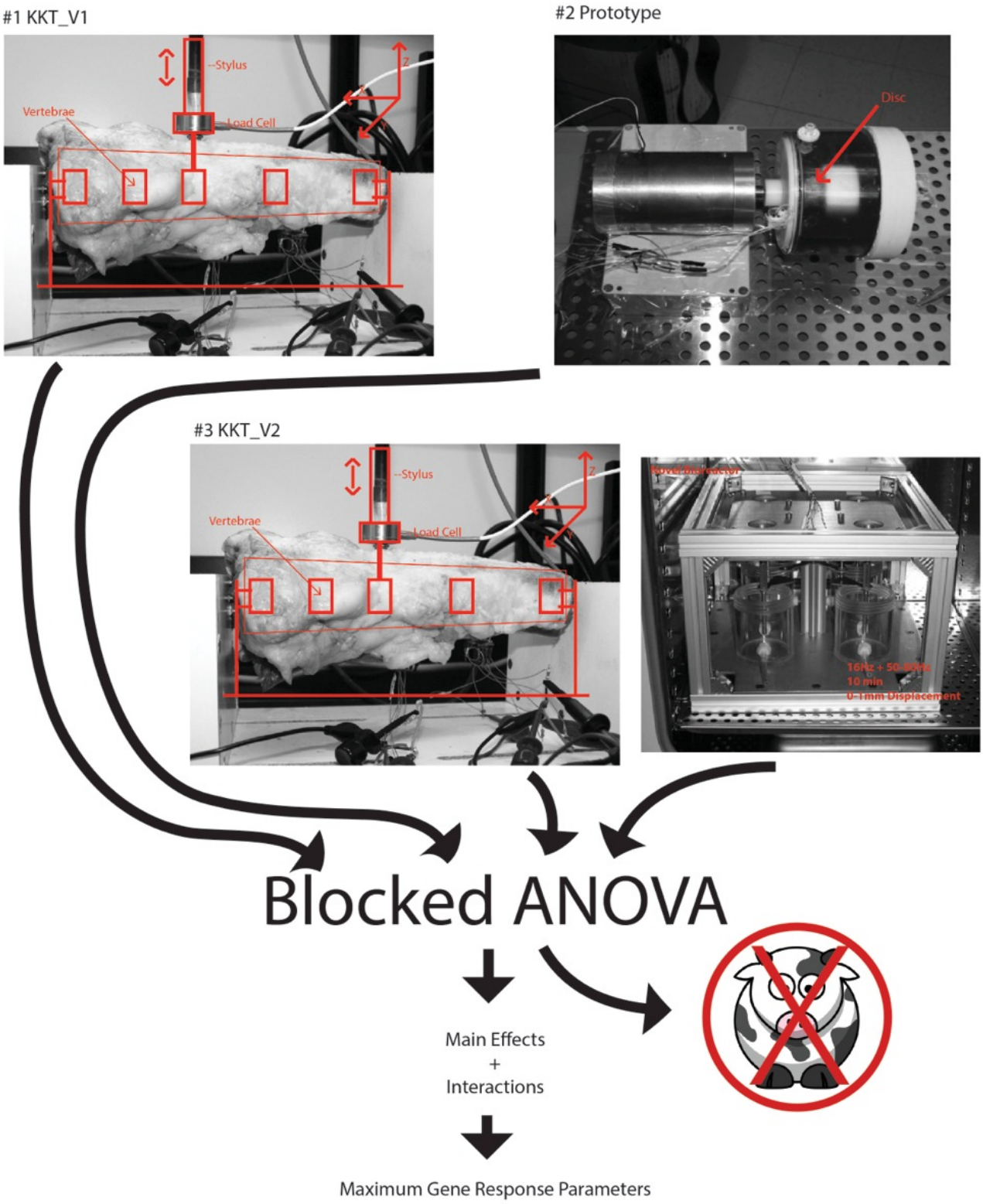

Figure 32 Overview of analysis for chapter 5. All data from all previous experiments have been collated and the effects of animal variance accounted for (noted by marked cow). Categorization of the data (3 groups of each parameter) allowed for main effects tests, interactions and maximum response parameters for each gene to be determined.

As discussed previously, bovine disc tissue was used as it has been deemed an ideal candidate to model human disc tissues. These bovine disc experiments consisted of: a) an initial evaluation of the unmodified intervention (KKT_v1) on disc metabolism; b) a basic research test matrix of a range of vibration frequencies, amplitudes, and durations to optimize expression of genes responsible for maintaining disc matrix (G.T. Desmoulin et al., 2010); c) and once optimized, evaluating a modified intervention (KKT_v2) of its effects on disc metabolism (G.T. Desmoulin et al., 2011). Conclusions included that the modified intervention (KKT_v2) was capable of increasing expression of key genes associated with disc health, indicating a potential therapeutic stimulus. Once it was discovered that the vibration pattern could be "tuned" to create a tissue-specific potential therapeutic response, it was desired to create a new research tool so that other tissues could be tested and "tuned" in future experiments. Hence, a new research device was designed and constructed with closed-loop positional control of disc tissue compression. The device also improved fluid flow between bioreactors, was capable of loading up to four discs independently, and could switch vibration-loading patterns instantly and automatically. By confirming the positive influence of mRNA expression from applied vibration patterns with an entirely new device, this research has moved past the proof of concept stage (G.T. Desmoulin et al., 2013; G.T. Desmoulin, Hunter, et al., 2012). However, the current data remains unable to determine whether the gene expression changes translate into altered protein expression necessary for long-term disc health.

5.2 Analysis of All Data as Whole

In this section the data were considered across all experiments (KKT_v1, Prototype, KKT_v2, and Bioreactor (240 samples on ave.)) in order to see the effects of the animals that

were used in the various experiments. However, in this analysis each parameter (frequency, load, and duration) value that caused greatest amount of gene expression for each gene in the assay was also determined.

Specifically, a blocked 3-way fixed effect ANOVA including all two-way interactions were included in the model. The blocks, the animals (n=84), were considered random factors. The three fixed-effect factors were frequency, load, and duration. All post hoc tests were carried out using Tukey's method. All statistical analyses were performed using SAS^{TM} statistical software version 9.2. After transformation all models run satisfied the assumptions that the residuals are normally distributed random variables centered about 0 with constant variance. A natural logarithm transformation was used for all response variables in the models. Outliers were noted and some observations were deleted (I.e. Collagen I >3000 and Collagen II >30).

Due to the different levels of the fixed effects factors between experiments the only way to combine the analysis of all studies was to recode the variables into levels. It was desired to test the data set across three levels; controls, low, and high. However, the parameter estimates for the two way interactions between these three level factors are not estimable. The reason for this is that there are not enough samples in the control group for all three variables repeated in each block. In a complete block design it is required to have data for all levels of these variables within each block (animal). This is not the case here. However, two categories does work (Low and High). Hence, in order to achieve the interactions, the data were coded with either a 0 or a 1. The cutoff for each fixed effect factor was: frequency >50 Hz = 1, load >0.4 g = 1, and duration >10 min = 1; all other values were coded as 0. The cutoff for each fixed effect was chosen logically from an actual finite number that was measured in each category and found to create a separation between gene responses. For example, load amplitude had a threshold value of 0.4 g

before most genes would significantly increase expression. Hence, logically 0.4 g was chosen to maximize the difference between the two groups. A similar approach was taken with the other fixed effect factors. All raw data and full ANOVA tables can be found in the Appendix.

The analysis showed a significant effect (p-value <0.05) due to animals (blocks) for all 6 genes tested. There was considerable animal-to-animal variation in all models tested. The results of the analysis of variance are given for each of the six genes below. The tables of fixed effects with the p-values (automatically labeled by SAS^{TM} software as "Pr > F" in tables below) determine which factors or interactions have significant effects on the response variable (i.e. gene expression). The tables below show the least square mean estimates on the natural logarithm scale for all six genes tested. Which means that the higher the number the more expression of that gene for the particular set of parameters. The "full" ANOVA tables and residual plots are also available with each raw data section in the appendix for each gene.

5.2.1 Collagen Type I

The main effect due to amplitude (load_rms_cat) and the interaction between load amplitude and duration (load_dur_cat) were both statistically significant ($p < 0.05$). No other effects were found to be statistically significant (Table 10).

Table 10: Fixed main effects and interactions for Collagen I.

Type 3 Tests of Fixed Effects				
Effect	**Num DF**	**Den DF**	**F Value**	**Pr > F**
load_freq_cat	1	149	1.43	0.2338
load_rms_cat	1	149	23.55	<.0001
load_freq*load_rms_c	1	149	1.10	0.2957
load_dur_cat	1	149	0.25	0.6159
load_freq*load_dur_c	1	149	0.97	0.3262
load_rms*load_dur_c	1	149	20.97	<.0001

Table Legend:
load_freq_cat = Frequency
load_rms_cat = Amplitude
load_dur_cat = Duration
load_freq*load_rms_c = Frequency * amplitude
load_freq*load_dur_c = Frequency * duration
load_rms*load_dur_c = Amplitude * duration

There was a statistically significant difference ($p < 0.05$) in mean responses of Collagen I between load amplitude level 0 (<0.4g) and level 1 (>0.4g). The analysis showed a statistically significant ($p < 0.05$) difference in mean responses between low load duration (<10min) versus high load duration (>10min) when load amplitude was at the low level 0 (<0.4g). The analysis showed a statistically significant ($p < 0.05$) difference in mean Collagen I responses between levels load_rms = 0 (<0.4g) load duration =1 (>10min) and load rms =1 (>0.4g) load duration=0 (<10min) (Figure 33). The analysis showed a statistically significant ($p < 0.05$) difference in mean responses between levels load rms = 0 (<0.4g) load duration =1 (>10min) and load rms =1 (>0.4g) load duration=1 (>10min). Collagen I response was a maximum (estimate =3.82) when load rms=0 (<0.4g) and load duration=1 (>10min).

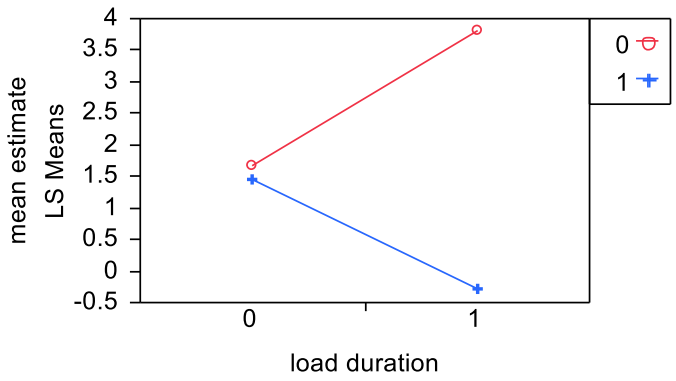

Figure 33: Interaction plot of load duration (x-axis; 0 < 10min; 1 >10min) and load rms amplitude (red = 0 <0.4g; blue = 1 >0.4g) for Collagen I response (y-axis).

5.2.2 Collagen Type II

The main effect due to amplitude (load_rms_cat) and the interaction between amplitude and duration (load_duration_cat) were both statistically significant (p-value <0.05) (Table 11). No other effects were found to be statistically significant.

Table 11: Fixed main effects and interactions for Collagen II.

Type 3 Tests of Fixed Effects				
Effect	**Num DF**	**Den DF**	**F Value**	**Pr > F**
load_freq_cat	1	156	2.17	0.1428
load_rms_cat	1	156	4.76	0.0306
load_freq*load_rms_c	1	156	0.01	0.9323
load_dur_cat	1	156	0.00	0.9945
load_freq*load_dur_c	1	156	0.08	0.7720
load_rms_*load_dur_c	1	156	8.62	0.0038

Table Legend:
load_freq_cat = Frequency
load_rms_cat = Amplitude
load_dur_cat = Duration
load_freq*load_rms_c = Frequency * amplitude
load_freq*load_dur_c = Frequency * duration
load_rms*load_dur_c = Amplitude * duration

There was a statistically significant difference (p <0.05) in mean Collagen II responses between load rms level 0 (<0.4g) and level 1 (>0.4g) (Figure 34). The analysis showed a statistically significant (p <0.05) difference in mean responses between levels load rms = 0 (<0.4g) load duration =1 (>10min) and load rms =1 (>0.4g) load duration=0 (<10min). The analysis showed a statistically significant (p-value <0.05) difference in mean responses between levels load rms = 0 (<0.4g) load duration =1 (>10min) and load rms =1 (>0.4g) load duration=1 (>10min). Collagen II response was a maximum (estimate =1.68) when load rms=0 (<0.4g) and load duration=1 (>10min).

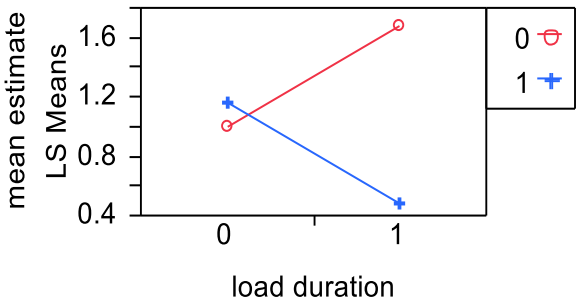

Figure 34: Interaction plot of load duration (x-axis; 0 <10min; 1 >10min) and load rms amplitude (red = 0 <0.4g; blue = 1 >0.4gS) for Collagen II.

5.2.3 Aggrecan

The main effects of Aggrecan expression due to frequency (load_freq_cat), duration (load_dur_cat), and the interaction between frequency and duration were all found to be statistically significant (p <0.05) (Table 12). No other effects were found to be statistically significant.

Table 12: Fixed main effects and interactions for Aggrecan.

Type 3 Tests of Fixed Effects				
Effect	Num DF	Den DF	F Value	Pr > F
load_freq_cat	1	157	9.63	0.0023
load_rms_cat	1	157	1.86	0.1743
load_freq*load_rms_c	1	157	0.03	0.8729
load_dur_cat	1	157	8.75	0.0036
load_freq*load_dur_c	1	157	11.94	0.0007
load_rms_*load_dur_c	1	157	2.13	0.1467

Table Legend:
load_freq_cat = Frequency
load_rms_cat = Amplitude
load_dur_cat = Duration
load_freq*load_rms_c = Frequency * amplitude
load_freq*load_dur_c = Frequency * duration
load_rms*load_dur_c = Amplitude * duration

No conclusion can be drawn about the main effects frequency and duration on their own since there is a significant interaction between them. The analysis showed a statistically significant ($p < 0.05$) difference in mean responses between levels load freq = 0 (<50 Hz) load duration =0 (<10 min) and load freq =0 (<50 Hz) load duration=1 (>10 min) (Figure 35). The analysis showed a statistically significant ($p < 0.05$) difference in mean Aggrecan responses between levels load freq = 0 (< 50Hz) load duration = 1 (>10 min) and load freq = 1 (>50 Hz) load duration = 0 (< 10min). The analysis showed a statistically significant (p-value <0.05) difference in mean responses between levels load freq = 0 (<50Hz) load duration = 1 (>10 min) and load freq = 1 (>50 Hz) load duration = 1 (>10 min). The response was a maximum (estimate =1.45) when load freq=0 (<50 Hz) and load duration=1 (>10 min).

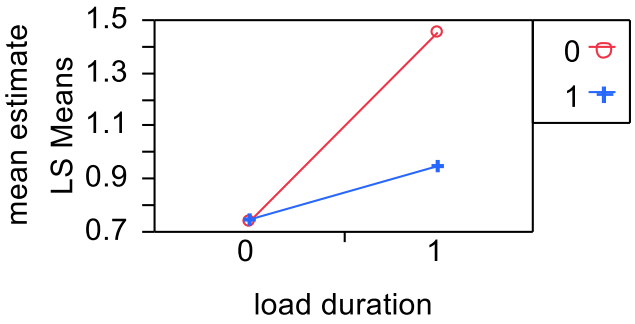

Figure 35: Interaction plot of load duration (x-axis; 0 < 10min; 1 >10min) and load frequency (red = 0 <50Hz; blue = 1 >50Hz) for Aggrecan.

5.2.4 Biglycan

The interaction between frequency (load_freq_cat) and amplitude (load_rms_cat) was found to be statistically significant ($p < 0.05$) (Table 13). No other effects were found to be statistically significant.

Table 13: Fixed main effects and interactions for Biglycan.

Type 3 Tests of Fixed Effects				
Effect	**Num DF**	**Den DF**	**F Value**	**Pr > F**
load_freq_cat	1	156	2.57	0.1110
load_rms_cat	1	156	0.00	0.9600
load_freq*load_rms_c	1	156	5.82	0.0170
load_dur_cat	1	156	0.42	0.5200
load_freq*load_dur_c	1	156	2.95	0.0879
load_rms_*load_dur_c	1	156	2.86	0.0929

Table Legend:
load_freq_cat = Frequency
load_rms_cat = Amplitude
load_dur_cat = Duration
load_freq*load_rms_c = Frequency * amplitude
load_freq*load_dur_c = Frequency * duration
load_rms*load_dur_c = Amplitude * duration

No conclusion can be drawn about any main effects on their own since there is a significant interaction between frequency and amplitude. The analysis showed a statistically

significant ($p < 0.05$) difference in mean responses between levels load freq = 1 (>50 Hz) load rms =0 (<0.4 g) and load freq =0 (<50 Hz) load rms=1 (>0.4g) (Figure 36). The response was a maximum (estimate =1.08) when load duration=0 (<10 min) and load rms=1 (>0.4 g).

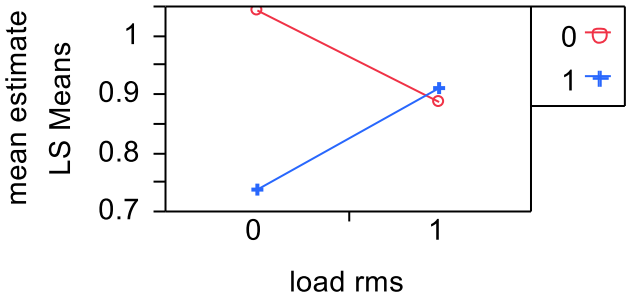

Figure 36: Interaction plot of load rms (x-axis; 0 <0.4g; 1 >0.4g) and load frequency (red = 0 <50Hz; blue = 1 >50Hz) for Biglycan.

5.2.5 Versican

No main effects or interactions were found to be statistically significant at the alpha=0.05 level of significance for Versican (Table 14). The response was a maximum (estimate =1.61) when load duration=0 (<10min) and load frequency =1 (>50Hz).

Table 14: Fixed main effects and interactions for Versican.

Type 3 Tests of Fixed Effects				
Effect	**Num DF**	**Den DF**	**F Value**	**Pr > F**
load_freq_cat	1	157	0.01	0.9139
load_rms_cat	1	157	0.35	0.5530
load_freq*load_rms_c	1	157	0.97	0.3270
load_dur_cat	1	157	1.41	0.2370
load_freq*load_dur_c	1	157	0.29	0.5903
load_rms_*load_dur_c	1	157	0.03	0.8653

Table Legend:
load_freq_cat = Frequency
load_rms_cat = Amplitude
load_dur_cat = Duration
load_freq*load_rms_c = Frequency * amplitude
load_freq*load_dur_c = Frequency * duration
load_rms*load_dur_c = Amplitude * duration

5.2.6 Decorin

No main effects or interactions were found to be statistically significant at the alpha=0.05 level of significance for Decorin (Table 15). The response was a maximum (estimate =1.47) when load rms=1 (>0.4g) and load frequency =1 (>50Hz).

Table 15: Fixed main effects and interactions for Decorin.

Type 3 Tests of Fixed Effects				
Effect	**Num DF**	**Den DF**	**F Value**	**Pr > F**
load_freq_cat	1	157	0.02	0.8946
load_rms_cat	1	157	1.19	0.2772
load_freq*load_rms_c	1	157	3.51	0.0629
load_dur_cat	1	157	1.24	0.2663
load_freq*load_dur_c	1	157	0.06	0.8062
load_rms_*load_dur_c	1	157	0.74	0.3907

Table Legend:
load_freq_cat = Frequency
load_rms_cat = Amplitude
load_dur_cat = Duration
load_freq*load_rms_c = Frequency * amplitude
load_freq*load_dur_c = Frequency * duration
load_rms*load_dur_c = Amplitude * duration

5.2.7 Discussion

Data were pooled across all experiments (KKT_v1, Prototype, KKT_v2, and Bioreactor); in order to see the effects of the animals that were used in the various experiments and to identify what level of each parameter (frequency, load, and duration) would cause the greatest increase of gene expression for each gene in the assay. Below, Table 16 shows a summary of the significant ($p < 0.05$) main effects, interactions, and maximum response parameters for each gene when data from all experiments were pooled and the effects of the various animals used in the experiments were removed.

Table 16 Summary of significant (p<0.05) Main Effects, Interactions, and maximum response parameters for each genes mRNA.

Outcome	Collagen I	Collagen II	Aggrecan	Biglycan	Versican	Decorin
Main Effect	Amp	Amp	Freq and Dur	-	-	-
Interaction	Amp * Dur	Amp * Dur	Freq * Dur	Freq * Amp	-	-
Max Response	>10 min + <0.4 g	>10 min + <0.4 g	>10 min + <50 Hz	<50 Hz + <0.4 g	Any Treatment Level	Any Treatment Level

Amp = Amplitude
Dur = Duration
Freq = Frequency

The table above shows a complex array of conditions and interactions necessary to cause up-regulation of specific genes. As with the modified intervention (KKT_v2) where two windows of vibration loading patterns were required to increase desired gene response across a chosen gene assay, one may pick a gene of interest from the table above and "tune" their loading pattern to up-regulate its response.

5.3 Summary of Completed Research

The first experiment, a clinical study using the Khan Kinetic Treatment (KKT_v1) vibration, corrected 62 percent of abnormal cervical Mean Axis of Rotations (MAR) with significantly larger MAR vector magnitude differences [pre-post] at the C5-C6 level than shams and MAR correction was significantly related to improving pain across all subjects (G.T. Desmoulin, Hunter, et al., 2012; G.T. Desmoulin, Szostek, et al., 2012).

The second experiment and first objective of this dissertation (**Objective 1**) looked primarily at evaluating version 1 of a spine vibration treatment (KKT_v1) as it pertained to imparted mechanics to the vertebrae and the biological effects on cells of the disc. While initial

vibration protocols used by KKT_v1 could effectively replace abnormal pivot points back to normal, as discussed in the first paragraph, the cells in the discs were unaffected in the original device (KKT_v1). Since disc health plays a significant role in MAR normality and chronic pain, long-term changes may not occur unless disc health is addressed. Hence, other experiments (**Objective 2**) identified the optimal vibration patterns (load, frequency, and duration) to increase relative expression in genes that produce proteins responsible for disc health. Implementing these optimal vibration patterns into a modified KKT device (KKT_v2) (**Objective 3**) was able to describe the imparted mechanics. This was presented by detailing disc tissue strain in 3D and notes the changes from passive effects of the original vibration pattern (KKT_v1) to one that stimulates gene expression in the modified device (KKT_v2). Hence, the design of the bioreactor (**Objective 4**) ensured the ability to load tissue with a wide variety of parameter magnitudes while mimicking in-vivo conditions. After validating the parameters, the new device was then used to confirm the results achieved with the previous experiments.

Comparing the experiments from Chapters 3 (complex shear loading) and 4 (constrained axial loading), loading orientation effects could be assessed. Controlled constrained axial vibration had similar positive gene expression response as unconstrained shear vibration or complex shear. Table 17 below describes the direct comparison between the load condition and gene expression to assess the load orientation affects on gene expression. Five of six genes had comparable responses to completely different loading orientations, and one gene--while significantly up regulated in constrained axial loading--was not significantly affected in complex shear loading.

This result is not surprising, since the cells of the nucleus are oriented in a random omni-directional way both in-vivo and in-situ as tested in this dissertation. Further, pressure is the

force per unit area acting in a fluid, and is typically the same as measured in different directions and locations because fluids deform to equalize the pressure despite the direction of the applied load. This phenomenon is found to be in-part true in the nucleus pulposus of normal intervertebral discs (A. L. Nachemson, 1960), as tested in this dissertation. Hence, the changing mechanical environment when the tissue is loaded should affect each cell similarly despite the orientation of the load direction. However, in the constrained axial experiment there was a tare load of 40 N that was not present in the complex shear experiments. Since the nucleus pulposus does not act purely like a fluid and is also capable of stress gradients typical of solids (Skrzypiec et al., 2007), loading orientation may affect specific cells or genes differently. Further, as discussed in chapter 2, decorin is involved in the organization of collagen fibrils leading to increased tensile strength of the tissue (Gotz et al., 1997). Hence, decorin mRNA expression may have been more sensitive to the tare load that was experienced in the constrained axial load experiments.

Table 17 Load condition vs gene expression.

	Gene Expression					
Load Condition	**Collagen I**	**Collagen II**	**Aggrecan**	**Byglycan**	**Versican**	**Decorin**
Complex Shear	ns	ns	s/up	ns	s/up	ns
Constrained Axial	ns	ns	s/up	ns	s/up	s/up

s = significant compared to control
ns = non-significant compared to control
up = upregulated

Further, to reiterate from chapter 2 it is important to understand that the expression of mRNA does correlate to protein expression (Guo et al., 2008). When specifically looking at genes responsible for extracellular regions of tissues similar to the ones used in this study, Guo et

al., 2008 found that mRNA accounted for a significant portion (41%) of the protein expression variance ($r=0.643$; $p<0.0001$). Hence, while relying on mRNA expression to predict protein expression is not perfect it could be considered reliable and valid in this case.

Other meaningful questions that have yet to be answered are "What happens to the disc if the proteins are up-regulated?", "How would that affect long-term disc health?", and "How often would the vibration intervention needs to be applied to maintain the effect?".

The hypothesis is that increasing gene expression would also increase the amount of protein present and would help "restore" tissue integrity as various other, more invasive, approaches have achieved. For example, tissue-engineering strategies of rescuing native disc cells, and repopulating the disc with cells in order to increase matrix synthesis; stem cells isolated from bone marrow offer an obtainable cell population with the capacity to generate disc matrix (Kalson, Richardson, & Hoyland, 2008). Experiments such as western blot analysis are required to test this hypothesis.

The effect of increasing disc matrix and proteoglycans of the disc is believed to be two folds. One is that the altered mechanical behavior of the disc, discussed in chapter 2, when proteoglycans are reduced will be restored. The second is that increased proteoglycans will inhibit neural and vascular disc ingrowth that is typically associated with back pain at a specific spinal level, also discussed in chapter 2. More complex experiments would be required to test this hypothesis. Perhaps an animal injury model, demonstrating altered mechanics and biology, ends with short term improvement with continued vibration intervention.

The remaining question is "How often would the vibration intervention need to be applied to maintain the effect?". Similar to neural adaptation effects, such as adapting to constant stimuli, it is believed that the intervention would be required often (2-3 week or more),

over a longer period of time (1-3 yrs), and may require additional "tuning" in order to continue the response. Although it is too soon to even speculate this would require a long-term human study in-vivo. Hence, MRI or another suitable imaging source would be required along with advanced analysis techniques in order to detect any proteoglycan changes in the disc itself; although symptom and functional changes could be tracked relatively easily via questionaries' and clinician tests.

5.4 Novel Outcomes of Dissertation

Scientific journal articles are published based in part on their novel outcomes. Detailing the conclusions of the resulting published articles of this dissertation will assist in summarizing its novel outcomes.

The first step was to publish preliminary data and literature surveys. The preliminary data showed that the interventions` effect could be significant and the literature surveys detailed information critical to further developing the novel vibration-based spinal intervention. This was achieved with a total of three publications, G. Desmoulin & Khan, 2007, G. T. Desmoulin et al., 2007, and Hill, Desmoulin, & Hunter, 2009. The first of two preliminary data manuscripts cited above compared a control group with a KKT_v1 treatment group, significant decreases in neck pain and decreased pain medication use were found. There were, however, no changes in functional measures. Limitations of this first preliminary data study included a) not having sham controls or b) blinding patients/clinicians to experimental groups. The second of the two preliminary data manuscripts included sham controls with significantly improved clinical outcomes.

The literature survey publication detailed the theory behind the success of the treatment and where improvements could be made. The important of stylus control is discussed as the force impulse (force x time characteristic) delivered to the spine relates highly to vertebral motion and associated reflex activity and how treatment might change for patients with hypomobile joints (adjustment) or hypermobile joints (strength exercises). The literature survey also discusses the interventions mechanisms of pain relief, like vibration analgesia and the gate theory of pain. Further, mechanisms of muscle relaxation with vibration are explored as gamma motor units, controlling muscle length, may reduce their input with application effectively lengthening the muscle and finally cellular biosynthesis potential was discussed. Since over 40% of the patients seen in KKT International Clinics have some form of disc degeneration associated with their pain, the mechanism most desired to be developed was the non-invasive ability to restore disc tissue.

Degeneration is known to cause many changes in the disc. As discussed in chapter 2 nucleus pulposus (NP) tissue changes include increased breakdown of matrix and altered matrix synthesis, specifically, increases in type I collagen synthesis and decreased synthesis of aggrecan (M. Adams & P. Roughley, 2006; W. Johnson & Roberts, 2007; Le Maitre, Pockert, et al., 2007). As the amount of aggrecan and swelling pressure of the NP fall, loss of disc height altars joint loading patterns eventually leading to microtrauma and pain.

Consequently, a series of gene expression experiments designed to assess vibrations ability to stimulate up regulation of genes important in maintaining disc health were conducted. Initial experiment results showed that the vibration-based intervention in its original form (KKT_v1) did not influence gene expression. It was thought that the intervention needed to

change its mechanical vibration pattern in order to suit the appropriate stimulus for the genes of interest.

The second gene expression experiment utilized a prototype bioreactor that was capable of 0-200 Hz frequencies, 0-2 g amplitudes and 0-60 min durations. This experiment allowed testing of a wide variety of vibration loading patterns. Maximum gene expression was determined in order to identify the optimal parameters for a potential non-invasive therapy. Results showed that axial free vibration of disc influences expression of mRNA for biglycan, collagen type I, collagen type II, decorin, and versican in bovine nucleus pulposi (G. T. Desmoulin et al., 2010). Vibration amplitude had the most substantial effect on disc gene expression (G. T. Desmoulin et al., 2010) and vibration within the ranges tested had no detectable effect on cellular apoptosis rates (G. T. Desmoulin et al., 2010, 2011).

Once the optimal vibration parameters for maximizing gene expression had been identified, it was possible to modify the current intervention's firmware to include the "ideal" vibration patterns and retest with a third gene expression experiment. Using KKT_v2 with optimal vibration patterns, found in earlier experiments, gene expression and imparted mechanics were determined (G. T. Desmoulin et al., 2011). KKT_v2 with the optimal vibration pattern caused aggrecan, collagen type I, and versican (genes largely responsible for disc health) of the bovine nucleus pulposus to be up regulated (G. T. Desmoulin, Hunter, et al., 2012; G. T. Desmoulin et al., 2011). Further, genes of proteins normally found in low concentration in the nucleus pulposus such as collagen type I were not significantly influenced by the modified KKT vibration (KKT_v2) (G. T. Desmoulin et al., 2011). In combination these findings suggest a disc regenerative effect of the modified KKT vibration treatment (KKT_v2) (G. T. Desmoulin, Hunter, et al., 2012; G. T. Desmoulin et al., 2011).

In summary of the above, KKT vibration intervention (KKT_v1) was modified (KKT_v2) based on basic research and could now be used on patients with degenerative disc disease and discogenic back pain (G. T. Desmoulin, Hunter, et al., 2012; G. T. Desmoulin et al., 2011).

Since "tuning" mechanical vibrations to stimulate specific genes was shown to be past the proof of concept stage via previous experiments it was thought that other tissues of the vertebrae-disc system such as endplates, vertebral bodies, or even ligaments could also be "tuned". Resulting in a novel bioreactor to be developed in the latter portion of this dissertation and was found to be more efficient at loading tissues due to its multi-unit platform approach (G. T. Desmoulin et al., 2013). Its controlled constrained axial vibration has similar positive gene expression responses as unconstrained axial and complex shear vibration demonstrating its validity and potential use for other tissues (G. T. Desmoulin et al., 2013). Further, the novel bioreactor more accurately mimicks in-vivo conditions by circulating cell culture medium (0.05 L/min). Fluid dynamics modeling results also show minimal stagnation locations (G. T. Desmoulin et al., 2013).

As discussed previously loading orientation effects could be generally assessed. Controlled constrained axial vibration had similar positive gene expression responses as unconstrained shear vibration or complex shear. This result was expected, since the cells of the nucleus are oriented in a random omni-directional way and fluids deform to equalize the pressure despite the direction of the applied load. This phenomenon is found to be in-part true in the nucleus pulposus of normal intervertebral discs (A. L. Nachemson, 1960). Hence, despite the load orientation each cell should be affected similarly. However, the nucleus pulposus does not act purely like a fluid and is also capable of stress gradients typical of solids (Skrzypiec et al.,

2007), therefore load orientation may affect specific cells or genes differently as one of the six genes was not the same between load orientation conditions.

The dissertation covers detailed information from literature review to proof of concept stages and the development of a novel bioreactor that could be used for additional experiments. However, the most beneficial portions of this thesis detail that a non-invasive vibrational-based therapy for disc tissue is on the horizon and currently being tested in clinics. The goal now is to see what proteins actually do change with the intervention and to show results, if any, in human tissue. Although it may be too soon to speculate in humans it would require a long-term in-vivo study. Hence, MRI would be required along with advanced image analysis techniques to detect any proteoglycan changes in the disc itself.

5.5 Limitations and Assumptions

There are several limitations and assumptions of the research performed in this dissertation. First and foremost is that bovine disc tissue was used ex-vivo in place of human disc tissue in vivo. As discussed in previous chapters, while bovine disc tissue is considered the best model to perform these types of experiments, there remain limitations to the conclusions that can be made: a) despite being bovine in nature the discs were healthy to begin with and may behave differently than what was presented here under various stages of disc degeneration as the number of viable cells are comparatively higher in healthy tissue; b) bovine discs have some remnant notochord cells, which regulate proteoglycan production, and therefore may have influenced the nature of the responses; c) all experiments were ex-vivo although in-vivo conditions were mimicked; d) there is both a physical size and anatomical difference between the bovine tail segments used and what would be applied to humans so pure mechanics differences exist,

specifically, dynamic responses of the system and the systems boundary conditions. Dynamic responses would change due to the greater mass and additional tissues (adding damping and stiffness) of the human system with respect to the bovine segments chosen for these experiments. Boundary conditions would also be different since the bovine segments were fixed on end while the human cervical spine is attached to a large mass (head and torso) at either end. While the head and shoulder of the patient are at rest on the treatment bed they are not fixed and hence would present a different boundary conditions for the cervical spine during vibration loading; e) as discussed in chapter 2, transmissibility is the ratio of energy output of the system to the input energy. The transmissibility model in chapter 2 showed that the energy output is greatest at the systems natural frequency. Since the natural frequency of the human system would be different than the natural frequency of the bovine segments it is likely the amount of energy transmitted to human discs would also be different further this was not a parameter in the data collection; f) on this note its likely that different sized patients would also have various responses to the vibration as the amount of energy that actually reaches the discs in-vivo would vary; g) since the hypothesis is based on stimulating healthy cells to produce more protein for long-term disc health, its likely that discs with more healthy cells such as those in younger or non-degenerated discs would respond more favorably to vibration; h) The up-regulation of gene expression does not necessarily mean that additional protein is being produced. While correlation studies have determined that mRNA levels generally correlate to protein expression levels (Guo et al., 2008), this has not been confirmed specifically for the nucleus pulposus of either bovine or human disc tissue. However, structural tissue genes of different areas of the body were the most correlated to protein expression and therefore it reasons that it would be likely in this case although it was not confirmed; i) All experimental time frames were short-term. Only single treatment time periods

were tested. This is not indicative of the intervention treatment sessions that typically occur 2-3 times per week over 6-8 weeks with human patients in the clinic. If possible, it is likely that any disc change in human would occur over at least the entire treatment period and most likely could not be detected via MRI unless long-term treatment was maintained over years. However, human in-vivo detection of disc changes should remain the ultimate goal of this research. Objectives and a study design for such an investigation could be coupled with other assessments and is summarized in the following section on "Future Work".

In chapter 4 the device grip used to fix the tissue sample was difficult to work with in general and made consistent initial compression laborious. It would be desirable in any future experiments to redesign the grippers. Further, when publishing the results of chapter 4 it was argued by one reviewer that force feedback should have been utilized in place of displacement control. This would have the advantage of knowing the tare load prior to and during vibration but would lack the amount of disc strain and it's likely that as the disc compressed over time the force, while kept the same, would have decreasing influence over the disc tissue strain which may alter results. In a perfect world displacement control or force control with accompanied monitoring to the other variable would be best to characterize imparted mechanics that effect disc cells most greatly. Finally, having all four bioreactor cells sharing medium may have caused cross contamination. While test conditions were the same in each cell during a run the location of each sample should have been recorded. Since the cross contamination issue could, at least in part, be accounted for by including location as a random variable in a blocked ANOVA during analysis.

In chapter 5 the new analysis does shed additional light on the vibration parameters necessary to maximize expression of each gene in the assay. However, since discrete

measurement resolution was somewhat low it was not possible to obtain interactions or determine parameters using mathematical methods (maximums and minimums). So, results were collated into 2 groups each (high and low) so that interactions and parameter combinations to stimulate maximum gene response could be determined albeit lower resolution.

Overall the experiments only looked at NP tissue as pilot studies showed that AF tissue did not respond as readily to vibration. However, both AF and endplate tissue are clearly involved in disc degeneration and so AF samples have been stored for future analysis if need be. Further, other tissues including ligaments, tendons, and muscles may also be involved in discogenic back pain but were not analyzed in this dissertation.

5.6 Future Work

The goal of future research should work toward validating the hypothesis of non-invasive tissue regeneration. This may consist of additional basic research experiments at the tissue level that confirm changes in protein levels via western blot techniques. However, this may also consist of in-vivo human trials utilizing magnetic resonance imaging to detect changes in proteoglycan levels of the disc with continued treatment with the modified KKT device (KKT_v2). This is feasible since KKT has already been cleared for the frequencies, loads, and amplitudes found to maximize expression of desirable genes. Objectives and a study design for such an investigation could be coupled with other assessments and might look like this:

Proposed Objectives

The first objective of this study would be to show that long-term regular vibrational based treatment over the period of 2 yrs could effectively maintain the normality of cervical spinal pivot points found to be abnormal at the beginning of the study when compared to a gold

standard treatment and pain medication. The hypothesis of this objective would be based on previous research and state that the majority of the treatment group (~60%) would maintain cervical spinal pivot points throughout the treatment period (2-3 treatments per week for up to 2yrs) and would be greater than the gold standard treatment.

The second objective of the proposed study would be to show long-term regular vibration based treatment over the period of 2 yrs can result in decreased pain, decreased disability, and increased quality of life when compared to a gold standard treatment and pain medication. The hypothesis of this objective would be that the vibration based treatment group would improve symptoms over that of the gold standard treatment. The basis for these hypotheses are based on short-term clinical studies with similar outcomes using the vibration based treatment.

The third and main objective of the proposed study would be to be able to detect changes in the state of intervertebral disc degeneration through periodic quantitative MRI while undergoing long-term KKT treatment when compared to a gold standard treatment and pain medication. The basis for this hypothesis is the experiments performed in this dissertation that identified a specific vibration loading pattern capable of up regulating mRNA expression in genes responsible for producing proteins that support disc extracellular matrix.

Proposed Study Design

This proposed study would be a longitudinal comparative study investigating the ability of the vibration based treatment to cause long-term changes in spinal joint pivot points, patient outcome in self-reported levels of spine related pain, a disability index, and quality of life and changes to the state of intervertebral disc degeneration. The design could only be single blinded, but would be comparative, and randomly assigned longitudinal study of the vibration and a gold standard and pain medication. All subjects signing the consent form would first be matched on

sex, age, and diagnosis. We would then randomly split the matched pairs into two groups ("vibration based treatment" and "gold standard"). Then all subjects would undergo treatment and data collection once prior to treatment and once every 6 months for the duration of two years after treatment initiation.

In addition to the proposed study above, additional basic research should utilize the new research device developed in Chapter 4 of this dissertation to test the ability of specific loading patterns that affect the metabolism of other load bearing tissues of the spine such as ligaments. In doing so potential therapeutic responses can be devised to specifically target the affected tissue. Justification, Aims, and Objectives of a study for such an investigation might look like this:

Justification

The project would aim to implement sustained mechanical vibration, known to increase specific gene expression in intervertebral disc (IVD) tissue, to ligament tissues to determine whether similar mechano-biology exists. The application of free axial vibration has already been shown to positively affect target messenger RNA in the nucleus pulposi of bovine IVDs via this dissertation. However, the effect of vibration on surrounding ligament tissue in the neck and spine remains unknown. Exploring the resulting mechano-biology in ligament tissue is the next logical step in understanding the full effect of vibration on soft tissues in the neck and spine.

Proposed Aim 1: To design, build, and test custom tissue grips that can effectively transmit vibration forces from the loading platform of chapter 4 to ligament tissue.

Proposed Aim 2: To determine whether the positive expression of target mRNA observed in IVDs after specific sustained vibrations, also exists in ligament tissue under similarly "tuned" loading conditions.

Proposed Future Tasks

Ligament Grip Design: The existing multi-unit vibration-loading platform detailed in chapter 4 would be modified to transmit mechanical vibrations to ligament tissue. The modifications would be modular tissue grips that would be designed and fabricated over the course of this proposed project.

RT-PCR Analysis: Using the vibration-loading platform with modified tissue grips, vibrations would be applied to isolated rabbit knee ligaments over a range of amplitudes, frequencies, and durations. To measure the resulting biosynthesis, the mRNA expression of aggrecan, biglycan, collagen type I, collagen type II, decorin, and versican would be measured using Real Time – Polymerase Chain Reaction (RT_PCR). The normalized expression of these genes (relative to GAPDH, a 'housekeeping' gene) would be compared between treatment and control groups.

5.6.1 Future Work Summary

While the two above-proposed experiments would require much more detail they do provide the basic framework of the overall goal of future research determining if non-invasive tissue regeneration is possible. This may consist of additional basic research experiments at the tissue level that confirm changes in protein levels via western blot techniques however; it will

ultimately require in-vivo human data to be achieved. This is feasible since the vibration-based treatment (KKT) highlighted in this dissertation has already been cleared for a wide range of frequencies, loads, and amplitudes.

REFERENCES

Adams, M., Dolan, A., & WC., H. (1986). The stages of disc degeneration as revealed by discogram. *J. Bone Joint Surg. [Br.], 68*, r36-41.

Adams, M., & Dolan, P. (2005). Spine biomechanics. *J Biomech, 38*, 1972–1983.

Adams, M., Freeman, B., Morrison, H., Nelson, I., & Dolan, P. (2000). Mechanical initiation of intervertebral disc degeneration. *Spine, 25*, 1625-1636.

Adams, M., Pollintine, P., Tobias, J., Wakley, G., & Dolan, P. (2006). Intervertebral disc degeneration can predispose to anterior vertebral fractures in the thoracolumbar spine. *J Bone Miner Res 21*, 1409–1416.

Adams, M., & Roughley, P. (2006). What is intervertebral disc degeneration, and what causes it? *Spine, 31*, 2151-2161.

Adams, M. A., Freeman, B. J., Morrison, H. P., Nelson, I. W., & Dolan, P. (2000). Mechanical initiation of intervertebral disc degeneration. *Spine, 25*, 1625–1636.

Adams, M. A., & Hutton, W. C. (1981). The effect of posture on the strength of the lumbar spine. *Engineering in Medicine, 10*(4), 199-202.

Adams, M. A., & Hutton, W. C. (1981). The relevance of torsion to the mechanical derangement of the lumbar spine. [Research Support, Non-U.S. Gov't]. *Spine (Phila Pa 1976), 6*(3), 241-248.

Adams, M. A., & Roughley, P. J. (2006). What is intervertebral disc degeneration, and what causes it? . *Spine, 31*, 2151–2161.

Adams, P., Eyre, D., & Muir, H. (1977). Biochemical aspects of development and aging of human lumbar intervertebral discs. *Rheum. Rehabil., 16*, 22-29.

Alem, N. (2005). Application of the new ISO 2631-5 to health hazard assessment of repeated shocks in U.S. Army vehicles. *Ind Health, 43*, 403-412.

Amevo, B., Worth, D., & Bogduk, N. (1991). Instantaneous axes of rotation of the typical cervical motion segments: a study in normal volunteers. *Clin Biomech, 6*, 111-117.

Anderson, D., Izzo, M., & Hall, D. (2002). Comparative gene expression profiling of normal and degenerative discs: analysis of a rabbit annular laceration model. *Spine, 27*, 1291–1296.

Aoki, Y., Akeda, K., An, H., Muehleman, C., Takahashi, K., Moriya, H., & Masuda, K. (2006). Nerve fiber ingrowth into scar tissue formed following nucleus pulposus extrusion in the rabbit anular-puncture disc degeneration model: effects of depth of puncture. *Spine (Phila Pa 1976), 31*(21), E774-780. doi: 10.1097/01.brs.0000238681.71537.41 [doi]

00007632-200610010-00022 [pii]

Aoki, Y., Ohtori, S., Ino, H., Douya, H., Ozawa, T., Saito, T., . . . Takahashi, K. (2004). Disc inflammation potentially promotes axonal regeneration of dorsal root ganglion neurons innervating lumbar intervertebral disc in rats. *Spine (Phila Pa 1976), 29*(23), 2621-2626. doi: 00007632-200412010-00005 [pii]

Aoki, Y., Ohtori, S., Takahashi, K., Ino, H., Takahashi, Y., Chiba, T., & Moriya, H. (2004). Innervation of the lumbar intervertebral disc by nerve growth factor-dependent neurons related to inflammatory pain. *Spine (Phila Pa 1976), 29*(10), 1077-1081. doi: 00007632-200405150-00005 [pii]

Aoki, Y., Takahashi, Y., Takahashi, K., Chiba, T., Kurokawa, M., Ozawa, T., & Moriya, H. (2004). Sensory innervation of the lateral portion of the lumbar intervertebral disc in rats. *Spine J, 4*(3), 275-280. doi: 10.1016/j.spinee.2003.10.005 [doi]

S1529943003005540 [pii]

Armstrong, J. (Ed.). (1958). *Lumbar Disc Lesions*. Edinburgh E.S. Livingstone Limited.

Arnau, J., Vallano, A., Lopez, A., Pellise, F., Delgado, M., & Prat, N. (2006). A critical review of guidelines for low back pain treatment. *Eur Spine J, 15*(5), 543-553.

Assendelft, W., Morton, S., Yu, E., Suttorp, M., & Shekelle, P. (2003). Spinal manipulative therapy for low back pain. A meta-analysis of effectiveness relative to other therapies. *Ann Intern Med, 138*, 871-881.

Baranto, A., Hellstrom, M., & Sward, L. Acute Injury of an Intervertebral Disc in an Elite Tennis Player: A Case Report. *Spine (Phila Pa 1976)*. doi: 10.1097/BRS.0b013e3181bf12b5 [doi]

Barrick, W., Schofferman, J., & Reynolds, J. (2000). Anterior lumbar fusion improves discogenic pain at levels of prior posterolateral fusion. *Spine, 25*, 853-857.

Battie´, M., Videman, T., Levalahti, E., Gill, K., & Kaprio, J. (2007). Heritability of low back pain and the role of disc degeneration. *Pain, 131*, 272-280.

Benjamin, M., & Ralphs, J. R. (2004). Biology of fibrocartilage cells. *Int Rev Cytol, 233*, 1-45. doi: 10.1016/S0074-7696(04)33001-9 [doi]

S0074769604330019 [pii]

Bishop, B. (1980). Pain: its physiology and rationale for management. Part III. Consequences of current concepts of pain mechanisms related to pain management. *Phys Ther, 60*, 24-37.

Bogduk, N., Amevo, B., & Pearcy, M. (1995). A biological basis for instantaneous centres of rotation of the vertebral column. *Proc Inst Mech Eng [H], 209*(3), 177-183.

Bogduk, N., & Mercer, S. (2000). Biomechanics of the cervical spine. I: Normal kinematics. *Clin Biomech (Bristol, Avon), 15*(9), 633-648. doi: S0268-0033(00)00034-6 [pii]

Brinckmann, P. (1986). Injury of the annulus fibrosus and disc protrusions. An in-vitro investigation on human lumbar discs. *Spine, 11*, 149-153.

Brinckmann, P., & Horst, M. (1985). The influence of vertebral body fracture, intradiscal injection, and partial discectomy on the radial bulge and height of human lumbar discs. *Spine, 10*, 138-145.

Brisby, H. (2006). Pathology and possible mechanisms of nervous system response to disc degeneration. *J Bone Joint Surg Am, 88(Suppl. 2)*, 68-71.

Brown, K., Pollintine, P., & Adams, M. (2008). Biomechanical implications of degenerative joint disease in the apophyseal joints of human thoracic and lumbar vertebrae. *Am J Phys Anthropol, 136*, 318–326.

Chen J, Y. W., Setton LA. . (2004). Static compression induces zonal-specific changes in gene expression for extracellular matrix and cytoskeletal proteins in intervertebral disc cells in vitro. *Matrix Biol, 22*, 573-583.

Cherkin, D., Eisenberg, D., Sherman, K., Barlow, W., Kaptchuk, T., Street, J., & Deyo, R. (2001). Randomized trial comparing traditional Chinese medical acupuncture, therapeutic massage, and self-care education for chronic low back pain. *Arch Intern Med 161*, 1081-1088.

Cheung, J. T. M., Zhang, M., & Chow, D. H. K. (2003). Biomechanical responses of the intervertebral joints to static and vibrational loading: a finite element study. *Clinical Biomechanics, 18*, 790-799.

Cobb, C., deVries, H., Urban, R., Luekens, C., & Bagg, R. (1945). Electrical activity in muscle pain *Am J Phys Med Rehabil, 54*, 80-87.

Coermann, R. R. (1962). The mechanical impedance of the human body in sitting and standing position at low frequencies. *Human Factors, 4*, 227-253.

Cong, L., Pang, H., Xuan, D., & Tu, G. The interaction between aggrecan gene VNTR polymorphism and cigarette smoking in predicting incident symptomatic intervertebral disc degeneration. *Connect Tissue Res*. doi: 10.3109/03008200903564455 [doi]

Costi, J. J., Stokes, I. A., Gardner-Morse, M., Laible, J. P., Scoffone, H. M., & Iatridis, J. C. (2007). Direct measurement of intervertebral disc maximum shear strain in six degrees of freedom: motions

that place disc tissue at risk of injury. [Research Support, N.I.H., Extramural]. *J Biomech, 40*(11), 2457-2466. doi: 10.1016/j.jbiomech.2006.11.006

Cs-Szabo, G., Ragasa-San Juan, D., Turumella, V., Masuda, K., & Thonar, E. J. (2002). Changes in mRNA and protein levels of proteoglycans of the anulus fibrosus and nucleus pulposus during intervertebral disc degeneration. *Spine, 27*(20), 2212-2219.

Demers, C. N., Antoniou, J., & Mwale, F. (2004). Value and limitations of using the bovine tail as a model for the human lumbar spine. . *Spine (Phila Pa 1976), 29*, 2793-2799.

Derby, R., Lettice, J., Kula, T., Lee, S., Seo, K., & Kim, B. (2005). Single-level lumbar fusion in chronic discogenic low-back pain: psychological and emotional status as a predictor of outcome measured using the 36-item Short Form. *J Neurosurg Spine, 3*, 255-261.

Desmoulin, G., & Khan, A. (2007). Spinal Mechanisms of Chronic Pain. *AJPM, 17*, 27-43.

Desmoulin, G. T., Enns-Bray, W. S., Hewitt, C. R., & Hunter, C. J. (2013). Multi-unit sustained vibration loading platform for biological tissues: design, validation and experimentation. *Journal of Biomechanics, 46*(1), 116-121.

Desmoulin, G. T., & Hunter, C. J. (2010). International Patent No. WO/2011/145069.

Desmoulin, G. T., Hunter, C. J., Hewitt, C. R., Bogduk, N., & Al-Ameri, O. S. (2012). Noninvasive Intervention Corrects Biomechanics and Up-Regulates Disc Genes for Longterm Spinal Health. *Global Spine J. , 02*(S01 - World Forum for Spine Research 2012 The Intervertebral Disc—from Degeneration to Pain.), S1.12. doi: 10.1055/s-0032-1318607.

Desmoulin, G. T., Reno, C. R., & Hunter, C. J. (2010). Free Axial Vibrations At 0 to 200 Hz Positively Affect Extracellular Matrix Messenger Ribonucleic Acid Expression in Bovine Nucleus Pulposi. *SPINE, 35* (15), 1437 - 1444.

Desmoulin, G. T., Reno, C. R., & Hunter, C. J. (2011). Disc strain and resulting positive mRNA expression from application of a non-invasive treatment. *SPINE, 36*(14), E921-E928.

Desmoulin, G. T., Szostek, J. S., Khan, A. H., Al-Ameri, O. S., Hunter, C. J., & Bogduk, N. (2012). Spinal Intervention Efficacy on Correcting Cervical Vertebral Axes of Rotation and the Resulting Improvements in Pain, Disability, and Psychsocial Measures. *Journal of Musculoskeletal Pain, 20*(1), 31-40.

Desmoulin, G. T., Yasin, N. I., & Chen, D. W. (2007). Spinal Mechanisms of Pain Control. *Clinical Journal of Pain, 23*(7), 576-585.

Dickenson, A. (2002). Gate control theory of pain stands the test of time. *Br J Anaesth, 88*, 755-757.

Drake, J. D., Aultman, C. D., McGill, S. M., & Callaghan, J. P. (2005). The influence of static axial torque in combined loading on intervertebral joint failure mechanics using a porcine model. [In Vitro

Research Support, Non-U.S. Gov't]. *Clin Biomech (Bristol, Avon), 20*(10), 1038-1045. doi: 10.1016/j.clinbiomech.2005.06.007

Dungan, T. (May 8, 2001).

Ekblom, A., & Hansson, P. (1985). Extra-segmental transcutaneous electrical nerve stimulation and mechanical vibratory stimulation as compared to placebo for the relief of acute oro-facial pain. *Pain, 23*, 223-229.

Elliot, T. (April 8, 1997).

Ernst, E. (1999). Massage therapy for low back pain: a systematic review. *J Pain Symptom Manage, 17*, 65-69.

Evans, J., & Moore, E. (June 27, 1989).

Ferguson, S. J., & Steffen, T. (2003). Biomechanics of the aging spine. *Eur Spine J, 12 Suppl 2*, S97-S103. doi: 10.1007/s00586-003-0621-0 [doi]

Fontana, T. L., Richardson, C. A., & Stanton, W. R. (2005). The effect of weight-bearing exercise with low frequency, whole body vibration on lumbosacral proprioception: a pilot study on normal subjects. *Aust J Physiother, 51*(4), 259-263.

Fox, E., & Melzack, R. (1976). Transcutaneous electrical stimulation and acupuncture: comparison of treatment for low-back pain. *Pain, 2*, 141-148.

Freemont, A. (2009). The cellular pathobiology of the degenerate intervertebral disc and discogenic back pain. *Rheumatology, 48*, 5-10.

Freemont, A., Peacock, T., Goupille, P., Hoyland, J., O'Brien, J., & Jayson, M. (1997). Nerve ingrowth into diseased intervertebral disc in chronic back pain. *Lancet 350*, 178-181.

Friedenberg, Z. B., & Miller, W. T. (1963). Degenerative disc diseases of the cervical spine. *J Bone Joint Surg, 45A*, 1171-1178.

Fritz, J., Whitman, J., & Childs, J. (2005). Lumbar spine segmental mobility assessment: an examination of validity for determining intervention strategies in patients with low back pain. *Arch Phys Med Rehabil, 86*, 1745-1752.

Fritz, M., Fischer, S., & Brode, P. (2005). Vibration induced low back disorders--comparison of the vibration evaluation according to ISO 2631 with a force-related evaluation. *Appl Ergon, 36*(4), 481-488. doi: S0003-6870(05)00027-X [pii]

10.1016/j.apergo.2005.01.008

Fromm, C., & Noth, J. (1976). Reflex responses of gamma motoneurons to vibration of the muscle they innervate. *J Physiol 256*, 117-136.

Fromm, C., Noth, J., & Thilmann, A. (1976). Inhibition of extensor gamma motoneurons by antagonistic primary and secondary spindle afferents. *Pflugers Arch, 363*, 81-86.

Furlan, A., Brosseau, L., Imamura, M., & Irvin, E. (2002). Massage for low-back pain: a systematic review within the framework of the Cochrane Collaboration Back Review Group. *Spine 27*, 1896-1910.

Furukawa, T., Ito, K., Nuka, S., Hashimoto, J., Takei, H., Takahara, M., . . . Shinomura, T. (2009). Absence of biglycan accelerates the degenerative process in mouse intervertebral disc. [Research Support, Non-U.S. Gov't]. *Spine (Phila Pa 1976), 34*(25), E911-917. doi: 10.1097/BRS.0b013e3181b7c7ec

Geisser, M., Wiggert, E., Haig, A., & Colwell, M. (2005). A randomized, controlled trial of manual therapy and specific adjuvant exercise for chronic low back pain. *Clin J Pain 21*, 463-470.

Gilson, A., Dreger, M., & Urban, J. (2010). Differential expression level of cytokeratin 8 in cells of the bovine nucleus pulposus complicates the search for specific intervertebral disc cell markers. . *Arthritis Research & Therapy, 12*(24).

Goldring, S., & Goldring, M. (2004). The role of cytokines in cartilage matrix degeneration in osteoarthritis. *Clin Orthop Relat Res, 427 (Suppl.)*, S27–36.

Gore, D. R., Sepic, S. B., & Gardner, G. M. (1986). Roentgenographic findings of the cervical spine in asymptomatic people. *Spine, 11*(6), 521-524.

Gotz, W., Barnert, S., Bertagnoli, R., Miosge, N., Kresse, H., & Herken, R. (1997). Immunohistochemical localization of the small proteoglycans decorin and biglycan in human intervertebral discs. *Cell Tissue Res, 289*(1), 185-190.

Graven-Nielsen, T., Svensson, P., & Arendt-Nielsen, L. (1997). Effects of experimental muscle pain on muscle activity and coordination during static and dynamic motor function. *Electroencephalogr Clin Neurophysiol 105*, 156-164.

Guieu, R., Tardy-Gervet, M., & Giraud, P. (1992). Met-enkephalin and beta-endorphin are not involved in the analgesic action of transcutaneous vibratory stimulation. *Pain, 48*, 83-88.

Guieu, R., Tardy-Gervet, M., & J., R. (1991). Analgesic effects of vibration and transcutaneous electrical nerve stimulation applied separately and simultaneously to patients with chronic pain. *Can J Neurol Sci, 18*, 113-119.

Guo, Y., Xiao, P., Lei, S., Deng, F., Xiao, G. G., Liu, Y., . . . Deng, H. (2008). How is mRNA expression predictive for protein expression? A correlation study on human circulating monocytes. [Research Support, N.I.H., Extramural

Research Support, Non-U.S. Gov't]. *Acta Biochim Biophys Sin (Shanghai), 40*(5), 426-436.

Haigh, R., & Clarke, A. (1999). Effectiveness of rehabilitation for spinal pain. *Clin Rehabil, 13*, 63-81.

Haigh, R., & Clarke, A. (1999). Effectiveness of rehabilitation for spinal pain. . *Clin Rehabil, 13*, 63-81.

Hall, A. C., Urban, J. P., & Gehl, K. A. (1991). The effects of hydrostatic pressure on matrix synthesis in articular cartilage. *J. Orthop. Res., 9*, 1-10.

Handa, T., Ishihara, H., Ohshima, H., Osada, R., Tsuji, H., & Obata, K. (1997a). Effects of hydrostatic pressure on matrix synthesis and matrix metalloproteinase production in the human lumbar intervertebral disc. . *Spine, 22*, 1085-1091.

Handa, T., Ishihara, H., Ohshima, H., Osada, R., Tsuji, H., & Obata, K. (1997b). Effects of hydrostatic pressure on matrix synthesis and matrix metalloproteinase production in the human lumbar intervertebral disc. . *Spine, 22*, 1085–1091.

Happey, F., Johnson, A., Naylor, A., & Turner, R. (1964). Preliminary observations concerning the fine structure of the intervertebral disc. *J. Bone Joint Surg. [Br.], 46*, 563-567.

Hayashi, S., Taira, A., & Inoue, G. (2008). TNF-alpha in nucleus pulposus induces sensory nerve growth: a study of the mechanism of discogenic low back pain using TNF-alpha-deficient mice. *Spine, 33*, 1542-1546.

Heller, C. A., Stanley, P., Lewis-Jones, B., & Heller, R. F. (1983). Value of x ray examinations of the cervical spine. *Br Med J (Clin Res Ed), 287*(6401), 1276-1278.

Henzel, J. H., Mohr, G. C., & H.E., v. G. (1968). Reappraisal of biodynamic implications of human ejections. *Aerospace Med, 39*, 231-240.

Hill, E. T., Desmoulin, G. T., & Hunter, C. J. (2009). Is vibration truly an injurious stimulus in the human spine? *J of Biomechanics, 42*(16), 2631–2635.

Hilton, R., & Ball, J. (1984). Vertebral rim lesions in the dorsolumbar spine. *Ann Rheum Dis, 43*, 302–307.

Hodge, J. (2005). Facet, nerve root and epidural block. *Semin Ultrasound CT MR, 26*, 98-102.

Holm, S., Holm, A. K., Ekstrom, L., Karladani, A., & Hansson, T. (2004). Experimental disc degeneration due to endplate injury. *J. Spinal. Disord. Tech., 17*, 64–71.

Horton, W. (1958). Further observations on the elastic mechanisms of the intervertebral disc. *J. Bone Joint Surg. [Br.], 40*, 552-557.

Hoyland, J., Le Maitre, C., & Freemont, A. (2008). Investigation of the role of IL-1 and TNF in matrix degradation in the intervertebral disc. *Rheumatology, 47*, 809-814.

Hult, E., Ekstrom, L., Kaigle, A., Holm, S., & Hansson, T. (1995). In vivo measurement of spinal column viscoelasticity-an animal model. *Journal of Engineering in Medicine, 209*, 105-110.

Hutton, W. C., Toribatake, Y., Elmer, W. A., Ganey, T. M., Tomita, K., & Whitesides, T. E. (1998). The effect of compressive force applied to the intervertebral disc in vivo. A study of proteoglycans and collagen. *Spine (Phila Pa 1976), 23*(23), 2524-2537.

Iatridis, J., MacLean, J., Roughley, P., & Alini, M. (2006). Effects of mechanical loading on intervertebral disc metabolism in vivo. *J Bone Joint Surg Am, 88 (Suppl. 2)*, 41-46.

Iatridis, J. C., MacLean, J. J., Roughley, P. J., & Alini, M. (2006). Effects of mechanical loading on intervertebral disc metabolism in vivo. [Comparative Study

Research Support, N.I.H., Extramural

Research Support, Non-U.S. Gov't

Review]. *J Bone Joint Surg Am, 88 Suppl 2*, 41-46. doi: 10.2106/JBJS.E.01407

Inoue, G., Ohtori, S., Aoki, Y., Ozawa, T., Doya, H., Saito, T., . . . Takahashi, K. (2006). Exposure of the nucleus pulposus to the outside of the anulus fibrosus induces nerve injury and regeneration of the afferent fibers innervating the lumbar intervertebral discs in rats. *Spine (Phila Pa 1976), 31*(13), 1433-1438. doi: 10.1097/01.brs.0000219946.25103.db [doi]

00007632-200606010-00007 [pii]

Inoue, H. (1973). Three dimensional observations of collagen framework of intervertebral disc in rats, dogs and humans. *Arch. Histol. Jpn., 36*, 39-56.

Ishihara, H., McNally, D. S., Urban, J. P., & Hall, A. C. (1996). Effects of hydrostatic pressure on matrix synthesis in different regions of the intervertebral disc. . *J. Appl. Physiol., 80*, 839-846.

Iwamoto, J., Takeda, T., Sato, Y., & Uzawa, M. (2005). Effect of whole-body vibration exercise on lumbar bone mineral density, bone turnover, and chronic back pain in post-menopausal osteoporotic women treated with alendronate. *Aging Clin Exp Res, 17*(2), 157-163. doi: 2844 [pii]

Izambert, O., Mitton, D., Thourot, M., & Lavaste, F. (2003). Dynamic stiffness and damping of human intervertebral disc using axial oscillatory displacement under a free mass system. *European Spine Journal, 12*, 562-566.

Jensen, A., Kaerlev, L., Tuchsen, F., Hannerz, H., Dahl, S., Nielsen, P. S., & Olsen, J. (2008). Locomotor diseases among male long-haul truck drivers and other professional drivers. *Int Arch Occup Environ Health, 81*(7), 821-827. doi: 10.1007/s00420-007-0270-4

Jimbo, K., Park, J., Yokosuka, K., Sato, K., & Nagata, K. (2005). Positive feedback loop of interleukin-1beta upregulating production of inflammatory mediators in human intervertebral disc cells in vitro. *J Neurosurg Spine, 2*, 589-595.

Johannessen, W., Vresilovic, E., Wright, A., & Elliott, D. (2004). Intervertebral disc mechanics are restored following cyclic loading and unloaded recovery. *Ann Biomed Eng, 32*, 70-76.

Johnson, E., Chetty, K., Moore, I., Stewart, A., & Jones, A. (1982). Distribution and arrangement of elastic fibres in intervertebral discs of adult humans. *J. Anat., 135*, 301-309.

Johnson, W., Caterson, B., Eisenstein, S., Hynds, D., Snow, D., & Roberts, S. (2002). Human intervertebral disc aggrecan inhibits nerve growth in vitro. *Arthritis Rheum 46*, 2658-2664.

Johnson, W., & Roberts, S. (2007). 'Rumours of my death may have been greatly exaggerated': a brief review of cell death in human intervertebral disc disease and implications for cell transplantation therapy. *Biochem Soc Trans, 35*, 680-682.

Jünger, S., Gantenbein-Ritter, B., Lezuo, P., Alini, M., Ferguson, S. J., & Ito, K. (2009). Effect of limited nutrition on in situ intervertebral disc cells under simulated-physiological loading. *Spine (Phila Pa 1976), 34*(12), 1264-1271.

Kaigle, A., Ekström, L., Holm, S., Rostedt, M., & Hansson, T. (1998). In vivo dynamic stiffness of the porcine lumbar spine exposed to cyclic loading: influence of load and degeneration. *J Spinal Disord, 11*(1), 65-70.

Kalson, N. S., Richardson, S., & Hoyland, J. A. (2008). Strategies for regeneration of the intervertebral disc. [Review]. *Regen Med, 3*(5), 717-729. doi: 10.2217/17460751.3.5.717

Kang, Y., Choi, W., & Pickar, J. (2002). Electrophysiologic evidence for an intersegmental reflex pathway between lumbar paraspinal tissues. *Spine, 27*, E56-E63.

Kasra, M., Goel, V., Martin, J., Wang, S., Choi, W., & Buckwalter, J. (2003). Effect of dynamic hydrostatic pressure on rabbit intervertebral disc cells. *J Orthop Res, 21*, 597-603.

Kasra, M., Goel, V., Martin, J., Wang, S. T., Choi, W., & J., B. (2003). Effect of dynamic hydrostatic pressure on rabbit intervertebral disc cells. *Journal of Orthopaedic Research, 21*, 597-603.

Kasra, M., Shirazi-Adl, A., & Drouin, G. (1992). Dynamics of Human Lumbar Intervertebral Joints: Experimental and Finite-Element Investigations. *Spine, 17*(1), 93-102.

Katz, J., Pennella-Vaughan, J., Hetzel, R., Kanazi, G., & Dworkin, R. (2005). A randomized, placebo-controlled trial of bupropion sustained release in chronic low back pain. . *J Pain, 6*, 656-661.

Kawchuk, G., & Herzog, W. (1993). Biomechanical characterization [fingerprinting] of five novel methods of cervical spine manipulation. *J Manipulative Physiol Ther 16*, 573-577.

Kazarian, L. (1981). Injuries to the human spinal column: Biomechanics and injury classification. *Exerc. Sport Sci. Rev., 9*, 297-352.

Kelgren, J. (1977). The anatomical source of back pain. *Rheumatol Rehab, 16*, 3–12.

Kerr, D., Walsh, D., & Baxter, D. (2003). Acupuncture in the management of chronic low back pain: a blinded randomized controlled trial. *Clin J Pain, 19*, 364-370.

Keyes, D., & Compere, E. (1932). The normal pathophysiology of the nucleus pulposus of the intervertebral disc. *J. Bone Joint Surg, 14*, 897-938.

Khadilkar, A., Milne, S., Brosseau, L., Wells, G., Tugwell, P., Robinson, V., . . . Saginur, M. (2005). Transcutaneous electrical nerve stimulation for the treatment of chronic low back pain: A systematic review. . *Spine, 30*, 2657-2666.

Kluba, T., Niemeyer, T., Gaissmaier, C., & Grunder, T. (2005). Human anulus fibrosis and nucleus pulposus cells of the intervertebral disc: effect of degeneration and culture system on cell phenotype. [Comparative Study

Research Support, Non-U.S. Gov't]. *Spine (Phila Pa 1976), 30*(24), 2743-2748.

Kofoed, H., & Levander, B. (1987). Respiratory gas pressures in the spine. Measurements in goats. *Acta Orthop Scand, 58*(4), 415-418.

Korecki, C. L., Jeffrey, J. M., & Iatridis, J. C. (2007). Characterization of an in vitro intervertebral disc organ culture system. *Eur Spine J, 16*, 1029-1037.

Korecki, C. L., MacLean, J. J., & Iatridis, J. C. (2008). Dynamic compression effects on intervertebral disc mechanics and biology. [Research Support, N.I.H., Extramural]. *Spine (Phila Pa 1976), 33*(13), 1403-1409. doi: 10.1097/BRS.0b013e318175cae7

Kumar, A., Varghese, M., Mohan, D., Mahajan, P., Gulati, P., & Kale, S. (1999). Effect of whole-body vibration on the low back. A study of tractor-driving farmers in north India. *Spine, 24*(23), 2506-2515.

Kuslich, S., Ulstrom, C., & Michael, C. (1991). The tissue origin of low back pain and sciatica: a report of pain response to tissue stimulation during operations on the lumbar spine using local anesthesia. *Orthop Clin North Am 22*, 181-187.

Le Maitre, C., Hoyland, J., & Freemont, A. (2007). Catabolic cytokine expression in degenerate and herniated human intervertebral discs: IL-1beta and TNFalpha expression profile. *Arthritis Res Ther, 9*, R77.

Le Maitre, C., Pockert, A., Buttle, D., Freemont, A., & Hoyland, J. (2007). Matrix synthesis and degradation in human intervertebral disc degeneration. *Biochem Soc Trans, 35*, 652–655.

Lee, J. K., Desmoulin, G. T., Khan, A. H., & Park, E. J. (2011a). Comparison of 3D Spinal Motions during Stair-climbing between Individuals With and Without Low Back Pain. *Gait and Posture., 34*, 222-226.

Lee, J. K., Desmoulin, G. T., Khan, A. H., & Park, E. J. (2011b). A portable inertial sensing-based spinal motion measurement system for low back pain assessment. [Research Support, Non-U.S. Gov't]. *Conf Proc IEEE Eng Med Biol Soc, 2011*, 4737-4740. doi: 10.1109/IEMBS.2011.6091173

Licciardone, J., Brimhall, A., & King, L. (2005). Osteopathic manipulative treatment for low back pain: a systematic review and meta analysis of randomized controlled trials. *BMC Musculoskelet Disord, 6*, 1-12.

Lindahl, O. (1948). Uber den Wassergehalt des Knorpels *Acta Orthop. Scand., 17*, 134.

Lings, S., & Leboeuf-Yde, C. (2000). Whole-body vibration and low back pain: a systematic, critical review of the epidemiological literature 1992-1999. *International Archives of Occupational and Environmental Health, 73*, 290-297.

Liu, J., Sekiya, I., Asai, K., Tada, T., Kato, T., & Matsui, B. (2001). Biosynthetic response of cultured articular chondrocytes to mechanical vibration. *Research in Experimental Medicine, 200*, 193-193.

Luo, J., Skrzypiec, D. M., Pollintine, P., Adams, M. A., Annesley-Williams, D. J., & Dolan, P. (2007). Mechanical efficacy of vertebroplasty: influence of cement type, BMD, fracture severity, and disc degeneration. . *Bone, 40*, 1110-1119.

Luoma, K., Riihimaki, H., Luukkonen, R., Raininko, R., Viikari-Juntura, E., & Lamminen, A. (2000). Low back pain in relation to lumbar disc degeneration. *Spine, 25*, 487492.

MacGregor, A., Andrew, T., Sambrook, P., & Spector, T. (2004). Structural, psychological, and genetic influences on low back and neck pain: a study of adult female twins. *Arthritis Rheum 51*, 160-167.

MacLean, J. J., Lee, C. R., Alini, M., & Iatridis, J. C. (2005). The effects of short-term load duration on anabolic and catabolic gene expression in the rat tail intervertebral disc. *J Orthop Res., 23*, 1120-1127.

Maigne, J., & Vautravers, P. (2003). Mechanism of action of spinal manipulative therapy. *Joint Bone Spine, 70*, 336-341.

Malekian, M., Park, S. S., & Hunter, C. J. (2008, June 25-29). *EXPERIMENTAL MODAL ANALYSIS OF INTERVERTEBRAL DISC JOINT DYNAMICS.* Paper presented at the Proceedings of the ASME 2008 Summer Bioengineering Conference, Marriott Resort, Marco Island, Florida, USA.

Martin, J., & Buckwalter, J. (2002). Aging, articular cartilage chondrocyte senescence and osteoarthritis. *Biogerontology, 3*, 257-264.

Maruotti, N., Cantatore, F., Crivellato, E., Vacca, A., & Ribatti, D. (2006). Angiogenesis in rheumatoid arthritis. *Histol Histopathol, 21*, 557-566.

Matre, D., Sinkjaer, T., Svensson, P., & Arendt-Nielsen, L. (1998). Experimental muscle pain increases the human stretch reflex. *Pain, 75*, 331-339.

Meir, A., McNally, D., Fairbank, J., Jones, D., & Urban, J. (2008). The internal pressure and stress environment of the scoliotic intervertebral disc – a review. *Proc Inst Mech Eng [H], 222*, 209–219.

Melzack, R., Jeans, M., Stratford, J., & Monks, R. (1980). Ice massage and transcutaneous electrical stimulation comparison of treatment for low-back pain. *Pain 9* 209-217.

Melzack, R., Vetere, P., & Finch, L. (1983). Transcutaneous electrical nerve stimulation [TENS] for low back pain. A comparison of TENS and massage for pain and range of motion. *Phys Ther 63*, 489-493.

Melzack, R., & Wall, P. (1965). Pain mechanisms: a new theory. *Science, 150*, 971–979.

Mens, J. (2005). The use of medication in low back pain. *Best Pract Res Clin Rheumatol, 19*, 609-621.

Mertens, H. (1978). Nonlinear behavior of sitting humans under increasing gravity. *Aviat Space Environ Med 49*, 287-298.

Morril, B. (1957). Single Degree of Freedom *Mechanical Vibrations*. New York, NY: The Ronald Press Company.

Muksian, R., & Nash, C. D. (1974). A model for the response of seated humans to sinusoidal displacements of the seat. *J. Biomech, 7*(3), 209-215.

Nachemson, A., Lewin, T., Maroudas, A., & Freeman, M. (1970). In vitro diffusion of dye through the end plates and the annulus fibrosus of human lumbar intervertebral disc. *Acta Orthop. Scand., 41*, 589-607.

Nachemson, A. L. (1960). Lumbar intradiscal pressure. *Acta Orthop. Scand. (supplement 43).*

Nahum, A. M., & Melvin, J. W. (2010). *Accidental Injury: Biomechanics and Prevention* (2nd ed.). New York, NY: Springer Science + Business Media.

Oborne, D. J. (1983). Whole-body vibration and International Standard ISO 2631: a critique. *Hum Factors, 25*(1), 55-69.

Ohtori, S., Takahashi, K., Chiba, T., Yamagata, M., Sameda, H., & Moriya, H. (2001). Sensory innervation of the dorsal portion of the lumbar intervertebral discs in rats. *Spine (Phila Pa 1976), 26*(8), 946-950.

Ohtori, S., Takahashi, Y., Takahashi, K., Yamagata, M., Chiba, T., Tanaka, K., . . . Moriya, H. (1999). Sensory innervation of the dorsal portion of the lumbar intervertebral disc in rats. *Spine (Phila Pa 1976), 24*(22), 2295-2299.

Okunribido, O. O., Magnusson, M., & Pope, M. H. (2008). The role of whole body vibration, posture and manual materials handling as risk factors for low back pain in occupational drivers. *Ergonomics, 51*(3), 308-329. doi: 791086598 [pii]

10.1080/00140130701637262 [doi]

Oshima, H., Ishihara, H., Urban, J. P., & Tsuji, H. (1993). The use of coccygeal discs to study intervertebral disc metabolism. . *J Orthop Res 11*, 332–338.

Palmer, K. T., Harris, C. E., Griffin, M. J., Bennett, J., Reading, I., Sampson, M., & Coggon, D. (2008). Case-control study of low-back pain referred for magnetic resonance imaging, with special focus on whole-body vibration. *Scand J Work Environ Health, 34*(5), 364-373. doi: 1282 [pii]

Pang, W., Ho, S., & Huang, M. (1999). Selective lumbar spinal nerve block, a review. *Acta Anaesthesiol Sin, 37*, 21-26.

Peate, W. (1994). Occupational musculoskeletal disorders. *Prim care 21*, 313-327.

Peloso, P., Fortin, L., Beaulieu, A., Kamin, M., & Rosenthal, N. (2004). Protocol TRP-CAN-1 Study Group. Analgesic efficacy and safety of tramadol/acetaminophen combination tablets [Ultracet] in treatment of chronic low back pain: a multicenter, outpatient, randomized, double blind, placebo controlled trial *J Rheumatol 31*, 2454-2463.

Perle, S., & Kawchuk, G. (2005). Pressures generated during spinal manipulation and their association with hand anatomy. *J Manipulative Physiol Ther 28*, e1-7.

Pompeiano, O., Wand, P., & Sontag, K. (1975). Response of Renshaw cells to sinusoidal stretch of hind limb extensor muscles. *Arch Ital Biol, 113*, 205-237.

Przybyla, A., Pollintine, P., Bedzinski, R., & Adams, M. A. (2006). Outer annulus tears have less effect than endplate fracture on stress distributions inside intervertebral discs: relevance to disc degeneration. *Clin Biomech (Bristol, Avon), 21*, 1013–1019.

Pye, S., Reid, D., Adams, J., Silman, A., & O'Neill, T. (2007). Influence of weight, body mass index and lifestyle factors on radiographic features of lumbar disc degeneration. *Ann Rheum Dis, 66*, 426-427.

Qassem, W., Othman, M. O., & Abdul-Majeed, S. (1994). The effects of vertical and horizontal vibrations on the human body. *Med Eng Phys, 16*(2), 151-161.

Rabischong, P., Louis, R., Vegraud, J., & Massacre, C. (1978). The inter-vertebral disc. *Anat. Clin., 1*, 55-64.

Reno, C., Marchuk, L., Sciore, P., Frank, C. B., & Hart, D. A. (1997). Rapid isolation of total RNA from small samples of hypocellular, dense connective tissues. *Biotechniques, 22*(6), 1082-1086.

Repanti, M., Korovessis, P., Stamatakis, M., Spastris, P., & Kosti, P. (1998). Evolution of disc degeneration in lumbar spine: a comparative histological study between herniated and postmortem retrieved disc specimens. *J Spinal Disord, 11*, 41-45.

Rittweger, J., Just, K., Kautzsch, K., Reeg, P., & Felsenberg, D. (2002). Treatment of chronic lower back pain with lumbar extension and whole-body vibration exercise: a randomized controlled trial. *SPINE, 27*(17), 1829-1834.

Roaf, R. (1960). A study of the mechanics of spinal injuries. . *J Bone Joint Surg, 42B*, 810-823.

Robb, M. J., & Mansfield, N. J. (2007). Self-reported musculoskeletal problems amongst professional truck drivers. *Ergonomics, 50*(6), 814-827. doi: 777640352 [pii]

10.1080/00140130701220341 [doi]

Robert, R., Raoul, S., Hamel, O., Doe, K., Lanoiselee, J., Berthelot, J., . . . Bord, E. (2004). Chronic lower back pain: A new therapeutic approach. *Neurochirurgie, 50*, 117-122.

Roughley, P. J. (2004). Biology of intervertebral disc again and degeneration: involvement of the extracellular matrix. . *Spine, 29*, 2691-2699.

Roughley, P. J., Melching, L. I., Heathfield, T. F., Pearce, R. H., & Mort, J. S. (2006). The structure and degradation of aggrecan in human intervertebral disc. *Eur Spine J, 15 Suppl 3*, S326-332. doi: 10.1007/s00586-006-0127-7 [doi]

Roy, E., Hollins, M., & Maixner, W. (2003). Reduction of TMD pain by high frequency vibration: a spatial and temporal analysis. . *Pain, 101 Erratum in: Pain 104: 717*, 267-274.

Rufai, A., Benjamin, M., & Ralphs, J. R. (1995). The development of fibrocartilage in the rat intervertebral disc. *Anat Embryol (Berl), 192*(1), 53-62.

Rymer, Z., & Hasan, Z. (1981). Prolonged time course for vibratory suppression of stretch reflex in the decebrate cat. *Exp Brain Res, 44*, 101-112.

Salo, J., Kaigle Holm, A., Indahl, A., Mackiewicz, Z., Sukura, A., Holm, S., . . . Konttinen, Y. T. (2008). Expression of vascular endothelial growth factor receptors coincide with blood vessel in-growth and reactive bone remodelling in experimental intervertebral disc degeneration. *Clin Exp Rheumatol, 26*(6), 1018-1026. doi: 2518 [pii]

Saunders, J., & Inman, V. (1940). Pathology of the intervertebral disc. *Arch. Surg., 40*, 384-416.

Schmidt, H., Shirazi-Adl, A., Galbusera, F., & Wilke, H. J. Response analysis of the lumbar spine during regular daily activities--a finite element analysis. *J Biomech, 43*(10), 1849-1856. doi: S0021-9290(10)00180-6 [pii]

10.1016/j.jbiomech.2010.03.035 [doi]

Schnake, K., Putzier, M., Haas, N., & Kandziora, F. (2006). Mechanical concepts for disc regeneration. *Eur Spine J 15(Suppl. 3)* S354-360.

Setton, L., & Chen, J. (2006). Mechanobiology of the intervertebral disc and relevance to disc degeneration. *J Bone Joint Surg Am, 88 (Suppl. 2)*, 52-57.

Sharma, S., Sing, R., Sharma, A., & Mittal, R. (2003). Incidence of low back pain in workage adults in rural North India. *Indian J Med Sci 57*, 145-147.

Shen, B., Melrose, J., Ghosh, P., & F., T. (2003). Induction of matrix metalloproteinase-2 and -3 activity in ovine nucleus pulposus cells grown in three-dimensional agarose gel culture by interleukin-1beta: a potential pathway of disc degeneration. *Eur Spine J, 12*, 66-67.

Skikic, E., & Suad, T. (2003). The effects of McKenzie exercises for patients with low back pain, our experience. *Bosn J Basic Med Sci 3*, 70-75.

Skrzypiec, D. M., Pollintine, P., Przybyla, A., Dolan, P., & Adams, M. A. (2007). The internal mechanical properties of cervical intervertebral discs as revealed by stress profilometry. *Eur. Spine J., 16*, 1701-1709.

Smith, H. L. (2006). The discrete dynamics of monotonically decomposable maps. *J Math Biol 53*(4), 747-758.

Soukane, D., Shirazi-Adl, A., & Urban, J. (2007). Computation of coupled diffusion of oxygen, glucose and lactic acid in an intervertebral disc. *J Biomech 40*, 2645-2654.

Strayer, A. (2005). Lumbar spine; common pathology and interventions. *J Neurosci Nurs, 37*, 181-193.

Studer, R., Gilbertson, L., Georgescu, H., Sowa, G., Vo, N., & Kang, J. (2008). p38 MAPK inhibition modulates rabbit nucleus pulposus cell response to IL-1. *J Orthop Res, 26*, 991-998.

Sugiura, A., Ohtori, S., Yamashita, M., Inoue, G., Yamauchi, K., Koshi, T., . . . Takahashi, K. (2008). Existence of nerve growth factor receptors, tyrosine kinase a and p75 neurotrophin receptors in intervertebral discs and on dorsal root ganglion neurons innervating intervertebral discs in rats. *Spine (Phila Pa 1976), 33*(19), 2047-2051. doi: 10.1097/BRS.0b013e31817f8d58 [doi]

00007632-200809010-00006 [pii]

Sweat, R. (July 24, 1984).

Sylven, B., Paulson, S., Hirsch, C., & Snellman, O. (1951). Biophysical and physiological investigation on cartilage and other mesenchyma tissues: II. Ultrastructure of bovine and human nucleus pulposus. *J. Bone Joint Surg. [Am.], 33*, 333-340.

Sztrolovics, R., Grover, J., Cs-Szabo, G., Shi, S. L., Zhang, Y., Mort, J. S., & Roughley, P. J. (2002). The characterization of versican and its message in human articular cartilage and intervertebral disc. *J Orthop Res, 20*(2), 257-266.

Takeda, T. (1975). Three dimensional observation of collagen framework of human lumbar disc. *J. Jpn. Orthop. Assoc., 49*, 47-75.

Tamrin, S. B., Yokoyama, K., Jalaludin, J., Aziz, N. A., Jemoin, N., Nordin, R., . . . Abdullah, M. (2007). The Association between risk factors and low back pain among commercial vehicle drivers in peninsular Malaysia: a preliminary result. *Ind Health, 45*(2), 268-278. doi: JST.JSTAGE/indhealth/45.268 [pii]

Tardy-Gervet, M., Guieu, R., Ribot-Ciscar, E., & Roll, J. (1993). Transcutaneous mechanical vibrations: analgesic effect and antinociceptive mechanisms. . *Rev Neurol (Paris), 149*, 177-185.

Taylor, T., Ghosh, P., & GR., B. (1981). The contribution of the intervertebral disc to the scoliotic deformity. *Clin. Orthop., 156*, 79-90.

Tiemessen, I. J., Hulshof, C. T., & Frings-Dresen, M. H. (2008). Low back pain in drivers exposed to whole body vibration: analysis of a dose-response pattern. *Occup Environ Med, 65*(10), 667-675. doi: oem.2007.035147 [pii]

10.1136/oem.2007.035147 [doi]

Tucek, K. (Aug 5, 2003). U.S. Patent 6,602,211.

Ulrich, J. A., Liebenberg, E. C., Thuillier, D. U., & Lotz, J. C. (2007). ISSLS prize winner: repeated disc injury causes persistent inflammation. . *Spine, 32*, 2812–2819.

van Tulder, M., Koes, B., Seitsalo, S., & Malmivaara, A. (2006). Outcome of invasive treatment modalities on back pain and sciatica: an evidence-based review. *Eur Spine J, 15*(Suppl 1), S82-92.

Videman, T., Simonen, R., Usenius, J., Osterman, K., & Battie, M. (2000). The long-term effects of rally driving on spinal pathology. *Clin Biomech (Bristol, Avon), 15*(2), 83-86. doi: S0268003399000479 [pii]

Voronov, E., Carmi, Y., & Apte, R. (2007). Role of IL-1-mediated inflammation in tumor angiogenesis. *Adv Exp Med Biol, 601*, 265–270.

Walsh, A. J., & Lotz, J. C. (2004). Biological response of the intervertebral disc to dynamic loading. [Comparative Study

Research Support, Non-U.S. Gov't

Research Support, U.S. Gov't, P.H.S.]. *J Biomech, 37*(3), 329-337.

Walsh, A. J., & Lotz, J. C. (2004). Biological response of the intervertebral disc to dynamic loading. *Journal of Biomechanics, 37*(3), 329-337.

Wang, D., Jiang, S., & Dai, L. (2007). Biologic response of the intervertebral disc to static and dynamic compression in vitro. *Spine, 32*, 2521-2528.

Weiler, C., Nerlich, A. G., Zipperer, J., Bachmeier, B. E., & Boos, N. (2002). 2002 SSE Award Competition in Basic Science: expression of major matrix metalloproteinases is associated with intervertebral disc degradation and resorption. *Eur. Spine J., 11*, 308–320.

Wiesel, S. W., & International Society for Study of the Lumbar Spine. (1996). *The lumbar spine* (2nd ed.). Philadelphia: W. B. Saunders Co.

Wilke, H. J., Neef, P., Caimi, M., Hoogland, T., & Claes Lutz, E. (1999). New in vivo measurement of pressure in the intervetebral disc in daily life. *SPINE, 24*(8), 755-762.

Wing, T. (October 29, 1985).

Yoganandan, N., Cusick, J. F., Pintar, F. A., & Rao, R. D. (2001). Whiplash Injury Determination With Conventional Spine Imaging and Cryomicrotomy. *Spine, 26*(22), 2443-2448.

Zhao, C., Liu, D., Li, H., Jiang, L., & Dai, L. (2007). Interleukin-1beta enhances the effect of serum deprivation on rat annular cell apoptosis *Apoptosis, 12*, 2155–2161.

Zhao, C., Wang, L., Jiang, L., & Dai, L. (2007). The cell biology of intervertebral disc aging and degeneration. *Ageing Res Rev, 6*, 247-261.

APPENDIX

A.1 MATLAB CODE

A.1.1 Frequency Response Function

```
natural_frequency = 1;

damping_ratio = 0.1;

excitation_frequency = linspace(0,3,201);


numerator = natural_frequency.^2;

denominator = sqrt((natural_frequency^2 - excitation_frequency.^2).^2 +
(2*damping_ratio*natural_frequency*excitation_frequency).^2);

k_times_magnitude_of_FRF = numerator./denominator;


numerator = -2*damping_ratio*natural_frequency*excitation_frequency;

denominator = natural_frequency^2 - excitation_frequency.^2;

phase_of_FRF = atand(numerator./denominator);

phase_of_FRF(excitation_frequency > natural_frequency) = phase_of_FRF(excitation_frequency > natural_frequency) - 180;


subplot(211)
```

```
plot(excitation_frequency, k_times_magnitude_of_FRF)
xlabel('\omega/\omega_n')
ylabel('k|H(\omega)|')
title('Magnitude of the Frequency Response Function as a function of the Excitation Frequency \omega');
grid on

subplot(212)
plot(excitation_frequency, phase_of_FRF)
xlabel('\omega/\omega_n')
ylabel('\phi(\omega) in deg')
title('Phase of the Frequency Response Function as a function of the Excitation Frequency \omega');
grid on
```

A.1.2 Transmissibility

```
natural_frequency = 2;
damping_ratio = 0.1;
excitation_frequency = linspace(0,3*natural_frequency,201);
```

```
numerator = sqrt( natural_frequency^4 + (2*damping_ratio*natural_frequency*excitation_frequency).^2);

denominator = sqrt((natural_frequency^2 - excitation_frequency.^2).^2 +
(2*damping_ratio*natural_frequency*excitation_frequency).^2);

transmissibility = numerator./denominator;


figure(1), clf

plot(excitation_frequency./natural_frequency, transmissibility)

xlabel('\omega/\omega_n')

ylabel('TR(\omega)')

title('Transmissibility TR as a function of the normalized base excitation frequency \omega/\omega_n', 'fontsize', 14);

grid on
```

A.2 LABVIEW Virtual Instrument (VI)

A.2.1 VI Graphical User Interface

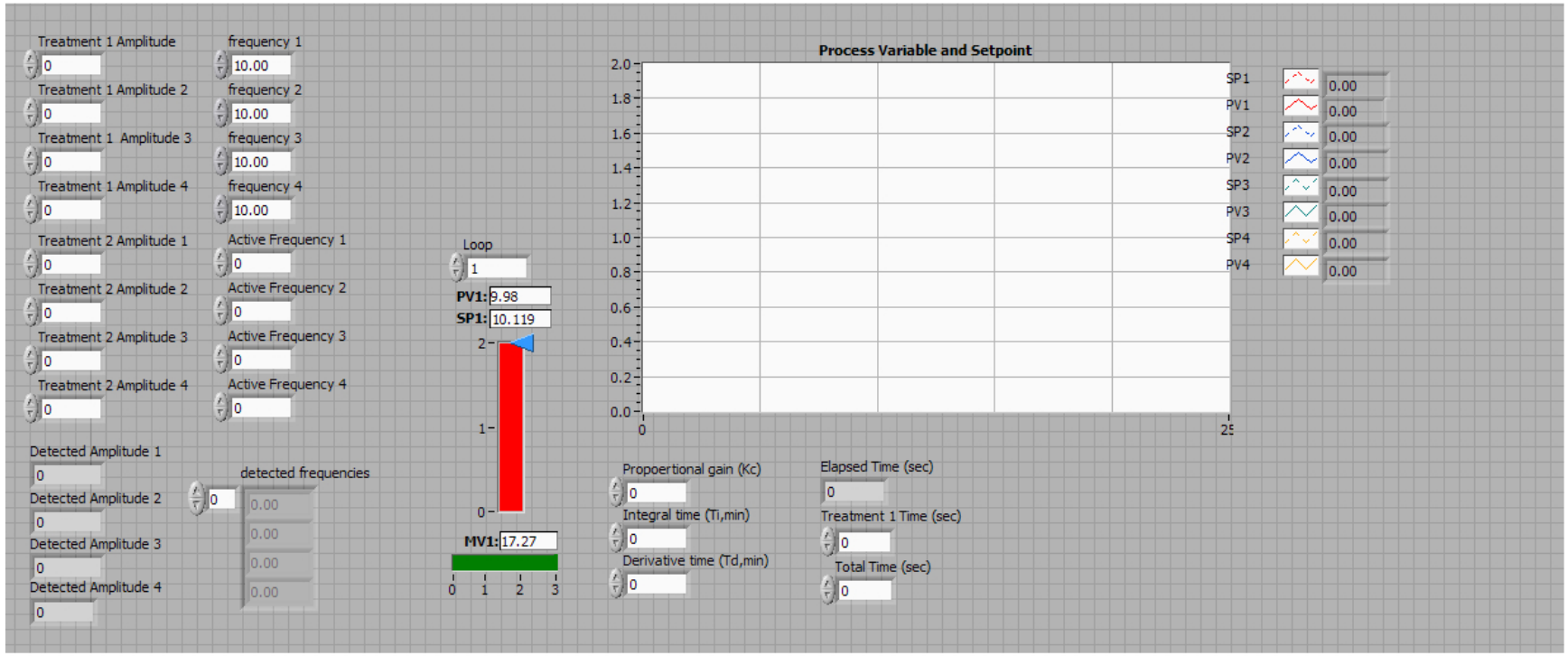

A.2.2 VI Code Block Diagram

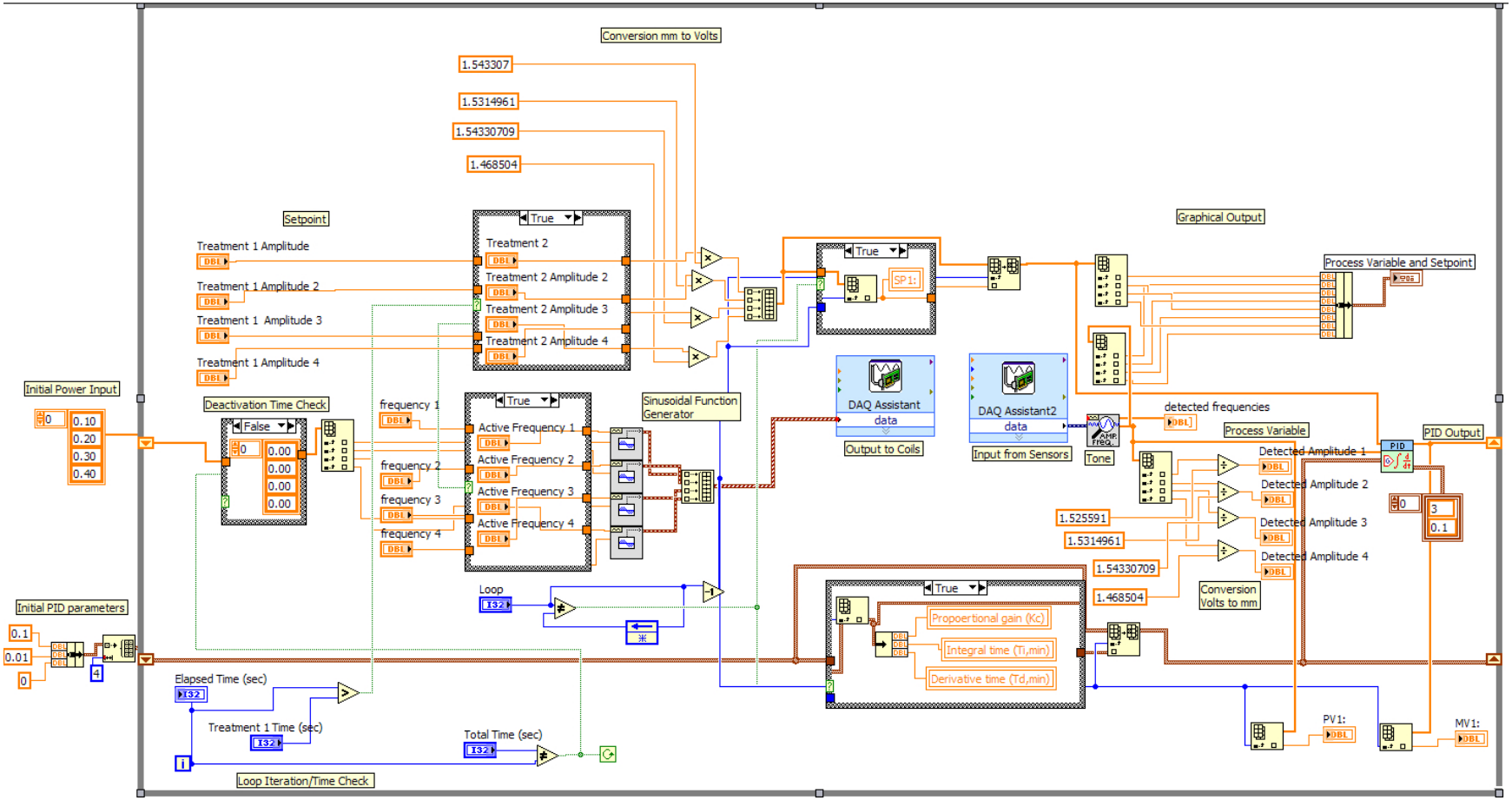

A.3 PCB board layout for accelerometer mounts

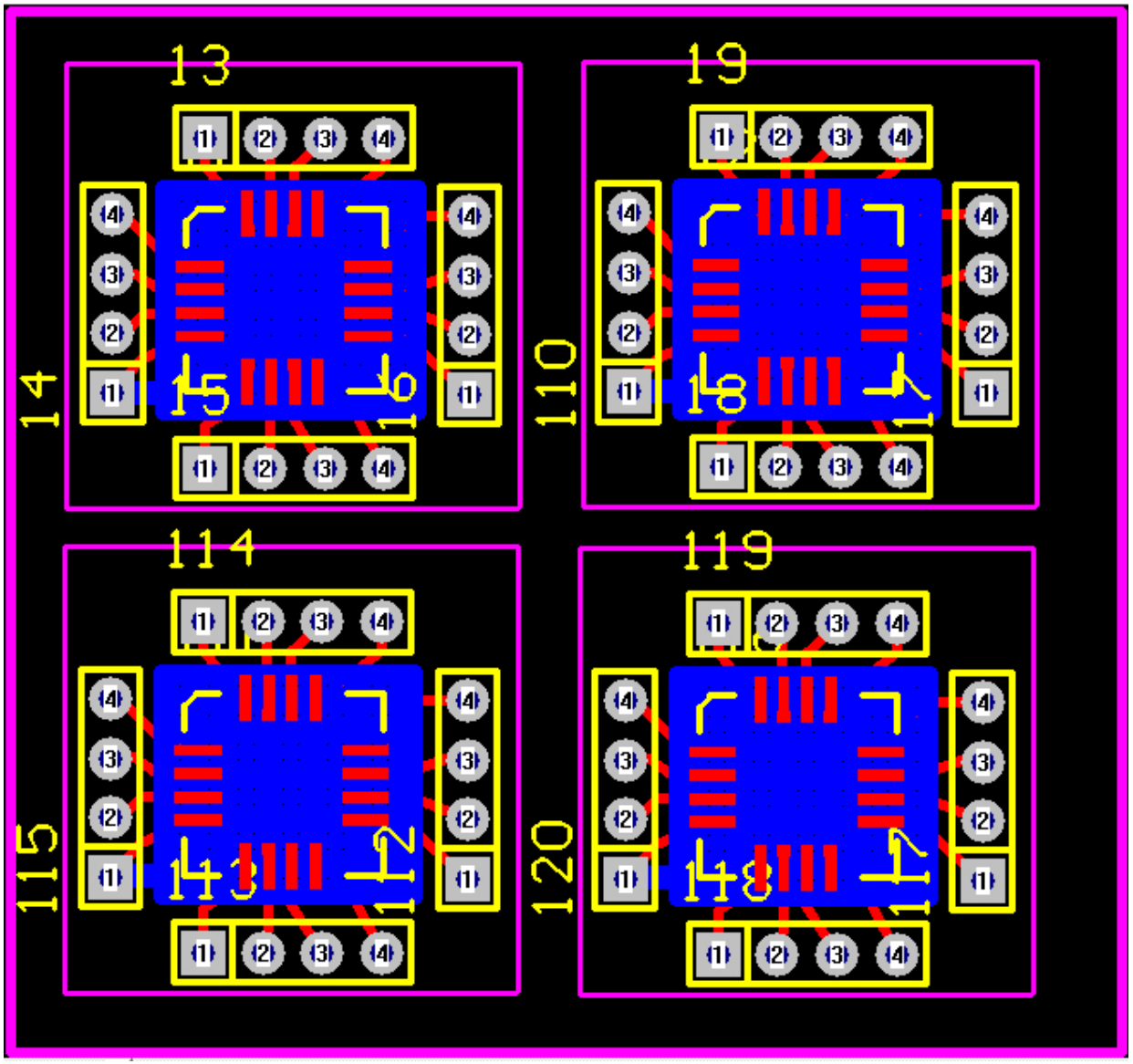

A.4 RAW DATA AND ANOVA TABLES
A.4.1 Objective 1 Data

Specimen #	Load Freq (Hz)	Load-(Intensity %)	Load Duration	Aggrecan	Biglycan	Collagen 1	Collagen II	Decorin	Versican
132	KKT	20	60 pulses	2.55	3.86	1.93	3.73	6.73	9.85
133	KKT	20	60 pulses	1.80	4.14	1.19	1.80	3.61	7.21
134	KKT	80	60 pulses	1.23	1.32	4.76	1.00	3.03	2.83
135	KKT	80	60 pulses	1.19	1.00	5.46	1.19	2.07	1.00
136	KKT	50	60 pulses	1.00	1.62	3.03	1.00	3.61	3.73
137	KKT	50	60 pulses	1.04	1.52	2.73	1.11	4.14	3.73
138	KKT	20	60 pulses	1.04	2.00	4.59	2.22	3.03	5.10
139	KKT	20	60 pulses	1.68	2.55	6.96	2.64	4.76	6.06
140	KKT	50	60 pulses	1.68	1.68	8.28	2.22	2.22	8.00
141	KKT	50	60 pulses	1.62	2.73	5.86	1.62	2.38	4.92
142	KKT	50	60 pulses	1.27	1.80	1.00	1.37	2.46	2.46
143	KKT	50	60 pulses	1.46	2.55	4.00	2.00	5.46	5.28
144	KKT	80	60 pulses	1.52	1.93	4.14	2.00	2.83	3.86
145	KKT	80	60 pulses	1.41	1.68	3.25	1.07	2.00	2.22
146	KKT	20	1000pulses	2.83	2.64	2.55	1.68	1.46	2.38
147	KKT	20	1000pulses	2.93	3.73	7.46	3.25	1.87	5.10
148	KKT	80	1000pulses	1.74	2.22	5.86	1.68	7.21	7.73
149	KKT	80	1000pulses	1.32	2.55	10.93	2.07	4.29	10.20
150	KKT	50	1000pulses	2.00	2.83	8.88	1.41	4.00	9.19
151	KKT	50	1000pulses	1.87	6.73	6.50	2.22	8.57	6.06
152	KKT	20	1000pulses	1.62	2.14	6.06	1.37	5.46	5.28
153	KKT	20	1000pulses	2.07	2.46	9.85	2.22	9.85	8.28
154	KKT	50	1000pulses	1.62	5.46	4.92	2.73	8.28	6.28
155	KKT	50	1000pulses	1.62	5.66	7.46	2.73	5.10	9.51
156	KKT	80	1000pulses	3.48	3.48	12.13	5.86	4.44	9.85
157	KKT	80	1000pulses	2.38	4.92	4.29	2.46	6.06	6.96
158	KKT	80	1000pulses	3.14	4.29	20.39	3.61	6.50	9.51
159	KKT	80	1000pulses	1.68	2.46	13.93	3.86	8.88	12.55

Specimen #	Load Freq (Hz)	Load-(Intensity %)	Load Duration	Aggrecan	Biglycan	Collagen 1	Collagen II	Decorin	Versican
160	KKT	50	1000pulses	5.28	4.76	17.15	7.73	7.21	16.56
161	KKT	50	1000pulses	1.80	4.76	9.19	2.00	5.10	4.59
162	KKT	20	1000pulses	2.07	5.28	6.73	1.52	4.14	4.29
163	KKT	20	1000pulses	2.83	5.46	7.21	1.62	4.59	4.29
164	KKT	80	60pulses	3.03	5.46	9.85	3.25	2.07	13.45
165	KKT	80	60pulses	1.52	2.55	4.00	1.93	1.00	7.46
166	KKT	20	60pulses	2.73	4.59	7.21	4.44	3.86	16.56
167	KKT	20	60pulses	1.62	2.07	1.74	1.62	1.57	5.86
168	0	0	0	1.62	3.14	6.28	4.14	1.74	8.28
169	0	0	0	2.07	4.44	17.15	4.14	3.73	8.28
170	0	0	0	2.73	3.48	7.73	3.14	4.29	17.15
171	0	0	0	2.14	3.36	8.00	2.83	6.28	6.50
172	0	0	0	2.14	1.80	9.85	1.41	1.27	3.14
173	0	0	0	2.30	2.55	17.75	2.38	3.61	6.06
174	0	0	0	1.87	3.48	4.44	3.14	6.73	8.57
175	0	0	0	2.64	2.64	13.00	3.86	1.46	11.71
176	0	0	0	2.73	4.76	15.45	5.66	10.20	7.21
177	0	0	0	4.59	8.57	20.39	4.14	6.50	14.93
178	KKT	50	1000pulses over 6days	3.25	3.03	3.48	2.30	2.30	6.06
179	KKT	50	1000pulses over 6days	2.07	2.46	2.22	1.15	3.25	5.10
180	KKT	50	1000pulses over 6days	2.93	3.48	3.86	2.07	4.14	3.86
181	KKT	50	1000pulses over 6days	2.30	3.03	5.10	2.07	3.61	5.10
182	KKT	50	1000pulses over 6days	2.73	3.03	5.28	2.83	3.73	6.28
183	KKT	50	1000pulses over 6days	3.61	5.10	7.21	3.73	6.06	6.73
184	0	0	0	2.00	2.07	4.14	1.37	6.73	1.00
185	0	0	0	2.83	2.38	2.64	1.46	4.59	2.83
186	0	0	0	2.07	2.55	2.14	1.62	6.50	1.93
187	0	0	0	1.37	2.00	1.57	1.74	3.86	4.76

A.4.2 Objective 2 Pilot Data

Nucleus Pulposus

Specimen #	Load Freq (Hz)	Load-ave (RMS-g)	Load Duration (min)	Aggrecan	Biglycan	Collagen 1	Collagen II	Decorin	Versican
1	8	0.13	60	9.85	2.93	2896.3	9.51	4.59	2.22
2	160	0.15	60	2.73	1.00	1260.7	3.36	2.30	1.41
3	16	0.16	60	10.93	2.64	1910.9	6.73	5.10	2.93
4	80	0.29	60	5.86	3.73	12416.8	48.50	5.66	13.93
5	16	0.28	60	19.03	6.28	1097.5	18.38	6.28	5.28
6	80	0.31	60	9.85	3.61	14263.1	142.02	4.59	22.63
7	160	0.29	60	7.21	3.25	5404.7	9.19	3.48	8.28
8	8	0.32	60	10.20	2.38	2272.4	12.13	1.00	8.57
9	16	0.33	60	16.56	7.73	19484.0	27.86	17.15	14.93
10	80	0.32	60	3.25	2.30	861.1	4.00	1.04	1.00
11	8	0.31	60	6.50	1.93	1176.3	7.46	2.93	2.93
12	160	0.28	60	4.44	1.41	891.4	4.92	3.86	1.52
13	80	0.30	60	4.76	1.32	1398.8	3.61	2.30	3.25
14	16	0.27	60	10.56	2.93	2610.3	10.56	5.10	8.57
15	160	0.28	60	5.10	1.68	1024.0	5.28	3.36	3.73
16	80	0.31	60	6.50	1.00	1910.9	6.96	1.68	2.64
17	8	0.30	60	6.96	1.15	2352.5	4.92	1.04	1.80
18	16	0.31	60	10.93	3.48	5996.9	14.93	6.06	7.46
19	160	0.29	60	13.00	4.44	3213.7	15.45	4.14	8.57
20	8	0.29	60	12.55	5.86	922.9	14.93	1.93	8.57

Annulus Fibrosus

Specimen #	Load Freq (Hz)	Load-ave (RMS-g)	Load Duration (min)	Aggrecan	Biglaycan	Collagen 1	Collagen II	Decorin	Versican
1	8	0.13	60	4.44	6.28	191900.6	3.36	22.63	8.88
2	160	0.15	60	6.73	6.73	191900.6	7.73	18.38	6.96
3	16	0.16	60	8.00	10.56	489178.0	8.57	21.11	16.56
4	80	0.29	60	1.00	2.64	49667.0	1.00	10.20	2.22
5	16	0.28	60	7.46	5.66	55109.0	7.73	17.75	4.59
6	80	0.31	60	4.14	5.66	118128.7	1.80	10.56	10.56
7	160	0.29	60	5.66	9.51	205674.0	7.73	27.86	7.73
8	8	0.32	60	2.55	3.36	145433.5	1.87	36.76	6.73
9	16	0.33	60	4.00	7.46	358099.3	2.55	59.71	9.19
10	80	0.32	60	1.93	3.73	114104.8	1.00	23.43	6.73
11	8	0.31	60	3.25	2.64	53231.8	1.27	23.43	3.86
12	160	0.28	60	1.19	2.73	212927.1	1.00	23.43	4.14
13	80	0.30	60	5.46	6.73	205674.0	6.28	21.11	11.71
14	16	0.27	60	7.21	6.28	140479.5	9.19	14.93	8.00
15	160	0.28	60	4.59	7.73	126607.2	5.66	18.38	8.88
16	80	0.31	60	10.93	8.57	179049.6	13.93	26.91	8.00
17	8	0.30	60	4.44	6.96	506428.8	6.73	35.51	9.85
18	16	0.31	60	2.93	6.28	244589.0	2.64	17.75	8.88

Specimen #	Load Freq (Hz)	Load-ave (RMS-g)	Load Duration (min)	Aggrecan	Biglaycan	Collagen 1	Collagen II	Decorin	Versican
19	160	0.29	60	5.10	7.73	358099.3	5.66	35.51	12.55
20	8	0.29	60	4.00	7.73	1.0	5.10	36.76	9.19

A.4.3 Objective 2 Data

Specimen #	Load Freq (Hz)	Load-ave (RMS-g)	Load Duration (min)	Aggrecan	Biglycan	Collagen 1	Collagen II	Decorin	Versican
21	160	0.29	60	1.87	1.93	2.00	3.03	1.19	5.10
22	200	0.31	60	1.68	2.38	2.07	1.57	1.32	5.46
23	200	0.29	60	1.93	1.80	2.64	1.80	1.15	7.46
24	0	0.00	60	2.07	4.14	2.14	2.07	1.52	8.00
25	160	0.26	60	3.61	4.92	13.93	4.92	3.61	5.86
26	200	0.28	60	1.80	3.61	2.83	1.87	1.00	4.76
27	160	0.28	60	1.57	1.52	1.41	1.80	1.04	2.22
28	200	0.34	60	1.80	1.93	8.00	1.62	1.15	4.44
29	0	0.00	60	1.46	2.14	1.19	1.41	1.46	3.61
30	160	0.29	60	2.64	2.46	6.50	3.86	2.46	3.36
31	200	0.30	60	1.74	2.64	5.66	2.07	4.92	3.03
32	160	0.30	60	1.00	1.00	1.00	1.46	1.27	1.00
33	0	0.00	60	1.27	1.62	1.74	1.00	3.61	2.07
34	0	0.00	60	2.38	5.28	7.46	3.86	1.93	4.92
35	8	0.33	10	1.27	1.07	1.32	1.00	3.48	4.60
36	200	0.33	10	1.80	1.80	3.61	1.46	6.50	11.31
37	80	0.31	10	1.23	1.28	2.07	1.19	3.73	12.55
38	0	0.00	10	1.52	2.00	3.03	2.46	5.28	12.13
39	16	0.30	10	1.04	1.46	17.75	1.15	2.22	2.14
40	160	0.32	10	1.00	1.19	4.60	2.46	5.86	10.93
42	0	0.00	10	2.38	1.74	3.36	2.64	4.44	15.46
43	0	0.00	60	2.07	2.14	2.30	3.14	1.52	2.93
44	8	0.24	10	2.14	1.93	5.86	2.14	11.31	21.86
45	160	0.24	10	3.48	1.93	1.57	4.44	5.10	22.63
46	16	0.25	10	1.68	1.93	1.23	1.57	4.14	10.93
47	200	0.28	10	2.55	1.46	2.07	2.30	4.14	9.85
52	0	0.00	10	1.62	1.68	4.00	1.80	3.14	9.51
53	200	0.28	10	1.68	1.74	1.93	2.30	1.93	3.14
54	0	0.00	10	1.87	1.87	3.25	2.00	1.00	1.00
55	16	0.27	10	1.37	1.63	2.30	1.80	3.14	4.60
56	160	0.26	10	1.00	1.00	1.00	1.37	1.04	1.87
57	8	0.24	10	2.14	3.14	14.42	3.48	21.86	16.56
58	16	0.26	10	4.00	3.48	8.57	7.73	11.31	15.46
59	200	0.30	10	4.59	2.73	6.28	4.60	9.19	16.56
60	160	0.26	10	1.93	1.46	2.38	2.22	2.93	8.28
61	80	0.28	10	2.55	2.07	6.06	4.44	6.50	11.31
62	80	0.28	10	3.36	2.30	3.61	4.60	4.29	13.00
63	8	0.26	10	2.83	4.00	17.75	4.14	27.86	24.25
64	200	0.27	10	3.61	1.93	3.36	1.80	5.46	8.57

Specimen #	Load Freq (Hz)	Load-ave (RMS-g)	Load Duration (min)	Aggrecan	Biglycan	Collagen 1	Collagen II	Decorin	Versican
65	200	0.29	10	3.14	2.22	4.29	4.29	4.76	8.88
66	16	0.27	10	3.03	3.61	3.86	5.28	10.56	16.00
67	8	0.26	10	3.36	3.36	3.36	5.66	7.73	11.71
68	160	0.28	10	3.14	1.93	1.23	3.36	1.68	6.28
69	80	0.25	10	3.48	3.14	3.61	4.60	2.38	9.19
70	80	0.27	10	4.00	3.25	4.00	6.73	6.50	18.38
71	16	0.15	10	3.03	2.93	10.20	4.00	6.28	2.38
72	200	0.12	10	2.07	2.14	8.28	4.29	7.73	2.46
73	8	0.13	10	1.93	1.52	5.66	2.22	2.73	2.30
74	160	0.13	10	2.00	1.37	4.44	2.07	5.66	3.61
75	80	0.12	10	2.00	1.62	4.59	2.64	3.25	1.52
76	80	0.11	10	1.74	1.74	6.96	3.03	4.76	1.80
77	200	0.13	10	1.37	1.11	2.22	2.73	1.57	1.32
78	8	0.13	10	1.52	1.19	7.21	2.38	6.06	2.14
79	160	0.13	10	1.52	1.41	10.20	2.38	4.00	1.11
80	16	0.13	10	3.61	1.80	4.44	2.64	3.25	3.48
81	80	0.13	10	2.64	1.74	5.28	4.92	5.46	4.00
82	8	0.13	10	5.28	3.36	8.88	8.57	6.96	6.73
83	200	0.13	10	2.07	1.57	2.73	1.68	8.88	2.55
84	16	0.14	10	2.93	2.64	10.20	4.14	6.73	1.80
85	160	0.12	10	1.00	1.27	6.73	1.00	2.22	1.19
86	80	0.13	10	2.83	2.55	16.00	4.29	3.73	3.14
87	8	0.13	10	1.15	1.27	1.62	2.55	6.06	4.76
88	200	0.13	10	1.57	1.93	3.73	1.37	2.30	2.22
89	160	0.13	10	1.32	2.38	1.41	1.93	6.73	1.52
91	80	0.13	10	1.00	1.57	2.22	1.57	4.14	2.64
92	16	0.13	10	2.07	1.68	4.14	2.46	2.22	2.14
93	200	0.13	10	1.93	2.07	3.25	1.27	2.14	2.38
94	8	0.13	10	1.41	1.00	1.00	1.93	1.00	1.00
95	160	0.13	10	1.57	1.41	2.73	1.68	1.62	2.00
96	160	0.50	10	1.27	1.74	1.62	2.00	1.80	1.00
97	8	0.54	10	1.19	1.11	1.00	1.00	1.11	1.11
98	200	0.51	10	2.00	2.46	3.03	3.73	1.41	1.27
99	16	0.51	10	3.14	1.74	3.14	4.44	2.30	3.36
100	80	0.49	10	2.46	2.93	2.93	3.61	2.38	1.87
101	80	0.50	10	2.30	3.73	5.46	4.92	7.46	2.93
103	200	0.51	10	1.93	5.10	10.93	5.10	7.46	2.83
104	8	-	10	2.00	4.00	3.14	4.14	5.10	2.64
105	160	0.51	10	2.00	4.14	6.96	4.76	13.00	2.14
106	0	0.00	10	3.14	2.14	3.14	3.14	2.38	7.21

Specimen #	Load Freq (Hz)	Load-ave (RMS-g)	Load Duration (min)	Aggrecan	Biglycan	Collagen 1	Collagen II	Decorin	Versican
107	160	0.50	10	1.74	3.86	16.00	4.29	9.85	2.07
108	8	0.50	10	1.80	3.25	3.25	3.61	10.56	1.87
109	200	0.51	10	1.87	3.14	4.00	3.14	4.44	3.03
110	16	0.51	10	2.83	7.21	15.45	8.57	8.28	3.61
111	80	0.50	10	4.29	5.66	8.57	9.51	8.88	4.44
112	80	0.50	10	2.83	3.14	5.10	3.73	4.44	2.64
113	16	0.50	10	1.68	2.55	3.61	2.73	4.00	1.74
114	200	0.53	10	1.87	5.28	29.86	6.73	18.38	3.86
114	200	0.53	10	2.07	6.06	9.51	5.66	9.51	4.76
115	8	0.49	10	1.00	1.00	1.15	1.04	1.00	1.11
116	160	0.50	10	2.22	4.59	3.48	4.76	6.28	3.36
117	160	0.50	10	2.14	4.92	6.28	4.92	13.00	2.73
118	8	0.50	10	2.93	5.66	32.00	9.85	15.45	4.29
120	16	0.50	10	2.46	4.59	24.25	5.86	15.45	2.55
121	80	0.50	10	2.46	3.73	5.10	6.50	5.10	2.30
122	0	0.00	10	1.62	2.22	5.46	2.22	3.36	4.76
123	0	0.00	10	3.73	5.66	3.73	6.28	5.10	7.46
124	0	0.00	10	1.32	2.07	5.46	2.22	3.48	3.03
125	0	0.00	10	1.80	3.86	4.59	2.73	7.46	6.06
126	0	0.00	10	2.22	3.36	4.59	3.86	2.55	4.76
127	0	0.00	10	3.73	4.29	7.21	5.66	4.00	7.21
128	0	0.00	10	2.83	4.00	6.96	7.21	7.73	6.28
129	0	0.00	10	1.52	1.15	2.46	2.00	4.14	2.55
130	0	0.00	10	2.00	2.64	3.25	3.73	4.76	6.96
131	0	0.00	10	1.62	2.22	6.28	4.59	5.86	2.93
189	20	0.25	10	2.64	4.44	21.11	1.80	10.20	8.57
190	30	0.27	10	1.93	2.22	3.14	1.57	2.38	6.50
191	40	0.25	10	2.00	1.41	3.03	1.46	1.41	6.06
192	50	0.26	10	2.83	3.36	6.06	3.03	10.93	7.73
193	60	0.25	10	3.48	3.48	7.21	2.83	4.29	14.42
194	70	0.25	10	1.19	1.93	1.57	1.87	3.03	6.06
195	0	0.00	10	1.80	2.07	2.83	2.55	3.03	8.57
196	20	0.25	10	1.00	1.41	1.00	1.07	1.57	2.73
197	30	0.26	10	1.52	1.32	1.62	2.30	1.62	3.36
198	40	0.25	10	2.38	2.46	3.73	2.14	2.00	3.73
199	50	0.23	10	3.14	2.83	3.36	3.73	4.29	6.96
200	60	0.26	10	1.80	2.30	2.55	1.62	6.06	5.10
201	70	0.25	10	4.76	5.10	11.31	3.73	3.61	7.21
202	0	0.00	10	2.30	2.83	2.93	2.64	2.30	2.00
203	20	0.26	10	1.68	2.14	2.00	1.27	4.44	5.10

Specimen #	Load Freq (Hz)	Load-ave (RMS-g)	Load Duration (min)	Aggrecan	Biglycan	Collagen 1	Collagen II	Decorin	Versican
204	30	0.26	10	2.22	3.03	1.74	1.37	5.46	8.57
205	40	0.26	10	1.68	1.68	1.62	1.62	1.23	4.44
206	50	0.24	10	2.83	4.00	6.28	4.76	2.55	12.55
207	60	0.28	10	1.87	2.46	3.61	2.22	1.46	6.28
208	70	0.25	10	3.86	4.00	4.92	3.61	1.19	6.50
209	0	0.00	10	2.55	2.83	1.93	2.30	1.00	6.28
210	20	0.25	10	2.46	3.25	7.73	4.00	5.28	9.51
211	30	0.26	10	2.55	3.73	5.28	2.64	8.88	8.00
212	40	0.25	10	2.73	3.36	6.96	4.29	2.46	15.45
213	50	0.25	10	3.36	4.59	5.46	3.48	1.62	13.45
214	60	0.26	10	1.57	1.41	2.83	1.23	3.86	4.76
215	70	0.26	10	3.61	3.86	6.96	3.36	5.10	4.92
216	0	0.00	10	2.55	2.55	3.03	1.87	6.96	4.44
217	20	0.26	10	1.32	1.00	1.19	1.00	2.07	2.93
218	30	0.25	10	2.73	4.29	6.28	2.83	5.28	9.51
219	40	0.25	10	2.64	2.38	4.29	3.36	4.59	5.46
220	50	0.25	10	3.14	2.83	4.29	2.07	2.93	7.21
221	60	0.24	10	3.14	3.36	3.25	3.25	2.73	7.21
222	70	0.25	10	2.64	2.22	4.44	2.07	3.03	6.96

Obj. 2 Data Aggrecan ANOVA Results

Model Information	
Data Set	WORK.ANIM
Dependent Variable	sqrt_aggrecan
Covariance Structure	Variance Components
Estimation Method	REML
Residual Variance Method	Profile
Fixed Effects SE Method	Model-Based
Degrees of Freedom Method	Containment

Class Level Information		
Class	**Levels**	**Values**
load_freq_cat	2	0 1
load_rms_cat	2	0 1
load_dur_cat	2	0 1
block	54	1 2 3 4 5 6 7 8 9 10 11 12 13 14 15 16 17 18 19 20 21 22 23 24 25 26 27 28 29 30 31 32 33 34 35 36 37 38 39 40 41 42 57 58 59 60 61 62 63 64 65 66 67 68

Dimensions	
Covariance Parameters	2
Columns in X	18
Columns in Z	54
Subjects	1
Max Obs Per Subject	158

Number of Observations	
Number of Observations Read	158
Number of Observations Used	158
Number of Observations Not Used	0

Iteration History			
Iteration	**Evaluations**	**-2 Res Log Like**	**Criterion**
0	1	227.27609848	
1	2	192.99880198	0.00000001

Convergence criteria met.

Covariance Parameter Estimates				
Cov Parm	**Estimate**	**Standard Error**	**Z Value**	**Pr > Z**
block	0.1183	0.03248	3.64	0.0001
Residual	0.1170	0.01658	7.06	<.0001

Fit Statistics	
-2 Res Log Likelihood	193.0
AIC (smaller is better)	197.0
AICC (smaller is better)	197.1
BIC (smaller is better)	201.0

Type 3 Tests of Fixed Effects				
Effect	**Num DF**	**Den DF**	**F Value**	**Pr > F**
load_freq_cat	1	99	7.66	0.0067
load_rms_cat	1	99	0.43	0.5160
load_freq*load_rms_c	1	99	0.26	0.6140
load_dur_cat	1	99	28.38	<.0001
load_freq*load_dur_c	1	99	18.83	<.0001
load_rms_*load_dur_c	0	.	.	.

Least Squares Means								
Effect	load_freq_cat	load_rms_cat	load_dur_cat	Estimate	Standard Error	DF	t Value	Pr > |t|
load_freq_cat	0			Non-est	.	.	.	.
load_freq_cat	1			Non-est	.	.	.	.
load_rms_cat		0		1.8650	0.06607	99	28.23	<.0001
load_rms_cat		1		Non-est	.	.	.	.
load_freq*load_rms_c	0	0		2.0305	0.07559	99	26.86	<.0001
load_freq*load_rms_c	0	1		Non-est	.	.	.	.
load_freq*load_rms_c	1	0		1.6996	0.07629	99	22.28	<.0001
load_freq*load_rms_c	1	1		Non-est	.	.	.	.
load_dur_cat			0	1.4839	0.07778	99	19.08	<.0001
load_du			1	Non-est	.	.	.	.

r_cat								
load_freq*load_dur_c	0		0	1.4630	0.09626	99	15.20	<.0001
load_freq*load_dur_c	0		1	Non-est	.	.	.	.
load_freq*load_dur_c	1		0	1.5047	0.08357	99	18.01	<.0001
load_freq*load_dur_c	1		1	Non-est	.	.	.	.
load_rms_*load_dur_c		0	0	1.5321	0.06636	99	23.09	<.0001
load_rms_*load_dur_c		0	1	2.1980	0.1102	99	19.95	<.0001
load_rms_*load_dur_c		1	0	1.4356	0.1365	99	10.51	<.0001

Differences of Least Squares Means						
Effect	**load_freq_cat**	**load_rms_cat**	**load_dur_cat**	**_load_freq_cat**	**_load_rms_cat**	**_load_dur_cat**
load_freq_cat	0			1		
load_rms_cat		0			1	
load_freq*load_rms_c	0	0		0	1	
load_freq*load_rms_c	0	0		1	0	
load_freq*load_rms_c	0	0		1	1	
load_freq*load_rms_c	0	1		1	0	
load_freq*load_rms_c	0	1		1	1	
load_freq*load_rms_c	1	0		1	1	
load_dur_cat			0			1
load_freq*load_dur_c	0		0	0		1
load_freq*load_dur_c	0		0	1		0
load_freq*l	0		0	1		1

oad_dur_c						
load_freq*load_dur_c	0		1	1		0
load_freq*load_dur_c	0		1	1		1
load_freq*load_dur_c	1		0	1		1
load_rms_*load_dur_c		0	0		0	1
load_rms_*load_dur_c		0	0		1	0
load_rms_*load_dur_c		0	1		1	0

Differences of Least Squares Means								
Effect	**load_freq_cat**	**load_rms_cat**	**load_dur_cat**	**_load_freq_cat**	**Estimate**	**Standard Error**	**DF**	**t Value**
load_freq_cat	0			1	0.2846	0.1029	99	2.77
load_rms_cat		0			Non-est	.	.	.
load_freq*load_rms_c	0	0		0	Non-est	.	.	.
load_fre	0	0		1	0.3309	0.07488	99	4.42

q*load_rms_c								
load_freq*load_rms_c	0	0		1	Non-est	.	.	.
load_freq*load_rms_c	0	1		1	Non-est	.	.	.
load_freq*load_rms_c	0	1		1	0.2383	0.1797	99	1.33
load_freq*load_rms_c	1	0		1	Non-est	.	.	.
load_dur_cat			0		Non-est	.	.	.
load_freq*load_dur_c	0		0	0	Non-est	.	.	.
load_freq*load_dur_c	0		0	1	-0.04163	0.09112	99	-0.46
load_freq*load_dur_c	0		0	1	Non-est	.	.	.
load_freq*load_dur_c	0		1	1	Non-est	.	.	.
load_freq*load_dur_c	0		1	1	0.6109	0.1555	99	3.93

load_freq*load_dur_c	1		0	1	Non-est	.	.	.
load_rms_*load_dur_c		0	0		-0.6659	0.1250	99	-5.33
load_rms_*load_dur_c		0	0		0.09647	0.1480	99	0.65
load_rms_*load_dur_c		0	1		0.7624	0.1751	99	4.35

Differences of Least Squares Means							
Effect	**load_freq_cat**	**load_rms_cat**	**load_dur_cat**	**_load_freq_cat**	**Pr > |t|**	**Adjustment**	**Adj P**
load_freq_cat	0			1	0.0067	Tukey	0.0067
load_rms_cat		0			.	Tukey-Kramer	.
load_freq*load_rms_c	0	0		0	.	Tukey-Kramer	.
load_freq*load_rms_c	0	0		1	<.0001	Tukey-Kramer	0.0001

load_freq *load_rms_c	0	0		1	.	Tukey-Kramer	.
load_freq *load_rms_c	0	1		1	.	Tukey-Kramer	.
load_freq *load_rms_c	0	1		1	0.1878	Tukey-Kramer	0.5485
load_freq *load_rms_c	1	0		1	.	Tukey-Kramer	.
load_dur_cat			0		.	Tukey-Kramer	.
load_freq *load_dur_c	0		0	0	.	Tukey-Kramer	.
load_freq *load_dur_c	0		0	1	0.6488	Tukey-Kramer	0.9681
load_freq *load_dur_c	0		0	1	.	Tukey-Kramer	.
load_freq *load_dur_c	0		1	1	.	Tukey-Kramer	.
load_freq *load_dur_c	0		1	1	0.0002	Tukey-Kramer	0.0009
load_freq *load_dur	1		0	1	.	Tukey-Kramer	.

_c							
load_rms_*load_dur_c		0	0		<.0001	Tukey-Kramer	<.0001
load_rms_*load_dur_c		0	0		0.5160	Tukey-Kramer	0.7917
load_rms_*load_dur_c		0	1		<.0001	Tukey-Kramer	<.0001
Moments							
N	158	**Sum Weights**	158				
Mean	0.0010897 3	**Sum Observations**	0.172178				
Std Deviation	0.4767085	**Variance**	0.2272509 9				
Skewness	0.6448302 4	**Kurtosis**	2.7930536				
Uncorrected SS	35.678593 7	**Corrected SS**	35.678406 1				
Coeff Variation	43745.392 8	**Std Error Mean**	0.0379248 9				

Basic Statistical Measures			
Location	**Variability**		
Mean	0.00109	**Std Deviation**	0.47671
Median	-0.04724	**Variance**	0.22725
Mode	-0.52976	**Range**	3.23540
		Interquartile Range	0.51449

Note: The mode displayed is the smallest of 3 modes with a count of 4.

Tests for Location: Mu0=0				
Test	**Statistic**	**p Value**		
Student's t	**t**	0.028734	**Pr > |t|**	0.9771
Sign	**M**	-5	**Pr >= |M|**	0.4741
Signed Rank	**S**	-357.5	**Pr >= |S|**	0.5365

Tests for Normality				
Test	**Statistic**	**p Value**		
Shapiro-Wilk	**W**	0.946703	**Pr < W**	<0.0001
Kolmogorov-Smirnov	**D**	0.078623	**Pr > D**	0.0179
Cramer-von	**W-Sq**	0.283729	**Pr > W-Sq**	<0.0050

Mises				
Anderson-Darling	A-Sq	1.924588	Pr > A-Sq	<0.0050

Quantiles (Definition 5)	
Quantile	Estimate
100% Max	1.835753
99%	1.736144
95%	0.779469
90%	0.591647
75% Q3	0.237723
50% Median	-0.047241
25% Q1	-0.276762
10%	-0.527767
5%	-0.573259
1%	-1.318281
0% Min	-1.399643

Extreme Observations			
Lowest	Highest		
Value	Obs	Value	Obs
-1.399643	33	1.01601	20
-1.318281	29	1.26906	6

-1.087836	42	1.54281	9
-1.087836	24	1.73614	19
-0.983861	34	1.83575	5

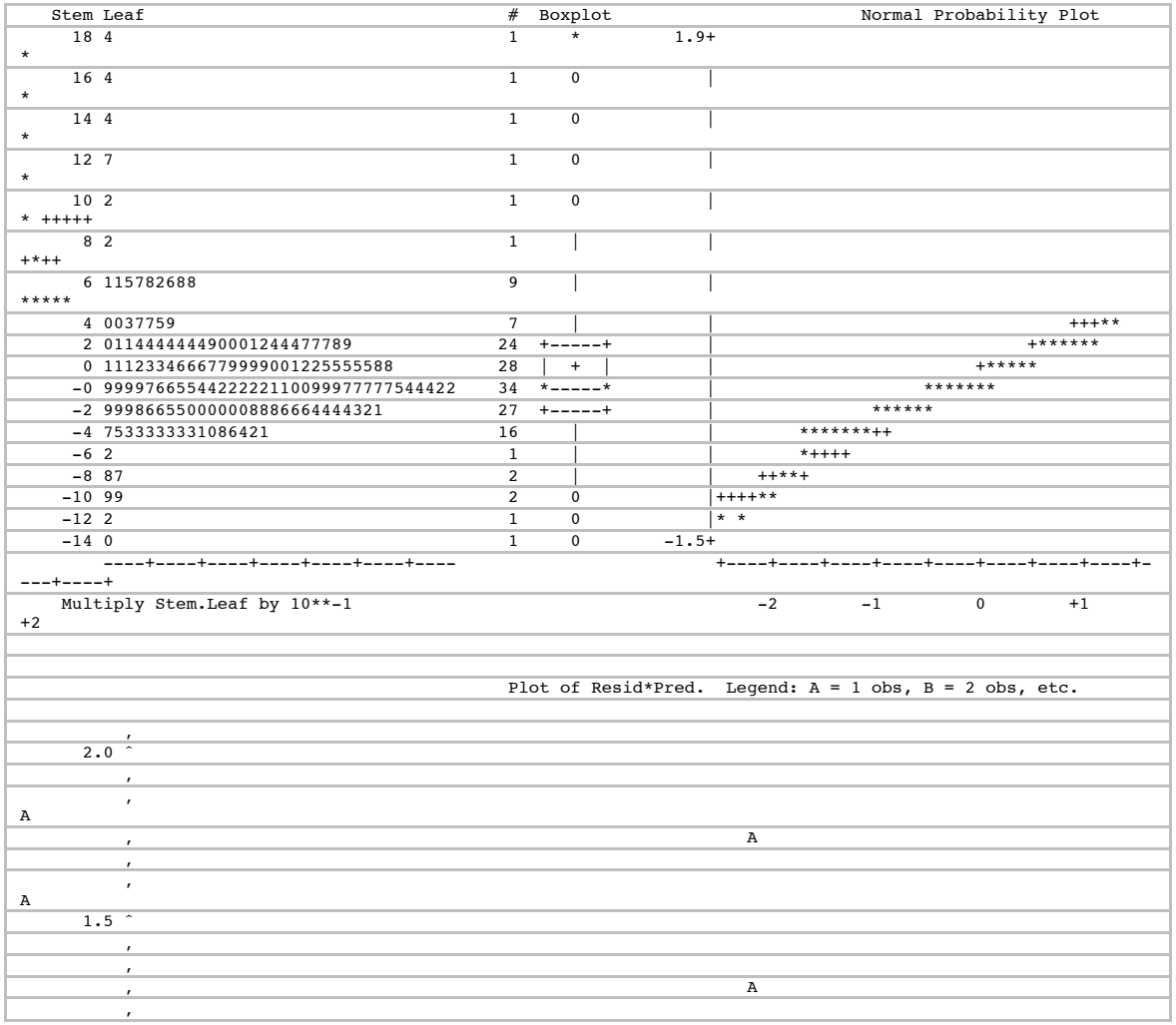

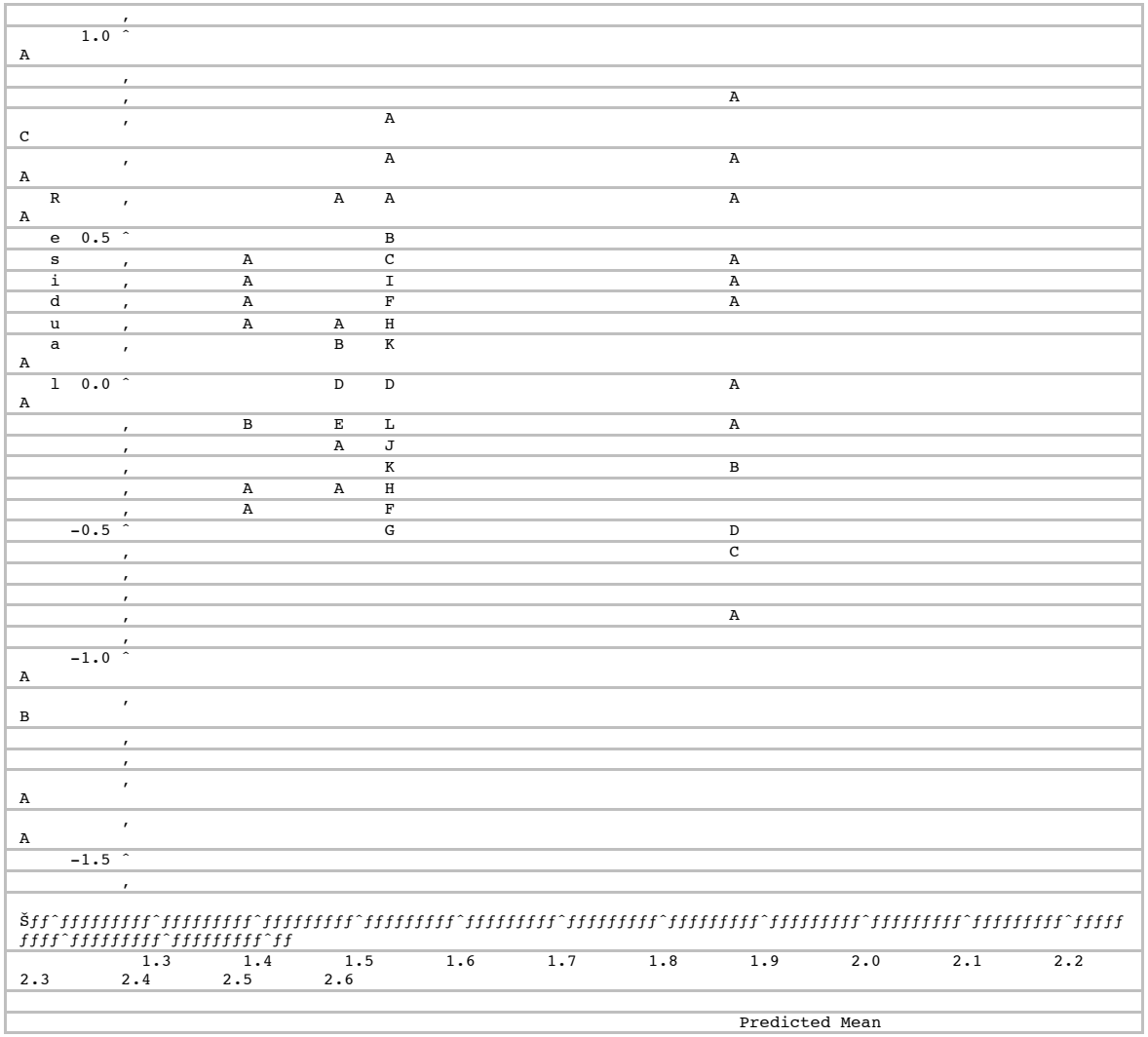
1.0
0.5
0.0
-0.5
-1.0
-1.5
A
C
B
D
E
F
G
H
I
J
K
L
1.3
1.4
1.5
1.6
1.7
1.8
1.9
2.0
2.1
2.2
2.3
2.4
2.5
2.6
Predicted Mean

Obj. 2 Data Biglycan ANOVA Results

Model Information	
Data Set	WORK.ANIM
Dependent Variable	sqrt_Biglycan
Covariance Structure	Variance Components
Estimation Method	REML
Residual Variance Method	Profile
Fixed Effects SE Method	Model-Based
Degrees of Freedom Method	Containment

Class Level Information		
Class	**Levels**	**Values**
load_freq_cat	2	0 1
load_rms_cat	2	0 1
load_dur_cat	2	0 1
block	54	1 2 3 4 5 6 7 8 9 10 11 12 13 14 15 16 17 18 19 20 21 22 23 24 25 26 27 28 29 30 31 32 33 34 35 36 37 38 39 40 41 42 57 58 59 60 61 62 63 64 65 66 67 68

Dimensions	
Covariance Parameters	2
Columns in X	18
Columns in Z	54
Subjects	1
Max Obs Per Subject	158

Number of Observations	
Number of Observations Read	158
Number of Observations Used	158
Number of Observations Not Used	0

Iteration History			
Iteration	**Evaluations**	**-2 Res Log Like**	**Criterion**
0	1	140.18697502	
1	2	129.55886087	0.00000001

Convergence criteria met.

Covariance Parameter Estimates				
Cov Parm	**Estimate**	**Standard Error**	**Z Value**	**Pr > Z**
block	0.03772	0.01480	2.55	0.0054
Residual	0.09417	0.01327	7.09	<.0001

Fit Statistics	
-2 Res Log Likelihood	129.6
AIC (smaller is better)	133.6
AICC (smaller is better)	133.6
BIC (smaller is better)	137.5

Type 3 Tests of Fixed Effects				
Effect	**Num DF**	**Den DF**	**F Value**	**Pr > F**
load_freq_cat	1	99	0.52	0.4736
load_rms_cat	1	99	10.92	0.0013
load_freq*load_rms_c	1	99	4.71	0.0325
load_dur_cat	1	99	3.69	0.0578
load_freq*load_dur_c	1	99	3.59	0.0610
load_rms_*load_dur_c	0	.	.	.

Least Squares Means								
Effect	load_freq_cat	load_rms_cat	load_dur_cat	Estimate	Standard Error	DF	t Value	Pr > |t|
load_freq_cat	0			Non-est	.	.	.	.
load_freq_cat	1			Non-est	.	.	.	.
load_rms_cat		0		1.5936	0.04449	99	35.82	<.0001
load_rms_cat		1		Non-est	.	.	.	.
load_freq*load_rms_c	0	0		1.7123	0.05556	99	30.82	<.0001
load_freq*load_rms_c	0	1		Non-est	.	.	.	.
load_freq*load_rms_c	1	0		1.4750	0.05473	99	26.95	<.0001
load_freq*load_rms_c	1	1		Non-est	.	.	.	.
load_dur_cat			0	1.6826	0.05317	99	31.65	<.0001
load_du			1	Non-est	.	.	.	.

r_cat								
load_freq*load_dur_c	0		0	1.6531	0.07179	99	23.03	<.0001
load_freq*load_dur_c	0		1	Non-est	.	.	.	.
load_freq*load_dur_c	1		0	1.7121	0.06035	99	28.37	<.0001
load_freq*load_dur_c	1		1	Non-est	.	.	.	.
load_rms_*load_dur_c		0	0	1.5103	0.04512	99	33.47	<.0001
load_rms_*load_dur_c		0	1	1.6770	0.07546	99	22.22	<.0001
load_rms_*load_dur_c		1	0	1.8549	0.09515	99	19.49	<.0001

Differences of Least Squares Means						
Effect	**load_freq_cat**	**load_rms_cat**	**load_dur_cat**	**_load_freq_cat**	**_load_rms_cat**	**_load_dur_cat**
load_freq_cat	0			1		
load_rms_cat		0			1	
load_freq*load_rms_c	0	0		0	1	
load_freq*load_rms_c	0	0		1	0	
load_freq*load_rms_c	0	0		1	1	
load_freq*load_rms_c	0	1		1	0	
load_freq*load_rms_c	0	1		1	1	
load_freq*load_rms_c	1	0		1	1	
load_dur_cat			0			1
load_freq*load_dur_c	0		0	0		1
load_freq*load_dur_c	0		0	1		0
load_freq*l	0		0	1		1

oad_dur_c						
load_freq*load_dur_c	0		1	1		0
load_freq*load_dur_c	0		1	1		1
load_freq*load_dur_c	1		0	1		1
load_rms_*load_dur_c		0	0		0	1
load_rms_*load_dur_c		0	0		1	0
load_rms_*load_dur_c		0	1		1	0

Differences of Least Squares Means								
Effect	**load_freq_cat**	**load_rms_cat**	**load_dur_cat**	**_load_freq_cat**	**Estimate**	**Standard Error**	**DF**	**t Value**
load_freq_cat	0			1	0.06480	0.09007	99	0.72
load_rms_cat		0			Non-est	.	.	.
load_freq*load_rms_c	0	0		0	Non-est	.	.	.
load_fre	0	0		1	0.2373	0.06517	99	3.64

q*load_rms_c								
load_freq*load_rms_c	0	0		1	Non-est	.	.	.
load_freq*load_rms_c	0	1		1	Non-est	.	.	.
load_freq*load_rms_c	0	1		1	-0.1077	0.1569	99	-0.69
load_freq*load_rms_c	1	0		1	Non-est	.	.	.
load_dur_cat			0		Non-est	.	.	.
load_freq*load_dur_c	0		0	0	Non-est	.	.	.
load_freq*load_dur_c	0		0	1	-0.05904	0.07928	99	-0.74
load_freq*load_dur_c	0		0	1	Non-est	.	.	.
load_freq*load_dur_c	0		1	1	Non-est	.	.	.
load_freq*load_dur_c	0		1	1	0.1886	0.1360	99	1.39

load_freq*load_dur_c	1		0	1	Non-est	.	.	.
load_rms_*load_dur_c		0	0		-0.1667	0.08685	99	-1.92
load_rms_*load_dur_c		0	0		-0.3446	0.1043	99	-3.30
load_rms_*load_dur_c		0	1		-0.1779	0.1214	99	-1.47

Differences of Least Squares Means							
Effect	**load_freq_cat**	**load_rms_cat**	**load_dur_cat**	**_load_freq_cat**	**Pr > |t|**	**Adjustment**	**Adj P**
load_freq_cat	0			1	0.4736	Tukey	0.4736
load_rms_cat		0			.	Tukey-Kramer	.
load_freq*load_rms_c	0	0		0	.	Tukey-Kramer	.
load_freq*load_rms_c	0	0		1	0.0004	Tukey-Kramer	0.0024
load_freq	0	0		1	.	Tukey-	.

***load_rms_c**						Kramer	
load_freq *load_rms_c	0	1		1	.	Tukey-Kramer	.
load_freq *load_rms_c	0	1		1	0.4941	Tukey-Kramer	0.9021
load_freq *load_rms_c	1	0		1	.	Tukey-Kramer	.
load_dur_cat			0		.	Tukey-Kramer	.
load_freq *load_dur_c	0		0	0	.	Tukey-Kramer	.
load_freq *load_dur_c	0		0	1	0.4582	Tukey-Kramer	0.8787
load_freq *load_dur_c	0		0	1	.	Tukey-Kramer	.
load_freq *load_dur_c	0		1	1	.	Tukey-Kramer	.
load_freq *load_dur_c	0		1	1	0.1684	Tukey-Kramer	0.5101
load_freq *load_dur_c	1		0	1	.	Tukey-Kramer	.

load_rms_*load_dur_c		0	0		0.0578	Tukey-Kramer	0.1385
load_rms_*load_dur_c		0	0		0.0013	Tukey-Kramer	0.0038
load_rms_*load_dur_c		0	1		0.1460	Tukey-Kramer	0.3121

Moments							
N	158	**Sum Weights**	158				
Mean	-0.0016765	**Sum Observations**	-0.2648866				
Std Deviation	0.35611766	**Variance**	0.12681979				
Skewness	0.3227538	**Kurtosis**	-0.336775				
Uncorrected SS	19.911150 7	**Corrected SS**	19.910706 7				
Coeff Variation	-21241.762	**Std Error Mean**	0.0283312				

Basic Statistical Measures			
Location	**Variability**		
Mean	-0.00168	**Std Deviation**	0.35612
Median	-0.05145	**Variance**	0.12682
Mode	0.11526	**Range**	1.73123
		Interquartile Range	0.53214

Note: The mode displayed is the smallest of 3 modes with a count of 4.

Tests for Location: Mu0=0				
Test	**Statistic**	**p Value**		
Student's t	**t**	-0.05917	**Pr > |t|**	0.9529
Sign	**M**	-6	**Pr >= |M|**	0.3816
Signed Rank	**S**	-245.5	**Pr >= |S|**	0.6714

Tests for Normality				
Test	**Statistic**	**p Value**		
Shapiro-Wilk	**W**	0.986198	**Pr < W**	0.1193
Kolmogorov-Smirnov	**D**	0.069	**Pr > D**	0.0656
Cramer-von	**W-Sq**	0.128258	**Pr > W-Sq**	0.0470

Mises				
Anderson-Darling	A-Sq	0.708849	Pr > A-Sq	0.0664

Quantiles (Definition 5)	
Quantile	Estimate
100% Max	0.9460421
99%	0.9227238
95%	0.6107049
90%	0.4910623
75% Q3	0.2660323
50% Median	-0.0514518
25% Q1	-0.2661097
10%	-0.4400552
5%	-0.5316237
1%	-0.7391022
0% Min	-0.7851834

Extreme Observations			
Lowest	Highest		
Value	Obs	Value	Obs
-0.785183	17	0.721681	25
-0.739102	109	0.804774	137

-0.685537	91	0.812077	116
-0.651554	90	0.922724	9
-0.584772	33	0.946042	103

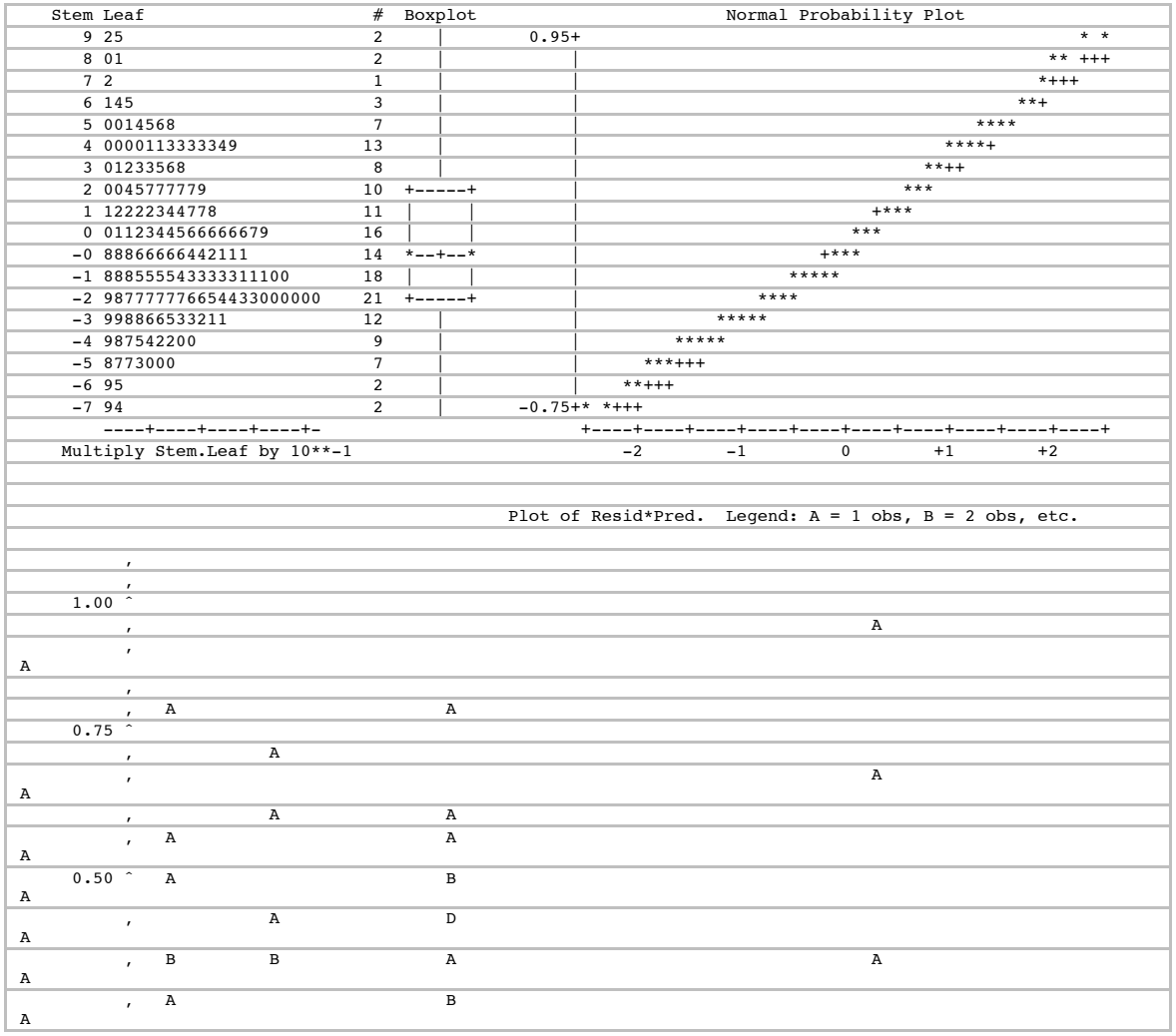

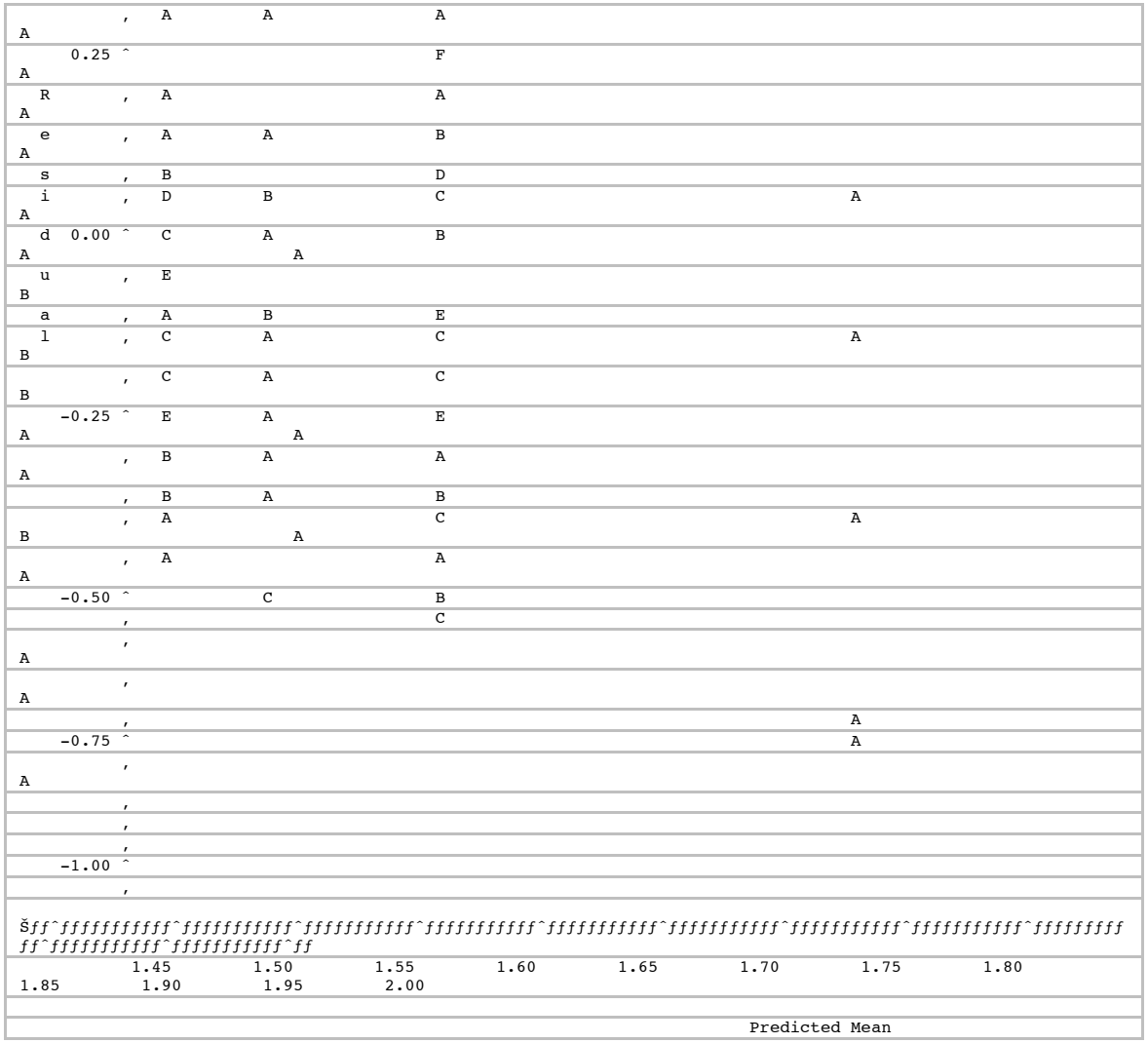
A A A
A
0.25 ^ F
A
R , A A
A
e , A A B
A
s , B D
i , D B C A
A
d 0.00 ^ C A B
A A
u , E
B
a , A B E
l , C A C A
B
, C A C
B
-0.25 ^ E A E
A A
, B A A
A
, B A B
, A C A
B A
, A A
A
-0.50 ^ C B
, C
,
A
,
A
, A
-0.75 ^ A
,
A
,
,
,
-1.00 ^
,
Šƒƒˆƒƒƒƒƒƒƒƒˆƒƒƒƒƒƒƒƒˆƒƒƒƒƒƒƒƒˆƒƒƒƒƒƒƒƒˆƒƒƒƒƒƒƒƒˆƒƒƒƒƒƒƒƒˆƒƒƒƒƒƒƒƒˆƒƒƒƒƒƒƒƒˆƒƒƒƒƒƒƒƒˆƒƒƒƒƒƒƒƒˆƒƒƒƒƒƒƒƒˆƒƒ
1.45 1.50 1.55 1.60 1.65 1.70 1.75 1.80
1.85 1.90 1.95 2.00
Predicted Mean

Obj. 2 Data Collagen Type I ANOVA Results

Model Information	
Data Set	WORK.ANIM
Dependent Variable	sqrt_Collagen1
Covariance Structure	Variance Components
Estimation Method	REML
Residual Variance Method	Profile
Fixed Effects SE Method	Model-Based
Degrees of Freedom Method	Containment

Class Level Information		
Class	**Levels**	**Values**
load_freq_cat	2	0 1
load_rms_cat	2	0 1
load_dur_cat	2	0 1
block	54	1 2 3 4 5 6 7 8 9 10 11 12 13 14 15 16 17 18 19 20 21 22 23 24 25 26 27 28 29 30 31 32 33 34 35 36 37 38 39 40 41 42 57 58 59 60 61 62 63 64 65 66 67 68

Dimensions	
Covariance Parameters	2
Columns in X	18
Columns in Z	54
Subjects	1
Max Obs Per Subject	152

Number of Observations	
Number of Observations Read	152
Number of Observations Used	152
Number of Observations Not Used	0

Iteration History			
Iteration	**Evaluations**	**-2 Res Log Like**	**Criterion**
0	1	1049.87644833	
1	2	927.49855149	0.02116857
2	1	918.27837086	0.01231063
3	1	913.14258650	0.00489827
4	1	911.21846767	0.00094918
5	1	910.87570965	0.00004471
6	1	910.86087810	0.00000011
7	1	910.86084122	0.00000000

Convergence criteria met.

Covariance Parameter Estimates				
Cov Parm	**Estimate**	**Standard Error**	**Z Value**	**Pr > Z**
block	119.43	28.3018	4.22	<.0001
Residual	6.7031	1.0853	6.18	<.0001

Fit Statistics	
-2 Res Log Likelihood	910.9
AIC (smaller is better)	914.9
AICC (smaller is better)	914.9
BIC (smaller is better)	918.8

Type 3 Tests of Fixed Effects				
Effect	**Num DF**	**Den DF**	**F Value**	**Pr > F**
load_freq_cat	1	93	16.10	0.0001
load_rms_cat	1	93	0.07	0.7914
load_freq*load_rms_c	1	93	0.07	0.7892
load_dur_cat	1	93	2.87	0.0934
load_freq*load_dur_c	1	93	27.34	<.0001

load_rms_*load_dur_c	0	.	.	.

Least Squares Means								
Effect	**load_freq_cat**	**load_rms_cat**	**load_dur_cat**	**Estimate**	**Standard Error**	**DF**	**t Value**	**Pr > |t|**
load_freq_cat	0			Non-est	.	.	.	.
load_freq_cat	1			Non-est	.	.	.	.
load_rms_cat		0		7.6541	1.6266	93	4.71	<.0001
load_rms_cat		1		Non-est	.	.	.	.
load_freq*load_rms_c	0	0		9.4739	1.6334	93	5.80	<.0001
load_freq*load_rms_c	0	1		Non-est	.	.	.	.
load_freq*load_rms_c	1	0		5.8344	1.6858	93	3.46	0.0008
load_freq*load_rms_c	1	1		Non-est	.	.	.	.

load_dur_cat			0	5.7062	1.7231	93	3.31	0.0013
load_dur_cat			1	Non-est	.	.	.	.
load_freq*load_dur_c	0		0	5.6995	1.8003	93	3.17	0.0021
load_freq*load_dur_c	0		1	Non-est	.	.	.	.
load_freq*load_dur_c	1		0	5.7129	1.7201	93	3.32	0.0013
load_freq*load_dur_c	1		1	Non-est	.	.	.	.
load_rms_*load_dur_c		0	0	5.9826	1.5942	93	3.75	0.0003
load_rms_*load_dur_c		0	1	9.3257	2.1669	93	4.30	<.0001
load_rms_*load_dur_c		1	0	5.4298	2.3596	93	2.30	0.0236

Differences of Least Squares Means						
Effect	**load_freq_cat**	**load_rms_cat**	**load_dur_cat**	**_load_freq_cat**	**_load_rms_cat**	**_load_dur_cat**
load_freq_cat	0			1		
load_rms_cat		0			1	
load_freq*load_rms_c	0	0		0	1	
load_freq*load_rms_c	0	0		1	0	
load_freq*load_rms_c	0	0		1	1	
load_freq*load_rms_c	0	1		1	0	
load_freq*load_rms_c	0	1		1	1	
load_freq*load_rms_c	1	0		1	1	
load_dur_cat			0			1
load_freq*load_dur_c	0		0	0		1
load_freq*load_dur_c	0		0	1		0
load_freq*l	0		0	1		1

oad_dur_c						
load_freq*load_dur_c	0		1	1		0
load_freq*load_dur_c	0		1	1		1
load_freq*load_dur_c	1		0	1		1
load_rms_*load_dur_c		0	0		0	1
load_rms_*load_dur_c		0	0		1	0
load_rms_*load_dur_c		0	1		1	0

Differences of Least Squares Means								
Effect	**load_freq_cat**	**load_rms_cat**	**load_dur_cat**	**_load_freq_cat**	**Estimate**	**Standard Error**	**DF**	**t Value**
load_freq_cat	0			1	3.4454	0.8588	93	4.01
load_rms_cat		0			Non-est	.	.	.
load_freq*load_rms_c	0	0		0	Non-est	.	.	.
load_fre	0	0		1	3.6396	0.6601	93	5.51

q*load_rms_c								
load_freq*load_rms_c	0	0		1	Non-est	.	.	.
load_freq*load_rms_c	0	1		1	Non-est	.	.	.
load_freq*load_rms_c	0	1		1	3.2511	1.4454	93	2.25
load_freq*load_rms_c	1	0		1	Non-est	.	.	.
load_dur_cat			0		Non-est	.	.	.
load_freq*load_dur_c	0		0	0	Non-est	.	.	.
load_freq*load_dur_c	0		0	1	-0.01345	0.7233	93	-0.02
load_freq*load_dur_c	0		0	1	Non-est	.	.	.
load_freq*load_dur_c	0		1	1	Non-est	.	.	.
load_freq*load_dur_c	0		1	1	6.9042	1.3517	93	5.11

load_freq*load_dur_c	1		0	1	Non-est	.	.	.
load_rms_*load_dur_c		0	0		-3.3432	1.9722	93	-1.70
load_rms_*load_dur_c		0	0		0.5527	2.0837	93	0.27
load_rms_*load_dur_c		0	1		3.8959	2.7897	93	1.40

Differences of Least Squares Means							
Effect	**load_freq_cat**	**load_rms_cat**	**load_dur_cat**	**_load_freq_cat**	**Pr > |t|**	**Adjustment**	**Adj P**
load_freq_cat	0			1	0.0001	Tukey	0.0001
load_rms_cat		0			.	Tukey-Kramer	.
load_freq*load_rms_c	0	0		0	.	Tukey-Kramer	.
load_freq*load_rms_c	0	0		1	<.0001	Tukey-Kramer	<.0001
load_freq	0	0		1	.	Tukey-	.

***load_rms_c**						Kramer	
load_freq *load_rms_c	0	1		1	.	Tukey-Kramer	.
load_freq *load_rms_c	0	1		1	0.0268	Tukey-Kramer	0.1177
load_freq *load_rms_c	1	0		1	.	Tukey-Kramer	.
load_dur_cat			0		.	Tukey-Kramer	.
load_freq *load_dur_c	0		0	0	.	Tukey-Kramer	.
load_freq *load_dur_c	0		0	1	0.9852	Tukey-Kramer	1.0000
load_freq *load_dur_c	0		0	1	.	Tukey-Kramer	.
load_freq *load_dur_c	0		1	1	.	Tukey-Kramer	.
load_freq *load_dur_c	0		1	1	<.0001	Tukey-Kramer	<.0001
load_freq *load_dur_c	1		0	1	.	Tukey-Kramer	.

load_rms_*load_dur_c		0	0		0.0934	Tukey-Kramer	0.2125
load_rms_*load_dur_c		0	0		0.7914	Tukey-Kramer	0.9620
load_rms_*load_dur_c		0	1		0.1659	Tukey-Kramer	0.3469

Moments							
N	152	**Sum Weights**	152				
Mean	-0.9004039	**Sum Observations**	-136.86139				
Std Deviation	10.083219	**Variance**	101.671305				
Skewness	2.93701388	**Kurtosis**	7.6208806				
Uncorrected SS	15475.5976	**Corrected SS**	15352.3671				
Coeff Variation	-1119.8551	**Std Error Mean**	0.81785706				

Basic Statistical Measures			
Location	**Variability**		
Mean	-0.90040	**Std Deviation**	10.08322
Median	-3.80733	**Variance**	101.67131
Mode	-4.80015	**Range**	52.72641
		Interquartile Range	1.15808

Note: The mode displayed is the smallest of 4 modes with a count of 3.

Tests for Location: Mu0=0				
Test	**Statistic**	**p Value**		
Student's t	**t**	-1.10093	**Pr > |t|**	0.2727
Sign	**M**	-61	**Pr >= |M|**	<.0001
Signed Rank	**S**	-3775	**Pr >= |S|**	<.0001

Tests for Normality				
Test	**Statistic**	**p Value**		
Shapiro-Wilk	**W**	0.465949	**Pr < W**	<0.0001
Kolmogorov-Smirnov	**D**	0.407733	**Pr > D**	<0.0100
Cramer-von	**W-Sq**	7.448182	**Pr > W-Sq**	<0.0050

Mises				
Anderson-Darling	**A-Sq**	36.30292	**Pr > A-Sq**	<0.0050

Quantiles (Definition 5)	
Quantile	**Estimate**
100% Max	40.9423622
99%	38.2161738
95%	29.7298001
90%	-0.0692516
75% Q3	-3.1709095
50% Median	-3.8073312
25% Q1	-4.3289902
10%	-4.7765373
5%	-4.9820693
1%	-11.5558307
0% Min	-11.7840501

Extreme Observations			
Lowest	**Highest**		
Value	**Obs**	**Value**	**Obs**
-11.7841	23	34.7948	5
-11.5558	27	35.6277	13

-11.4120	18	37.9373	12
-11.3583	36	38.2162	10
-10.1436	28	40.9424	1

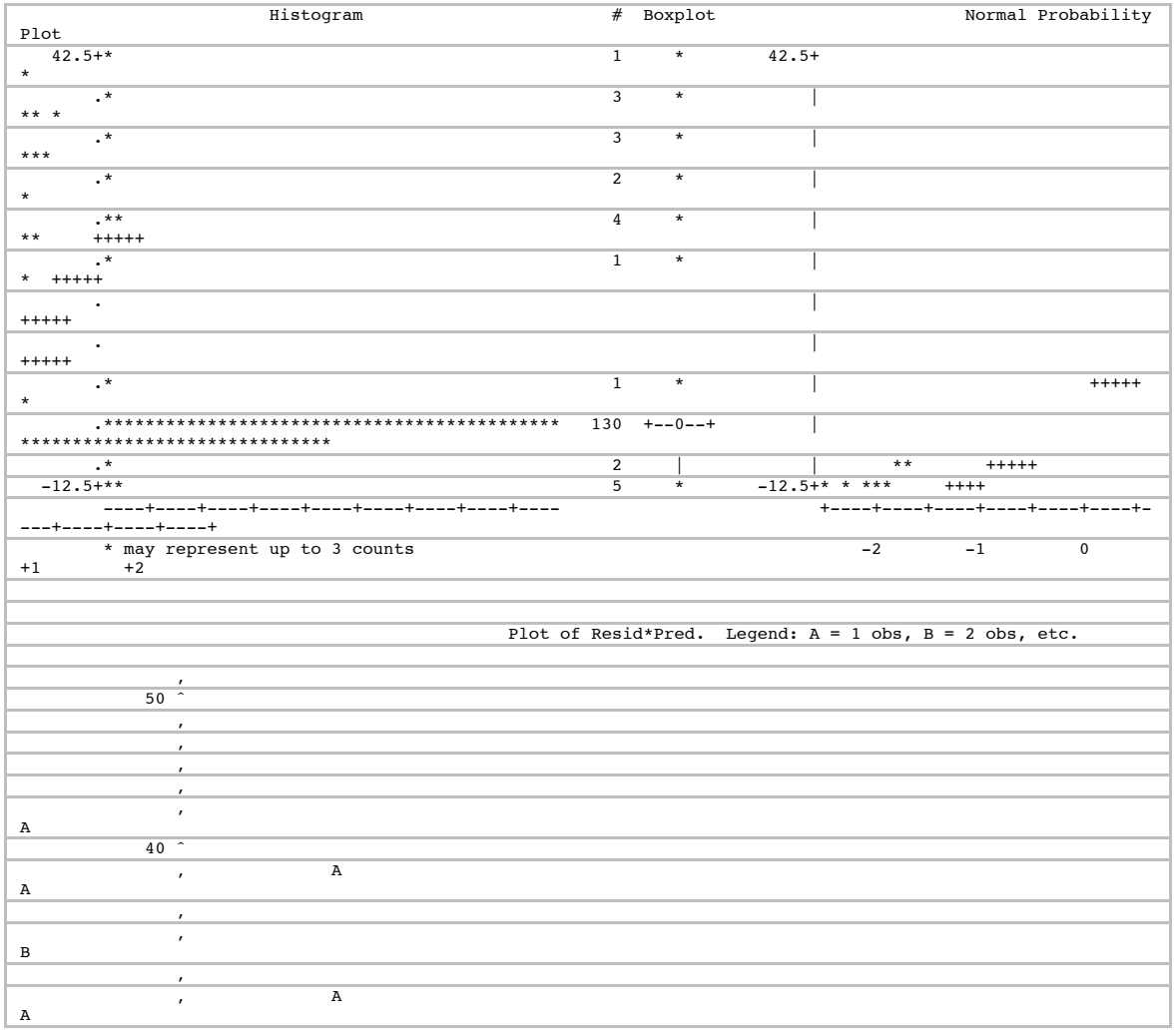

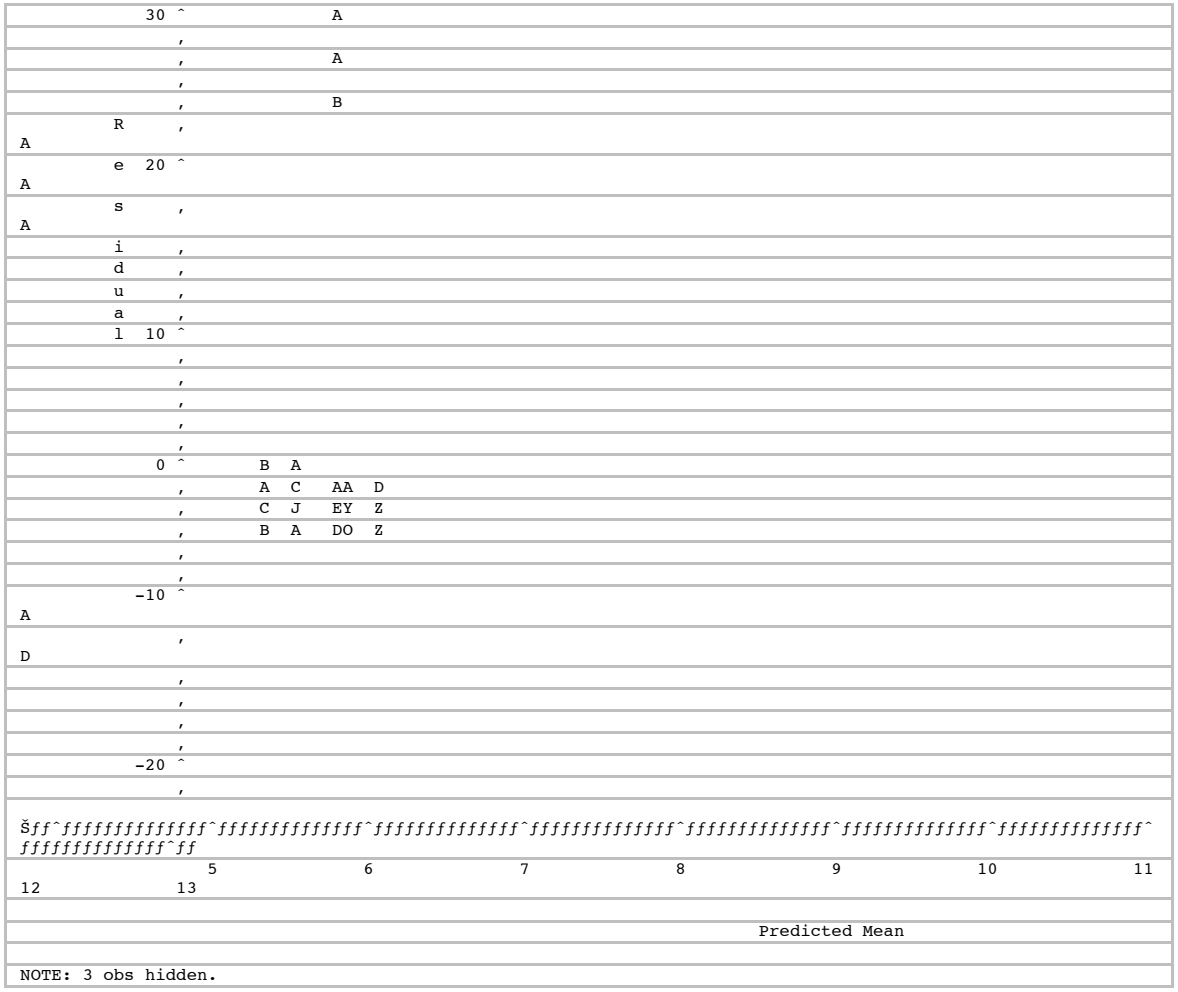

NOTE: 3 obs hidden.

Obj. 2 Data Collagen Type II ANOVA Results

Model Information	
Data Set	WORK.ANIM
Dependent Variable	sqrt_Collagen2
Covariance Structure	Variance Components
Estimation Method	REML
Residual Variance Method	Profile
Fixed Effects SE Method	Model-Based
Degrees of Freedom Method	Containment

Class Level Information		
Class	**Levels**	**Values**
load_freq_cat	2	0 1
load_rms_cat	2	0 1
load_dur_cat	2	0 1
block	54	1 2 3 4 5 6 7 8 9 10 11 12 13 14 15 16 17 18 19 20 21 22 23 24 25 26 27 28 29 30 31 32 33 34 35 36 37 38 39 40 41 42 57 58 59 60 61 62 63 64 65 66 67 68

Dimensions	
Covariance Parameters	2
Columns in X	18
Columns in Z	54
Subjects	1
Max Obs Per Subject	157

Number of Observations	
Number of Observations Read	157
Number of Observations Used	157
Number of Observations Not Used	0

Iteration History			
Iteration	**Evaluations**	**-2 Res Log Like**	**Criterion**
0	1	346.68072115	
1	2	316.57894907	0.01300529
2	1	316.29760005	0.00045304
3	1	316.28860247	0.00000064
4	1	316.28859006	0.00000000

Convergence criteria met.

Covariance Parameter Estimates				
Cov Parm	**Estimate**	**Standard Error**	**Z Value**	**Pr > Z**
block	0.2925	0.08094	3.61	0.0002
Residual	0.2593	0.03749	6.92	<.0001

Fit Statistics	
-2 Res Log Likelihood	316.3
AIC (smaller is better)	320.3
AICC (smaller is better)	320.4
BIC (smaller is better)	324.3

Type 3 Tests of Fixed Effects				
Effect	**Num DF**	**Den DF**	**F Value**	**Pr > F**
load_freq_cat	1	98	0.14	0.7132
load_rms_cat	1	98	2.31	0.1317
load_freq*load_rms_c	1	98	1.45	0.2322
load_dur_cat	1	98	17.28	<.0001
load_freq*load_dur_c	1	98	1.25	0.2659
load_rms_*load_dur_c	0	.	.	.

Least Squares Means								
Effect	load_freq_cat	load_rms_cat	load_dur_cat	Estimate	Standard Error	DF	t Value	Pr > |t|
load_freq_cat	0			Non-est	.	.	.	.
load_freq_cat	1			Non-est	.	.	.	.
load_rms_cat		0		2.0923	0.1025	98	20.40	<.0001
load_rms_cat		1		Non-est	.	.	.	.
load_freq*load_rms_c	0	0		2.2028	0.1159	98	19.01	<.0001
load_freq*load_rms_c	0	1		Non-est	.	.	.	.
load_freq*load_rms_c	1	0		1.9817	0.1182	98	16.77	<.0001
load_freq*load_rms_c	1	1		Non-est	.	.	.	.
load_dur_cat			0	1.8639	0.1201	98	15.52	<.0001

load_dur_cat			1	Non-est	.	.	.	.
load_freq*load_dur_c	0		0	1.8289	0.1471	98	12.43	<.0001
load_freq*load_dur_c	0		1	Non-est	.	.	.	.
load_freq*load_dur_c	1		0	1.8988	0.1283	98	14.80	<.0001
load_freq*load_dur_c	1		1	Non-est	.	.	.	.
load_rms_*load_dur_c		0	0	1.6912	0.1026	98	16.49	<.0001
load_rms_*load_dur_c		0	1	2.4933	0.1707	98	14.61	<.0001
load_rms_*load_dur_c		1	0	2.0366	0.2101	98	9.69	<.0001

Differences of Least Squares Means						
Effect	**load_freq_cat**	**load_rms_cat**	**load_dur_cat**	**_load_freq_cat**	**_load_rms_cat**	**_load_dur_cat**

load_freq_cat	0			1		
load_rms_cat		0			1	
load_freq*load_rms_c	0	0		0	1	
load_freq*load_rms_c	0	0		1	0	
load_freq*load_rms_c	0	0		1	1	
load_freq*load_rms_c	0	1		1	0	
load_freq*load_rms_c	0	1		1	1	
load_freq*load_rms_c	1	0		1	1	
load_dur_cat			0			1
load_freq*load_dur_c	0		0	0		1
load_freq*load_dur_c	0		0	1		0
load_freq*load_dur_c	0		0	1		1
load_freq*load_dur_c	0		1	1		0
load_freq*load_dur_c	0		1	1		1

load_freq*load_dur_c	1		0	1		1
load_rms_*load_dur_c		0	0		0	1
load_rms_*load_dur_c		0	0		1	0
load_rms_*load_dur_c		0	1		1	0

Differences of Least Squares Means								
Effect	**load_freq_cat**	**load_rms_cat**	**load_dur_cat**	**_load_freq_cat**	**Estimate**	**Standard Error**	**DF**	**t Value**
load_freq_cat	0			1	0.05684	0.1542	98	0.37
load_rms_cat		0			Non-est	.	.	.
load_freq*load_rms_c	0	0		0	Non-est	.	.	.
load_freq*load_rms_c	0	0		1	0.2211	0.1128	98	1.96
load_freq*load_rms_c	0	0		1	Non-est	.	.	.

load_freq*load_rms_c	0	1		1	Non-est	.	.	.
load_freq*load_rms_c	0	1		1	-0.1074	0.2686	98	-0.40
load_freq*load_rms_c	1	0		1	Non-est	.	.	.
load_dur_cat			0		Non-est	.	.	.
load_freq*load_dur_c	0		0	0	Non-est	.	.	.
load_freq*load_dur_c	0		0	1	-0.06992	0.1360	98	-0.51
load_freq*load_dur_c	0		0	1	Non-est	.	.	.
load_freq*load_dur_c	0		1	1	Non-est	.	.	.
load_freq*load_dur_c	0		1	1	0.1836	0.2339	98	0.78
load_freq*load_dur_c	1		0	1	Non-est	.	.	.
load_rms_*load_		0	0		-0.8021	0.1930	98	-4.16

dur_c								
load_rms_*load_dur_c		0	0		-0.3454	0.2272	98	-1.52
load_rms_*load_dur_c		0	1		0.4568	0.2701	98	1.69

Differences of Least Squares Means							
Effect	**load_freq_cat**	**load_rms_cat**	**load_dur_cat**	**_load_freq_cat**	**Pr > |t|**	**Adjustment**	**Adj P**
load_freq_cat	0			1	0.7132	Tukey	0.7132
load_rms_cat		0			.	Tukey-Kramer	.
load_freq*load_rms_c	0	0		0	.	Tukey-Kramer	.
load_freq*load_rms_c	0	0		1	0.0529	Tukey-Kramer	0.2105
load_freq*load_rms_c	0	0		1	.	Tukey-Kramer	.
load_freq*load_rms_c	0	1		1	.	Tukey-Kramer	.

load_freq *load_rms_c	0	1		1	0.6902	Tukey-Kramer	0.9783
load_freq *load_rms_c	1	0		1	.	Tukey-Kramer	.
load_dur_cat			0		.	Tukey-Kramer	.
load_freq *load_dur_c	0		0	0	.	Tukey-Kramer	.
load_freq *load_dur_c	0		0	1	0.6084	Tukey-Kramer	0.9556
load_freq *load_dur_c	0		0	1	.	Tukey-Kramer	.
load_freq *load_dur_c	0		1	1	.	Tukey-Kramer	.
load_freq *load_dur_c	0		1	1	0.4344	Tukey-Kramer	0.8611
load_freq *load_dur_c	1		0	1	.	Tukey-Kramer	.
load_rms_*load_dur_c		0	0		<.0001	Tukey-Kramer	0.0002
load_rms_*load_d		0	0		0.1317	Tukey-Kramer	0.2860

ur_c							
load_rms_*load_dur_c		0	1		0.0939	Tukey-Kramer	0.2136

Moments							
N	157	**Sum Weights**	157				
Mean	-0.0138743	**Sum Observations**	-2.1782695				
Std Deviation	0.70947769	**Variance**	0.5033586				
Skewness	2.19358346	**Kurtosis**	12.050803 6				
Uncorrected SS	78.554163 1	**Corrected SS**	78.523941 1				
Coeff Variation	-5113.6004	**Std Error Mean**	0.0566224 8				

Basic Statistical Measures			
Location	**Variability**		
Mean	-0.01387	**Std Deviation**	0.70948
Median	-0.11352	**Variance**	0.50336
Mode	-0.24837	**Range**	6.31203
		Interquartile Range	0.68740

Note: The mode displayed is the smallest of 3 modes with a count of 3.

Tests for Location: Mu0=0				
Test	**Statistic**	**p Value**		
Student's t	**t**	-0.24503	**Pr > |t|**	0.8068
Sign	**M**	-12.5	**Pr >= |M|**	0.0551
Signed Rank	**S**	-839.5	**Pr >= |S|**	0.1417

Tests for Normality				
Test	**Statistic**	**p Value**		
Shapiro-Wilk	**W**	0.860306	**Pr < W**	<0.0001
Kolmogorov-Smirnov	**D**	0.100138	**Pr > D**	<0.0100
Cramer-von Mises	**W-Sq**	0.553162	**Pr > W-Sq**	<0.0050
Anderson-Darling	**A-Sq**	3.25444	**Pr > A-Sq**	<0.0050

Quantiles (Definition 5)	
Quantile	**Estimate**
100% Max	4.644779
99%	2.611009

95%	1.189124
90%	0.712086
75% Q3	0.296366
50% Median	-0.113525
25% Q1	-0.391038
10%	-0.738333
5%	-0.977774
1%	-1.479814
0% Min	-1.667248

Extreme Observations			
Lowest	**Highest**		
Value	**Obs**	**Value**	**Obs**
-1.66725	32	1.21899	111
-1.47981	28	1.61123	18
-1.22850	23	1.61994	5
-1.11111	31	2.61101	8
-1.06642	21	4.64478	4

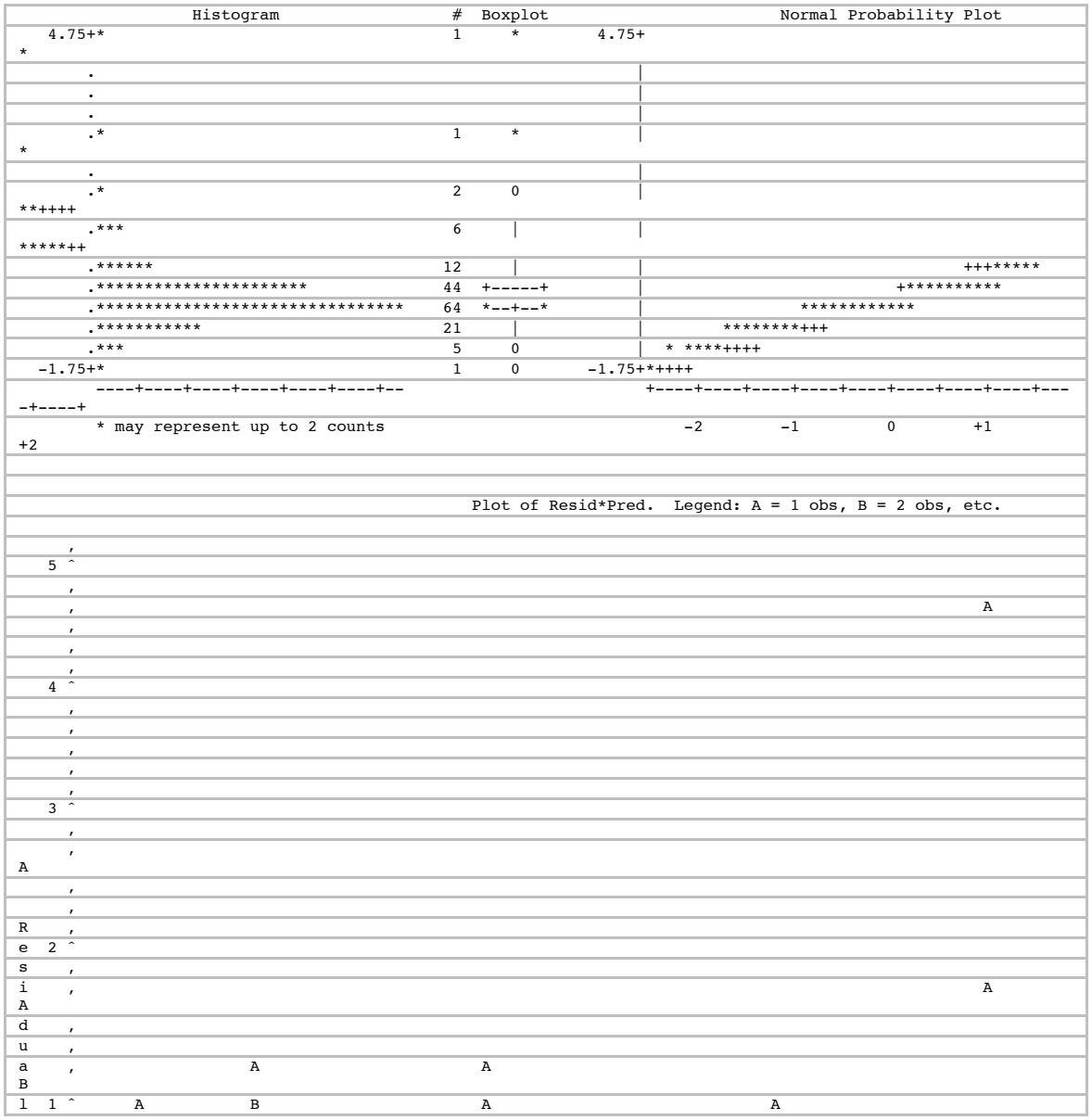
Histogram
Boxplot
Normal Probability Plot
4.75+*
4.75+
*
.
.
.
.*
*
.
.*
**++++
.***
*****++
.******
++++++++
.**********
++++++++++
.**********
****
.**********
**********+++
.***
* ****++++
-1.75+*
-1.75+*++++
----+----+----+----+----+----+--
+----+----+----+----+----+----+----+----+---
-+----+
* may represent up to 2 counts
-2
-1
0
+1
+2
Plot of Resid*Pred. Legend: A = 1 obs, B = 2 obs, etc.
5 ^
4 ^
3 ^
2 ^
1 ^
Residual
A
B

A	,		A			
	,		B			A
A	,	I	B	A	A	
A	,	B	G		A	A
	,	D	F	A	B	
B	0 ˆ	D	C	A	E	A
	,	G	O		B	B
	,	G	J	A	B	B
A	,	F	E			C
A	,	A	E		A	
A	,			A		A
	-1 ˆ			A		E
A	,					A
	,					
A	,					
A	,					
	,					
	-2 ˆ					
	,					
Šˆƒƒƒƒƒƒƒƒƒƒƒƒˆƒƒƒƒƒƒƒƒƒƒƒƒˆƒƒƒƒƒƒƒƒƒƒƒƒˆƒƒƒƒƒƒƒƒƒƒƒƒˆƒƒƒƒƒƒƒƒƒƒƒƒˆƒƒƒƒƒƒƒƒƒƒƒƒˆƒƒƒƒƒƒƒƒƒƒƒƒˆƒƒƒƒƒƒƒƒƒƒƒƒˆƒƒƒ ƒƒƒƒƒƒƒƒƒˆƒƒƒƒƒƒƒƒƒƒƒƒˆƒƒƒƒƒƒƒƒƒƒƒƒˆ						
1.6 1.7 1.8 1.9 2.0 2.1 2.2 2.3 2.4 2.5 2.6 2.7						
				Predicted Mean		

Obj. 2 Data Decorin ANOVA Results

Model Information	
Data Set	WORK.ANIM
Dependent Variable	sqrt_Decorin
Covariance Structure	Variance Components
Estimation Method	REML
Residual Variance Method	Profile
Fixed Effects SE Method	Model-Based
Degrees of Freedom Method	Containment

Class Level Information		
Class	**Levels**	**Values**
load_freq_cat	2	0 1
load_rms_cat	2	0 1
load_dur_cat	2	0 1
block	54	1 2 3 4 5 6 7 8 9 10 11 12 13 14 15 16 17 18 19 20 21 22 23 24 25 26 27 28 29 30 31 32 33 34 35 36 37 38 39 40 41 42 57 58 59 60 61 62 63 64 65 66 67 68

Dimensions	
Covariance Parameters	2
Columns in X	18
Columns in Z	54
Subjects	1
Max Obs Per Subject	158

Number of Observations	
Number of Observations Read	158
Number of Observations Used	158
Number of Observations Not Used	0

Iteration History			
Iteration	**Evaluations**	**-2 Res Log Like**	**Criterion**
0	1	361.03329125	
1	2	353.28257572	0.00000000

Convergence criteria met.

Covariance Parameter Estimates				
Cov Parm	**Estimate**	**Standard Error**	**Z Value**	**Pr > Z**
block	0.1357	0.05987	2.27	0.0117
Residual	0.4267	0.05993	7.12	<.0001

Fit Statistics	
-2 Res Log Likelihood	353.3
AIC (smaller is better)	357.3
AICC (smaller is better)	357.4
BIC (smaller is better)	361.3

Type 3 Tests of Fixed Effects				
Effect	**Num DF**	**Den DF**	**F Value**	**Pr > F**
load_freq_cat	1	99	0.05	0.8236
load_rms_cat	1	99	5.37	0.0226
load_freq*load_rms_c	1	99	1.48	0.2264
load_dur_cat	1	99	4.95	0.0284
load_freq*load_dur_c	1	99	0.04	0.8391
load_rms_*load_dur_c	0	.	.	.

Least Squares Means								
Effect	load_freq_cat	load_rms_cat	load_dur_cat	Estimate	Standard Error	DF	t Value	Pr > |t|
load_freq_cat	0			Non-est	.	.	.	.
load_freq_cat	1			Non-est	.	.	.	.
load_rms_cat		0		1.8657	0.08948	99	20.85	<.0001
load_rms_cat		1		Non-est	.	.	.	.
load_freq*load_rms_c	0	0		1.9892	0.1141	99	17.44	<.0001
load_freq*load_rms_c	0	1		Non-est	.	.	.	.
load_freq*load_rms_c	1	0		1.7423	0.1117	99	15.60	<.0001
load_freq*load_rms_c	1	1		Non-est	.	.	.	.
load_dur_cat			0	2.3054	0.1072	99	21.51	<.0001
load_du			1	Non-est	.	.	.	.

r_cat								
load_freq*load_dur_c	0		0	2.3127	0.1477	99	15.66	<.0001
load_freq*load_dur_c	0		1	Non-est	.	.	.	.
load_freq*load_dur_c	1		0	2.2982	0.1233	99	18.64	<.0001
load_freq*load_dur_c	1		1	Non-est	.	.	.	.
load_rms_*load_dur_c		0	0	2.0609	0.09089	99	22.67	<.0001
load_rms_*load_dur_c		0	1	1.6706	0.1521	99	10.98	<.0001
load_rms_*load_dur_c		1	0	2.5500	0.1924	99	13.26	<.0001

Differences of Least Squares Means						
Effect	**load_freq_cat**	**load_rms_cat**	**load_dur_cat**	**_load_freq_cat**	**_load_rms_cat**	**_load_dur_cat**
load_freq_cat	0			1		
load_rms_cat		0			1	
load_freq*load_rms_c	0	0		0	1	
load_freq*load_rms_c	0	0		1	0	
load_freq*load_rms_c	0	0		1	1	
load_freq*load_rms_c	0	1		1	0	
load_freq*load_rms_c	0	1		1	1	
load_freq*load_rms_c	1	0		1	1	
load_dur_cat			0			1
load_freq*load_dur_c	0		0	0		1
load_freq*load_dur_c	0		0	1		0

load_freq*load_dur_c	0		0	1		1
load_freq*load_dur_c	0		1	1		0
load_freq*load_dur_c	0		1	1		1
load_freq*load_dur_c	1		0	1		1
load_rms_*load_dur_c		0	0		0	1
load_rms_*load_dur_c		0	0		1	0
load_rms_*load_dur_c		0	1		1	0

Differences of Least Squares Means								
Effect	**load_freq_cat**	**load_rms_cat**	**load_dur_cat**	**_load_freq_cat**	**Estimate**	**Standard Error**	**DF**	**t Value**
load_freq_cat	0			1	0.04258	0.1905	99	0.22
load_rms_cat		0			Non-est	.	.	.
load_freq*load_rms_c	0	0		0	Non-est	.	.	.

load_freq*load_rms_c	0	0		1	0.2469	0.1377	99	1.79
load_freq*load_rms_c	0	0		1	Non-est	.	.	.
load_freq*load_rms_c	0	1		1	Non-est	.	.	.
load_freq*load_rms_c	0	1		1	-0.1618	0.3317	99	-0.49
load_freq*load_rms_c	1	0		1	Non-est	.	.	.
load_dur_cat			0		Non-est	.	.	.
load_freq*load_dur_c	0		0	0	Non-est	.	.	.
load_freq*load_dur_c	0		0	1	0.01449	0.1674	99	0.09
load_freq*load_dur_c	0		0	1	Non-est	.	.	.
load_freq*load_dur_c	0		1	1	Non-est	.	.	.
load_freq*load_	0		1	1	0.07068	0.2875	99	0.25

dur_c								
load_freq*load_dur_c	1		0	1	Non-est	.	.	.
load_rms_*load_dur_c		0	0		0.3902	0.1755	99	2.22
load_rms_*load_dur_c		0	0		-0.4891	0.2111	99	-2.32
load_rms_*load_dur_c		0	1		-0.8794	0.2452	99	-3.59

Differences of Least Squares Means							
Effect	**load_freq_cat**	**load_rms_cat**	**load_dur_cat**	**_load_freq_cat**	**Pr > |t|**	**Adjustment**	**Adj P**
load_freq_cat	0			1	0.8236	Tukey	0.8236
load_rms_cat		0			.	Tukey-Kramer	.
load_freq*load_rms_c	0	0		0	.	Tukey-Kramer	.
load_freq*load_rms_c	0	0		1	0.0759	Tukey-Kramer	0.2824

load_freq *load_rms_c	0	0		1	.	Tukey-Kramer	.
load_freq *load_rms_c	0	1		1	.	Tukey-Kramer	.
load_freq *load_rms_c	0	1		1	0.6268	Tukey-Kramer	0.9617
load_freq *load_rms_c	1	0		1	.	Tukey-Kramer	.
load_dur_cat			0		.	Tukey-Kramer	.
load_freq *load_dur_c	0		0	0	.	Tukey-Kramer	.
load_freq *load_dur_c	0		0	1	0.9312	Tukey-Kramer	0.9998
load_freq *load_dur_c	0		0	1	.	Tukey-Kramer	.
load_freq *load_dur_c	0		1	1	.	Tukey-Kramer	.
load_freq *load_dur_c	0		1	1	0.8063	Tukey-Kramer	0.9947
load_freq *load_dur	1		0	1	.	Tukey-Kramer	.

_c							
load_rms_*load_dur_c		0	0		0.0284	Tukey-Kramer	0.0721
load_rms_*load_dur_c		0	0		0.0226	Tukey-Kramer	0.0581
load_rms_*load_dur_c		0	1		0.0005	Tukey-Kramer	0.0015

Moments							
N	158	**Sum Weights**	158				
Mean	-0.0038918	**Sum Observations**	-0.6149038				
Std Deviation	0.73574516	**Variance**	0.54132094				
Skewness	0.905516	**Kurtosis**	2.15562191				
Uncorrected SS	84.9897808	**Corrected SS**	84.9873877				
Coeff Variation	-18905.028	**Std Error Mean**	0.05853274				

Basic Statistical Measures			
Location	**Variability**		

Mean	-0.00389	**Std Deviation**	0.73575
Median	-0.02398	**Variance**	0.54132
Mode	-1.17027	**Range**	4.56527
		Interquartile Range	0.94959

Note: The mode displayed is the smallest of 2 modes with a count of 3.

Tests for Location: Mu0=0				
Test	**Statistic**	**p Value**		
Student's t	**t**	-0.06649	**Pr > |t|**	0.9471
Sign	**M**	-4	**Pr >= |M|**	0.5777
Signed Rank	**S**	-466.5	**Pr >= |S|**	0.4198

Tests for Normality				
Test	**Statistic**	**p Value**		
Shapiro-Wilk	**W**	0.95579	**Pr < W**	<0.0001
Kolmogorov-Smirnov	**D**	0.070798	**Pr > D**	0.0507
Cramer-von Mises	**W-Sq**	0.142334	**Pr > W-Sq**	0.0309
Anderson-Darling	**A-Sq**	1.043013	**Pr > A-Sq**	0.0095

Quantiles (Definition 5)	
Quantile	**Estimate**
100% Max	3.1077962
99%	2.5048754
95%	1.1933574
90%	0.8459793
75% Q3	0.4315921
50% Median	-0.0239765
25% Q1	-0.5180005
10%	-0.8605594
5%	-1.1021855
1%	-1.4550491
0% Min	-1.4574762

```
     Stem Leaf                           # Boxplot                        Normal Probability Plot
       30 1                              1    0         3.1+                                                  *
       28                                                  |
       26                                                  |
       24 0                              1    0            |                                                *
       22 3                              1    0            |                                              *
       20                                                  |
       18                                                  |                                                  +
       16 4                              1    |            |                                             *  +++
       14 88                             2    |            |                                           **++
       12                                     |            |                                          +++
       10 2388499                        7    |            |                                       ****
        8 13566                          5    |            |                                    +***
        6 00011145909                   11    |            |                                  +***
        4 22334557779016                14 +-----+         |                               *****
        2 335990113344799               15 |     |         |                            ****
        0 11458899999223337             17 |     |         |                          ***
       -0 754440066532222               15 *--+--*         |                       ****
       -2 98740004411                   11 |     |         |                    +***
       -4 88776443211966666433221100    26 +-----+         |                ******
       -6 96430888553300                14    |            |             ****
       -8 84320061                       8    |            |          ***++
      -10 77706                          5    |            |      *****++
      -12 0                              1    |            |     *  ++
      -14 660                            3    |        -1.5+* * *++
          ----+----+----+----+----+-                        +----+----+----+----+----+----+----+----+----+----+
      Multiply Stem.Leaf by 10**-1                              -2        -1         0        +1        +2


                                                Plot of Resid*Pred.  Legend: A = 1 obs, B = 2 obs, etc.

          ,
        4 ˆ
          ,
          ,
          ,
          ,
          ,
          ,                                                                           A
        3 ˆ
          ,
          ,
          ,                                                                           A
          ,
          ,                                    A
          ,
        2 ˆ
          ,
          ,
     R    ,                                                                                                                              A
     e    ,                                                                                                         B
     s    ,
     i    ,                                                   A                       D
     d  1 ˆ                                                   A                       A                                                  B
     u    ,      A                                            A                       A                             A
     a    ,      A                             B
     l    ,      B                                            E                       C
```

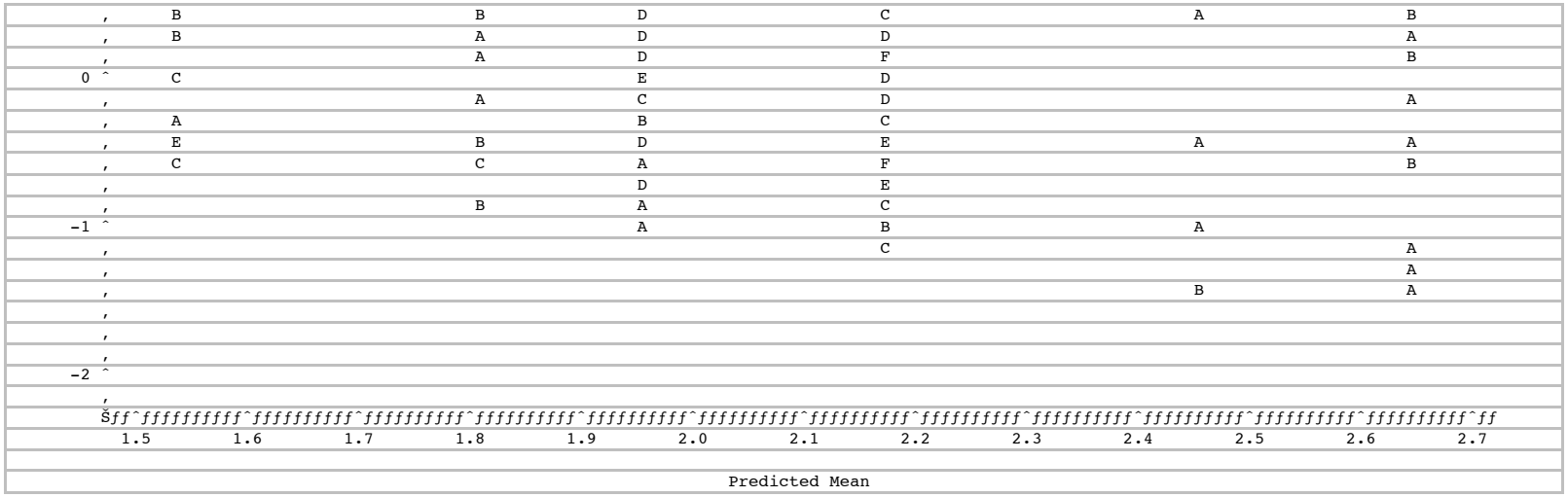
B B D C A B
B A D D A
A D F B
0 ^ C E D
A C D A
A B C
E B D E A A
C C A F B
D E
B A C
-1 ^ A B A
C A
A
B A
-2 ^
1.5 1.6 1.7 1.8 1.9 2.0 2.1 2.2 2.3 2.4 2.5 2.6 2.7
Predicted Mean

Obj. 2 Data Versican ANOVA Results

Model Information	
Data Set	WORK.ANIM
Dependent Variable	sqrt_Versican
Covariance Structure	Variance Components
Estimation Method	REML
Residual Variance Method	Profile
Fixed Effects SE Method	Model-Based
Degrees of Freedom Method	Containment

Class Level Information		
Class		**Values**
load_freq_cat		0 1
load_rms_cat		0 1
load_dur_cat		0 1
block		1 2 3 4 5 6 7 8 9 10 11 12 13 14 15 16 17 18 19 20 21 22 23 24 25 26 27 28 29 30 31 32 33 34 35 36 37 38 39 40 4 66 67 68

Dimensions	
Covariance Parameters	2
Columns in X	18
Columns in Z	54
Subjects	1
Max Obs Per Subject	158

Number of Observations	
Number of Observations Read	158
Number of Observations Used	158
Number of Observations Not Used	0

Iteration History			
Iteration	**Evaluati**	**-2 Res Log Like**	**Criterion**
0	1	401.03315036	
1	2	358.95729734	0.00000785
2	1	358.95698330	0.00000000

Convergence criteria met.

Covariance Parameter Estimates				
Cov Parm	**Estimate**	**Standard**	**Z Val**	**Pr > Z**
block	0.4009	0.1039	3.86	<.0001
Residual	0.3337	0.04705	7.09	<.0001

Fit Statistics	
-2 Res Log Likelihood	359.0
AIC (smaller is better)	363.0
AICC (smaller is better)	363.0
BIC (smaller is better)	366.9

Type 3 Tests of Fixed Effects				
Effect	**Num**	**Den**	**F Value**	**Pr > F**
load_freq_cat	1	99	0.08	0.7790
load_rms_cat	1	99	10.71	0.0015
load_freq*load_rms_c	1	99	0.67	0.4159
load_dur_cat	1	99	3.25	0.0747
load_freq*load_dur_c	1	99	0.00	0.9849
load_rms_*load_dur_c	0	.	.	.

Least Squares Means								
Effect	**load_freq_cat**	**load_rms_cat**	**load_dur_cat**	**Estimate**	**Standard**	**DF**	**t Value**	**Pr > |t|**
load_freq_cat	0			Non-est	.	.	.	.
load_freq_cat	1			Non-est	.	.	.	.
load_rms_cat		0		2.2938	0.1187	99	19.32	<.0001
load_rms_cat		1		Non-est	.	.	.	.
load_freq*load_rms_c	0	0		2.3327	0.1338	99	17.44	<.0001
load_freq*load_rms_c	0	1		Non-est	.	.	.	.
load_freq*load_rms_c	1	0		2.2549	0.1355	99	16.64	<.0001
load_freq*load_rms_c	1	1		Non-est	.	.	.	.
load_dur_cat			0	2.0648	0.1392	99	14.83	<.0001
load_dur_cat			1	Non-est	.	.	.	.
load_freq*load_dur_c	0		0	2.0390	0.1696	99	12.02	<.0001
load_freq*load_dur_c	0		1	Non-est	.	.	.	.
load_freq*load_dur_c	1		0	2.0905	0.1482	99	14.11	<.0001
load_freq*load_dur_c	1		1	Non-est	.	.	.	.
load_rms_*load_dur_c		0	0	2.4943	0.1190	99	20.97	<.0001
load_rms_*load_dur_c		0	1	2.0933	0.1970	99	10.63	<.0001
load_rms_*load_dur_c		1	0	1.6353	0.2430	99	6.73	<.0001

Differences of Least Squares Means						
Effect	**load_freq_cat**	**load_rms_cat**	**load_dur_cat**	**_load_freq_cat**	**_load_rms_cat**	**_load_dur_cat**
load_freq_cat	0			1		
load_rms_cat		0			1	
load_freq*load_rms_c	0	0		0	1	
load_freq*load_rms_c	0	0		1	0	
load_freq*load_rms_c	0	0		1	1	
load_freq*load_rms_c	0	1		1	0	
load_freq*load_rms_c	0	1		1	1	
load_freq*load_rms_c	1	0		1	1	
load_dur_cat			0			1
load_freq*load_dur_c	0		0	0		1
load_freq*load_dur_c	0		0	1		0
load_freq*load_dur_c	0		0	1		1
load_freq*load_dur_c	0		1	1		0
load_freq*load_dur_c	0		1	1		1
load_freq*load_dur_c	1		0	1		1
load_rms_*load_dur_c		0	0		0	1
load_rms_*load_dur_c		0	0		1	0
load_rms_*load_dur_c		0	1		1	0

Differences of Least Squares Means								
Effect	**load_freq_cat**	**load_rms_cat**	**load_dur_cat**	**_load_freq_cat**	**Estimate**	**Standard**	**DF**	**t Value**
load_freq_cat	0			1	-0.04907	0.1744	99	-0.28
load_rms_cat		0			Non-est	.	.	.
load_freq*load_rms_c	0	0		0	Non-est	.	.	.
load_freq*load_rms_c	0	0		1	0.07778	0.1271	99	0.61
load_freq*load_rms_c	0	0		1	Non-est	.	.	.
load_freq*load_rms_c	0	1		1	Non-est	.	.	.
load_freq*load_rms_c	0	1		1	-0.1759	0.3048	99	-0.58
load_freq*load_rms_c	1	0		1	Non-est	.	.	.
load_dur_cat			0		Non-est	.	.	.
load_freq*load_dur_c	0		0	0	Non-est	.	.	.
load_freq*load_dur_c	0		0	1	-0.05148	0.1546	99	-0.33
load_freq*load_dur_c	0		0	1	Non-est	.	.	.
load_freq*load_dur_c	0		1	1	Non-est	.	.	.
load_freq*load_dur_c	0		1	1	-0.04665	0.2636	99	-0.18
load_freq*load_dur_c	1		0	1	Non-est	.	.	.
load_rms_*load_dur_c		0	0		0.4010	0.2226	99	1.80
load_rms_*load_dur_c		0	0		0.8590	0.2625	99	3.27
load_rms_*load_dur_c		0	1		0.4581	0.3120	99	1.47

Differences of Least Squares Means							
Effect	**load_freq_cat**	**load_rms_cat**	**load_dur_cat**	**_load_freq_cat**	**Pr > |t|**	**Adjustment**	**Adj P**
load_freq_cat	0			1	0.7790	Tukey	0.7790
load_rms_cat		0			.	Tukey-Kramer	.
load_freq*load_rms_c	0	0		0	.	Tukey-Kramer	.
load_freq*load_rms_c	0	0		1	0.5419	Tukey-Kramer	0.9280
load_freq*load_rms_c	0	0		1	.	Tukey-Kramer	.
load_freq*load_rms_c	0	1		1	.	Tukey-Kramer	.
load_freq*load_rms_c	0	1		1	0.5651	Tukey-Kramer	0.9387
load_freq*load_rms_c	1	0		1	.	Tukey-Kramer	.
load_dur_cat			0		.	Tukey-Kramer	.
load_freq*load_dur_c	0		0	0	.	Tukey-Kramer	.
load_freq*load_dur_c	0		0	1	0.7399	Tukey-Kramer	0.9872
load_freq*load_dur_c	0		0	1	.	Tukey-Kramer	.
load_freq*load_dur_c	0		1	1	.	Tukey-Kramer	.
load_freq*load_dur_c	0		1	1	0.8599	Tukey-Kramer	0.9980
load_freq*load_dur_c	1		0	1	.	Tukey-Kramer	.
load_rms_*load_dur_c		0	0		0.0747	Tukey-Kramer	0.1744
load_rms_*load_dur_c		0	0		0.0015	Tukey-Kramer	0.0042
load_rms_*load_dur_c		0	1		0.1452	Tukey-Kramer	0.3106

Moments			
N	158	**Sum Weights**	158
Mean	0.00293443	**Sum Observations**	0.46364009

Std Deviation	0.84129676	**Variance**	0.70778023
Skewness	0.65544035	**Kurtosis**	0.37927854
Uncorrected SS	111.122857	**Corrected SS**	111.121497
Coeff Variation	28669.8436	**Std Error Mean**	0.06692998

Basic Statistical Measures			
Location	**Variability**		
Mean	0.00293	**Std Deviation**	0.84130
Median	-0.03408	**Variance**	0.70778
Mode	-0.42172	**Range**	4.23584
		Interquartile Range	1.11500

Note: The mode displayed is the smallest of 5 modes with a count of 3.

Tests for Location: Mu0=0				
Test	**Statistic**	**p Value**		
Student's t	**t**	0.043843	**Pr > |t|**	0.9651
Sign	**M**	-3	**Pr >= |M|**	0.6909
Signed Rank	**S**	-389.5	**Pr >= |S|**	0.5007

Tests for Normality				
Test	**Statistic**	**p Value**		
Shapiro-Wilk	**W**	0.969823	**Pr < W**	0.0016
Kolmogorov-Smirnov	**D**	0.062489	**Pr > D**	0.1340
Cramer-von Mises	**W-Sq**	0.131888	**Pr > W-Sq**	0.0428
Anderson-Darling	**A-Sq**	0.98186	**Pr > A-Sq**	0.0145

Quantiles (Definition 5)	
Quantile	**Estimate**
100% Max	2.703855
99%	2.392548
95%	1.613273
90%	1.135442
75% Q3	0.471522
50% Median	-0.034082
25% Q1	-0.643477
10%	-1.053245
5%	-1.190341
1%	-1.531982
0% Min	-1.531982

Extreme Observations			
Lowest		**Highest**	
Value	**Obs**	**Value**	**Obs**
-1.53198	88	1.83046	65
-1.53198	49	2.14313	43
-1.40305	74	2.30021	44
-1.36575	80	2.39255	58
-1.30770	72	2.70386	6

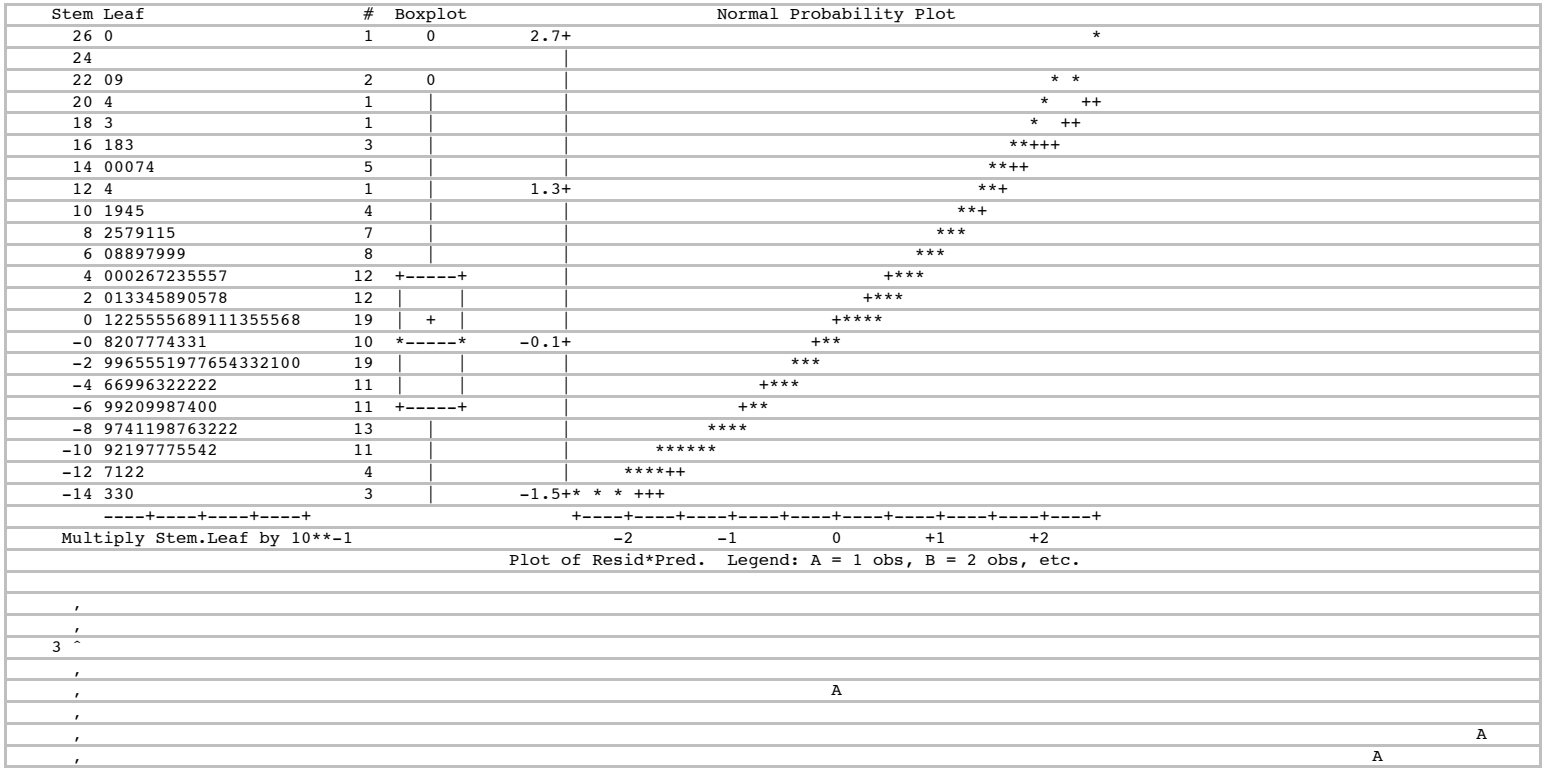

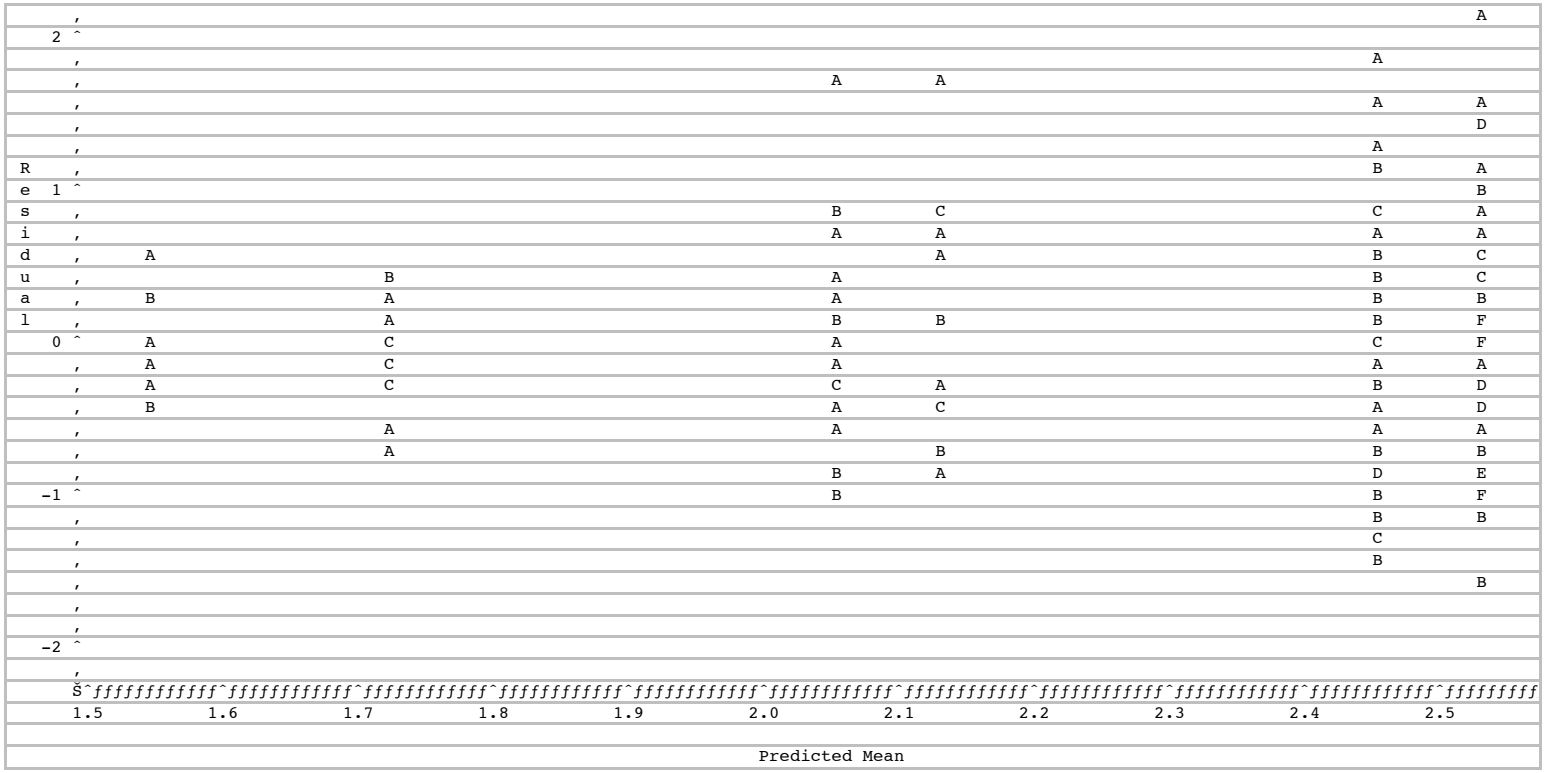
Residuals
2
1
0
-1
-2
A
B
C
D
E
1.5
1.6
1.7
1.8
1.9
2.0
2.1
2.2
2.3
2.4
2.5
Predicted Mean

A.4.4 Objective 3 Data

Specimen #	Load Freq (Hz)	Load-ave (RMS-g)	Load Duration (min)	Aggrecan	Biglycan	Collagen 1	Collagen II	Decorin	Versican
230	KKT(16)	0.5-1	10	1.87	6.96	19.70	16.00	1.00	7.21
231	KKT(16)	0.5-1	10	1.68	6.50	18.38	12.13	1.52	10.93
232	KKT(65)	0.5-1	10	2.14	4.92	14.42	8.57	2.55	5.86
233	KKT(65)	0.5-1	10	1.32	5.10	14.42	5.66	6.06	5.28
234	0	0	0	1.68	15.45	18.38	3.86	11.71	4.14
235	0	0	0	2.22	13.93	8.28	4.59	13.00	4.29
236	KKT(16-65)	0.5-1	5(5)	3.03	3.03	2.22	4.14	7.73	4.92
237	KKT(16-65)	0.5-1	5(5)	3.86	3.48	2.38	4.76	9.19	3.61
238	KKT(65)	0.5-1	10	2.38	2.73	4.14	4.59	6.96	6.50
239	KKT(65)	0.5-1	10	2.73	2.22	2.14	2.38	17.15	4.14
240	KKT(16)	0.5-1	10	1.74	4.14	17.15	4.29	7.46	8.88
241	KKT(16)	0.5-1	10	2.38	3.25	1.27	5.10	11.71	7.21
242	KKT(16-65)	0.5-1	5(5)	2.64	2.22	2.93	2.73	5.86	4.76
243	KKT(16-65)	0.5-1	5(5)	4.14	3.86	2.93	3.48	4.44	5.66
244	KKT(65)	0.5-1	10	2.73	3.25	1.00	2.55	7.21	4.59
245	KKT(65)	0.5-1	10	3.03	3.61	3.48	3.36	8.88	4.59
246	0	0	0	1.00	2.22	2.38	3.86	9.85	5.28
247	0	0	0	1.93	3.14	5.66	6.50	12.55	5.66
248	KKT(16)	0.5-1	10	2.55	3.25	5.10	6.73	16.56	8.00
249	KKT(16)	0.5-1	10	3.86	3.61	4.92	7.21	19.03	8.88
250	KKT(16-65)	0.5-1	5(5)	3.61	2.46	4.00	4.29	7.21	2.00
251	KKT(16-65)	0.5-1	5(5)	1.93	1.00	8.28	1.00	11.31	1.00
252	0	0	0	1.87	6.28	9.19	13.45	16.00	5.86
253	0	0	0	2.30	4.92	11.31	9.19	13.93	7.21

A.4.5 Objective 4 Data

Specimen #	Load Freq (Hz)	Load Amplitude (mm)	Load Duration (min)	Aggrecan	Biglycan	Collagen 1	Collagen II	Decorin	Versican
312	16-65	cDaq 0.6 axial	5(5)	3.14	4.29	1.19	3.36	2.73	4.44
313	16-65	cDaq 0.6 axial	5(5)	2.07	3.48	1.87	-	2.46	5.10
314	16-65	cDaq 0.6 axial	5(5)	1.93	-	1.04	2.46	-	-
317	0	0	0	1.74	1.46	1.68	2.07	2.07	4.14
318	0	0	0	1.00	1.00	1.00	-	1.80	1.00
319	16-65	cDaq 0.6 axial	5(5)	2.46	4.14	3.61	6.73	2.07	5.66
321	0	0	0	-	2.46	2.00	-	1.32	-
323	0	0	0	-	2.38	-	1.93	1.00	3.03
325	0	0	0	1.52	1.68	-	1.04	1.74	4.29
327	0	0	0	1.41	1.23	1.68	1.11	1.62	3.73
328	16-65	cDaq 0.6 axial	5(5)	-	-	-	-	-	-
329	16-65	cDaq 0.6 axial	5(5)	1.80	3.03	2.46	4.59	2.00	7.46

Entire Data Set (All objectives combined) Aggrecan ANOVA Results

Model Information	
Data Set	WORK.ANIM
Dependent Variable	ln_Aggrecan
Covariance Structure	Variance Components
Estimation Method	REML
Residual Variance Method	Profile
Fixed Effects SE Method	Model-Based
Degrees of Freedom Method	Containment

Class Level Information		
Class	**Levels**	**Values**
load_freq_cat	2	0 1
load_rms_cat	2	0 1
load_dur_cat	2	0 1
block	84	1 2 3 4 5 6 7 8 9 10 11 12 13 14 15 16 17 18 19 20 21 22 23 24 25 26 27 28 29 30 31 32 33 34 35 36 37 38 39 40 41 42 43 44 45 46 47 48 49 50 51 52 53 54 55 56 57 58 59 60 61 62 63 64 65 66 67 68 69 70 71 72 73 74 75 76 77 78 79 80 81 82 83 84

Dimensions	
Covariance Parameters	2
Columns in X	19
Columns in Z	84
Subjects	1
Max Obs Per Subject	250

Number of Observations	
Number of Observations Read	250
Number of Observations Used	247
Number of Observations Not Used	3

Iteration History			
Iteration	**Evaluations**	**-2 Res Log Like**	**Criterion**
0	1	330.74097172	
1	2	288.54534354	0.00000001
2	1	288.54534266	0.00000000

Convergence criteria met.

Covariance Parameter Estimates				
Cov Parm	**Estimate**	**Standard Error**	**Z Value**	**Pr > Z**
block	0.09662	0.02248	4.30	<.0001
Residual	0.1181	0.01331	8.88	<.0001

Fit Statistics	
-2 Res Log Likelihood	288.5
AIC (smaller is better)	292.5
AICC (smaller is better)	292.6
BIC (smaller is better)	297.4

Type 3 Tests of Fixed Effects				
Effect	**Num DF**	**Den DF**	**F Value**	**Pr > F**
load_freq_cat	1	157	9.63	0.0023
load_rms_cat	1	157	1.86	0.1743
load_freq*load_rms_c	1	157	0.03	0.8729
load_dur_cat	1	157	8.75	0.0036
load_freq*load_dur_c	1	157	11.94	0.0007
load_rms_*load_dur_c	1	157	2.13	0.1467

Least Squares Means								
Effect	load_freq_cat	load_rms_cat	load_dur_cat	Estimate	Standard Error	DF	t Value	Pr > |t|
load_freq_cat	0			1.0964	0.1026	157	10.69	<.0001
load_freq_cat	1			0.8440	0.07930	157	10.64	<.0001
load_rms_cat		0		1.0787	0.05997	157	17.99	<.0001
load_rms_cat		1		0.8617	0.1502	157	5.74	<.0001
load_freq*load_rms_c	0	0		1.1998	0.06916	157	17.35	<.0001
load_freq*load_rms_c	0	1		0.9931	0.1826	157	5.44	<.0001
load_freq*load_rms_c	1	0		0.9576	0.07172	157	13.35	<.0001
load_freq*load_rms_c	1	1		0.7303	0.1407	157	5.19	<.0001
load_dur_cat			0	0.7408	0.04472	157	16.57	<.0001
load_du			1	1.1996	0.1534	157	7.82	<.0001

r_cat								
load_freq*load_dur_c	0		0	0.7384	0.05631	157	13.11	<.0001
load_freq*load_dur_c	0		1	1.4544	0.1877	157	7.75	<.0001
load_freq*load_dur_c	1		0	0.7432	0.05467	157	13.59	<.0001
load_freq*load_dur_c	1		1	0.9447	0.1477	157	6.39	<.0001
load_rms_*load_dur_c		0	0	0.7356	0.05610	157	13.11	<.0001
load_rms_*load_dur_c		0	1	1.4218	0.1034	157	13.75	<.0001
load_rms_*load_dur_c		1	0	0.7459	0.06233	157	11.97	<.0001
load_rms_*load_dur_c		1	1	0.9774	0.2880	157	3.39	0.0009

Differences of Least Squares Means						
Effect	**load_freq_cat**	**load_rms_cat**	**load_dur_cat**	**_load_freq_cat**	**_load_rms_cat**	**_load_dur_cat**
load_freq_cat	0			1		
load_rms_cat		0			1	
load_freq*load_rms_c	0	0		0	1	
load_freq*load_rms_c	0	0		1	0	
load_freq*load_rms_c	0	0		1	1	
load_freq*load_rms_c	0	1		1	0	
load_freq*load_rms_c	0	1		1	1	
load_freq*load_rms_c	1	0		1	1	
load_dur_cat			0			1
load_freq*load_dur_c	0		0	0		1
load_freq*load_dur_c	0		0	1		0
load_freq*l	0		0	1		1

oad_dur_c						
load_freq*load_dur_c	0		1	1		0
load_freq*load_dur_c	0		1	1		1
load_freq*load_dur_c	1		0	1		1
load_rms_*load_dur_c		0	0		0	1
load_rms_*load_dur_c		0	0		1	0
load_rms_*load_dur_c		0	0		1	1
load_rms_*load_dur_c		0	1		1	0
load_rms_*load_dur_c		0	1		1	1
load_rms_*load_dur_c		1	0		1	1

Differences of Least Squares Means								
Effect	**load_freq_cat**	**load_rms_cat**	**load_dur_cat**	**_load_freq_cat**	**Estimate**	**Standard Error**	**DF**	**t Value**
load_freq_cat	0			1	0.2524	0.08135	157	3.10
load_rms_cat		0			0.2170	0.1590	157	1.36
load_freq*load_rms_c	0	0		0	0.2067	0.1848	157	1.12
load_freq*load_rms_c	0	0		1	0.2421	0.07392	157	3.28
load_freq*load_rms_c	0	0		1	0.4695	0.1555	157	3.02
load_freq*load_rms_c	0	1		1	0.03543	0.1991	157	0.18
load_freq*load_rms_c	0	1		1	0.2628	0.1268	157	2.07
load_freq*load_rms_c	1	0		1	0.2273	0.1573	157	1.45
load_du			0		-0.4588	0.1551	157	-2.96

r_cat								
load_freq*load_dur_c	0		0	0	-0.7161	0.1864	157	-3.84
load_freq*load_dur_c	0		0	1	-0.00480	0.06574	157	-0.07
load_freq*load_dur_c	0		0	1	-0.2064	0.1539	157	-1.34
load_freq*load_dur_c	0		1	1	0.7113	0.1941	157	3.66
load_freq*load_dur_c	0		1	1	0.5097	0.1414	157	3.60
load_freq*load_dur_c	1		0	1	-0.2016	0.1565	157	-1.29
load_rms_*load_dur_c		0	0		-0.6862	0.1153	157	-5.95
load_rms_*load_dur_c		0	0		-0.01032	0.07788	157	-0.13
load_rms_*load_dur_c		0	0		-0.2418	0.2902	157	-0.83
load_rms_*load_dur_c		0	1		0.6758	0.1204	157	5.61

load_rms_*load_dur_c		0	1		0.4444	0.3052	157	1.46
load_rms_*load_dur_c		1	0		-0.2315	0.2889	157	-0.80

Differences of Least Squares Means							
Effect	**load_freq_cat**	**load_rms_cat**	**load_dur_cat**	**_load_freq_cat**	**Pr > |t|**	**Adjustment**	**Adj P**
load_freq_cat	0			1	0.0023	Tukey-Kramer	0.0023
load_rms_cat		0			0.1743	Tukey-Kramer	0.1743
load_freq*load_rms_c	0	0		0	0.2652	Tukey-Kramer	0.6788
load_freq*load_rms_c	0	0		1	0.0013	Tukey-Kramer	0.0070
load_freq*load_rms_c	0	0		1	0.0030	Tukey-Kramer	0.0155
load_freq*load_rms_c	0	1		1	0.8590	Tukey-Kramer	0.9980
load_freq	0	1		1	0.0399	Tukey-	0.1667

***load_rms_c**						Kramer	
load_freq *load_rms_c	1	0		1	0.1502	Tukey-Kramer	0.4729
load_dur_cat			0		0.0036	Tukey-Kramer	0.0036
load_freq *load_dur_c	0		0	0	0.0002	Tukey-Kramer	0.0010
load_freq *load_dur_c	0		0	1	0.9419	Tukey-Kramer	0.9999
load_freq *load_dur_c	0		0	1	0.1819	Tukey-Kramer	0.5385
load_freq *load_dur_c	0		1	1	0.0003	Tukey-Kramer	0.0019
load_freq *load_dur_c	0		1	1	0.0004	Tukey-Kramer	0.0024
load_freq *load_dur_c	1		0	1	0.1995	Tukey-Kramer	0.5717
load_rms_*load_dur_c		0	0		<.0001	Tukey-Kramer	<.0001
load_rms_*load_dur_c		0	0		0.8947	Tukey-Kramer	0.9992

load_rms_*load_dur_c		0	0		0.4060	Tukey-Kramer	0.8386
load_rms_*load_dur_c		0	1		<.0001	Tukey-Kramer	<.0001
load_rms_*load_dur_c		0	1		0.1473	Tukey-Kramer	0.4665
load_rms_*load_dur_c		1	0		0.4241	Tukey-Kramer	0.8537

Moments							
N	247	**Sum Weights**	247				
Mean	0.0029533 5	**Sum Observations**	0.7294775 8				
Std Deviation	0.4565884 3	**Variance**	0.2084729 9				
Skewness	0.0095895 6	**Kurtosis**	0.2773134 2				
Uncorrected SS	51.286510 4	**Corrected SS**	51.284356				
Coeff Variation	15460.014 8	**Std Error Mean**	0.0290520 3				

Basic Statistical Measures			
Location	**Variability**		
Mean	0.00295	**Std Deviation**	0.45659
Median	-0.01562	**Variance**	0.20847
Mode	-0.30933	**Range**	2.82531
		Interquartile Range	0.57298

Note: The mode displayed is the smallest of 2 modes with a count of 5.

Tests for Location: Mu0=0				
Test	**Statistic**	**p Value**		
Student's t	**t**	0.101657	**Pr > |t|**	0.9191
Sign	**M**	-5.5	**Pr >= |M|**	0.5247
Signed Rank	**S**	102	**Pr >= |S|**	0.9279

Tests for Normality				
Test	**Statistic**	**p Value**		
Shapiro-Wilk	**W**	0.996119	**Pr < W**	0.7998
Kolmogorov-Smirnov	**D**	0.034827	**Pr > D**	>0.1500
Cramer-von	**W-Sq**	0.031711	**Pr > W-Sq**	>0.2500

Mises				
Anderson-Darling	**A-Sq**	0.23287	**Pr > A-Sq**	>0.2500

Quantiles (Definition 5)	
Quantile	**Estimate**
100% Max	1.3928609
99%	1.1355276
95%	0.7200488
90%	0.5960611
75% Q3	0.3122354
50% Median	-0.0156174
25% Q1	-0.2607399
10%	-0.5843018
5%	-0.7280413
1%	-1.1720885
0% Min	-1.4324456

Extreme Observations			
Lowest	**Highest**		
Value	**Obs**	**Value**	**Obs**
-1.432446	33	0.935885	77
-1.293026	29	1.115383	6

-1.172088	32	1.135528	9
-0.943914	42	1.274554	5
-0.943914	24	1.392861	19

```
    Stem Leaf                                                #  Boxplot                        Normal Probability Plot
      12 79                                                   2     0         1.3+                                                  *
      10 24                                                   2     |            |                                               **++
       8 002624                                               6     |            |                                           ****
       6 000124567901228                                     15     |            |                                      ******
       4 00000022267880000444699                             23     |            |                                  *****
       2 0111233444666788889000011112335677889               37  +-----+         |                             ******
       0 122333355777890001222244556679999                   33  |  +  |         |                         +****
      -0 999977666666443222220009999977765555533322222200    48  *-----*     -0.1+                     ******
      -2 88762221111199966666555533222211110                 35  +-----+         |                *****
      -4 988777754441009777755310                            24     |            |            *****
      -6 5444443332009521                                    16     |            |      ******
      -8 440                                                  3     |            |   ***++
     -10 7                                                    1     0            |++*+
     -12 9                                                    1     0            |*
     -14 3                                                    1     0        -1.5+*
         ----+----+----+----+----+----+----+----+----+---                         +----+----+----+----+----+----+----+----+----+----+
     Multiply Stem.Leaf by 10**-1                                                     -2        -1         0        +1        +2


                                                Plot of Resid*Pred.  Legend: A = 1 obs, B = 2 obs, etc.

        ,
    1.5 ^
        ,                                                                  A
        ,
        ,                                                                                                                                        A
        ,
        ,                                                                  A                                                                     A
        ,
    1.0 ^
        ,    A A
        ,                                                                                                                                        A
        ,    A B                                                           A
        ,      A                                                           A                                                                     C
        ,    A BA                                                                                                                                B
        ,    C BB                                                          A
    0.5 ^    B EA
        ,    C DB                                                          A
        ,    C CB                                                          A
 R      ,    H GA                                                          A                                                                     A
 e      ,    F EB                                                                                                                                A
 s      ,  A C DC                                                          A
 i      ,  A F BA
 d  0.0 ^    I GA                                                          A
 u      ,    F HC
 a      ,  A C HC                                                          A
```

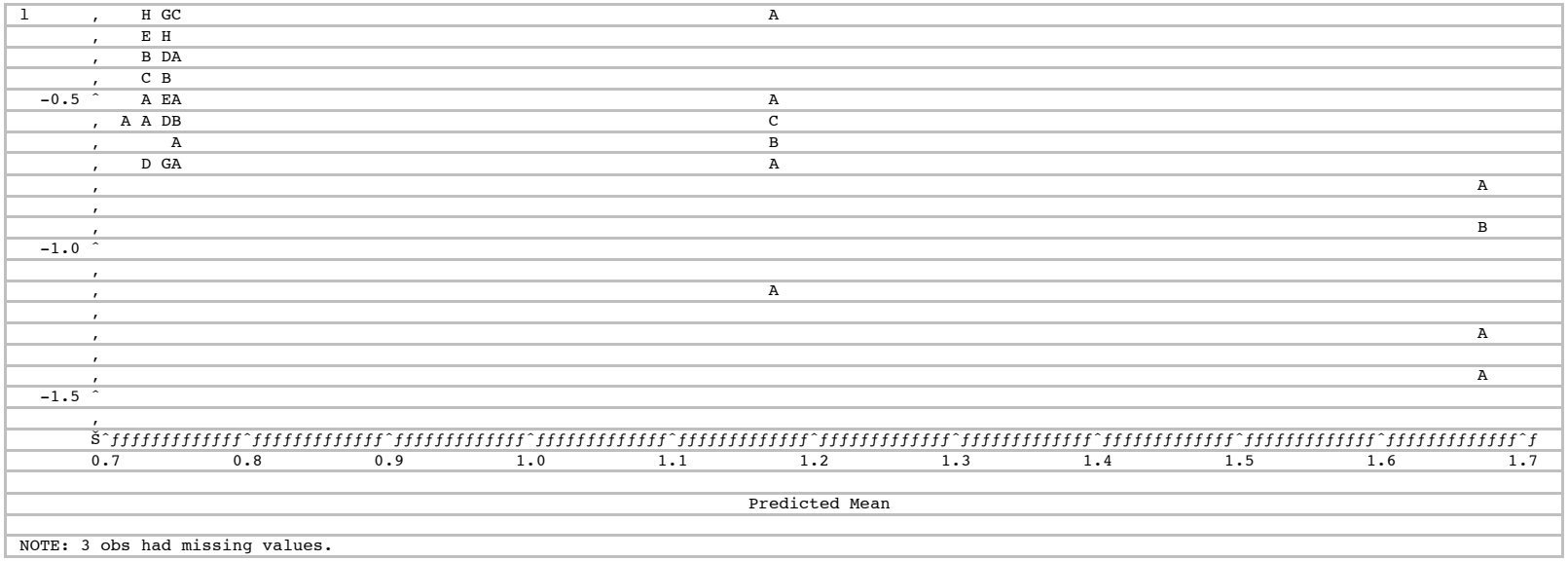

NOTE: 3 obs had missing values.

Entire Data Set (All objectives combined) Biglycan ANOVA Results

Model Information	
Data Set	WORK.ANIM
Dependent Variable	ln_Biglycan
Covariance Structure	Variance Components
Estimation Method	REML
Residual Variance Method	Profile
Fixed Effects SE Method	Model-Based
Degrees of Freedom Method	Containment

Class Level Information		
Class	**Levels**	**Values**
load_freq_cat	2	0 1
load_rms_cat	2	0 1
load_dur_cat	2	0 1
block	84	1 2 3 4 5 6 7 8 9 10 11 12 13 14 15 16 17 18 19 20 21 22 23 24 25 26 27 28 29 30 31 32 33 34 35 36 37 38 39 40 41 42 43 44 45 46 47 48 49 50 51 52 53 54 55 56 57 58 59 60 61 62 63 64 65 66 67 68 69 70 71 72 73 74 75 76 77 78 79 80 81 82 83 84

Dimensions	
Covariance Parameters	2
Columns in X	19
Columns in Z	84
Subjects	1
Max Obs Per Subject	248

Number of Observations	
Number of Observations Read	248
Number of Observations Used	246
Number of Observations Not Used	2

Iteration History			
Iteration	**Evaluations**	**-2 Res Log Like**	**Criterion**
0	1	340.87418998	
1	2	317.11762706	0.00000951
2	1	317.11704334	0.00000000

Convergence criteria met.

Covariance Parameter Estimates				
Cov Parm	**Estimate**	**Standard Error**	**Z Value**	**Pr > Z**
block	0.07866	0.02172	3.62	0.0001
Residual	0.1467	0.01661	8.83	<.0001

Fit Statistics	
-2 Res Log Likelihood	317.1
AIC (smaller is better)	321.1
AICC (smaller is better)	321.2
BIC (smaller is better)	326.0

Type 3 Tests of Fixed Effects				
Effect	**Num DF**	**Den DF**	**F Value**	**Pr > F**
load_freq_cat	1	156	2.57	0.1110
load_rms_cat	1	156	0.00	0.9600
load_freq*load_rms_c	1	156	5.82	0.0170
load_dur_cat	1	156	0.42	0.5200
load_freq*load_dur_c	1	156	2.95	0.0879
load_rms_*load_dur_c	1	156	2.86	0.0929

Least Squares Means								
Effect	**load_freq_cat**	**load_rms_cat**	**load_dur_cat**	**Estimate**	**Standard Error**	**DF**	**t Value**	**Pr > |t|**
load_freq_cat	0			0.9654	0.1065	156	9.06	<.0001
load_freq_cat	1			0.8239	0.08028	156	10.26	<.0001
load_rms_cat		0		0.8906	0.05881	156	15.14	<.0001
load_rms_cat		1		0.8987	0.1532	156	5.87	<.0001
load_freq*load_rms_c	0	0		1.0443	0.07063	156	14.79	<.0001
load_freq*load_rms_c	0	1		0.8865	0.1890	156	4.69	<.0001
load_freq*load_rms_c	1	0		0.7368	0.07230	156	10.19	<.0001
load_freq*load_rms_c	1	1		0.9109	0.1430	156	6.37	<.0001
load_dur_cat			0	0.9457	0.04385	156	21.57	<.0001
load_dur_cat			1	0.8436	0.1566	156	5.39	<.0001
load_freq*load_	0		0	0.9464	0.05726	156	16.53	<.0001

dur_c								
load_freq*load_dur_c	0		1	0.9845	0.1962	156	5.02	<.0001
load_freq*load_dur_c	1		0	0.9451	0.05514	156	17.14	<.0001
load_freq*load_dur_c	1		1	0.7026	0.1502	156	4.68	<.0001
load_rms_*load_dur_c		0	0	0.8072	0.05583	156	14.46	<.0001
load_rms_*load_dur_c		0	1	0.9740	0.1017	156	9.58	<.0001
load_rms_*load_dur_c		1	0	1.0842	0.06268	156	17.30	<.0001
load_rms_*load_dur_c		1	1	0.7132	0.2948	156	2.42	0.0167

Differences of Least Squares Means						
Effect	**load_freq_cat**	**load_rms_cat**	**load_dur_cat**	**_load_freq_cat**	**_load_rms_cat**	**_load_dur_cat**
load_freq_cat	0			1		
load_rms_cat		0			1	
load_freq*load_rms_c	0	0		0	1	
load_freq*load_rms_c	0	0		1	0	
load_freq*load_rms_c	0	0		1	1	
load_freq*load_rms_c	0	1		1	0	
load_freq*load_rms_c	0	1		1	1	
load_freq*load_rms_c	1	0		1	1	
load_dur_cat			0			1
load_freq*load_dur_c	0		0	0		1
load_freq*load_dur_c	0		0	1		0
load_freq*load_dur_c	0		0	1		1
load_freq*l	0		1	1		0

oad_dur_c						
load_freq*load_dur_c	0		1	1		1
load_freq*load_dur_c	1		0	1		1
load_rms_*load_dur_c		0	0		0	1
load_rms_*load_dur_c		0	0		1	0
load_rms_*load_dur_c		0	0		1	1
load_rms_*load_dur_c		0	1		1	0
load_rms_*load_dur_c		0	1		1	1
load_rms_*load_dur_c		1	0		1	1

Differences of Least Squares Means								
Effect	**load_freq_cat**	**load_rms_cat**	**load_dur_cat**	**_load_freq_cat**	**Estimate**	**Standard Error**	**DF**	**t Value**
load_freq_cat	0			1	0.1416	0.08834	156	1.60
load_rms_cat		0			-0.00812	0.1615	156	-0.05
load_freq*load_rms_c	0	0		0	0.1578	0.1899	156	0.83

load_freq*load_rms_c	0	0		1	0.3075	0.08123	156	3.79
load_freq*load_rms_c	0	0		1	0.1335	0.1587	156	0.84
load_freq*load_rms_c	0	1		1	0.1497	0.2064	156	0.73
load_freq*load_rms_c	0	1		1	-0.02432	0.1359	156	-0.18
load_freq*load_rms_c	1	0		1	-0.1740	0.1599	156	-1.09
load_dur_cat			0		0.1022	0.1585	156	0.64
load_freq*load_dur_c	0		0	0	-0.03815	0.1953	156	-0.20
load_freq*load_dur_c	0		0	1	0.001264	0.07033	156	0.02
load_freq*load_dur_c	0		0	1	0.2437	0.1576	156	1.55
load_freq*load_dur_c	0		1	1	0.03941	0.2024	156	0.19
load_freq*load_	0		1	1	0.2819	0.1550	156	1.82

dur_c								
load_freq*load_dur_c	1		0	1	0.2425	0.1594	156	1.52
load_rms_*load_dur_c		0	0		-0.1668	0.1144	156	-1.46
load_rms_*load_dur_c		0	0		-0.2770	0.08001	156	-3.46
load_rms_*load_dur_c		0	0		0.09405	0.2969	156	0.32
load_rms_*load_dur_c		0	1		-0.1103	0.1193	156	-0.92
load_rms_*load_dur_c		0	1		0.2608	0.3104	156	0.84
load_rms_*load_dur_c		1	0		0.3711	0.2962	156	1.25

Differences of Least Squares Means							
Effect	**load_freq_cat**	**load_rms_cat**	**load_dur_cat**	**_load_freq_cat**	**Pr > |t|**	**Adjustment**	**Adj P**
load_freq_cat	0			1	0.1110	Tukey-Kramer	0.1110
load_rms_cat		0			0.9600	Tukey-Kramer	0.9600

load_freq *load_rms_c	0	0		0	0.4074	Tukey-Kramer	0.8398
load_freq *load_rms_c	0	0		1	0.0002	Tukey-Kramer	0.0012
load_freq *load_rms_c	0	0		1	0.4018	Tukey-Kramer	0.8349
load_freq *load_rms_c	0	1		1	0.4693	Tukey-Kramer	0.8868
load_freq *load_rms_c	0	1		1	0.8582	Tukey-Kramer	0.9980
load_freq *load_rms_c	1	0		1	0.2781	Tukey-Kramer	0.6972
load_dur_cat			0		0.5200	Tukey-Kramer	0.5200
load_freq *load_dur_c	0		0	0	0.8454	Tukey-Kramer	0.9974
load_freq *load_dur_c	0		0	1	0.9857	Tukey-Kramer	1.0000
load_freq *load_dur_c	0		0	1	0.1241	Tukey-Kramer	0.4126
load_freq *load_dur	0		1	1	0.8459	Tukey-Kramer	0.9974

_c							
load_freq*load_dur_c	0		1	1	0.0708	Tukey-Kramer	0.2682
load_freq*load_dur_c	1		0	1	0.1303	Tukey-Kramer	0.4274
load_rms_*load_dur_c		0	0		0.1469	Tukey-Kramer	0.4656
load_rms_*load_dur_c		0	0		0.0007	Tukey-Kramer	0.0038
load_rms_*load_dur_c		0	0		0.7519	Tukey-Kramer	0.9890
load_rms_*load_dur_c		0	1		0.3567	Tukey-Kramer	0.7918
load_rms_*load_dur_c		0	1		0.4021	Tukey-Kramer	0.8353
load_rms_*load_dur_c		1	0		0.2122	Tukey-Kramer	0.5943

Moments			
N	246	**Sum Weights**	246
Mean	0.0015810 3	**Sum Observa**	0.38893341

		tions	
Std Deviation	0.46661474	**Variance**	0.21772932
Skewness	-0.140319	**Kurtosis**	-0.5160776
Uncorrected SS	53.3442976	**Corrected SS**	53.3436827
Coeff Variation	29513.3365	**Std Error Mean**	0.02975027

Basic Statistical Measures			
Location	**Variability**		
Mean	0.001581	**Std Deviation**	0.46661
Median	0.024637	**Variance**	0.21773
Mode	0.321158	**Range**	2.42405
		Interquartile Range	0.69977

Tests for Location: Mu0=0				
Test	**Statistic**	**p Value**		
Student's t	**t**	0.053143	**Pr > |t|**	0.9577
Sign	**M**	5	**Pr >= |M|**	0.5662
Signed Rank	**S**	325.5	**Pr >= |S|**	0.7714

Tests for Normality				
Test	**Statistic**	**p Value**		
Shapiro-Wilk	**W**	0.990665	**Pr < W**	0.1168
Kolmogorov-Smirnov	**D**	0.051204	**Pr > D**	0.1155
Cramer-von Mises	**W-Sq**	0.108564	**Pr > W-Sq**	0.0891
Anderson-Darling	**A-Sq**	0.691621	**Pr > A-Sq**	0.0741

Quantiles (Definition 5)	
Quantile	**Estimate**
100% Max	1.2574852
99%	0.9465875
95%	0.7025260
90%	0.5663393
75% Q3	0.3573188
50% Median	0.0246372
25% Q1	-0.3424528
10%	-0.6517656
5%	-0.8212564
1%	-1.0019314
0% Min	-1.1665612

Extreme Observations			
Lowest	**Highest**		
Value	**Obs**	**Value**	**Obs**
-1.166561	128	0.905615	183
-1.058087	17	0.938248	209
-1.001931	228	0.946587	229
-1.001931	109	0.973538	103
-0.897571	241	1.257485	170

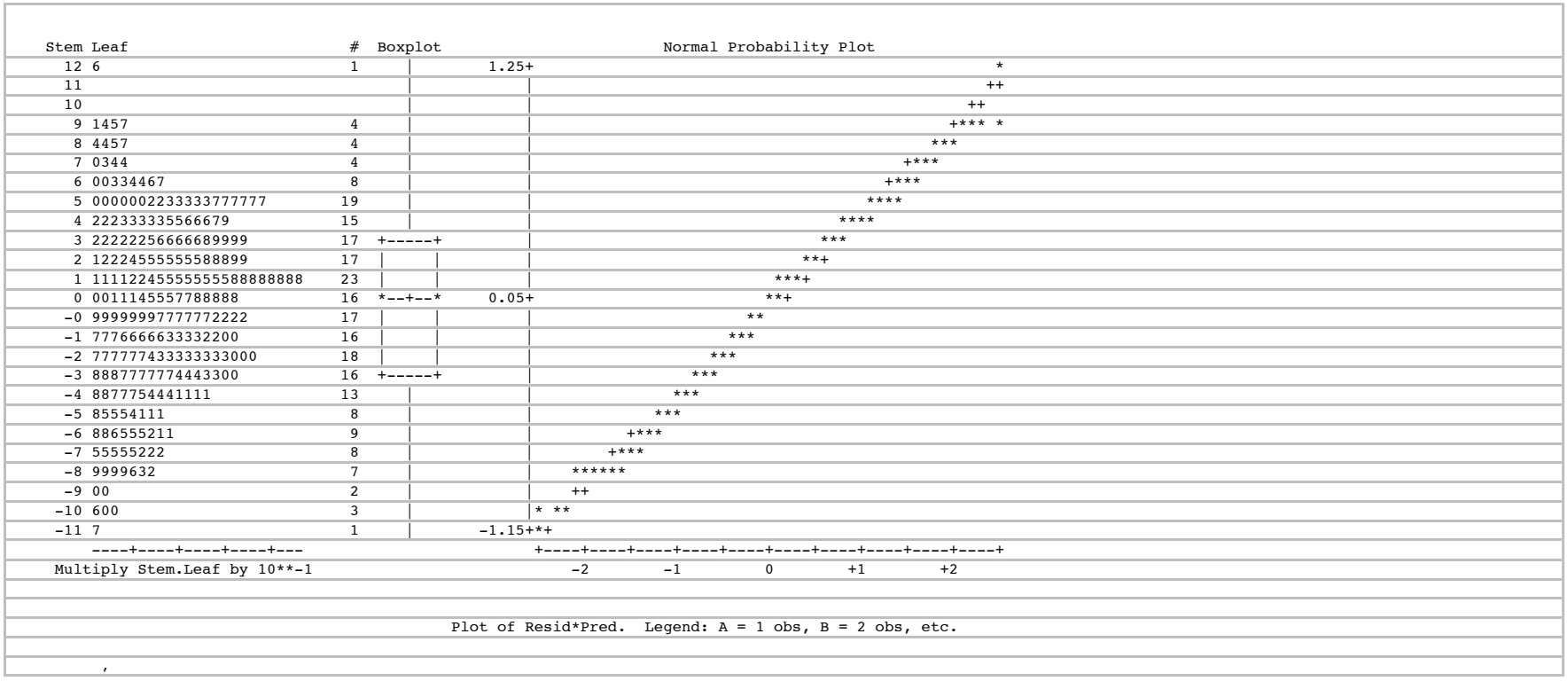

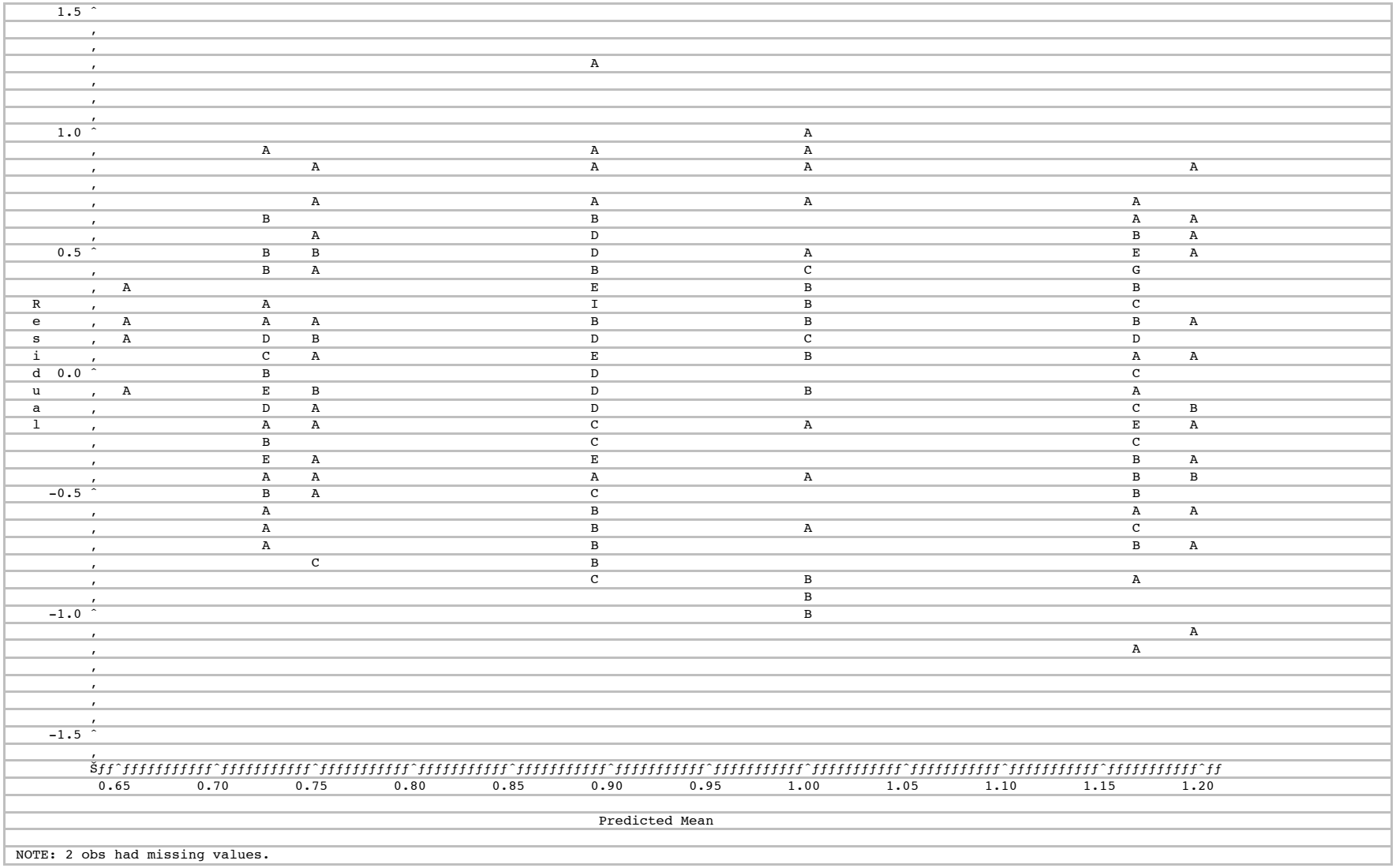

NOTE: 2 obs had missing values.

Entire Data Set (All objectives combined) Collagen Type I ANOVA Results

Model Information	
Data Set	WORK.ANIM
Dependent Variable	ln_Collagen1
Covariance Structure	Variance Components
Estimation Method	REML
Residual Variance Method	Profile
Fixed Effects SE Method	Model-Based
Degrees of Freedom Method	Containment

Class Level Information		
Class	**Levels**	**Values**
load_freq_cat	2	0 1
load_rms_cat	2	0 1
load_dur_cat	2	0 1
block	84	1 2 3 4 5 6 7 8 9 10 11 12 13 14 15 16 17 18 19 20 21 22 23 24 25 26 27 28 29 30 31 32 33 34 35 36 37 38 39 40 41 42 43 44 45 46 47 48 49 50 51 52 53 54 55 56 57 58 59 60 61 62 63 64 65 66 67 68 69 70 71 72 73 74 75 76 77 78 79 80 81 82 83 84

Dimensions	
Covariance Parameters	2
Columns in X	19
Columns in Z	84
Subjects	1
Max Obs Per Subject	244

Number of Observations	
Number of Observations Read	244
Number of Observations Used	239
Number of Observations Not Used	5

Iteration History			
Iteration	Evaluations	-2 Res Log Like	Criterion
0	1	804.08236457	
1	2	706.39486710	0.00352383
2	1	705.83981096	0.00017269
3	1	705.81485430	0.00000050
4	1	705.81478471	0.00000000

Convergence criteria met.

Covariance Parameter Estimates				
Cov Parm	**Estimate**	**Standard Error**	**Z Value**	**Pr > Z**
block	1.3624	0.2682	5.08	<.0001
Residual	0.5440	0.06530	8.33	<.0001

Fit Statistics	
-2 Res Log Likelihood	705.8
AIC (smaller is better)	709.8
AICC (smaller is better)	709.9
BIC (smaller is better)	714.7

Type 3 Tests of Fixed Effects				
Effect	**Num DF**	**Den DF**	**F Value**	**Pr > F**
load_freq_cat	1	149	1.43	0.2338
load_rms_cat	1	149	23.55	<.0001
load_freq*load_rms_c	1	149	1.10	0.2957
load_dur_cat	1	149	0.25	0.6159
load_freq*load_dur_c	1	149	0.97	0.3262
load_rms_*load_dur_c	1	149	20.97	<.0001

Least Squares Means								
Effect	**load_freq_cat**	**load_rms_cat**	**load_dur_cat**	**Estimate**	**Standard Error**	**DF**	**t Value**	**Pr > |t|**
load_freq_cat	0			1.7869	0.2777	149	6.43	<.0001
load_freq_cat	1			1.5470	0.2282	149	6.78	<.0001
load_rms_cat		0		2.7402	0.1948	149	14.07	<.0001
load_rms_cat		1		0.5937	0.4110	149	1.44	0.1507
load_freq*load_rms_c	0	0		2.9402	0.2044	149	14.38	<.0001
load_freq*load_rms_c	0	1		0.6335	0.4855	149	1.30	0.1939
load_freq*load_rms_c	1	0		2.5402	0.2241	149	11.34	<.0001
load_freq*load_rms_c	1	1		0.5538	0.3868	149	1.43	0.1543
load_dur_cat			0	1.5617	0.1466	149	10.65	<.0001
load_du			1	1.7722	0.4186	149	4.23	<.0001

r_cat								
load_freq*load_dur_c	0		0	1.5923	0.1679	149	9.48	<.0001
load_freq*load_dur_c	0		1	1.9814	0.4919	149	4.03	<.0001
load_freq*load_dur_c	1		0	1.5310	0.1644	149	9.31	<.0001
load_freq*load_dur_c	1		1	1.5630	0.4115	149	3.80	0.0002
load_rms_*load_dur_c		0	0	1.6583	0.1721	149	9.64	<.0001
load_rms_*load_dur_c		0	1	3.8221	0.3302	149	11.57	<.0001
load_rms_*load_dur_c		1	0	1.4651	0.1866	149	7.85	<.0001
load_rms_*load_dur_c		1	1	-0.2777	0.7730	149	-0.36	0.7199

Differences of Least Squares Means						
Effect	**load_freq_cat**	**load_rms_cat**	**load_dur_cat**	**_load_freq_cat**	**_load_rms_cat**	**_load_dur_cat**
load_freq_cat	0			1		
load_rms_cat		0			1	
load_freq*load_rms_c	0	0		0	1	
load_freq*load_rms_c	0	0		1	0	
load_freq*load_rms_c	0	0		1	1	
load_freq*load_rms_c	0	1		1	0	
load_freq*load_rms_c	0	1		1	1	
load_freq*load_rms_c	1	0		1	1	
load_dur_cat			0			1
load_freq*load_dur_c	0		0	0		1
load_freq*load_dur_c	0		0	1		0
load_freq*l	0		0	1		1

oad_dur_c						
load_freq*load_dur_c	0		1	1		0
load_freq*load_dur_c	0		1	1		1
load_freq*load_dur_c	1		0	1		1
load_rms_*load_dur_c		0	0		0	1
load_rms_*load_dur_c		0	0		1	0
load_rms_*load_dur_c		0	0		1	1
load_rms_*load_dur_c		0	1		1	0
load_rms_*load_dur_c		0	1		1	1
load_rms_*load_dur_c		1	0		1	1

Differences of Least Squares Means								
Effect	**load_freq_cat**	**load_rms_cat**	**load_dur_cat**	**_load_freq_cat**	**Estimate**	**Standard Error**	**DF**	**t Value**
load_freq_cat	0			1	0.2399	0.2007	149	1.20

load_rms_cat		0			2.1465	0.4423	149	4.85
load_freq*load_rms_c	0	0		0	2.3067	0.4965	149	4.65
load_freq*load_rms_c	0	0		1	0.4001	0.1796	149	2.23
load_freq*load_rms_c	0	0		1	2.3864	0.4241	149	5.63
load_freq*load_rms_c	0	1		1	-1.9066	0.5403	149	-3.53
load_freq*load_rms_c	0	1		1	0.07971	0.3080	149	0.26
load_freq*load_rms_c	1	0		1	1.9863	0.4374	149	4.54
load_dur_cat			0		-0.2105	0.4188	149	-0.50
load_freq*load_dur_c	0		0	0	-0.3891	0.4816	149	-0.81
load_freq*load_dur_c	0		0	1	0.06137	0.1564	149	0.39
load_freq*load_	0		0	1	0.02935	0.4184	149	0.07

dur_c								
load_freq*load_dur_c	0		1	1	0.4504	0.5061	149	0.89
load_freq*load_dur_c	0		1	1	0.4184	0.3490	149	1.20
load_freq*load_dur_c	1		0	1	-0.03202	0.4295	149	-0.07
load_rms_*load_dur_c		0	0		-2.1639	0.3544	149	-6.11
load_rms_*load_dur_c		0	0		0.1932	0.2070	149	0.93
load_rms_*load_dur_c		0	0		1.9360	0.7764	149	2.49
load_rms_*load_dur_c		0	1		2.3571	0.3730	149	6.32
load_rms_*load_dur_c		0	1		4.0999	0.8440	149	4.86
load_rms_*load_dur_c		1	0		1.7428	0.7675	149	2.27

Differences of Least Squares Means							
Effect	**load_freq_cat**	**load_rms_cat**	**load_dur_cat**	**_load_freq_cat**	**Pr > |t|**	**Adjustment**	**Adj P**
load_freq_cat	0			1	0.2338	Tukey-Kramer	0.2338
load_rms_cat		0			<.0001	Tukey-Kramer	<.0001
load_freq*load_rms_c	0	0		0	<.0001	Tukey-Kramer	<.0001
load_freq*load_rms_c	0	0		1	0.0274	Tukey-Kramer	0.1207
load_freq*load_rms_c	0	0		1	<.0001	Tukey-Kramer	<.0001
load_freq*load_rms_c	0	1		1	0.0006	Tukey-Kramer	0.0031
load_freq*load_rms_c	0	1		1	0.7962	Tukey-Kramer	0.9939
load_freq*load_rms_c	1	0		1	<.0001	Tukey-Kramer	<.0001
load_dur_			0		0.6159	Tukey-Kramer	0.6159

cat							
load_freq*load_dur_c	0		0	0	0.4205	Tukey-Kramer	0.8507
load_freq*load_dur_c	0		0	1	0.6953	Tukey-Kramer	0.9794
load_freq*load_dur_c	0		0	1	0.9442	Tukey-Kramer	0.9999
load_freq*load_dur_c	0		1	1	0.3749	Tukey-Kramer	0.8101
load_freq*load_dur_c	0		1	1	0.2324	Tukey-Kramer	0.6284
load_freq*load_dur_c	1		0	1	0.9407	Tukey-Kramer	0.9999
load_rms_*load_dur_c		0	0		<.0001	Tukey-Kramer	<.0001
load_rms_*load_dur_c		0	0		0.3521	Tukey-Kramer	0.7869
load_rms_*load_dur_c		0	0		0.0137	Tukey-Kramer	0.0650
load_rms_*load_dur_c		0	1		<.0001	Tukey-Kramer	<.0001

load_rms_*load_dur_c		0	1		<.0001	Tukey-Kramer	<.0001
load_rms_*load_dur_c		1	0		0.0246	Tukey-Kramer	0.1096
Moments							
N	239	**Sum Weights**	239				
Mean	-0.0338394	**Sum Observations**	-8.087628				
Std Deviation	1.32533316	**Variance**	1.75650798				
Skewness	0.47148112	**Kurtosis**	1.8453064				
Uncorrected SS	418.32258	**Corrected SS**	418.048899				
Coeff Variation	-3916.5331	**Std Error Mean**	0.08572868				

Basic Statistical Measures			
Location	**Variability**		
Mean	-0.03384	**Std Deviation**	1.32533
Median	-0.09378	**Variance**	1.75651
Mode	0.06833	**Range**	7.95996
		Interquartile Range	1.21247

Tests for Location: Mu0=0				
Test	**Statistic**	**p Value**		
Student's t	**t**	-0.39473	**Pr > |t|**	0.6934
Sign	**M**	-14.5	**Pr >= |M|**	0.0699
Signed Rank	**S**	-1432	**Pr >= |S|**	0.1813

Tests for Normality				
Test	**Statistic**	**p Value**		
Shapiro-Wilk	**W**	0.942943	**Pr < W**	<0.0001
Kolmogorov-Smirnov	**D**	0.095023	**Pr > D**	<0.0100
Cramer-von Mises	**W-Sq**	0.628426	**Pr > W-Sq**	<0.0050
Anderson-Darling	**A-Sq**	4.174279	**Pr > A-Sq**	<0.0050

Quantiles (Definition 5)	
Quantile	**Estimate**
100% Max	4.022492
99%	3.755796
95%	2.958705
90%	1.321950
75% Q3	0.518433
50% Median	-0.093777
25% Q1	-0.694036
10%	-1.415659
5%	-1.799414
1%	-3.532838
0% Min	-3.937471

Extreme Observations			
Lowest	**Highest**		
Value	**Obs**	**Value**	**Obs**
-3.93747	23	3.65181	13
-3.55754	27	3.71053	9
-3.53284	26	3.75580	10
-3.35062	18	3.85976	1
-3.27852	36	4.02249	12

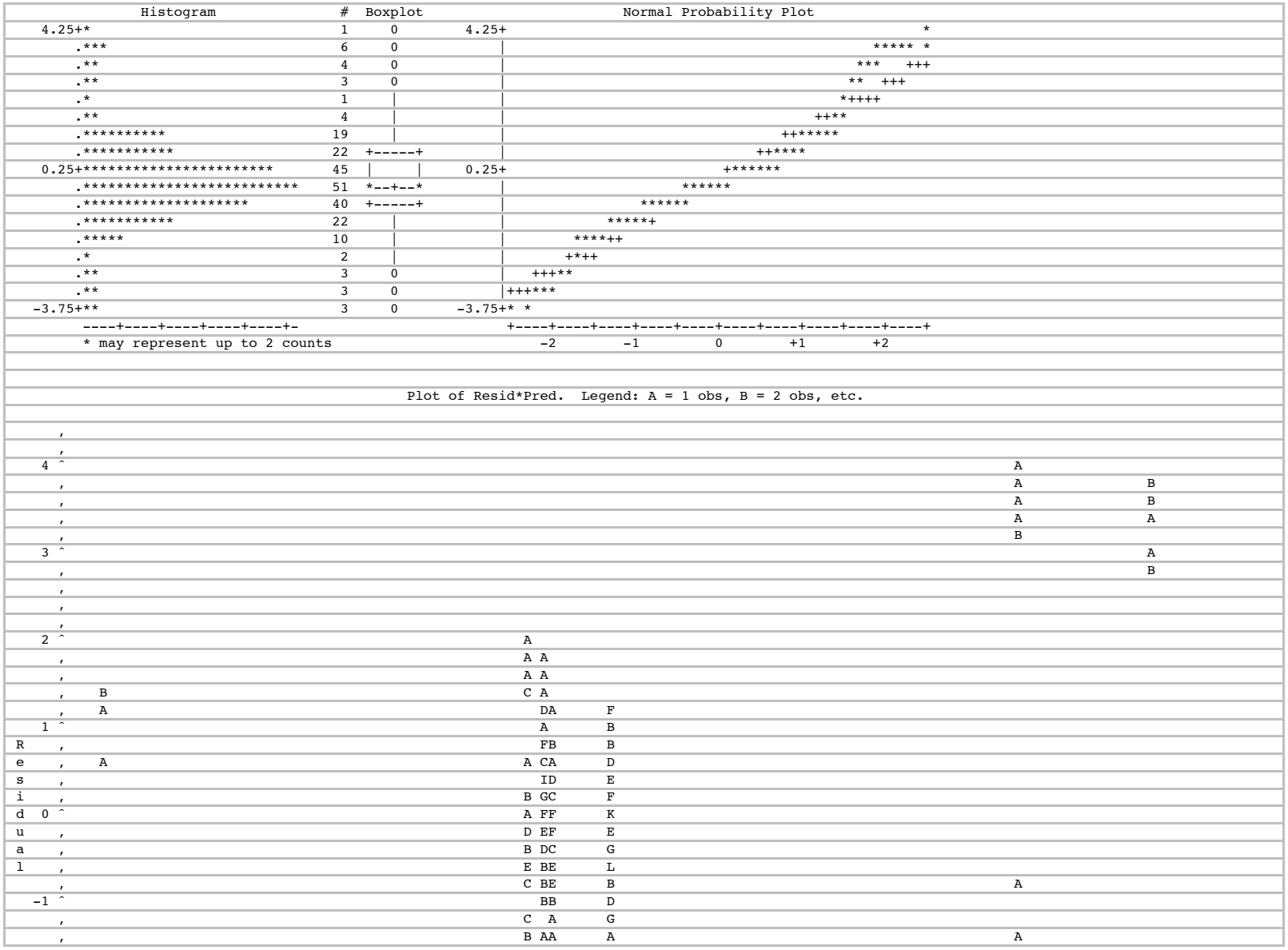
Histogram # Boxplot Normal Probability Plot
4.25+* 1 0 4.25+ *
.*** 6 0 ***** *
.** 4 0 *** +++
.** 3 0 ** +++
.* 1 * ++++
.** 4 ++**
.********** 19 ++******
.********** 22 +-----+ ++****
0.25+********** 45 | | 0.25+ +******
.************** 51 *--+--* ******
.********** 40 +-----+ ******
.********** 22 *****+
.***** 10 ****++
.* 2 +*++
.** 3 0 +++**
.** 3 0 +++***
-3.75+** 3 0 -3.75+* *
----+----+----+----+----+- +----+----+----+----+----+----+----+----+----+----+
* may represent up to 2 counts -2 -1 0 +1 +2
Plot of Resid*Pred. Legend: A = 1 obs, B = 2 obs, etc.
4 ^ A
A B
A B
A A
B
3 ^ A
B
2 ^ A
A A
A A
B C A
A DA F
1 ^ A B
R FB B
e A A CA D
s ID E
i B GC F
d 0 ^ A FF K
u D EF E
a B DC G
l E BE L
C BE B A
-1 ^ BB D
C A G
B AA A A

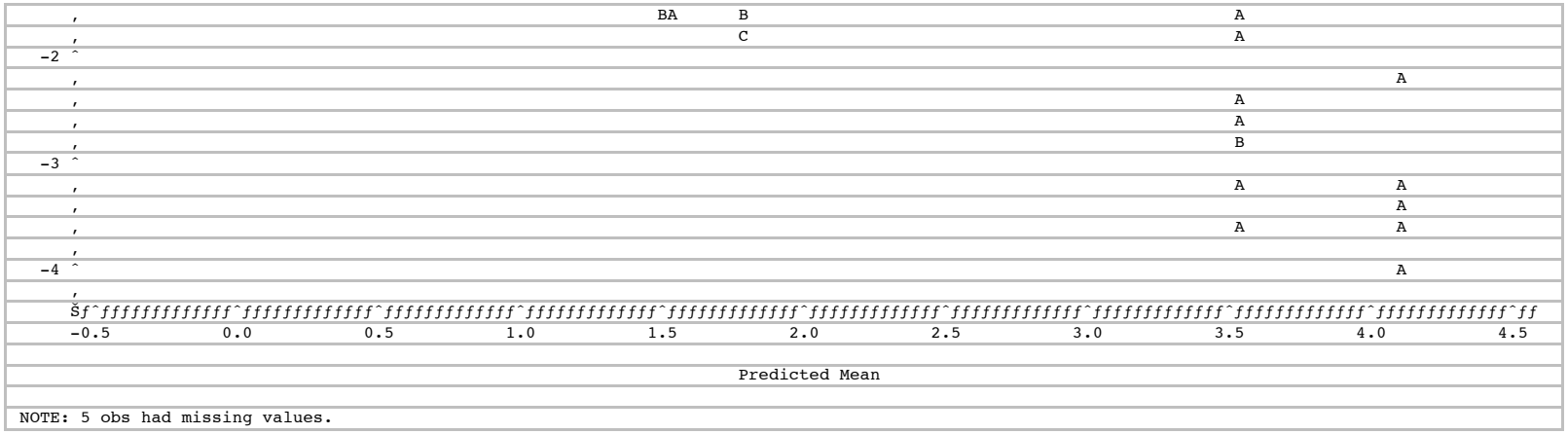

NOTE: 5 obs had missing values.

Entire Data Set (All objectives combined) Collagen Type II ANOVA Results

Model Information	
Data Set	WORK.ANIM
Dependent Variable	ln_Collagen2
Covariance Structure	Variance Components
Estimation Method	REML
Residual Variance Method	Profile
Fixed Effects SE Method	Model-Based
Degrees of Freedom Method	Containment

Class Level Information		
Class	**Levels**	**Values**
load_freq_cat	2	0 1
load_rms_cat	2	0 1
load_dur_cat	2	0 1
block	84	1 2 3 4 5 6 7 8 9 10 11 12 13 14 15 16 17 18 19 20 21 22 23 24 25 26 27 28 29 30 31 32 33 34 35 36 37 38 39 40 41 42 43 44 45 46 47 48 49 50 51 52 53 54 55 56 57 58 59 60 61 62 63 64 65 66 67 68 69 70 71 72 73 74 75 76 77 78 79 80 81 82 83 84

Dimensions	
Covariance Parameters	2
Columns in X	19
Columns in Z	84
Subjects	1
Max Obs Per Subject	249

Number of Observations	
Number of Observations Read	249
Number of Observations Used	245
Number of Observations Not Used	4

Iteration History			
Iteration	Evaluations	-2 Res Log Like	Criterion
0	1	487.90369682	
1	2	459.42599305	0.00137744
2	1	459.41043955	0.00000223
3	1	459.41041497	0.00000000

Convergence criteria met.

Covariance Parameter Estimates				
Cov Parm	**Estimate**	**Standard Error**	**Z Value**	**Pr > Z**
block	0.1690	0.04404	3.84	<.0001
Residual	0.2567	0.02947	8.71	<.0001

Fit Statistics	
-2 Res Log Likelihood	459.4
AIC (smaller is better)	463.4
AICC (smaller is better)	463.5
BIC (smaller is better)	468.3

Type 3 Tests of Fixed Effects				
Effect	**Num DF**	**Den DF**	**F Value**	**Pr > F**
load_freq_cat	1	155	4.56	0.0343
load_rms_cat	1	155	3.55	0.0615
load_freq*load_rms_c	1	155	0.04	0.8433
load_dur_cat	1	155	0.02	0.8891
load_freq*load_dur_c	1	155	0.80	0.3720
load_rms_*load_dur_c	1	155	7.23	0.0080

Least Squares Means								
Effect	**load_freq_cat**	**load_rms_cat**	**load_dur_cat**	**Estimate**	**Standard Error**	**DF**	**t Value**	**Pr > |t|**
load_freq_cat	0			1.2244	0.1461	155	8.38	<.0001
load_freq_cat	1			0.9694	0.1114	155	8.70	<.0001
load_rms_cat		0		1.3079	0.08291	155	15.78	<.0001
load_rms_cat		1		0.8859	0.2118	155	4.18	<.0001
load_freq*load_rms_c	0	0		1.4262	0.09722	155	14.67	<.0001
load_freq*load_rms_c	0	1		1.0226	0.2601	155	3.93	0.0001
load_freq*load_rms_c	1	0		1.1897	0.1013	155	11.75	<.0001
load_freq*load_rms_c	1	1		0.7491	0.1977	155	3.79	0.0002
load_dur_cat			0	1.0816	0.06167	155	17.54	<.0001

load_dur_cat			1	1.1122	0.2161	155	5.15	<.0001
load_freq*load_dur_c	0		0	1.1599	0.07924	155	14.64	<.0001
load_freq*load_dur_c	0		1	1.2888	0.2681	155	4.81	<.0001
load_freq*load_dur_c	1		0	1.0033	0.07640	155	13.13	<.0001
load_freq*load_dur_c	1		1	0.9355	0.2081	155	4.50	<.0001
load_rms_*load_dur_c		0	0	0.9971	0.07781	155	12.81	<.0001
load_rms_*load_dur_c		0	1	1.6188	0.1434	155	11.29	<.0001
load_rms_*load_dur_c		1	0	1.1662	0.08746	155	13.33	<.0001
load_rms_*load_dur_c		1	1	0.6055	0.4066	155	1.49	0.1384

Differences of Least Squares Means						
Effect	**load_freq_cat**	**load_rms_cat**	**load_dur_cat**	**_load_freq_cat**	**_load_rms_cat**	**_load_dur_cat**
load_freq_cat	0			1		
load_rms_cat		0			1	
load_freq*load_rms_c	0	0		0	1	
load_freq*load_rms_c	0	0		1	0	
load_freq*load_rms_c	0	0		1	1	
load_freq*load_rms_c	0	1		1	0	
load_freq*load_rms_c	0	1		1	1	
load_freq*load_rms_c	1	0		1	1	
load_dur_cat			0			1
load_freq*load_dur_c	0		0	0		1
load_freq*load_dur_c	0		0	1		0
load_freq*l	0		0	1		1

oad_dur_c						
load_freq*load_dur_c	0		1	1		0
load_freq*load_dur_c	0		1	1		1
load_freq*load_dur_c	1		0	1		1
load_rms_*load_dur_c		0	0		0	1
load_rms_*load_dur_c		0	0		1	0
load_rms_*load_dur_c		0	0		1	1
load_rms_*load_dur_c		0	1		1	0
load_rms_*load_dur_c		0	1		1	1
load_rms_*load_dur_c		1	0		1	1

Differences of Least Squares Means								
Effect	**load_freq_cat**	**load_rms_cat**	**load_dur_cat**	**_load_freq_cat**	**Estimate**	**Standard Error**	**DF**	**t Value**
load_freq_cat	0			1	0.2550	0.1194	155	2.14

load_rms_cat		0			0.4221	0.2241	155	1.88
load_freq*load_rms_c	0	0		0	0.4036	0.2624	155	1.54
load_freq*load_rms_c	0	0		1	0.2365	0.1092	155	2.17
load_freq*load_rms_c	0	0		1	0.6770	0.2189	155	3.09
load_freq*load_rms_c	0	1		1	-0.1671	0.2847	155	-0.59
load_freq*load_rms_c	0	1		1	0.2734	0.1845	155	1.48
load_freq*load_rms_c	1	0		1	0.4406	0.2214	155	1.99
load_dur_cat			0		-0.03052	0.2185	155	-0.14
load_freq*load_dur_c	0		0	0	-0.1289	0.2665	155	-0.48
load_freq*load_dur_c	0		0	1	0.1566	0.09496	155	1.65
load_freq*load_	0		0	1	0.2244	0.2176	155	1.03

dur_c								
load_freq*load_dur_c	0		1	1	0.2855	0.2769	155	1.03
load_freq*load_dur_c	0		1	1	0.3533	0.2089	155	1.69
load_freq*load_dur_c	1		0	1	0.06784	0.2206	155	0.31
load_rms_*load_dur_c		0	0		-0.6218	0.1605	155	-3.87
load_rms_*load_dur_c		0	0		-0.1692	0.1104	155	-1.53
load_rms_*load_dur_c		0	0		0.3916	0.4097	155	0.96
load_rms_*load_dur_c		0	1		0.4526	0.1677	155	2.70
load_rms_*load_dur_c		0	1		1.0133	0.4301	155	2.36
load_rms_*load_dur_c		1	0		0.5607	0.4080	155	1.37

Differences of Least Squares Means							
Effect	**load_freq_cat**	**load_rms_cat**	**load_dur_cat**	**_load_freq_cat**	**Pr > |t|**	**Adjustment**	**Adj P**
load_freq_cat	0			1	0.0343	Tukey-Kramer	0.0343
load_rms_cat		0			0.0615	Tukey-Kramer	0.0615
load_freq*load_rms_c	0	0		0	0.1261	Tukey-Kramer	0.4174
load_freq*load_rms_c	0	0		1	0.0318	Tukey-Kramer	0.1373
load_freq*load_rms_c	0	0		1	0.0023	Tukey-Kramer	0.0124
load_freq*load_rms_c	0	1		1	0.5581	Tukey-Kramer	0.9359
load_freq*load_rms_c	0	1		1	0.1403	Tukey-Kramer	0.4506
load_freq*load_rms_c	1	0		1	0.0484	Tukey-Kramer	0.1963
load_dur_			0		0.8891	Tukey-Kramer	0.8891

cat							
load_freq*load_dur_c	0		0	0	0.6293	Tukey-Kramer	0.9626
load_freq*load_dur_c	0		0	1	0.1012	Tukey-Kramer	0.3544
load_freq*load_dur_c	0		0	1	0.3040	Tukey-Kramer	0.7313
load_freq*load_dur_c	0		1	1	0.3042	Tukey-Kramer	0.7316
load_freq*load_dur_c	0		1	1	0.0928	Tukey-Kramer	0.3317
load_freq*load_dur_c	1		0	1	0.7588	Tukey-Kramer	0.9899
load_rms_*load_dur_c		0	0		0.0002	Tukey-Kramer	0.0009
load_rms_*load_dur_c		0	0		0.1276	Tukey-Kramer	0.4210
load_rms_*load_dur_c		0	0		0.3407	Tukey-Kramer	0.7747
load_rms_*load_dur_c		0	1		0.0077	Tukey-Kramer	0.0383

load_rms_*load_dur_c		0	1		0.0197	Tukey-Kramer	0.0901
load_rms_*load_dur_c		1	0		0.1713	Tukey-Kramer	0.5174
Moments							
N	245	**Sum Weights**	245				
Mean	-0.0041864	**Sum Observations**	-1.0256769				
Std Deviation	0.6390370 1	**Variance**	0.4083683				
Skewness	0.2419599 2	**Kurtosis**	0.3935664 7				
Uncorrected SS	99.646159 8	**Corrected SS**	99.641865 9				
Coeff Variation	-15264.463	**Std Error Mean**	0.0408265 8				

Basic Statistical Measures			
Location	**Variability**		
Mean	-0.00419	**Std Deviation**	0.63904
Median	-0.04182	**Variance**	0.40837
Mode	0.35457	**Range**	4.21641
		Interquartile Range	0.82119

Tests for Location: Mu0=0				
Test	**Statistic**	**p Value**		
Student's t	**t**	-0.10254	**Pr > |t|**	0.9184
Sign	**M**	-4.5	**Pr >= |M|**	0.6094
Signed Rank	**S**	-240.5	**Pr >= |S|**	0.8290

Tests for Normality				
Test	**Statistic**	**p Value**		
Shapiro-Wilk	**W**	0.993435	**Pr < W**	0.3578
Kolmogorov-Smirnov	**D**	0.034268	**Pr > D**	>0.1500
Cramer-von Mises	**W-Sq**	0.034389	**Pr > W-Sq**	>0.2500
Anderson-Darling	**A-Sq**	0.251574	**Pr > A-Sq**	>0.2500

Quantiles (Definition 5)	
Quantile	**Estimate**
100% Max	2.4301683
99%	1.5409545
95%	1.0337112
90%	0.7712454
75% Q3	0.4119779
50% Median	-0.0418193
25% Q1	-0.4092091
10%	-0.8271077
5%	-1.0269038
1%	-1.2537603
0% Min	-1.7862375

Extreme Observations			
Lowest	**Highest**		
Value	**Obs**	**Value**	**Obs**
-1.78624	32	1.51883	208
-1.44265	28	1.53285	230
-1.25376	246	1.54095	8
-1.25376	229	1.72686	244
-1.25376	90	2.43017	4

```
   Stem Leaf                                      #  Boxplot                        Normal Probability Plot
     24 3                                         1     0        2.5+                                                   *
     22                                                              |
     20                                                              |
     18                                                              |
     16 3                                         1     0            |                                                  *
     14 234                                       3     |            |                                              ***++
     12 49                                        2     |            |                                            **+
     10 378357                                    6     |        1.1+                                          ****
      8 1339122788                               10     |            |                                      ****
      6 000055557777912779                       18     |            |                                   ****
      4 155667889911133355667                    21  +-----+         |                                ****
      2 001112444455577788888912255555568899     36  |     |         |                            *****
      0 34478888001234457888                     20  |     |         |                          **+
     -0 98877743333100000007776643331            29  *--+--*         |                      ****
     -2 999977554444100888877775543310000        33  |     |    -0.3+                   ****
     -4 866539888854421111                       18  +-----+         |                ****
     -6 766554322299642221000                    21     |            |             ****
     -8 7763306633                               10     |            |          ***
    -10 8877763100                               10     |            |      ****
    -12 5551                                      4     |            |  ****+
    -14 4                                         1     |            |*+++
    -16 9                                         1     0       -1.7+*
        ----+----+----+----+----+----+----+-                         +----+----+----+----+----+----+----+----+----+----+
    Multiply Stem.Leaf by 10**-1                                         -2        -1         0        +1        +2


                                               Plot of Resid*Pred.  Legend: A = 1 obs, B = 2 obs, etc.

     ,
     ,
   3 ^
     ,
     ,
     ,
     ,                                                                                                          A
     ,
     ,
   2 ^
     ,
     ,                                                                                      A
     ,                                                                    A                 A                                                      A
     ,
     ,                                                                                      A                   A
R    ,                                                                    BA                                                                       A
e  1 ^                                                      A             AB                A
s    ,                                                                    BB                B                                                      B
i    ,                                                      A             DC                C                   A                                  A
d    ,   A                                                  H             AC                A                                                      A
u    ,   A                                                  A             DE                A                   A                                  A
a    ,   A                                                  D             ND                C                                                      A
l    ,                                                      C             FE                C                   C                                  A
   0 ^                                                      C             DA                C                   A
     ,   A                                                  F             JF                                    B                                  A
```

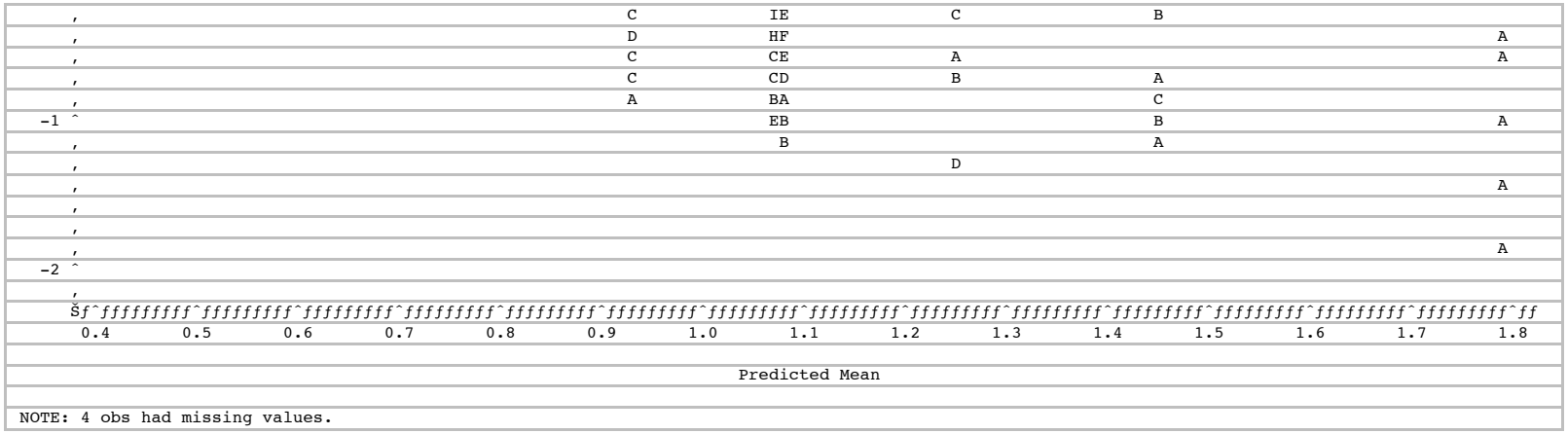

NOTE: 4 obs had missing values.

Entire Data Set (All objectives combined) Decorin ANOVA Results

Model Information	
Data Set	WORK.ANIM
Dependent Variable	ln_Decorin
Covariance Structure	Variance Components
Estimation Method	REML
Residual Variance Method	Profile
Fixed Effects SE Method	Model-Based
Degrees of Freedom Method	Containment

Class Level Information		
Class	**Levels**	**Values**
load_freq_cat	2	0 1
load_rms_cat	2	0 1
load_dur_cat	2	0 1
block	84	1 2 3 4 5 6 7 8 9 10 11 12 13 14 15 16 17 18 19 20 21 22 23 24 25 26 27 28 29 30 31 32 33 34 35 36 37 38 39 40 41 42 43 44 45 46 47 48 49 50 51 52 53 54 55 56 57 58 59 60 61 62 63 64 65 66 67 68 69 70 71 72 73 74 75 76 77 78 79 80 81 82 83 84

Dimensions	
Covariance Parameters	2
Columns in X	19
Columns in Z	84
Subjects	1
Max Obs Per Subject	250

Number of Observations	
Number of Observations Read	250
Number of Observations Used	247
Number of Observations Not Used	3

Iteration History			
Iteration	Evaluations	-2 Res Log Like	Criterion
0	1	549.02605909	
1	2	517.04595769	0.00001409
2	1	517.04541983	0.00000000

Convergence criteria met.

Covariance Parameter Estimates				
Cov Parm	**Estimate**	**Standard Error**	**Z Value**	**Pr > Z**
block	0.2141	0.05375	3.98	<.0001
Residual	0.3206	0.03617	8.86	<.0001

Fit Statistics	
-2 Res Log Likelihood	517.0
AIC (smaller is better)	521.0
AICC (smaller is better)	521.1
BIC (smaller is better)	525.9

Type 3 Tests of Fixed Effects				
Effect	**Num DF**	**Den DF**	**F Value**	**Pr > F**
load_freq_cat	1	157	0.02	0.8946
load_rms_cat	1	157	1.19	0.2772
load_freq*load_rms_c	1	157	3.51	0.0629
load_dur_cat	1	157	1.24	0.2663
load_freq*load_dur_c	1	157	0.06	0.8062
load_rms_*load_dur_c	1	157	0.74	0.3907

Least Squares Means								
Effect	**load_freq_cat**	**load_rms_cat**	**load_dur_cat**	**Estimate**	**Standard Error**	**DF**	**t Value**	**Pr > |t|**
load_freq_cat	0			1.2575	0.1634	157	7.69	<.0001
load_freq_cat	1			1.2399	0.1246	157	9.95	<.0001
load_rms_cat		0		1.1123	0.09253	157	12.02	<.0001
load_rms_cat		1		1.3851	0.2371	157	5.84	<.0001
load_freq*load_rms_c	0	0		1.2184	0.1087	157	11.21	<.0001
load_freq*load_rms_c	0	1		1.2966	0.2904	157	4.46	<.0001
load_freq*load_rms_c	1	0		1.0062	0.1123	157	8.96	<.0001
load_freq*load_rms_c	1	1		1.4736	0.2216	157	6.65	<.0001
load_dur_cat			0	1.3853	0.06934	157	19.98	<.0001
load_du			1	1.1121	0.2421	157	4.59	<.0001

r_cat								
load_freq*load_dur_c	0		0	1.3791	0.08912	157	15.47	<.0001
load_freq*load_dur_c	0		1	1.1359	0.2997	157	3.79	0.0002
load_freq*load_dur_c	1		0	1.3914	0.08563	157	16.25	<.0001
load_freq*load_dur_c	1		1	1.0884	0.2327	157	4.68	<.0001
load_rms_*load_dur_c		0	0	1.3547	0.08669	157	15.63	<.0001
load_rms_*load_dur_c		0	1	0.8699	0.1601	157	5.43	<.0001
load_rms_*load_dur_c		1	0	1.4158	0.09801	157	14.45	<.0001
load_rms_*load_dur_c		1	1	1.3544	0.4552	157	2.98	0.0034

Differences of Least Squares Means						
Effect	**load_freq_cat**	**load_rms_cat**	**load_dur_cat**	**_load_freq_cat**	**_load_rms_cat**	**_load_dur_cat**
load_freq_cat	0			1		
load_rms_cat		0			1	
load_freq*load_rms_c	0	0		0	1	
load_freq*load_rms_c	0	0		1	0	
load_freq*load_rms_c	0	0		1	1	
load_freq*load_rms_c	0	1		1	0	
load_freq*load_rms_c	0	1		1	1	
load_freq*load_rms_c	1	0		1	1	
load_dur_cat			0			1
load_freq*load_dur_c	0		0	0		1
load_freq*load_dur_c	0		0	1		0
load_freq*l	0		0	1		1

oad_dur_c						
load_freq*load_dur_c	0		1	1		0
load_freq*load_dur_c	0		1	1		1
load_freq*load_dur_c	1		0	1		1
load_rms_*load_dur_c		0	0		0	1
load_rms_*load_dur_c		0	0		1	0
load_rms_*load_dur_c		0	0		1	1
load_rms_*load_dur_c		0	1		1	0
load_rms_*load_dur_c		0	1		1	1
load_rms_*load_dur_c		1	0		1	1

Differences of Least Squares Means								
Effect	**load_freq_cat**	**load_rms_cat**	**load_dur_cat**	**_load_freq_cat**	**Estimate**	**Standard Error**	**DF**	**t Value**
load_freq_cat	0			1	0.01758	0.1325	157	0.13

load_rms_cat		0			-0.2728	0.2502	157	-1.09
load_freq*load_rms_c	0	0		0	-0.07820	0.2924	157	-0.27
load_freq*load_rms_c	0	0		1	0.2122	0.1209	157	1.76
load_freq*load_rms_c	0	0		1	-0.2552	0.2451	157	-1.04
load_freq*load_rms_c	0	1		1	0.2904	0.3166	157	0.92
load_freq*load_rms_c	0	1		1	-0.1770	0.2051	157	-0.86
load_freq*load_rms_c	1	0		1	-0.4674	0.2476	157	-1.89
load_dur_cat			0		0.2731	0.2448	157	1.12
load_freq*load_dur_c	0		0	0	0.2432	0.2977	157	0.82
load_freq*load_dur_c	0		0	1	-0.01232	0.1064	157	-0.12
load_freq*load_	0		0	1	0.2907	0.2434	157	1.19

dur_c								
load_freq*load_dur_c	0		1	1	-0.2555	0.3094	157	-0.83
load_freq*load_dur_c	0		1	1	0.04749	0.2311	157	0.21
load_freq*load_dur_c	1		0	1	0.3030	0.2467	157	1.23
load_rms_*load_dur_c		0	0		0.4848	0.1791	157	2.71
load_rms_*load_dur_c		0	0		-0.06109	0.1225	157	-0.50
load_rms_*load_dur_c		0	0		0.000310	0.4582	157	0.00
load_rms_*load_dur_c		0	1		-0.5459	0.1873	157	-2.91
load_rms_*load_dur_c		0	1		-0.4845	0.4808	157	-1.01
load_rms_*load_dur_c		1	0		0.06140	0.4569	157	0.13

Differences of Least Squares Means							
Effect	**load_freq_cat**	**load_rms_cat**	**load_dur_cat**	**_load_freq_cat**	**Pr > |t|**	**Adjustment**	**Adj P**
load_freq_cat	0			1	0.8946	Tukey-Kramer	0.8946
load_rms_cat		0			0.2772	Tukey-Kramer	0.2772
load_freq*load_rms_c	0	0		0	0.7894	Tukey-Kramer	0.9933
load_freq*load_rms_c	0	0		1	0.0811	Tukey-Kramer	0.2987
load_freq*load_rms_c	0	0		1	0.2994	Tukey-Kramer	0.7255
load_freq*load_rms_c	0	1		1	0.3604	Tukey-Kramer	0.7957
load_freq*load_rms_c	0	1		1	0.3894	Tukey-Kramer	0.8239
load_freq*load_rms_c	1	0		1	0.0609	Tukey-Kramer	0.2376
load_dur_			0		0.2663	Tukey-Kramer	0.2663

cat							
load_freq*load_dur_c	0		0	0	0.4152	Tukey-Kramer	0.8464
load_freq*load_dur_c	0		0	1	0.9079	Tukey-Kramer	0.9994
load_freq*load_dur_c	0		0	1	0.2342	Tukey-Kramer	0.6314
load_freq*load_dur_c	0		1	1	0.4101	Tukey-Kramer	0.8421
load_freq*load_dur_c	0		1	1	0.8374	Tukey-Kramer	0.9969
load_freq*load_dur_c	1		0	1	0.2211	Tukey-Kramer	0.6098
load_rms_*load_dur_c		0	0		0.0075	Tukey-Kramer	0.0374
load_rms_*load_dur_c		0	0		0.6187	Tukey-Kramer	0.9593
load_rms_*load_dur_c		0	0		0.9995	Tukey-Kramer	1.0000
load_rms_*load_dur_c		0	1		0.0041	Tukey-Kramer	0.0211

load_rms_*load_dur_c		0	1		0.3152	Tukey-Kramer	0.7452
load_rms_*load_dur_c		1	0		0.8933	Tukey-Kramer	0.9991
Moments							
N	247	**Sum Weights**	247				
Mean	0.0070172 9	**Sum Observations**	1.7332696 5				
Std Deviation	0.7193980 7	**Variance**	0.5175335 8				
Skewness	0.0786510 5	**Kurtosis**	-0.5652398				
Uncorrected SS	127.32542 3	**Corrected SS**	127.31326				
Coeff Variation	10251.799 1	**Std Error Mean**	0.0457742				

Basic Statistical Measures			
Location	**Variability**		
Mean	0.00702	**Std Deviation**	0.71940
Median	0.04480	**Variance**	0.51753
Mode	-1.44586	**Range**	3.40054
		Interquartile Range	1.11254

Tests for Location: Mu0=0				
Test	**Statistic**	**p Value**		
Student's t	**t**	0.153302	**Pr > |t|**	0.8783
Sign	**M**	6.5	**Pr >= |M|**	0.4452
Signed Rank	**S**	24	**Pr >= |S|**	0.9830

Tests for Normality				
Test	**Statistic**	**p Value**		
Shapiro-Wilk	**W**	0.989253	**Pr < W**	0.0634
Kolmogorov-Smirnov	**D**	0.056848	**Pr > D**	0.0496
Cramer-von Mises	**W-Sq**	0.124629	**Pr > W-Sq**	0.0525
Anderson-Darling	**A-Sq**	0.719259	**Pr > A-Sq**	0.0626

Quantiles (Definition 5)	
Quantile	**Estimate**
100% Max	1.8812609
99%	1.6386620
95%	1.1190901
90%	0.9202256
75% Q3	0.5329433
50% Median	0.0447951
25% Q1	-0.5795994
10%	-0.9314890
5%	-1.1682275
1%	-1.4458592
0% Min	-1.5192757

Extreme Observations			
Lowest	**Highest**		
Value	**Obs**	**Value**	**Obs**
-1.51928	158	1.49464	227
-1.44586	244	1.63367	228
-1.44586	191	1.63866	52
-1.44586	88	1.85106	9
-1.44586	49	1.88126	58

```
    Stem Leaf                                #  Boxplot                        Normal Probability Plot
      18 58                                  2     |         1.9+                                                  *
      16 34                                  2     |            |                                              **+
      14 339                                 3     |            |                                           ***+
      12 239                                 3     |            |                                         +**
      10 145581259                           9     |            |                                      ****
       8 014458811255888                    15     |            |                                   ****
       6 00011134446666703347788            23     |            |                                ****
       4 23336666666799990033469            23  +-----+         |                             ****
       2 2225889002256677999                19  |     |         |                           ***
       0 0112444557888891111256678888899    31  *--+--*         |                       ****
      -0 976663300866433332                 18  |     |         |                     ***
      -2 7433110076443300                   16  |     |         |                   +**
      -4 888877751111088877431110           24  +-----+         |                +****
      -6 999855422211755552211111           24     |            |             *****
      -8 99666539999997631                  17     |            |          ****
     -10 8740977                             7     |            |       ***+
     -12 114311                              6     |            |    ****
     -14 25555                               5     |        -1.5+* ***+
         ----+----+----+----+----+----+-                        +----+----+----+----+----+----+----+----+----+----+
     Multiply Stem.Leaf by 10**-1                                    -2        -1         0        +1        +2


                                                Plot of Resid*Pred.  Legend: A = 1 obs, B = 2 obs, etc.

                  ,
              2.0 ^
                  ,                                                                                                    A
                  ,                                        A
                  ,
                  ,                                                                                   A                A
                  ,
              1.5 ^                                                                                   A
                  ,                                                                                   B                          A
                  ,                                                                                                    A         A
                  ,
                  ,                                                                                   A                A
                  ,                                                                                   B                B         B
              1.0 ^        A                                                                                           C
                  ,                                                                            B      A                D
                  ,        A                               B                                          A                A
                  ,        A                                                                   A      A                A         C
                  ,        A                               B                                   A      B                          D
           R      ,        A                                                                   C                       C         A
           e  0.5 ^        C                               A                                   C                       D         B
           s      ,                                                                            B      A                C         E
           i      ,                                        A                                   D                       C         B
           d      ,                                                                                                    D         B
           u      ,        A                                                                   D      A              A B         B
           a      ,        B                               A                                   D      A                D         C
           l  0.0 ^                                                                            A                       D         E
                  ,                                                                            A                     A A         C
                  ,                                                                            C                       D         B
                  ,        A                                                                   A                       B         B
```

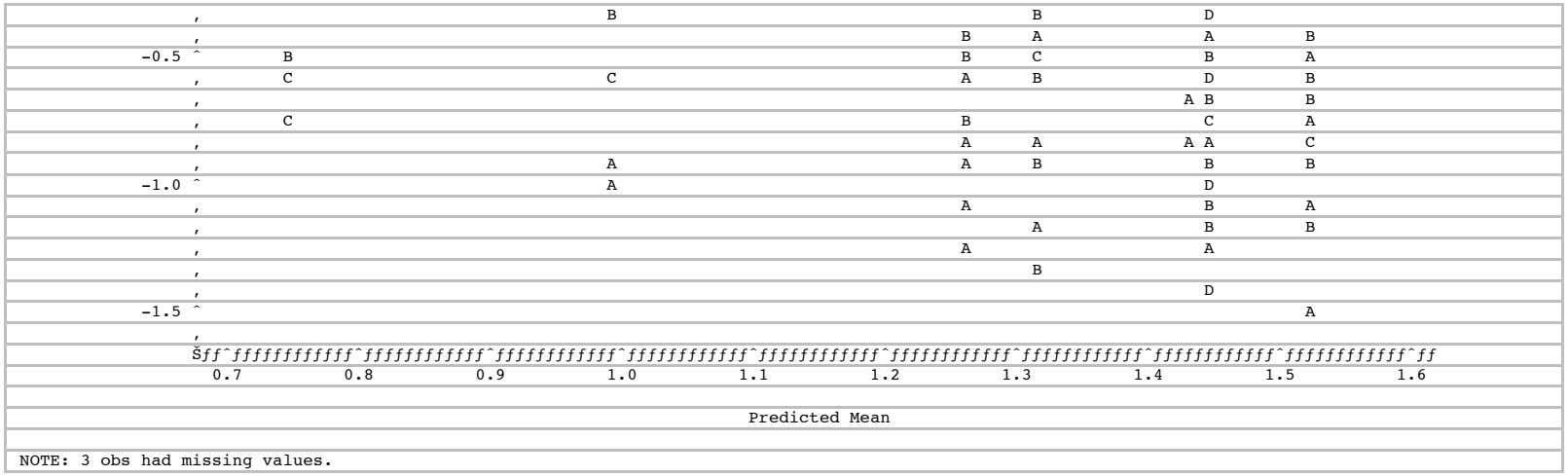

NOTE: 3 obs had missing values.

Entire Data Set (All objectives combined) Versican ANOVA Results

Model Information	
Data Set	WORK.ANIM
Dependent Variable	ln_Versican
Covariance Structure	Variance Components
Estimation Method	REML
Residual Variance Method	Profile
Fixed Effects SE Method	Model-Based
Degrees of Freedom Method	Containment

Class Level Information		
Class	**Levels**	**Values**
load_freq_cat	2	0 1
load_rms_cat	2	0 1
load_dur_cat	2	0 1
block	84	1 2 3 4 5 6 7 8 9 10 11 12 13 14 15 16 17 18 19 20 21 22 23 24 25 26 27 28 29 30 31 32 33 34 35 36 37 38 39 40 41 42 43 44 45 46 47 48 49 50 51 52 53 54 55 56 57 58 59 60 61 62 63 64 65 66 67 68 69 70 71 72 73 74 75 76 77 78 79 80 81 82 83 84

Dimensions	
Covariance Parameters	2
Columns in X	19
Columns in Z	84
Subjects	1
Max Obs Per Subject	250

Number of Observations	
Number of Observations Read	250
Number of Observations Used	247
Number of Observations Not Used	3

Iteration History			
Iteration	Evaluations	-2 Res Log Like	Criterion
0	1	536.58813398	
1	2	468.32184892	0.00001162
2	1	468.32169030	0.00000000

Convergence criteria met.

Covariance Parameter Estimates				
Cov Parm	**Estimate**	**Standard Error**	**Z Value**	**Pr > Z**
block	0.2791	0.05700	4.90	<.0001
Residual	0.2252	0.02526	8.91	<.0001

Fit Statistics	
-2 Res Log Likelihood	468.3
AIC (smaller is better)	472.3
AICC (smaller is better)	472.4
BIC (smaller is better)	477.2

Type 3 Tests of Fixed Effects				
Effect	**Num DF**	**Den DF**	**F Value**	**Pr > F**
load_freq_cat	1	157	0.01	0.9139
load_rms_cat	1	157	0.35	0.5530
load_freq*load_rms_c	1	157	0.97	0.3270
load_dur_cat	1	157	1.41	0.2370
load_freq*load_dur_c	1	157	0.29	0.5903
load_rms_*load_dur_c	1	157	0.03	0.8653

Least Squares Means								
Effect	**load_freq_cat**	**load_rms_cat**	**load_dur_cat**	**Estimate**	**Standard Error**	**DF**	**t Value**	**Pr > |t|**
load_freq_cat	0			1.4525	0.1531	157	9.48	<.0001
load_freq_cat	1			1.4400	0.1212	157	11.88	<.0001
load_rms_cat		0		1.5180	0.09523	157	15.94	<.0001
load_rms_cat		1		1.3744	0.2271	157	6.05	<.0001
load_freq*load_rms_c	0	0		1.5697	0.1057	157	14.84	<.0001
load_freq*load_rms_c	0	1		1.3352	0.2722	157	4.91	<.0001
load_freq*load_rms_c	1	0		1.4662	0.1109	157	13.22	<.0001
load_freq*load_rms_c	1	1		1.4137	0.2135	157	6.62	<.0001
load_dur_cat			0	1.5850	0.07146	157	22.18	<.0001

load_dur_cat			1	1.3074	0.2318	157	5.64	<.0001
load_freq*load_dur_c	0		0	1.5631	0.08696	157	17.97	<.0001
load_freq*load_dur_c	0		1	1.3418	0.2774	157	4.84	<.0001
load_freq*load_dur_c	1		0	1.6069	0.08452	157	19.01	<.0001
load_freq*load_dur_c	1		1	1.2730	0.2241	157	5.68	<.0001
load_rms_*load_dur_c		0	0	1.6767	0.08756	157	19.15	<.0001
load_rms_*load_dur_c		0	1	1.3592	0.1634	157	8.32	<.0001
load_rms_*load_dur_c		1	0	1.4932	0.09676	157	15.43	<.0001
load_rms_*load_dur_c		1	1	1.2557	0.4331	157	2.90	0.0043

Differences of Least Squares Means						
Effect	**load_freq_cat**	**load_rms_cat**	**load_dur_cat**	**_load_freq_cat**	**_load_rms_cat**	**_load_dur_cat**
load_freq_cat	0			1		
load_rms_cat		0			1	
load_freq*load_rms_c	0	0		0	1	
load_freq*load_rms_c	0	0		1	0	
load_freq*load_rms_c	0	0		1	1	
load_freq*load_rms_c	0	1		1	0	
load_freq*load_rms_c	0	1		1	1	
load_freq*load_rms_c	1	0		1	1	
load_dur_cat			0			1
load_freq*load_dur_c	0		0	0		1
load_freq*load_dur_c	0		0	1		0
load_freq*l	0		0	1		1

oad_dur_c						
load_freq*load_dur_c	0		1	1		0
load_freq*load_dur_c	0		1	1		1
load_freq*load_dur_c	1		0	1		1
load_rms_*load_dur_c		0	0		0	1
load_rms_*load_dur_c		0	0		1	0
load_rms_*load_dur_c		0	0		1	1
load_rms_*load_dur_c		0	1		1	0
load_rms_*load_dur_c		0	1		1	1
load_rms_*load_dur_c		1	0		1	1

Differences of Least Squares Means								
Effect	**load_freq_cat**	**load_rms_cat**	**load_dur_cat**	**_load_freq_cat**	**Estimate**	**Standard Error**	**DF**	**t Value**
load_freq_cat	0			1	0.01250	0.1154	157	0.11
load_rms_cat		0			0.1435	0.2414	157	0.59
load_freq*load_rms_c	0	0		0	0.2346	0.2770	157	0.85
load_freq*load_rms_c	0	0		1	0.1035	0.1034	157	1.00
load_freq*load_rms_c	0	0		1	0.1560	0.2350	157	0.66
load_freq*load_rms_c	0	1		1	-0.1310	0.2966	157	-0.44
load_freq*load_rms_c	0	1		1	-0.07854	0.1819	157	-0.43
load_freq*load_rms_c	1	0		1	0.05247	0.2386	157	0.22
load_du			0		0.2776	0.2338	157	1.19

r_cat								
load_freq*load_dur_c	0		0	0	0.2213	0.2742	157	0.81
load_freq*load_dur_c	0		0	1	-0.04376	0.09479	157	-0.46
load_freq*load_dur_c	0		0	1	0.2901	0.2317	157	1.25
load_freq*load_dur_c	0		1	1	-0.2651	0.2869	157	-0.92
load_freq*load_dur_c	0		1	1	0.06876	0.1984	157	0.35
load_freq*load_dur_c	1		0	1	0.3338	0.2365	157	1.41
load_rms_*load_dur_c		0	0		0.3176	0.1802	157	1.76
load_rms_*load_dur_c		0	0		0.1835	0.1168	157	1.57
load_rms_*load_dur_c		0	0		0.4211	0.4362	157	0.97
load_rms_*load_dur_c		0	1		-0.1341	0.1888	157	-0.71

load_rms_*load_dur_c		0	1		0.1035	0.4622	157	0.22
load_rms_*load_dur_c		1	0		0.2376	0.4332	157	0.55

Differences of Least Squares Means							
Effect	**load_freq_cat**	**load_rms_cat**	**load_dur_cat**	**_load_freq_cat**	**Pr > |t|**	**Adjustment**	**Adj P**
load_freq_cat	0			1	0.9139	Tukey-Kramer	0.9139
load_rms_cat		0			0.5530	Tukey-Kramer	0.5530
load_freq*load_rms_c	0	0		0	0.3984	Tukey-Kramer	0.8320
load_freq*load_rms_c	0	0		1	0.3182	Tukey-Kramer	0.7488
load_freq*load_rms_c	0	0		1	0.5076	Tukey-Kramer	0.9104
load_freq*load_rms_c	0	1		1	0.6592	Tukey-Kramer	0.9711
load_freq	0	1		1	0.6664	Tukey-	0.9729

***load_rms_c**						Kramer	
load_freq *load_rms_c	1	0		1	0.8262	Tukey-Kramer	0.9962
load_dur_cat			0		0.2370	Tukey-Kramer	0.2370
load_freq *load_dur_c	0		0	0	0.4208	Tukey-Kramer	0.8510
load_freq *load_dur_c	0		0	1	0.6450	Tukey-Kramer	0.9673
load_freq *load_dur_c	0		0	1	0.2124	Tukey-Kramer	0.5948
load_freq *load_dur_c	0		1	1	0.3569	Tukey-Kramer	0.7920
load_freq *load_dur_c	0		1	1	0.7294	Tukey-Kramer	0.9857
load_freq *load_dur_c	1		0	1	0.1601	Tukey-Kramer	0.4940
load_rms_*load_dur_c		0	0		0.0800	Tukey-Kramer	0.2955
load_rms_*load_dur_c		0	0		0.1181	Tukey-Kramer	0.3978

load_rms_*load_dur_c		0	0		0.3358	Tukey-Kramer	0.7692
load_rms_*load_dur_c		0	1		0.4787	Tukey-Kramer	0.8930
load_rms_*load_dur_c		0	1		0.8230	Tukey-Kramer	0.9960
load_rms_*load_dur_c		1	0		0.5841	Tukey-Kramer	0.9468
Moments							
N	247	**Sum Weights**	247				
Mean	-0.0001264	**Sum Observations**	-0.0312299				
Std Deviation	0.700624	**Variance**	0.49087399				
Skewness	-0.2131441	**Kurtosis**	-0.3004386				
Uncorrected SS	120.755006	**Corrected SS**	120.755002				
Coeff Variation	-554129.84	**Std Error Mean**	0.0445796 4				

Basic Statistical Measures			
Location	**Variability**		
Mean	-0.00013	**Std Deviation**	0.70062
Median	0.06776	**Variance**	0.49087
Mode	0.27508	**Range**	3.54037
		Interquartile Range	0.99774

Tests for Location: Mu0=0				
Test	**Statistic**	**p Value**		
Student's t	**t**	-0.00284	**Pr > |t|**	0.9977
Sign	**M**	5.5	**Pr >= |M|**	0.5247
Signed Rank	**S**	389	**Pr >= |S|**	0.7300

Tests for Normality				
Test	**Statistic**	**p Value**		
Shapiro-Wilk	**W**	0.991427	**Pr < W**	0.1583
Kolmogorov-Smirnov	**D**	0.047443	**Pr > D**	>0.1500
Cramer-von Mises	**W-Sq**	0.095427	**Pr > W-Sq**	0.1322
Anderson-Darling	**A-Sq**	0.562515	**Pr > A-Sq**	0.1477

Quantiles (Definition 5)	
Quantile	**Estimate**
100% Max	1.8399872
99%	1.4660603
95%	1.0722016
90%	0.8689785
75% Q3	0.4888603
50% Median	0.0677624
25% Q1	-0.5088792
10%	-0.9356996
5%	-1.2792893
1%	-1.7003872
0% Min	-1.7003872

Extreme Observations			
Lowest	**Highest**		
Value	**Obs**	**Value**	**Obs**
-1.70039	239	1.35476	4
-1.70039	88	1.38412	43
-1.70039	49	1.46606	44
-1.56065	128	1.48807	58
-1.56065	90	1.83999	6

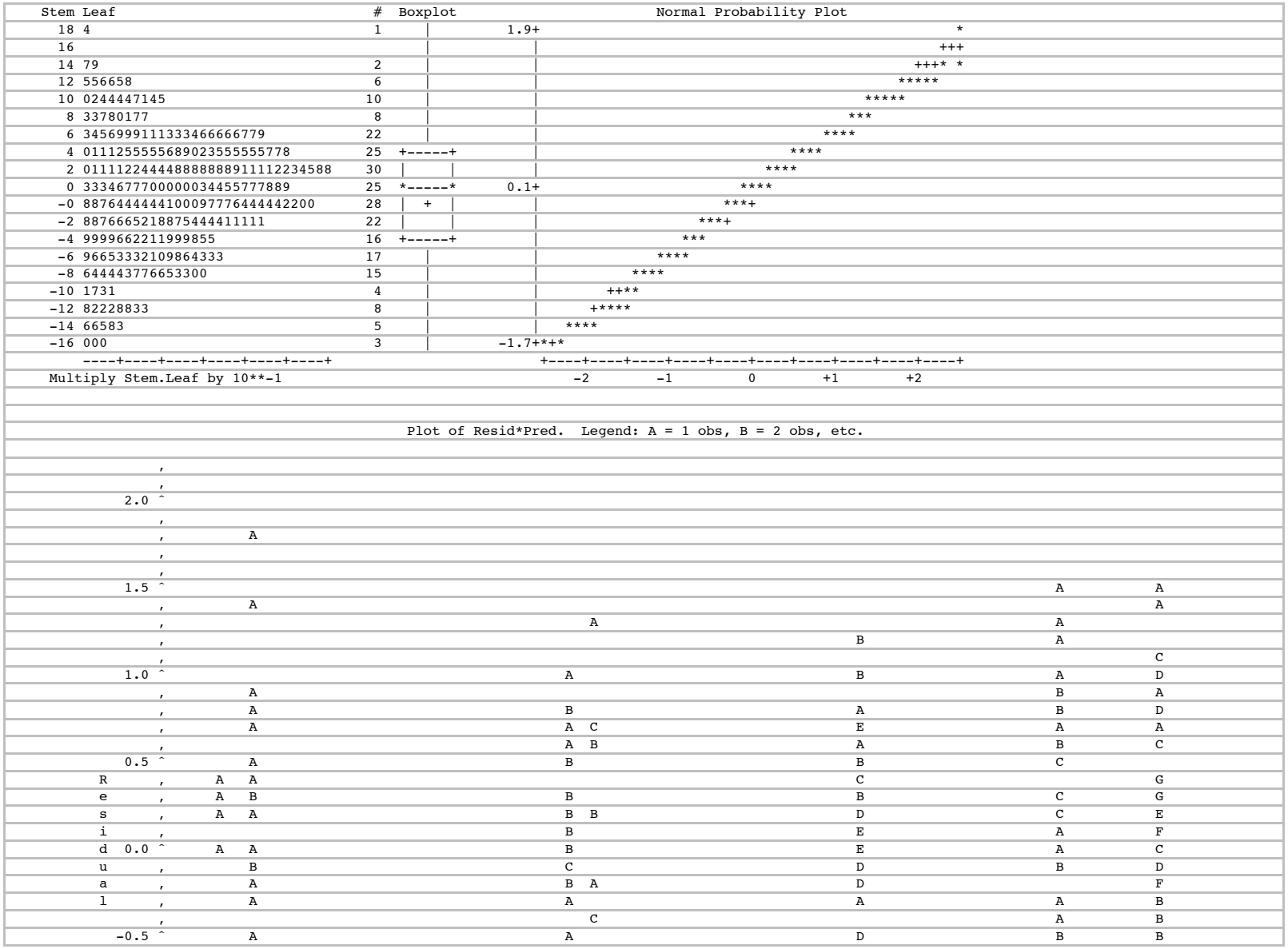
Stem Leaf # Boxplot Normal Probability Plot
18 4 1 1.9+ *
16 +++
14 79 2 +++* *
12 556658 6 *****
10 0244447145 10 *****
8 33780177 8 ***
6 3456999111333466666779 22 ****
4 0111255555689023555555778 25 +-----+ ****
2 01111224444888888891111234588 30 | | ****
0 3334677700000034455777889 25 *-----* 0.1+ ****
-0 8876444444100097776444442200 28 | + | ***+
-2 8876665218875444411111 22 | | ***+
-4 9999662211999855 16 +-----+ ***
-6 96653332109864333 17 ****
-8 644443776653300 15 ****
-10 1731 4 ++**
-12 82228833 8 +****
-14 66583 5 ****
-16 000 3 -1.7+*++
----+----+----+----+----+----+ +----+----+----+----+----+----+----+----+----+----+----+
Multiply Stem.Leaf by 10**-1 -2 -1 0 +1 +2
Plot of Resid*Pred. Legend: A = 1 obs, B = 2 obs, etc.
2.0 ^
1.5 ^
1.0 ^
0.5 ^
0.0 ^
-0.5 ^
R e s i d u a l

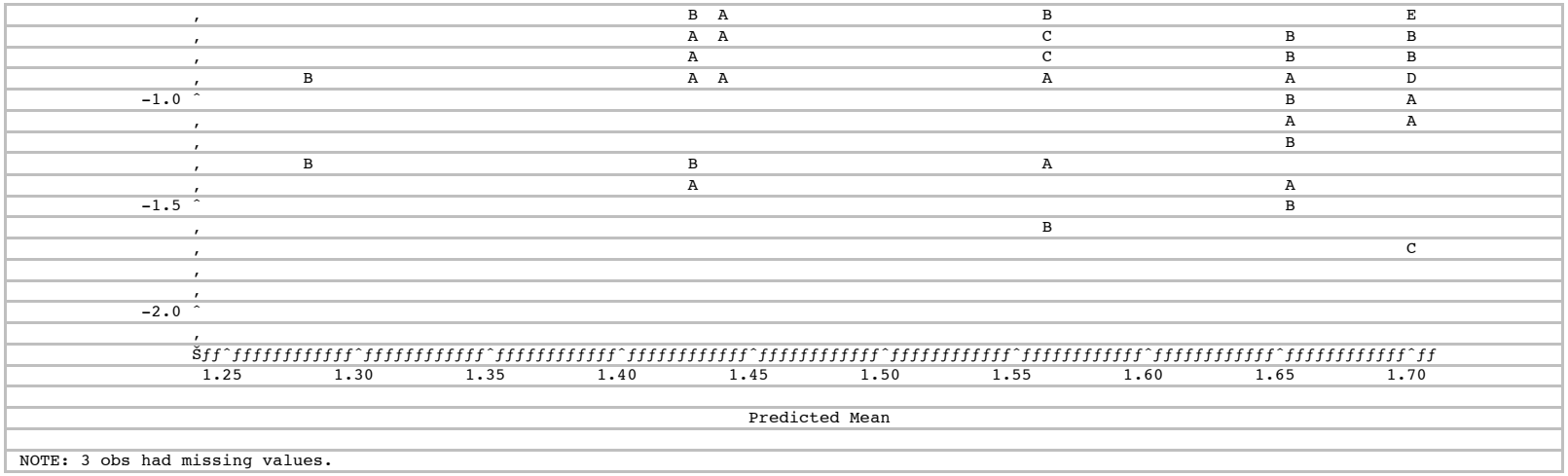

NOTE: 3 obs had missing values.

A.5 Copyright Permission

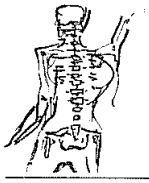

OPTIMA HEALTH SOLUTIONS
INTERNATIONAL CORPORATION

308—828 West 8th Avenue • Vancouver, BC • Canada V5Z 1E2 • Tel: (604) 266-5338 • Fax: (604) 267-0911 • www.khankinetic.com

April 16, 2013

Dr. Aslam H. Khan, D.C.
CEO, Optima Health Solutions International Corporation

Dear Dr. Khan:

I am a PhD Candidate at the University of Calgary. I would like your permission to reprint figure 1 of my thesis, which depicts a block diagram and two photographs of the cited intervention, the Khan Kinetic Treatment provided to me from you in December of 2006 for this exact purpose.

Please indicate your approval of this permission by signing the letter where indicated below and returning it to me as soon as possible. My email address is set forth below. Your signing of this letter will also confirm that you own the copyright to the above described material.

Thank you very much.
Sincerely,

PERMISSION GRANTED FOR THE USE REQUESTED ABOVE:

Dr. Aslam H. Khan
Date: April 16, 2013
Optima Health Solutions International Corporation

A.6 Bioreactor Schematics

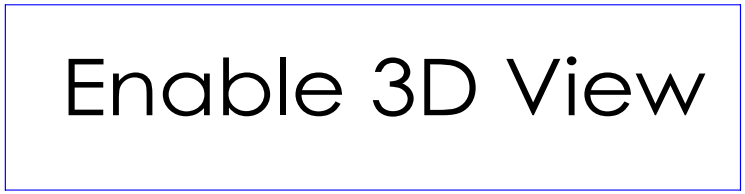
Enable 3D View

ITEM NO.	PART NUMBER	DESCRIPTION	QTY.
1	BR-006	FRAME	1
2	BR-002	TOP PLATE	1
3	BR-003	BASE PLATE	1
4	T7 round VC	VOICE COIL	4
5	4188T45	POLY JAR MCMASTER CARR	2
6	4188T45	POLY JAR MCMASTER CARR	2
7	84905A12	SERRATED GRIPPER MCMASTER CARR	8
8	HX-SHCS 0.25-20x0.5625x0.5625-N	SOCKET HEAD CAP SCREW 1/4-20	4
9	B18.3.5M - 6 x 1.0 x 12 Socket FCHS -- 12N	SOCKET COUNTERSUNK HEAD SCREW 6X1X12	24
10	BR-001	CLAMP PLATE	1
11	B18.3.1M - 6 x 1.0 x 20 Hex SHCS -- 20NHX	SOCKET HEAD CAP SCREW 6X1	8
12	B18.2.2.4M - Hex flange nut, M6 x 1 --N	FLANGE NUT M6X1	8
13	BR-004	GRIPPER ROD	4
14	BR-008	VC PUSH ROD	4
15	Preferred Narrow FW 0.164	8-32 WASHER	4
16	MSHXNUT 0.164-32-S-N	8-32 MACHINE SCREW HEX NUT	4
17	MSHXNUT 0.250-20-S-N	1/4-20 MACHINE SCREW HEX NUT	8
18	TUBE	MASTER FLEX L/S 25 TUBING	5
19	BR-007	TURNBUCKLE NUT	4
20	3842501753	BOSCH 8MM M6 T-NUT	24
21	2974K821	THRU WALL BARBED FITTING MCMASTER CARR	8
22	89585A1	BALL JOINT GRIPPER MCMASTER CARR (OPTIONAL)	4
23	HV-07575-10	COLE-PARMER PUMP	1

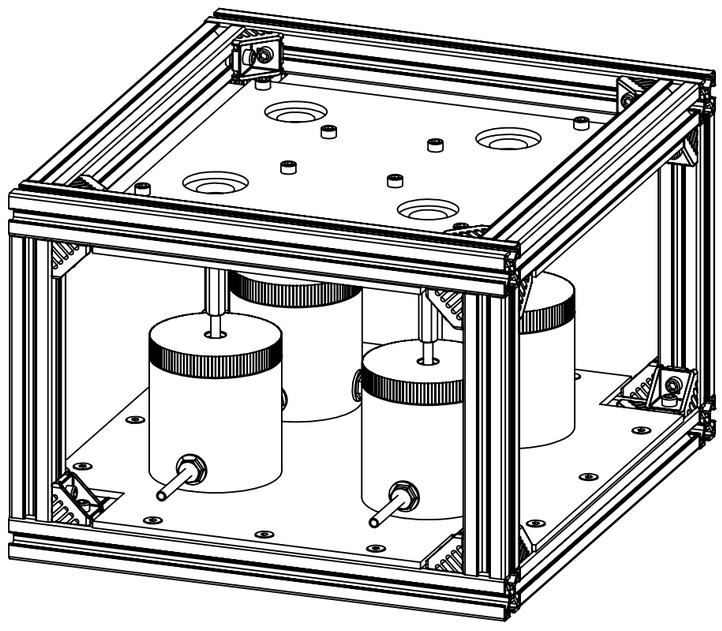

PROPRIETARY AND CONFIDENTIAL

THE INFORMATION CONTAINED IN THIS DRAWING IS THE SOLE PROPERTY OF <INSERT COMPANY NAME HERE>. ANY REPRODUCTION IN PART OR AS A WHOLE WITHOUT THE WRITTEN PERMISSION OF <INSERT COMPANY NAME HERE> IS PROHIBITED.

NEXT ASSY	USED ON
APPLICATION	

UNLESS OTHERWISE SPECIFIED:

DIMENSIONS ARE IN INCHES
TOLERANCES:
FRACTIONAL ±
ANGULAR: MACH ± BEND ±
TWO PLACE DECIMAL ±
THREE PLACE DECIMAL ±

INTERPRET GEOMETRIC TOLERANCING PER:

MATERIAL

FINISH

DO NOT SCALE DRAWING

	NAME	DATE
DRAWN		
CHECKED		
ENG APPR.		
MFG APPR.		
Q.A.		

COMMENTS:

TITLE:

BIO REACTOR ASSEMBLY

SIZE	DWG. NO.	REV
B	BR-009	

SCALE: 1:4	WEIGHT:	SHEET 1 OF 2

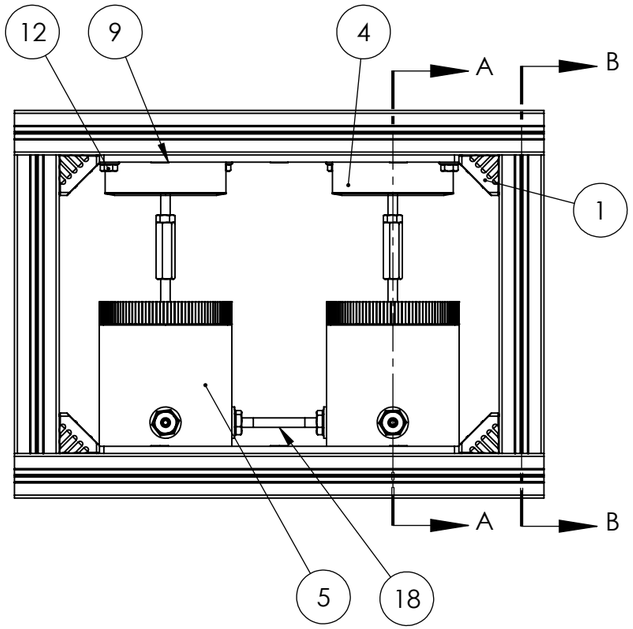

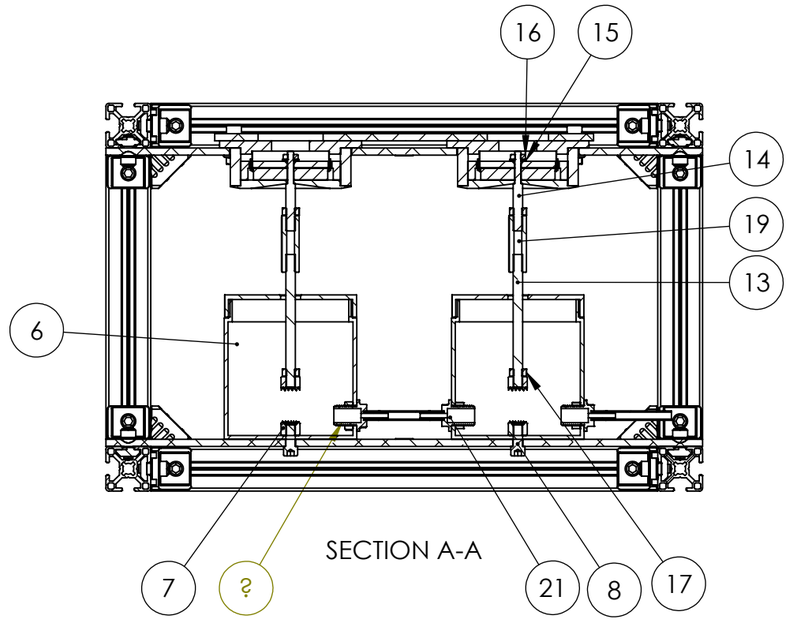

SECTION A-A

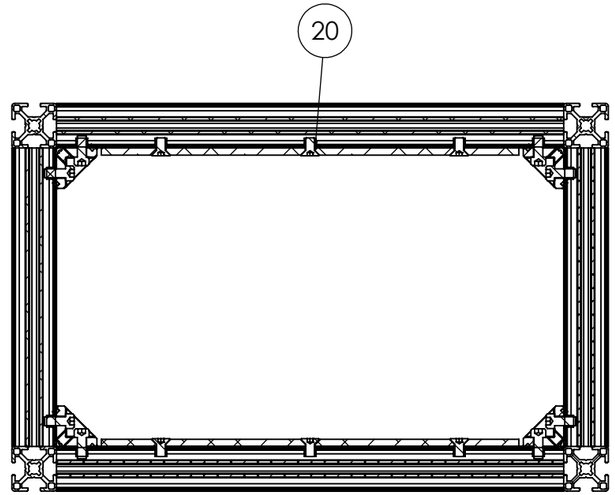

SECTION B-B

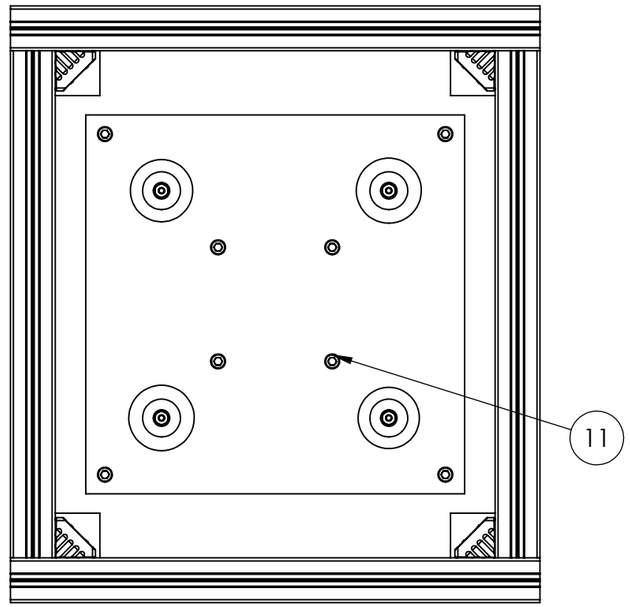

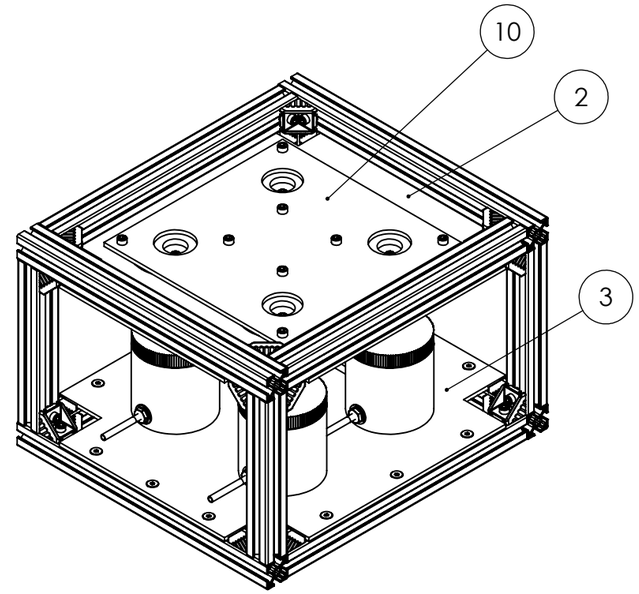

PROPRIETARY AND CONFIDENTIAL

THE INFORMATION CONTAINED IN THIS DRAWING IS THE SOLE PROPERTY OF <INSERT COMPANY NAME HERE>. ANY REPRODUCTION IN PART OR AS A WHOLE WITHOUT THE WRITTEN PERMISSION OF <INSERT COMPANY NAME HERE> IS PROHIBITED.

NEXT ASSY	USED ON
APPLICATION	

UNLESS OTHERWISE SPECIFIED:

DIMENSIONS ARE IN INCHES
TOLERANCES:
FRACTIONAL ±
ANGULAR: MACH ± BEND ±
TWO PLACE DECIMAL ±
THREE PLACE DECIMAL ±

INTERPRET GEOMETRIC TOLERANCING PER:

MATERIAL

FINISH

DO NOT SCALE DRAWING

	NAME	DATE
DRAWN		
CHECKED		
ENG APPR.		
MFG APPR.		
Q.A.		

COMMENTS:

TITLE:

SIZE	DWG. NO.	REV
B	BR-009	

SCALE: 1:4 | WEIGHT: | SHEET 2 OF 2

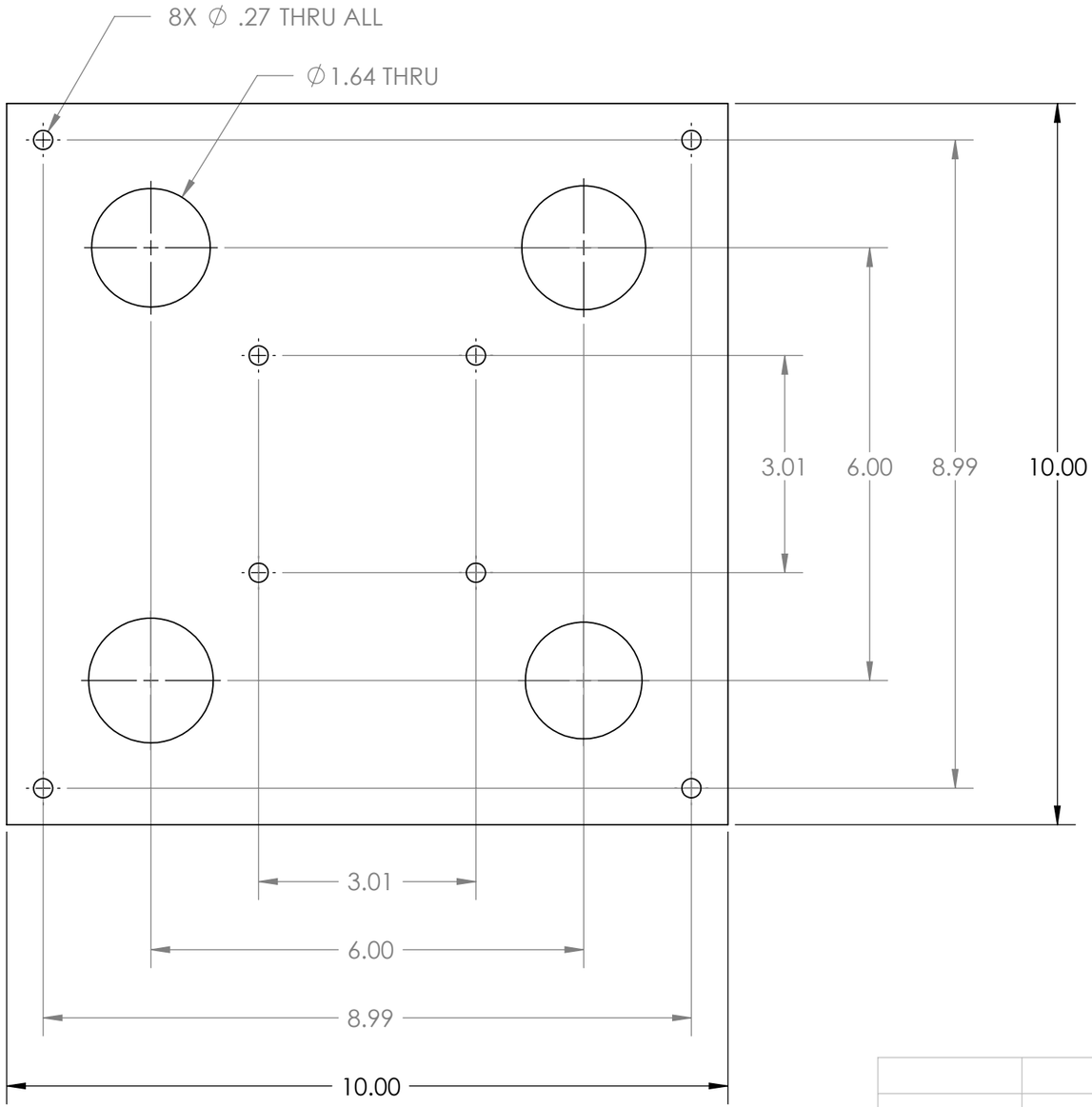

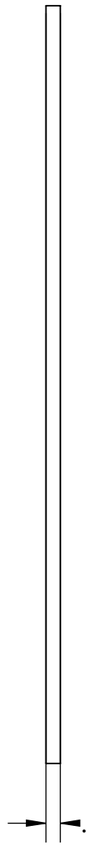

PROPRIETARY AND CONFIDENTIAL

THE INFORMATION CONTAINED IN THIS DRAWING IS THE SOLE PROPERTY OF <INSERT COMPANY NAME HERE>. ANY REPRODUCTION IN PART OR AS A WHOLE WITHOUT THE WRITTEN PERMISSION OF <INSERT COMPANY NAME HERE> IS PROHIBITED.

NEXT ASSY	USED ON
APPLICATION	

UNLESS OTHERWISE SPECIFIED:

DIMENSIONS ARE IN INCHES
TOLERANCES:
FRACTIONAL ±
ANGULAR: MACH ± BEND ±
TWO PLACE DECIMAL ±
THREE PLACE DECIMAL ±

INTERPRET GEOMETRIC TOLERANCING PER:

MATERIAL
6061-T6 (SS)

FINISH

DO NOT SCALE DRAWING

	NAME	DATE
DRAWN		
CHECKED		
ENG APPR.		
MFG APPR.		
Q.A.		

COMMENTS:

TITLE:

CLAMP PLATE

SIZE	DWG. NO.	REV
B	BR-001	

SCALE: 1:2	WEIGHT:	SHEET 1 OF 1

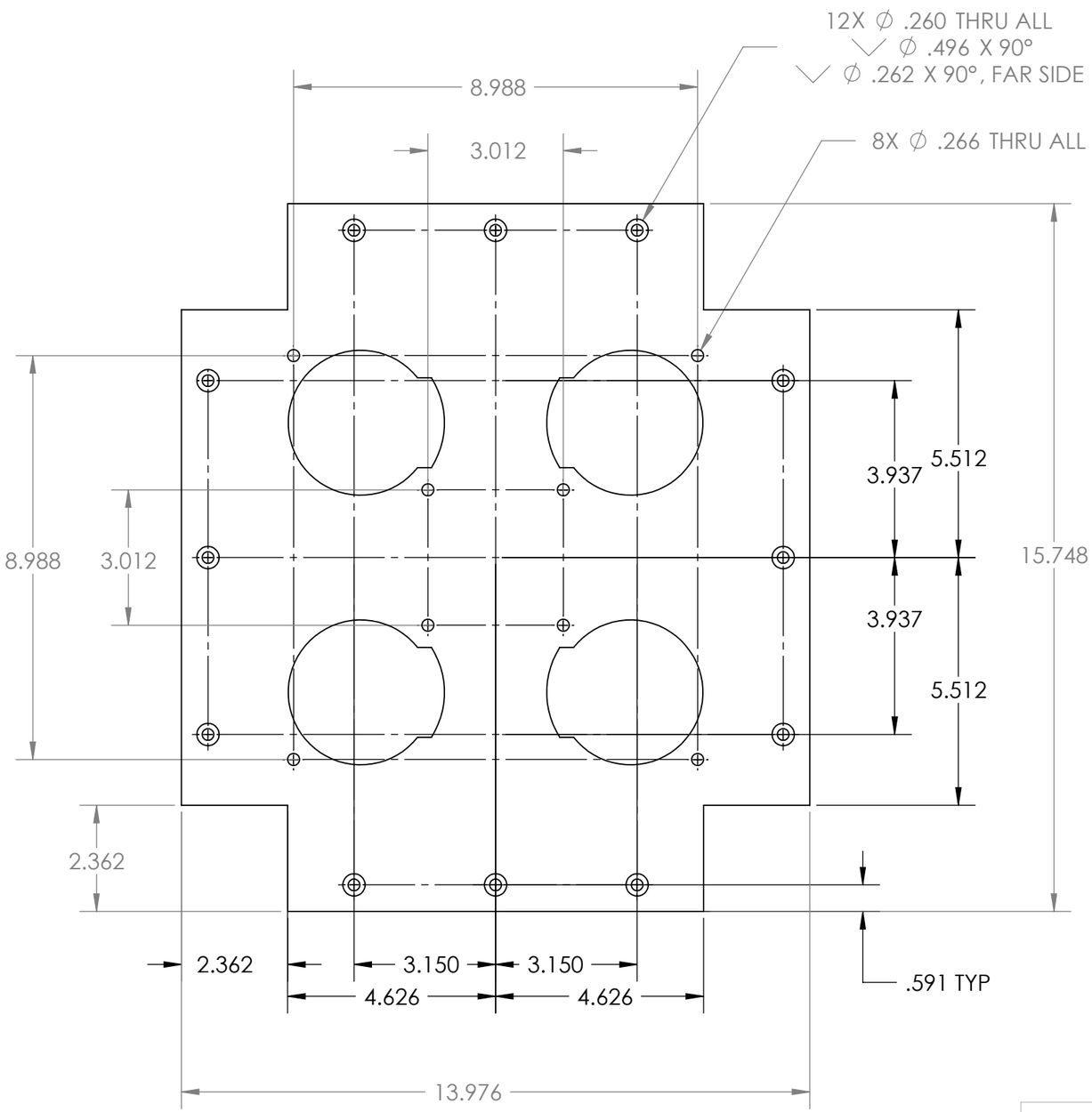

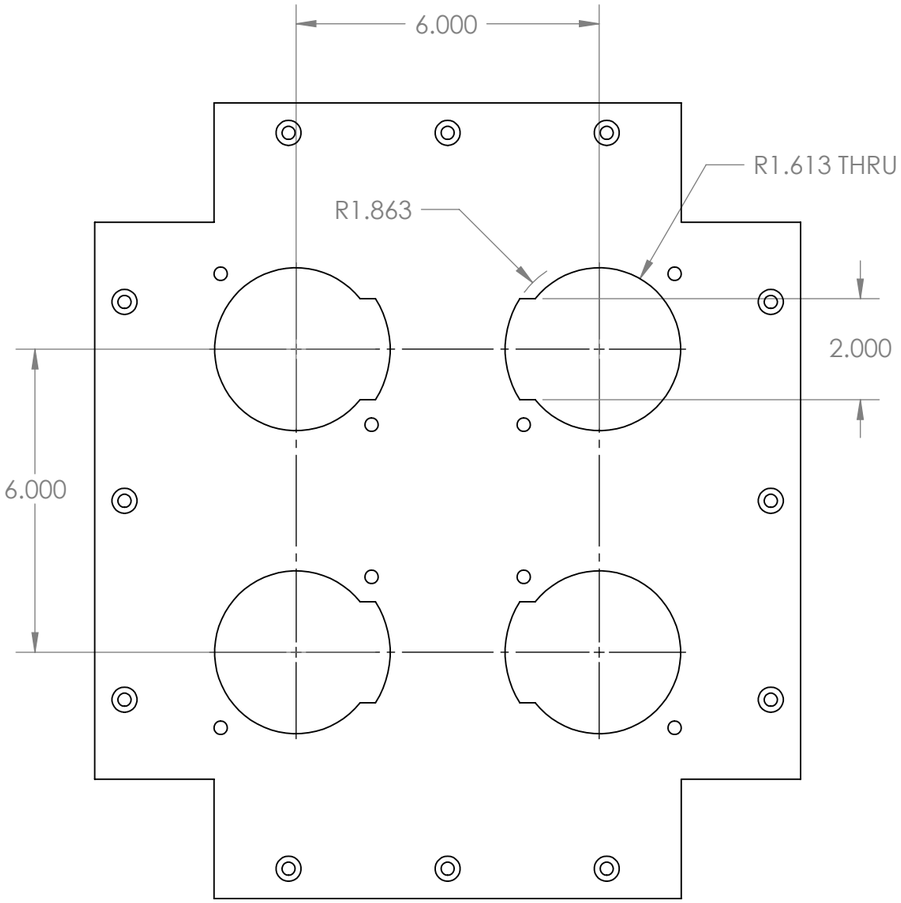

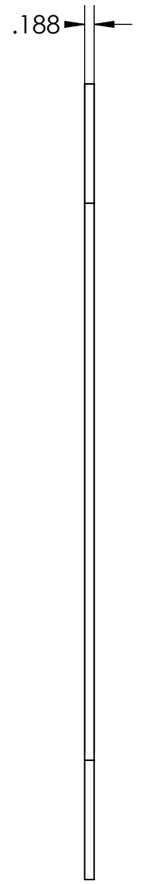

		UNLESS OTHERWISE SPECIFIED:		NAME	DATE
		DIMENSIONS ARE IN INCHES TOLERANCES: FRACTIONAL ± ANGULAR: MACH ± BEND ± TWO PLACE DECIMAL ± THREE PLACE DECIMAL ±	DRAWN		
			CHECKED		
			ENG APPR.		
			MFG APPR.		
		INTERPRET GEOMETRIC TOLERANCING PER:	Q.A.		
		MATERIAL 6061-T6 (SS)	COMMENTS:		
NEXT ASSY	USED ON	FINISH			
APPLICATION		DO NOT SCALE DRAWING			

PROPRIETARY AND CONFIDENTIAL

THE INFORMATION CONTAINED IN THIS DRAWING IS THE SOLE PROPERTY OF <INSERT COMPANY NAME HERE>. ANY REPRODUCTION IN PART OR AS A WHOLE WITHOUT THE WRITTEN PERMISSION OF <INSERT COMPANY NAME HERE> IS PROHIBITED.

TITLE:

TOP PLATE

SIZE	DWG. NO.	REV
B	BR-002	
SCALE: 1:3	WEIGHT:	SHEET 1 OF 1

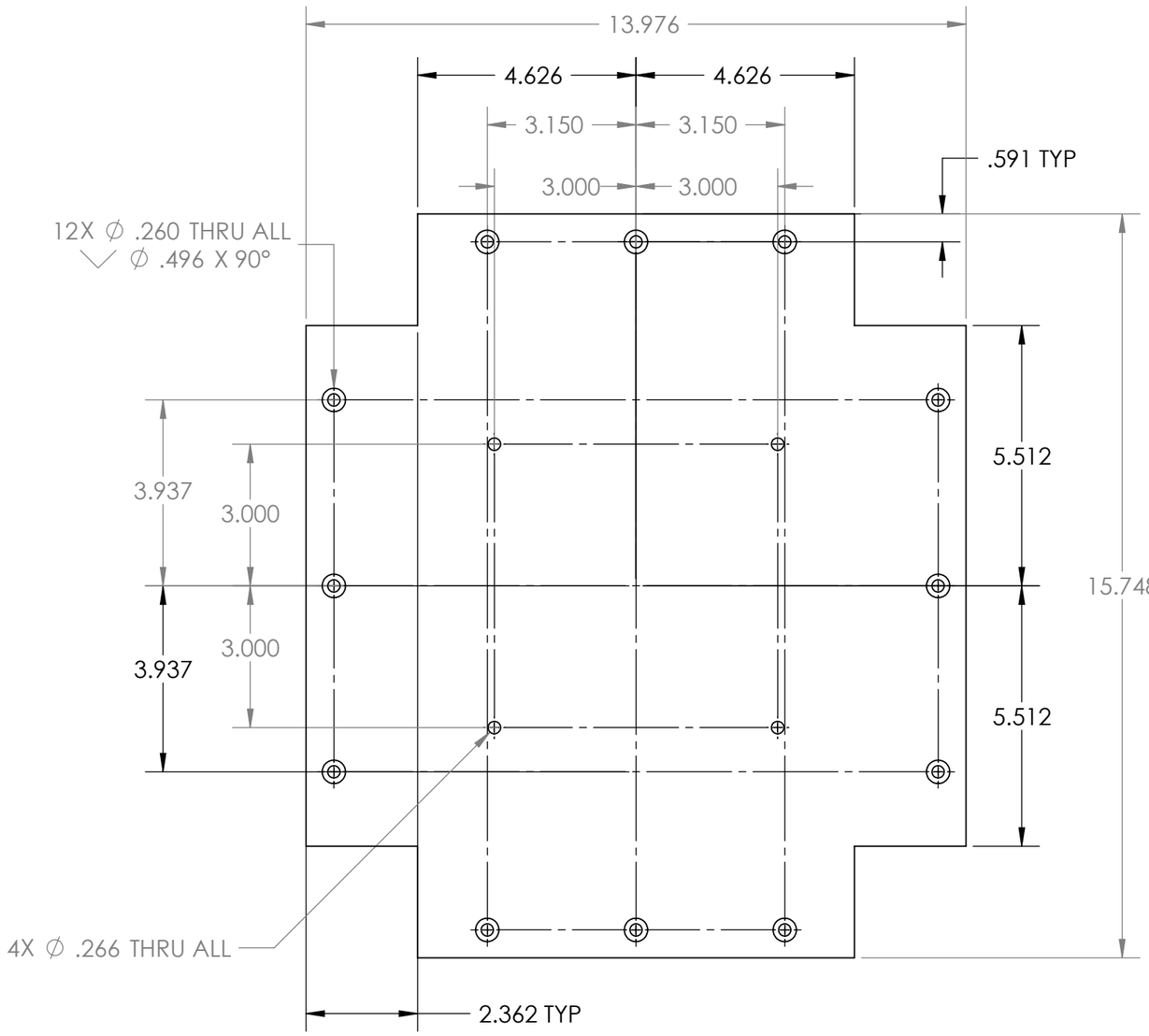

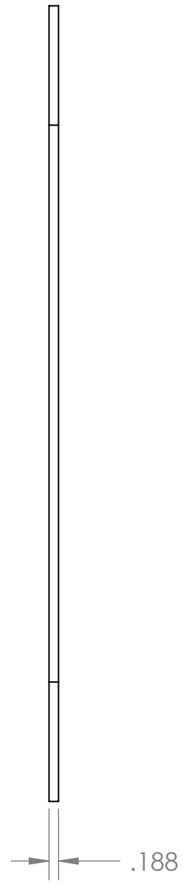

PROPRIETARY AND CONFIDENTIAL

THE INFORMATION CONTAINED IN THIS DRAWING IS THE SOLE PROPERTY OF <INSERT COMPANY NAME HERE>. ANY REPRODUCTION IN PART OR AS A WHOLE WITHOUT THE WRITTEN PERMISSION OF <INSERT COMPANY NAME HERE> IS PROHIBITED.

		UNLESS OTHERWISE SPECIFIED:		NAME	DATE
		DIMENSIONS ARE IN INCHES TOLERANCES: FRACTIONAL ± ANGULAR: MACH ± BEND ± TWO PLACE DECIMAL ± THREE PLACE DECIMAL ±	DRAWN	BE	6-18-10
			CHECKED		
			ENG APPR.		
			MFG APPR.		
		INTERPRET GEOMETRIC TOLERANCING PER:	Q.A.		
		MATERIAL 6061-T6 (SS)	COMMENTS:		
NEXT ASSY	USED ON	FINISH			
APPLICATION		DO NOT SCALE DRAWING			

TITLE:

BASE PLATE

SIZE	DWG. NO.	REV
B	BR-003	

SCALE: 1:3	WEIGHT:	SHEET 1 OF 1

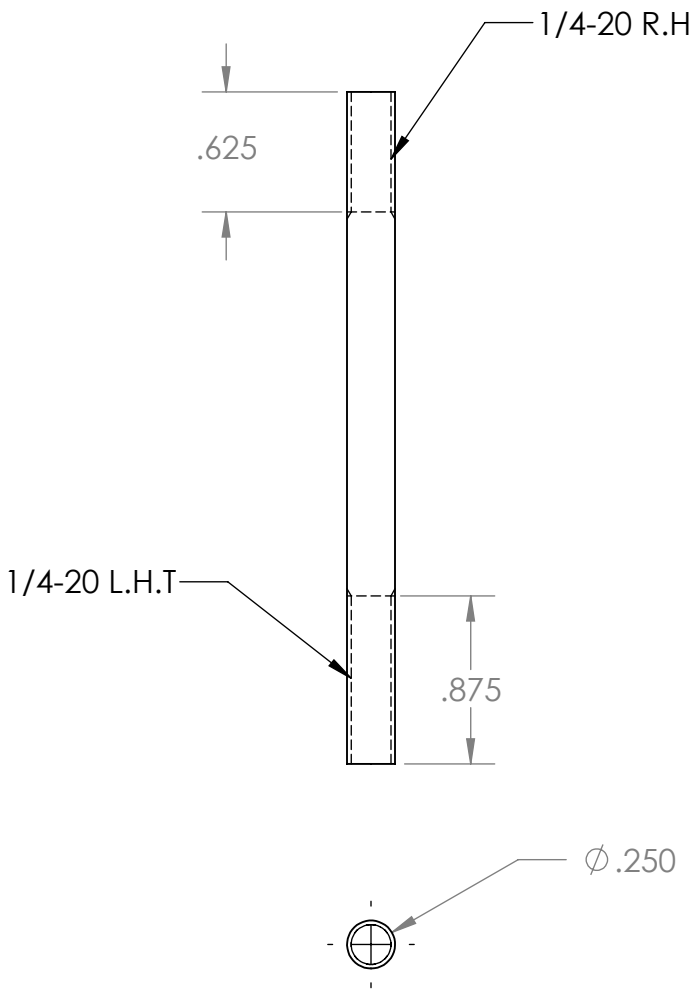

		UNLESS OTHERWISE SPECIFIED:		NAME	DATE
		DIMENSIONS ARE IN INCHES TOLERANCES: FRACTIONAL ± ANGULAR: MACH ± BEND ± TWO PLACE DECIMAL ± THREE PLACE DECIMAL ±	DRAWN		
			CHECKED		
			ENG APPR.		
			MFG APPR.		
		INTERPRET GEOMETRIC TOLERANCING PER:	Q.A.		
		MATERIAL Alloy Steel (SS)	COMMENTS:		
NEXT ASSY	USED ON	FINISH			
APPLICATION		DO NOT SCALE DRAWING			

PROPRIETARY AND CONFIDENTIAL

THE INFORMATION CONTAINED IN THIS DRAWING IS THE SOLE PROPERTY OF <INSERT COMPANY NAME HERE>. ANY REPRODUCTION IN PART OR AS A WHOLE WITHOUT THE WRITTEN PERMISSION OF <INSERT COMPANY NAME HERE> IS PROHIBITED.

TITLE:

GRIPPER ROD

SIZE	DWG. NO.	REV
A	BR-004	

SCALE: 1:1	WEIGHT:	SHEET 1 OF 1

5 4 3 2 1

ITEM NO.	QTY.	DESCRIPTION	LENGTH
1	4	REXROTH PN. 3 842 990 742	13.98
2	4	REXROTH PN. 3 842 990 742	7.87
3	4	REXROTH PN. 3 842 990 742	13.39

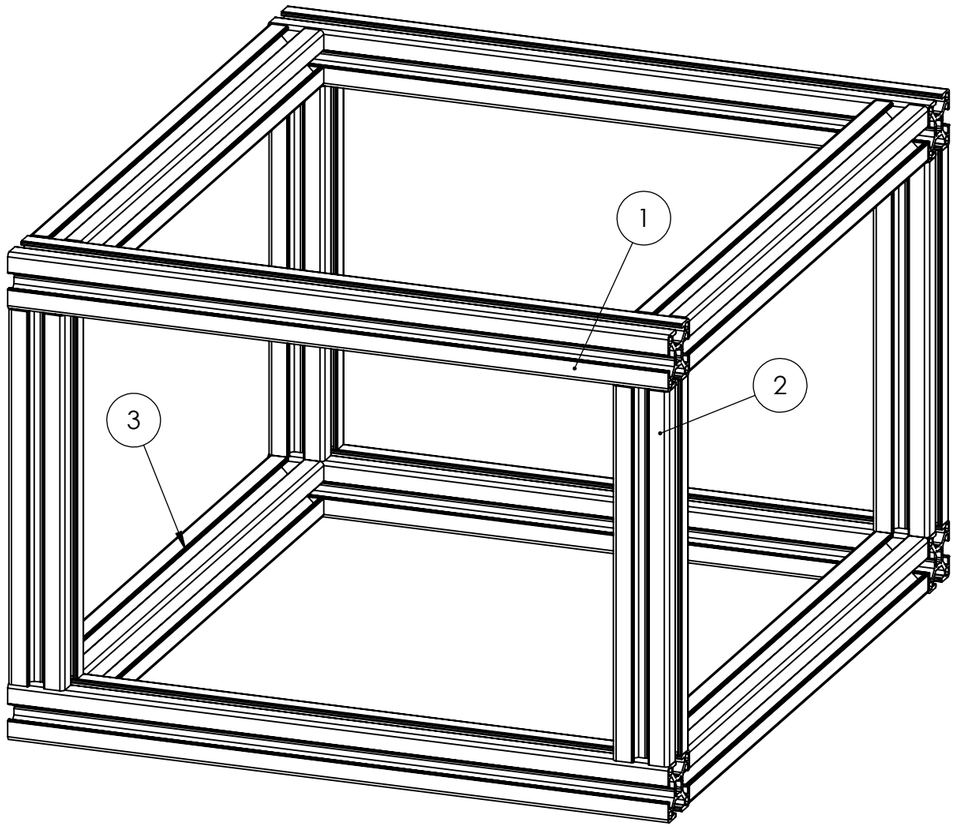

PROPRIETARY AND CONFIDENTIAL

THE INFORMATION CONTAINED IN THIS DRAWING IS THE SOLE PROPERTY OF <INSERT COMPANY NAME HERE>. ANY REPRODUCTION IN PART OR AS A WHOLE WITHOUT THE WRITTEN PERMISSION OF <INSERT COMPANY NAME HERE> IS PROHIBITED.

NEXT ASSY	USED ON	
APPLICATION		DO NOT SCALE DRAWING

UNLESS OTHERWISE SPECIFIED:

DIMENSIONS ARE IN INCHES
TOLERANCES:
FRACTIONAL ±
ANGULAR: MACH ± BEND ±
TWO PLACE DECIMAL ±
THREE PLACE DECIMAL ±

INTERPRET GEOMETRIC TOLERANCING PER:

MATERIAL
6061-T6 (SS)

FINISH

	NAME	DATE
DRAWN		
CHECKED		
ENG APPR.		
MFG APPR.		
Q.A.		

COMMENTS:

TITLE:

BOSCH 30X30 FRAME

SIZE	DWG. NO.	REV
B	BR-005	

SCALE: 1:3 | WEIGHT: | SHEET 1 OF 1

ITEM NO.	PART NUMBER	DESCRIPTION	QTY.
1	BR-005	BOSCH/REXROTH 30X30 FRAME	1
2	3 842 523 528	BOSCH/REXROTH GUSSET	24

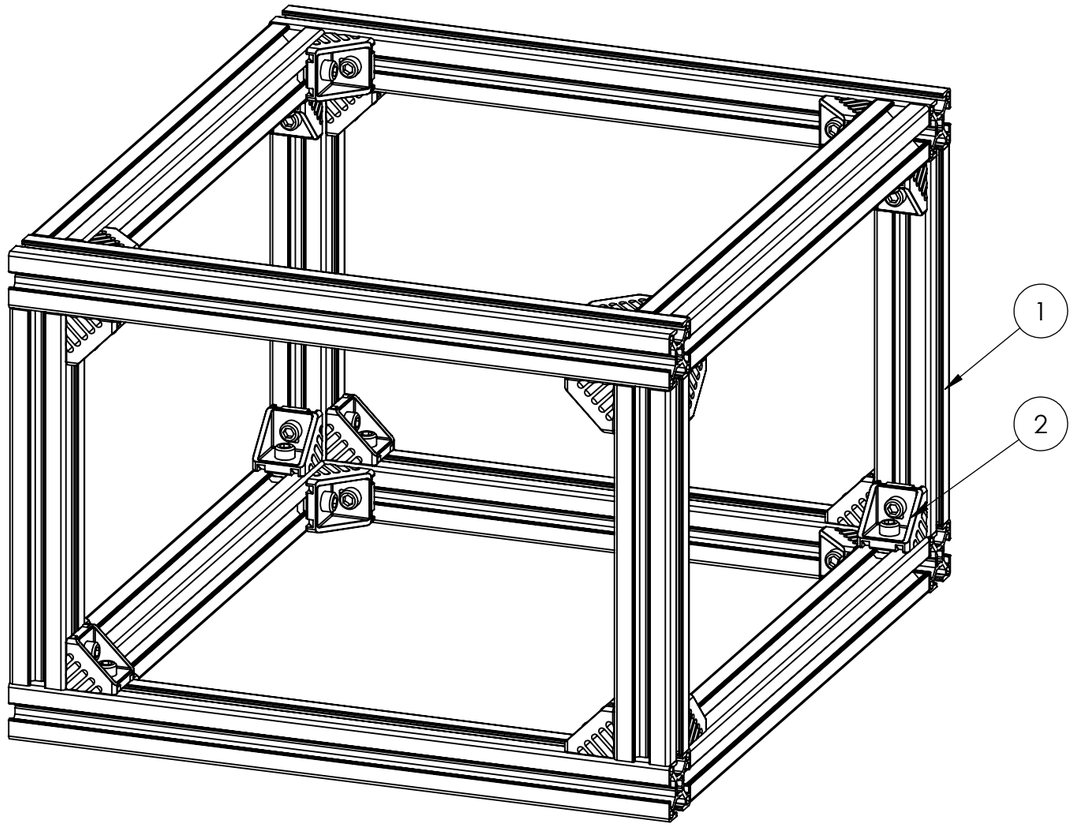

PROPRIETARY AND CONFIDENTIAL

THE INFORMATION CONTAINED IN THIS DRAWING IS THE SOLE PROPERTY OF <INSERT COMPANY NAME HERE>. ANY REPRODUCTION IN PART OR AS A WHOLE WITHOUT THE WRITTEN PERMISSION OF <INSERT COMPANY NAME HERE> IS PROHIBITED.

NEXT ASSY	USED ON	
APPLICATION		DO NOT SCALE DRAWING

UNLESS OTHERWISE SPECIFIED:

DIMENSIONS ARE IN INCHES
TOLERANCES:
FRACTIONAL ±
ANGULAR: MACH ± BEND ±
TWO PLACE DECIMAL ±
THREE PLACE DECIMAL ±

INTERPRET GEOMETRIC TOLERANCING PER:

MATERIAL

FINISH

	NAME	DATE
DRAWN		
CHECKED		
ENG APPR.		
MFG APPR.		
Q.A.		

COMMENTS:

TITLE:

FRAME

SIZE	DWG. NO.	REV
B	BR-006	

SCALE: 1:3	WEIGHT:	SHEET 1 OF 1

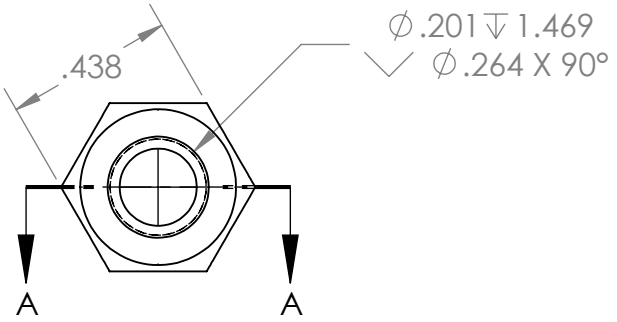

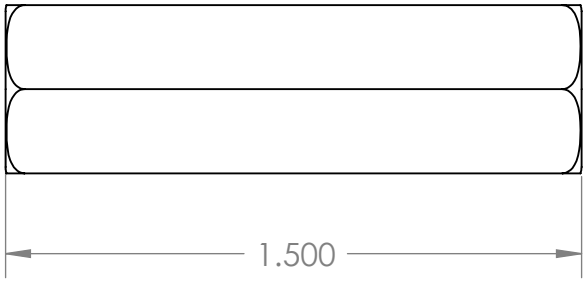

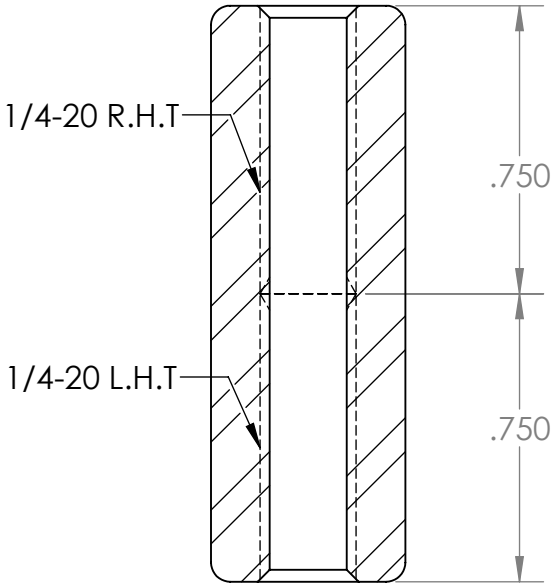

SECTION A-A

		UNLESS OTHERWISE SPECIFIED:		NAME	DATE
		DIMENSIONS ARE IN INCHES TOLERANCES: FRACTIONAL ± ANGULAR: MACH ± BEND ± TWO PLACE DECIMAL ± THREE PLACE DECIMAL ±	DRAWN		
			CHECKED		
			ENG APPR.		
			MFG APPR.		
		INTERPRET GEOMETRIC TOLERANCING PER:	Q.A.		
		MATERIAL Alloy Steel (SS)	COMMENTS:		
NEXT ASSY	USED ON	FINISH			
APPLICATION		DO NOT SCALE DRAWING			

PROPRIETARY AND CONFIDENTIAL

THE INFORMATION CONTAINED IN THIS DRAWING IS THE SOLE PROPERTY OF <INSERT COMPANY NAME HERE>. ANY REPRODUCTION IN PART OR AS A WHOLE WITHOUT THE WRITTEN PERMISSION OF <INSERT COMPANY NAME HERE> IS PROHIBITED.

TITLE:

TURNBUCKLE NUT

SIZE	DWG. NO.	REV
A	BR-007	

SCALE: 2:1	WEIGHT:	SHEET 1 OF 1

5 4 3 2 1

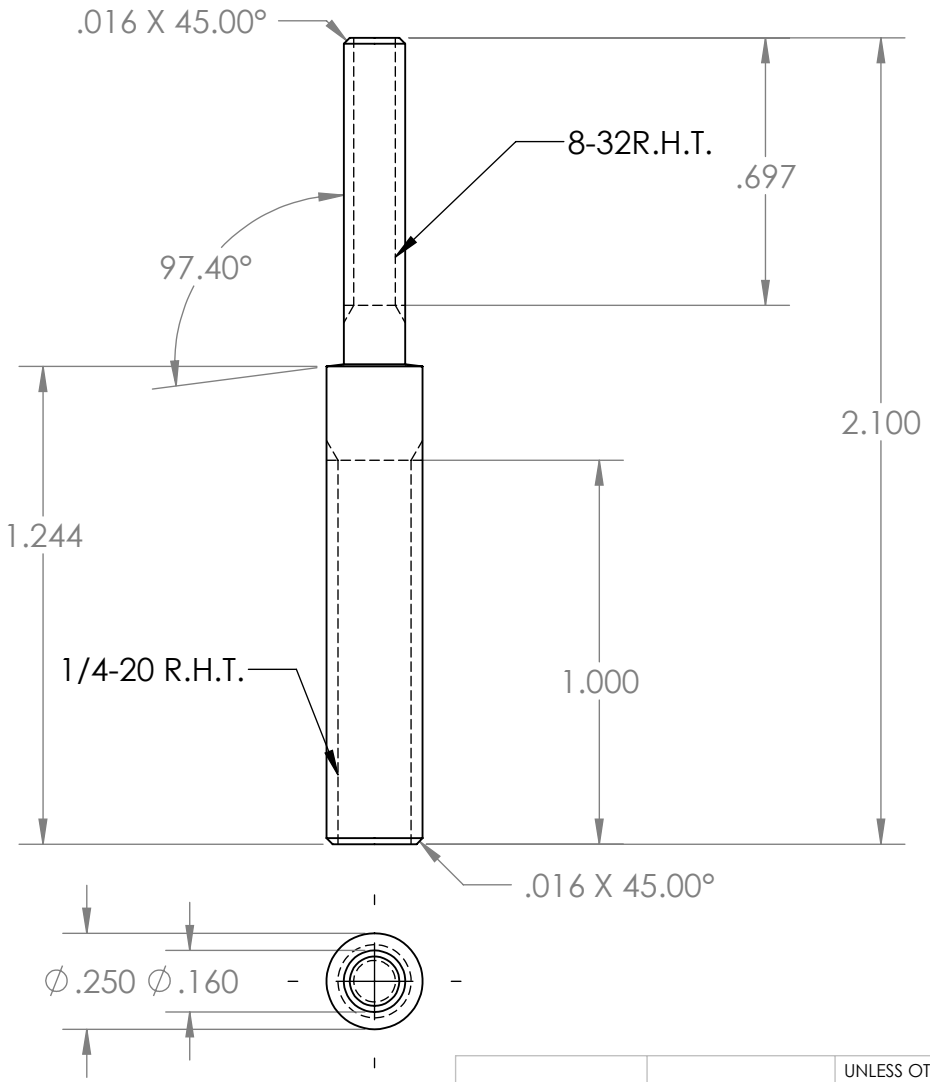

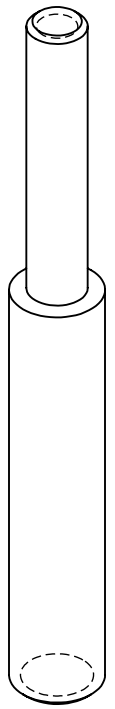

		UNLESS OTHERWISE SPECIFIED:		NAME	DATE
		DIMENSIONS ARE IN INCHES TOLERANCES: FRACTIONAL ± ANGULAR: MACH ± BEND ± TWO PLACE DECIMAL ± THREE PLACE DECIMAL ±	DRAWN		
			CHECKED		
			ENG APPR.		
			MFG APPR.		
		INTERPRET GEOMETRIC TOLERANCING PER:	Q.A.		
		MATERIAL Alloy Steel (SS)	COMMENTS:		
NEXT ASSY	USED ON	FINISH			
APPLICATION		DO NOT SCALE DRAWING			

PROPRIETARY AND CONFIDENTIAL

THE INFORMATION CONTAINED IN THIS DRAWING IS THE SOLE PROPERTY OF <INSERT COMPANY NAME HERE>. ANY REPRODUCTION IN PART OR AS A WHOLE WITHOUT THE WRITTEN PERMISSION OF <INSERT COMPANY NAME HERE> IS PROHIBITED.

TITLE:

VC PUSH ROD

SIZE	DWG. NO.	REV
A	BR-008	

SCALE: 2:1	WEIGHT:	SHEET 1 OF 1

5 4 3 2 1